Aspects of Supersymmetric Gauge Theories and Conformal Field Theories in Five and Three Dimensions



Julius Maurice Eckhard

Somerville College

University of Oxford

A thesis submitted for the degree of

Doctor of Philosophy

Michaelmas 2020

Abstract

Supersymmetric gauge theories and superconformal field theories have long played a central role in string theory. In this thesis, which is split into two parts, we explore multiple facets of this rich class of theories.

In the first part we establish a convenient way to describe 5d SCFTs and gauge theories — generalised toric polygons (GTPs). Based on insights from (p, q) 5-brane-webs we derive a dictionary between a 5d theory $\mathcal{T}_P$ and its associated GTP P. We provide an algorithm to describe the Higgs branch of $\mathcal{T}_P$ by computing its magnetic quiver. Furthermore, we identify the Hasse diagram and thereby the entire foliation structure of the Higgs branch. We apply this technique to a large class of 5d SCFTs with a weakly coupled $SU(N)$ gauge theory description. In this way we both recover known results and derive a series of new magnetic quivers.

In the second part we turn to the 3d-3d correspondence, that relates observables of supersymmetric 3d gauge theories $T[M_3]$ to partition functions of topological field theories on M_3. We study the sensitivity of this setup to the gauging of higher-form symmetries. We find a refinement of the 3d-3d correspondence for the Witten index, associated to the global structure of the gauge group of $T[M_3]$. For M_3 a Seifert manifold and gauge algebra $\mathfrak{g} = \mathfrak{su}(2)$ we verify this explicitly by counting the solutions to the resulting Bethe equations. We complement this analysis by a refined counting of the flat connections on M_3, accounting for the higher-form symmetries.

Finally, we investigate the so far unknown 3d-3d correspondences for theories with $\mathcal{N} = 1$ supersymmetry. We study the theories $T_{\mathcal{N}=1}[M_3]$ and analyse their connection to the geometry of G_2-manifolds. On the complementary side of the 3d-3d correspondence we determine the topological field theories whose partition functions compute the Witten index and the S^3-partition function of $T_{\mathcal{N}=1}[M_3]$. In the process we point out the relevance of a new generalisation of 3d Seiberg-Witten equations.

Statement of Originality

This thesis is based on research carried out in collaboration with Sakura Schäfer-Nameki, Jin-Mann Wong, Heeyeon Kim, Brian Willett, Yi-Nan Wang, Marieke van Beest and Antoine Bourget. I contributed substantially to all presented results.
Part I is based on the papers

- M. van Beest, A. Bourget, J. Eckhard and S. Schafer-Nameki, *(Symplectic) Leaves and (5d Higgs) Branches in the Poly(go)nesian Tropical Rain Forest*, 2008.05577 [1]
- M. van Beest, A. Bourget, J. Eckhard and S. Schafer-Nameki, *(5d RG-flow) Trees in the Tropical Rain Forest*, 2011.07033 [2]
- J. Eckhard, S. Schäfer-Nameki and Y.-N. Wang, *Trifectas for T_N in 5d*, *JHEP* **07** (2020) 199 [2004.15007] [3]

Part II is based on the papers

- J. Eckhard, H. Kim, S. Schafer-Nameki and B. Willett, *Higher-Form Symmetries, Bethe Vacua, and the 3d-3d Correspondence*, *JHEP* **01** (2020) 101 [1910.14086] [4]
- J. Eckhard, S. Schäfer-Nameki and J.-M. Wong, *An $\mathcal{N} = 1$ 3d-3d Correspondence*, *JHEP* **07** (2018) 052 [1804.02368] [5]

Acknowledgements

I am absolutely delighted to thank my supervisor Sakura Schäfer-Nameki for her constant support, both academically and personally. Her firm guidance and everlasting enthusiasm were truly invaluable and made this thesis possible. I could not have wished for a better supervisor.
During my research I was blessed with a set of fantastic collaborators, so I would also like to acknowledge Marieke van Beest, Antoine Bourget, Heeyeon Kim, Yi-Nan Wang, Brian Willett and Jenny Wong. Furthermore, I benefitted greatly from discussions with Fabio Apruzzi, Martin Bies, Andreas Braun, Cyril Closset, Andrés Collinucci, Marc-Antoine Fiset, Simone Giacomelli, Max Hübner and many more. Special thanks go to Cyril Closset and Amihay Hanany, who agreed to assess this thesis.
For financial support I would also like to thank the ERC Consolidator Grant 682608 (HIGGSBNDL), the ERC Starting Grant 306260 (DUALITIESHEPTH) and the Simons Foundation.
I would like to thank my friends and colleagues from the mathematical physics group for stimulating discussions during coffee breaks and wine receptions. For distracting me from physics, I would also like to thank my teammates at OUQC and Oxford Mammoths. I am thankful that so many of my friends and family visited me, although some of them deferred it to literally the last day. Finally, my gratitude goes to my parents, Corinna and Wolfgang, and to Antonia for their unwavering love, support and hospitality during the completion of this thesis.

Oxford, October 19, 2020

„Das ist, äh, eine Doktorarbeit.“
„Eine Doktorarbeit? Jetzt bin ich aber erleichtert. Ich dachte schon,
es sei eine schreckliche Krankheit.“
„Das ist eine Doktorarbeit gewissermaßen auch.“

Dr. Oztafan Kolibril und Volzotan Smeik
Rumo & Die Wunder im Dunkeln

Contents

1 Introduction **1**
1.1 Gauge Theories and SCFTs in String Theory 1
1.2 Content of this Thesis 7

I Five Dimensions **14**

2 Background in Five Dimensions **15**
2.1 5d SCFTs and Gauge Theories 15
2.2 (p, q) 5-Brane-Webs and Monodromies 19
2.3 Magnetic Quivers and Hasse Diagrams 22

3 The Tropical Rain Forest **26**
3.1 Generalised Toric Polygons of 5d SCFTs 28
3.2 Higgs Branches for 5d SCFTs from Edge Colourings 36
3.3 Application: $SU(N)$ with AS and F Matter 49
3.4 Derivation from the Tropics 62

II Three Dimensions **70**

4 Background in Three Dimensions **71**
4.1 $T[M_3]$ and the 3d-3d Correspondence 71
4.2 Higher-Form Symmetries 74

5 Higher-Form Symmetries, Bethe Vacua and the 3d-3d Correspondence **79**
5.1 $\widehat{T}[\Omega, G]$ from Graphs 82
5.2 $T[M_3, \mathfrak{g}, H]$ and Higher-Form Symmetries 96
5.3 Bethe Vacua for $T[M_3, \mathfrak{g}]$ 117

5.4 Flat Connections on M_3 and the 3d-3d Correspondence 132

6 An $\mathcal{N}=1$ 3d-3d Correspondence 140

6.1 $T_{\mathcal{N}=1}[M_3]$ 142

6.2 The BFH Model 152

6.3 S^3-Partition Function and Chern-Simons-Dirac Theory 158

7 Conclusion and Outlook 165

A Appendices to Part I 168

A.1 Brane-Webs for $SU(N)$ Gauge Theories 168

A.2 Detailed Analysis of the Submarginal SQCD 170

A.3 Tables of Magnetic Quivers 175

B Appendices to Part II 179

B.1 Positive Curvature Seifert Manifolds 179

B.2 Twisted Superpotential and Bethe Equations for $\widehat{T}[\Omega, SU(2)]$ 181

B.3 One-form Symmetries and Anomalies for Bethe Vacua 184

B.4 Flat Connections on S^3/Γ_{ADE} 186

B.5 G_2-holonomy, Associatives and Deformation Theory 189

B.6 Reduction of the Abelian 6d (2,0) Tensor Multiplet to 3d $\mathcal{N}=1$ . . . 191

B.7 M5-branes on S^3 197

B.8 Index Conventions for Section 6 199

Bibliography 201

List of Figures

3.1 Example of decoupling antisymmetric and fundamental matter 62

5.1 Plumbing graph for Seifert manifolds 84
5.2 Symmetries acting on plumbing data 86
5.3 Quiver description of $\widehat{T}[\Omega_{[k_1,k_2]}, G]]$ 91
5.4 Duality sequence between FT and trinion 93
5.5 Heegaard decomposition of $L(p,1)$ 114
5.6 Heegaard decomposition of $L(p,q)$ 116
5.7 Quiver corresponding to $\Omega_{[k_1,\cdots,k_n]}$ 122
5.8 Duality to trinion theory: Three copies of $T(SU(N)) \cong T_N$ 123
5.9 Quiver for two coupled trinions 123

6.1 $\mathcal{N}=1$ 3d-3d Correspondence for the Witten Index 141
6.2 Different compactification order of the 6d (2,0) on $M_3 \times S^1$ 147
6.3 Quiver of the $\mathcal{N}=2$ enhancement point of $\widehat{T}_{\mathcal{N}=1}[\Omega_{[k_1,\cdots,k_n]}, G]$ 150

List of Tables

1.1 Berger's list 3
1.2 List of calibrated cycles 5

2.1 Second index and triangle anomaly coefficient 18
2.2 List of assorted marginal 5d gauge theories 18
2.3 Summary of elementary transverse slices 25

3.1 Construction of polygons for the theories studied in this chapter . . . 32
3.2 Dictionary between brane-webs/tropics and coloured GTPs 69

4.1 TFTs obtained from 6d (2,0) on W_3 with a topological twist on M_3 . 74

5.1 Summary of the theories defined in this chapter 81
5.2 Quiver data and vacuum count for various Seifert manifolds for $G = U(2)$ 124
5.3 Dimensions of the eigenspaces $V_{\epsilon_A \epsilon_B}$ for $\Upsilon = \mathbb{Z}_2$ 130
5.4 Indices of $T[M_3, \mathfrak{su}(2), \mathbb{Z}_2^{(\delta)}]$ 130
5.5 Dimensions of the eigenspaces $V_{\epsilon_A^1 \epsilon_B^1 \epsilon_A^2 \epsilon_B^2}$ for $\Upsilon = \mathbb{Z}_2^{(1)} \times \mathbb{Z}_2^{(2)}$ 131
5.6 Refined index of $T[D_n, \mathfrak{su}(2), H]$ for $n = 0 \mod 4$ 131
5.7 Refined index of $T[D_n, \mathfrak{su}(2), H]$ for $n = 2 \mod 4$ 132
5.8 Refined counting of flat $PSL'(2, \mathbb{C})$ connections on S^3/Γ_{D_n} 139

A.1 UV-MQs for descendants of $SU(N)_0 + (2N+4)\boldsymbol{F}$ 176
A.2 UV-MQs for descendants of $SU(2n)_0 + 1\boldsymbol{AS} + (2n+6)\boldsymbol{F}$ 176
A.3 UV-MQs for descendants of $SU(2n+1)_0 + 1\boldsymbol{AS} + (2n+7)\boldsymbol{F}$ 177
A.4 UV-MQs for $SU(2n)_k + 2\boldsymbol{AS} + N_F\boldsymbol{F}$ 177
A.5 UV-MQs for $SU(2n+1)_k + 2\boldsymbol{AS} + N_F\boldsymbol{F}$ 178
A.6 UV-MQs for $[n_1] - SU(2)^m - [0]_{\theta=0}$ 178

B.1 The bosonic background fields for 5d $\mathcal{N} = 2$ supergravity 197
B.2 Summary of spacetime indices 200
B.3 Summary of R-symmetry indices 200

Chapter 1

Introduction

1.1 Gauge Theories and SCFTs in String Theory

Starting with the first approach to describe the standard model [6] there have been countless endeavours to engineer lower-dimensional supersymmetric quantum field theories (QFTs) as explicit solutions of string theory.[1] An obvious advantage of this programme is that string theory itself is rather constrained and consists of a small set of dynamical fields, whose behaviour is well understood — at least at low energies. Most importantly, it provides a UV-complete theory of (super-)gravity, which in lower dimensions is notoriously hard to come by. It is thus natural to ask for a description of lower-dimensional gravity, say on $\mathbb{R}^{1,d-1}$, in terms of string theory. Indeed, this can be achieved by putting string theory on a product space

$$\mathbb{R}^{1,d-1} \times X_n \,, \tag{1.1}$$

where the sum of n and d is the dimension of the string theory in question. In the IR, more precisely at energy scales $E \lesssim \frac{1}{r}$, where r is the length scale associated to X,[2] we can integrate out the details of the fields along X and obtain an effective theory of gravity in d dimensions. In the simple case (1.1) the lower-dimensional theory only depends on the choice of X and we denote it by $\mathcal{T}_X$.

[1] For notational ease we will denote by "string theory" any of the five dual 10d supergravities, 11d supergravity, and their UV-completion.

[2] To avoid clutter we will drop the subscript.

The d-dimensional gravitational constant depends on the volume of X

$$G_d \sim \frac{1}{\text{vol}(X)} \,. \tag{1.2}$$

Thus, gravity is decoupled whenever X is non-compact, which is the limit we will consider in this thesis. Gauge fields arise in string theory on (1.1) from the Kaluza-Klein reduction [7, 8] of the RR-fields C_{p+1} on compact cycles inside X.[3] Thus, the gauge group of the resulting theory depends heavily on the geometry of X. Clearly, this implies that gauge theories and geometry are very closely related in string theory. Understanding the dictionary

$$\text{Geometry of } X \longleftrightarrow \text{Physics of } \mathcal{T}_X \,, \tag{1.3}$$

i.e. the interplay between mathematics and physics in greater detail is one of the main motivations for the research presented in this thesis.

Evidence is accumulating that the universe we live in is not supersymmetric.[4] Nevertheless, the study of supersymmetric field theories remains highly relevant. First and foremost they provide a less troublesome arena for studying QFTs, which, despite almost a century of research, are still surprisingly mysterious. Observables that are incalculable in ordinary QFTs, like the partition function and correlators, may become accessible in the presence of supersymmetry. We will now review some of the appearances of supersymmetric QFTs in string theory, focussing on the ones relevant for this thesis.

In order for the theory $\mathcal{T}_X$ in (1.3) to be supersymmetric, the manifold X needs to obey certain conditions. Concretely, in the absence of fluxes, it has to admit covariantly constant spinors which requires it to be Ricci-flat. These manifolds were classified by Berger [9] and are summarised in table 1.1. It turns out that all these

[3] We will not be concerned with heterotic string theory, where gauge fields also arise explicitly from the 10d gauge bundle.

[4] Maybe this is the most relevant prediction of modern-age theoretical particle physics that is not supported by experiments.

X_n	n	Hol(X)	SUSY
Torus T^n	n	$\emptyset$	1
Calabi-Yau CY_k	$2k$	$SU(k)$	$\frac{2}{2^k}$
Hyper-Kähler HK_k	$4k$	$Sp(2k)$	$\frac{k+1}{2^{2k}}$
G_2	7	G_2	$\frac{1}{8}$
$Spin(7)$	8	$Spin(7)$	$\frac{1}{8}$

Table 1.1: Berger's list: Here, n is the real dimension and the number of preserved supercharges is given as a fraction of the original supersymmetry.

manifolds have a reduced holonomy group $\mathrm{Hol}(X_n) \subset SO(n)$, which determines the fraction of preserved supersymmetry. The prime candidates for X are Calabi-Yau manifolds CY_k, where the dictionary between the geometry of X and the physics of $\mathcal{T}_X$ is well-known. This approach has led to many seminal results. The manifolds of exceptional holonomy G_2 and $Spin(7)$ are much harder to study, due to their real geometry. After some initial advances [10–14], reductions on these spaces have not been considered for some time before they received a recent resurgence. This is a good example for a research area, in which string theorists and mathematicians can benefit from each other, as both sides of the dictionary (1.3) are so far poorly understood.

A natural generalisation to the above construction is the inclusion of background fluxes for the RR-fields C_{p+1}. This allows us to relax the Ricci-flatness condition of X and opens up a much larger class of possible theories $\mathcal{T}_X$. In recent years there has been a lot of discussion about which supergravities correspond to such a $\mathcal{T}_X$, i.e. are in the string theory landscape [15, 16]. In this thesis we will not be interested in turning on fluxes explicitly. However, the C_{p+1} still play a monumental role in the form of branes.

Since the second string revolution [17], branes have been an integral part of string theory. Classically, they act as $(p+1)$-dimensional sources for the RR-fields, but they turn out to be dynamical objects themselves. Importantly, their worldvolume

exhibits a supersymmetric gauge theory, with gravity decoupled. For example, the theory on a set of N Dp-branes is given by the $(p+1)$-dimensional gauge theory with 16 supercharges and gauge group $G = U(N)$. Most well-known is the 4d $\mathcal{N} = 4$ theory, which lives on D3-branes in type IIB. For other types of branes, the worldvolume theories are less explored. This includes the ABJM model on M2-branes [18] and the 6d (2,0) theory on M5-branes [19–21]. Although the latter is only partially understood, it is central to numerous pieces of research, including this thesis. For example, the Lagrangian and the non-abelian equations of motion are unknown. However, it makes up for this inconvenience by being the pinnacle of superconformal field theories (SCFTs). We will come back to this statement later.

Similar to (1.1) we can look at the theory on a brane and compactify it on

$$M_{p+1} \to W_d \times M_n \,, \tag{1.4}$$

i.e. dimensionally reduce it along M_n to study the resulting gauge theory on W_d. For reasons alluded to above, we are mostly interested in compactifications that preserve supersymmetry. For this, M_n needs to be a calibrated cycle, embedded into one of the manifolds in table 1.1. Calibrated cycles have minimal volume in their homology class, leading to a minimisation of energy and thus supersymmetry. We summarise some relevant calibrated cycles in table 1.2. In this thesis we are concerned with the reduction of the 6d (2,0) theory on calibrated three-cycles.

Of course, there is no reason to only consider coincident branes. Generic configurations of branes inside string theory break supersymmetry completely. However, in certain cases the participating branes preserve a common set of supercharges. Again, this setup features a supersymmetric gauge theory on its worldvolume, whose dynamics depend on the alignment of the branes. For example, the string modes stretching between different branes correspond to gauge modes of the effective theory. The first example involves D3-branes, suspended between 5-branes [22, 23]. Field theoretically, this corresponds to the 4d $\mathcal{N} = 4$ theory on an interval with certain boundary

Ambient X	M_n	n	Calibration
CY_k	Riemann surface	2	Kähler form ω
	Special Lagrangian	k	Holomorphic volume form Ω
	Kähler cycle	$2m$	ω^m
G_2	Associative	3	Associative form Φ
	Coassociative	4	$\star\Phi$
$Spin(7)$	Cayley	4	Cayley form Φ

Table 1.2: List of calibrated cycles

conditions. The details of the configuration directly translate to the properties of the effective three-dimensional gauge theory. Similar implementations of this basic concept have since then emerged. In this thesis we will encounter (p, q) 5-brane-webs [24–26], which are a convenient way to describe gauge theories and SCFTs in five dimensions.

As already advertised, another symmetry that plays a pivotal role in this thesis is the conformal symmetry, see e.g. [27]. In most gauge theories, the fundamental constants actually depend on the energy scale, governed by the equation

$$\frac{d}{d\log E}\,\lambda(E) = \beta_\lambda(E)\,, \tag{1.5}$$

where λ is some coupling constant. If all β-functions vanish, the theory is conformal, i.e. it does not depend on the energy scale. This is only possible if the theory in question does not exhibit any dimensionful parameters, that could be compared to the energy. By construction, CFTs are UV-complete, as there is no scale, where additional operators could appear. One of their most prominent applications in string theory is the AdS/CFT correspondence [28,29], or holography. It relates supergravity in $(d+1)$-dimensional anti-de Sitter (AdS) space, to a strongly coupled SCFT on the d-dimensional asymptotic boundary.

Combining conformality and supersymmetry allows for a classification of super-

conformal algebras, which was done by Nahm [30]. Crucially, it was shown that there are no SCFTs in dimensions larger than six. In two dimensions the list of possible theories is vast and has been studied extensively — for example leading to the discovery of string theory. On the other hand, for $d > 2$ the choices are significantly limited. The most famous SCFT is without a doubt the 4d $\mathcal{N} = 4$ SYM, which arises as the compactification of the 6d (2,0) theory on a T^2. Its only parameter is the dimensionless coupling constant

$$\tau = \frac{\theta}{2\pi} + \frac{4\pi i}{g^2}\,, \tag{1.6}$$

which can be identified with the complex structure of the torus. Due to its comparative simplicity and uniqueness, it has long been a playground for countless computational strategies and many of its properties are well-known. In 5d, all SCFTs have $\mathcal{N} = 1$ supersymmetry [31–34]. This is the class of theories that we will encounter in this thesis, both from a geometric and a brane-web point of view. All 6d SCFTs have $\mathcal{N} = (1, 0)$ supersymmetry [35–40], and many of them can be engineered in string theory from brane constructions. A full classification is possible in F-theory using geometric means. The 6d $\mathcal{N} = (2, 0)$ theory, which is solely classified by an ADE-algebra, is a special case. It sits on top of the table of SCFTs, as the theory with maximal supersymmetry in the top dimension.

We have seen that supersymmetric gauge theories and superconformal field theories can be studied from a multitude of different angles inside string theory. This thesis is an endeavour to make a small but relevant contribution to this vast and exciting field. We will concentrate on some specific aspects in five and three dimensions, which are outlined in the next subsection.

1.2 Content of this Thesis

In the first part of this thesis we are concerned with 5d $\mathcal{N} = 1$ gauge theories and SCFTs. In five dimensions the gauge coupling has negative mass dimension $\left[g_{5d}^{-2}\right] = 1$. This implies that any gauge theory is non-renormalisable. However, in many cases we can understand their UV completion in terms of a strongly coupled 5d SCFT [31]. Starting from these, one can include a relevant operator $\mathcal{O}$ to trigger an RG-flow [41]. Some of the deformations $\mathcal{O}$ can be identified with a SYM-term with gauge coupling $m_0 = g_{5d}^{-2}$ in the IR. A given SCFT might have multiple different gauge theory descriptions, triggered by different deformations. These are considered as UV dual gauge theory descriptions. Similarly, other deformations induce a flow to a descendant SCFT. In the IR these operators are interpreted as mass terms for matter fields with coefficient m_f. Diagrams of the RG flows of these two operations are shown below

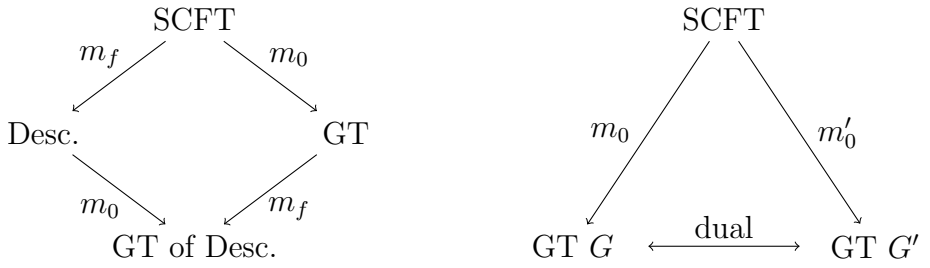

(1.7)

where we abbreviate a gauge theory with GT. Similar to other theories with eight supercharges, the moduli space of supersymmetric vacua of 5d $\mathcal{N} = 1$ theories is described by two distinct branches, the Coulomb branch (CB) and the Higgs branch (HB). In the gauge theory description these are parametrised by the scalars in the vector and hypermultiplet, respectively. We summarise details of this construction in section 2.1.

In the spirit of (1.3) we should compare this description to the geometry side. 5d $\mathcal{N} = 1$ theories are obtained by compactification of M-theory as in (1.1) with X_6 a Calabi-Yau manifold of complex dimension three. In order for this to describe an SCFT the Calabi-Yau needs to be non-compact and contain canonical singularities.

This prevents the appearance of any length scales. A gauge theory description of this SCFT then corresponds to a resolution of the singularities of X_6 that preserves the Calabi-Yau condition. The Coulomb branch of the gauge theory is parametrised by the Kähler deformations of the resolved manifold $\widetilde{X}_6$ and its origin, that is associated to the SCFT, exactly corresponds to the singular limit X_6. The Higgs branch is instead determined by the complex deformation space. In practice it is very challenging to compute this moduli space explicitly.

The smooth manifold $\widetilde{X}_6$ is characterised by compact divisors, S_i, and non-compact divisors, which determine the gauge and flavour symmetry, respectively. From the compact divisors and a choice of ruling, which corresponds to a gauge theory description, we can describe the full CB in the IR, from which the CB in the SCFT limit can be inferred. The hypermultiplets that transform in representations of the gauge group correspond to rational curves with self-intersection (-1) inside $\cup S_i$. Decoupling of such a hypermultiplet, and thus flowing to a different UV-fixed point is realised in terms of a flop that takes such a curve outside of $\cup S_i$. In the singular limit, its volume, and therefore the mass of the associated hypermultiplet, stays finite, and it thus decouples from the SCFT sector. Repeated decoupling gives rise to the complete descendant tree. This logic was used recently in [42–45] to create a systematic analysis of a large class of SCFTs. Given a geometry one can construct a graph called combined fibre diagram (CFD), which encodes the flavour symmetry and the possible mass deformations. In the geometry picture it is also possible to provide a classification of 5d SCFTs by starting with the geometries underlying the 6d classification of SCFTs in F-theory [37]. It was widely believed that all 5d SCFTs arise from 6d by circle-reduction and mass deformations, however recently some counter-examples were discovered [46]. The elliptically fibered Calabi-Yau geometries used in F-theory have a partial non-flat resolution, which characterise 5d SCFTs and their Coulomb branch descriptions. This is the approach taken in [42–45, 47–53]. Alternatively one

can directly classify the collection of surfaces that give rise to the Cartan generators of the 5d gauge theories, without constructing the full non-compact Calabi-Yau geometry [34, 54–58].

A particularly well-studied subset of geometries are toric Calabi-Yau threefold singularities [59, 60]. Although the class of SCFTs that can be studied in this fashion is quite limited, the description in terms of toric diagrams has striking advantages. For example it is straightforward to construct the toric diagrams of all descendants and weakly coupled gauge theory descriptions. One of the main features of chapter 3 is the definition of generalised toric polygons (GTPs) for more general SCFTs, and the description of their Higgs branch. Although these do not immediately specify the corresponding geometry there is justified hope that this approach can initiate further research from the geometry point of view.

A third way to describe 5d SCFTs is in terms of branes, more precisely webs of 5-branes and 7-branes [24, 25, 61–63] inside type IIB string theory, which we review in section 2.2. Not all 5d SCFTs have a description in terms of such webs, but in recent years the number of known constructions has steadily grown, by also including orientifold planes [64–69]. Given a brane-web it is possible to study the moduli space of the corresponding SCFT. The extended Coulomb branch, consisting of the CB and the mass parameters m_f and m_0, corresponds to the deformation space of the brane-web.

Furthermore, there has been recent progress towards a comprehensive description of the Higgs branch using magnetic quivers (MQ) and Hasse diagrams [70–82]. Magnetic quivers are graphs which, under certain conditions, provide a combinatorial description of a class of algebraic varieties. The key step of this construction is to interpret these graphs as 3d $\mathcal{N} = 4$ quiver gauge theories, whose Coulomb branch gives a physical realisation of these varieties. These 3d Coulomb branches can be quantitatively studied by computing the Hilbert series using the monopole formula

of [83]. For example, this allows us to deduce the enhanced flavour symmetry. For the 5d SCFTs studied in this thesis, the magnetic quiver is a unitary quiver gauge theory, whose Coulomb branch is conjectured to be the same symplectic singularity as the Higgs branch of the 5d theory. From a geometric point of view, studying the realisation of 5d SCFTs in M-theory on canonical singularities, magnetic quivers were derived in [46]. The Hasse diagram, introduced in [75], is a depiction of the partially ordered set corresponding to the foliation of the Higgs branch by symplectic leaves. Any pair of leaves which can be compared in the partial order defines a transverse slice between the two leaves, which is again a symplectic singularity, and to which one can associate a magnetic quiver. The leaves correspond physically to phases of the SCFT, while the transverse slices are associated to new theories obtained from the original theory by (a generalisation of) the Higgs mechanism. We summarise the necessary background material in section 2.3.

In chapter 3 we combine the advantages inherent in these various descriptions. Starting with the brane-web of a 5d SCFT, we translate its properties into a generalised toric polygon. From this we develop a procedure to read off the magnetic quiver of the theory itself and its descendants. We do this explicitly for 5d SCFTs with an $SU(N)$ description in the IR.

In the second part of this thesis we switch gears and consider another SCFT, the 6d (2,0) theory of gauge algebra $\mathfrak{u}(N)$. Putting this theory on a product manifold as in (1.4) we can choose the length scales on the two cycles independently, without changing the physics of the resulting theory. In fact, to a certain degree, this also holds in the compactification limit. To guarantee supersymmetry to be preserved, one of the cycles, say M_n, needs to be calibrated. Then, the compactification is accompanied by a topological twist [84], leading to a supersymmetric gauge theory that is called $T[M_n]$ on W_d, with $d = 6 - n$. On the other hand, one can reduce the 6d

(2,0) theory on W_d. Due to the topological twist this yields a topological field theory (TFT) on M_n. Conformality implies that the two theories have common observables

$$\mathcal{Z}_{W_d}(T[M_n]) = Z_{\mathrm{TFT}}(M_n)\,, \tag{1.8}$$

i.e. the partition function of $T[M_n]$ on W_d can be computed from the TFT on M_n. For M_2 a Riemann surface inside a $K3$ surface and $W_4 = S^4$ this is known as the AGT correspondence [85, 86]. It relates the sphere-partition function of theories of class $\mathcal{S}$ [87], to correlation functions of 2d Toda theory on M_2. For most types of calibrated cycles and various convenient choices for W_d similar correspondences of the type (1.8) have since then been developed for $n = 2$ [88–90] and $n = 4$ [91, 92].

In this thesis we are interested in the 3d-3d correspondence, first introduced in [93–95]. Here, M_3 is a special Lagrangian inside a Calabi-Yau three-fold and the relevant observable is the S^3-partition function. It was conjectured, that it agrees with the partition function of complex Chern-Simons theory on M_3, i.e.

$$Z_{S^3}\left(T_{\mathcal{N}=2}[M_3, G]\right) = \mathcal{Z}_{\mathrm{CS}_{\mathbb{C}},G}(M_3)\,, \tag{1.9}$$

where G is the gauge group. This correspondence has been tested extensively, supported by the concept of localisation [96–98], which provides a reliable tool to compute the S^3-partition function of 3d $\mathcal{N} = 2$ theories.[5] On the other side of the correspondence, the reduction of the 6d (2,0) theory on S^3, leading to complex Chern-Simons-theory, was explicitly performed in [100, 101]. These results were then extended to computing different observables, like the superconformal index on $S^2 \times S^1$, and the twisted index on $\Sigma_g \times S^1$ [102, 103]. In this thesis we are primarily interested in the Witten index $I = \mathrm{Tr}(-1)^F$, where F is the fermion number [104], which corresponds to the partition function on T^3. It is conjectured, that the 3d-3d correspondence relates it to the number of complex flat G-connections on M_3

$$I\left(T_{\mathcal{N}=2}[M_3, G]\right) = \#\left(\text{flat } G^{\mathbb{C}} \text{ connections on } M_3\right)\,. \tag{1.10}$$

[5] Recently, this technique was generalised to Seifert manifolds [99].

For Lagrangian theories a convenient technique to compute this observable is the Bethe/gauge correspondence [105,106] which relates the Witten index to the solutions to the Bethe equations. These are obtained by computing the twisted superpotential of $T[M_3]$, where the building blocks have been determined in [103, 106–109]. This approach was already used in [110] to test (1.10).

However, an important characteristic of $T[M_3]$ has so far been largely ignored: its higher-form (or q-form) symmetries [111]. These generalise global (zero-form) symmetries in the sense that the charged operators are q-dimensional and thus non-local. We give a summary of this concept in section 4.2. The 6d (2,0) theory itself has a three-form symmetry associated to the tensor field. Thus, the general correspondences (1.8) are expected to have refinements into different sectors, depending on the chosen higher-form symmetry. In fact, this is only true if W_d has non-trivial homology, so the T^d-partition function of $T[M_n, G]$ should be sensitive to this choice. For $n = 2$ this was discussed in [112] and related to the global structure of the gauge group. More precisely, theories of class $\mathcal{S}$ with a different choice of global structure of the gauge group can be obtained by compactification of the 6d (2,0) theory on the same M_2, after gauging part of the higher-form symmetry.[6] As expected, this concept also holds for 3d $\mathcal{N} = 2$ theories. In chapter 5 we refine the 3d-3d correspondence (1.10) to include the choice of higher-form symmetry, or equivalently the global structure of the gauge group. To substantiate this, we explicitly study the Bethe equations and compute the Witten index for $\mathfrak{g} = \mathfrak{su}(2)$ and M_3 a Seifert manifold and compare it to flat $SL(2, \mathbb{C})$ connections on M_3.

In table 1.2 we find another type of calibrated three-cycles — associative cycles inside manifolds of holonomy G_2. Although little is known about this class of manifolds [114, 115], there have been recent advances in their explicit construction [116–118]. Wrapping M5-branes around an associative three-cycle yields a 3d

[6] In [113] this was subsequently also discussed for other choices of n.

$\mathcal{N} = 1$ theory, denoted by $T_{\mathcal{N}=1}[M_3]$. These theories have two supercharges and no R-symmetry. Thus, localisation techniques can not be applied, as these rely on a $U(1)_R$ R-symmetry, and the knowledge about these theories is relatively limited. However, recently some dualities of 3d $\mathcal{N} = 1$ theories have been proposed [119–122]. Field theoretically, these theories appear on domain walls inside 4d $\mathcal{N} = 1$ theories [123–125]. Geometrically this can be understood by considering the ambient G_2-manifold inside M-theory [12, 14, 126–131]. It is natural to assume that there also exist 3d-3d correspondences for $\mathcal{N} = 1$, relating the observables of $T_{\mathcal{N}=1}[M_3]$ to TFTs. In chapter 6 we propose these dualities for both the Witten index and the S^3-partition function.

This thesis is constructed in the following way. Chapter 2 acts as background material for chapter 3, which is based on the results in [1–3]. Similarly, in chapter 4 we review some content necessary for chapters 5 and 6, which are drawn from [4] and [5], respectively. Each of the main chapters 3, 5 and 6 starts with a short introduction, where the main results are summarised. We conclude with section 7 and give some outlook towards further research. The appendices A and B, one for each of the two parts, contain technical details, further background material and additional results.

Part I

Five Dimensions

Chapter 2

Background in Five Dimensions

2.1 5d SCFTs and Gauge Theories

In this first part we are interested in 5d $\mathcal{N} = 1$ SCFTs which admit a weakly coupled gauge theory description. Field theoretically, the best way to understand this is by starting with an SCFT in the UV and turning on a relevant mass deformation. A subset of these trigger an RG-flow to a weakly coupled SYM in the IR, where we identify the deformation parameter with the gauge coupling $m_0 = g^{-2}$. We say that two weakly coupled gauge theory descriptions are "dual" if they have the same UV-completion, i.e. they are two deformations of the same SCFT. From the gauge theory perspective we can reach the UV limit by taking the gauge coupling to infinity $g \to \infty$.

Let us consider a specific 5d $\mathcal{N} = 1$ gauge theory with gauge group G of rank r, associated to a Lie algebra $\mathfrak{g}$ with generators T_i, and matter hypermultiplets transforming in some representation $\boldsymbol{R}$ of G. We take G to be simple for now, but can relax this condition to quiver gauge theories. The vector multiplet contains the gauge field A and a real scalar whose vevs ϕ_i, $i = 1, \ldots, r$, parametrise the Coulomb branch. The Coulomb branch is described by the effective Lagrangian

$$\mathcal{L}_{\text{CB}} = \tau_{ij} \left(d\phi^i \wedge \star\, d\phi^j + dA^i \wedge \star\, dA^j \right) + \frac{c_{ijk}}{24\pi^2} dA^i \wedge dA^j \wedge A^k + \ldots \,, \tag{2.1}$$

where τ_{ij} and c_{ijk} are the effective gauge coupling and Chern-Simons level, respectively. They can be conveniently obtained from a single function, the prepotential $\mathcal{F}(\phi^i)$

$$\tau_{ij} = \frac{\partial^2 \mathcal{F}}{\partial\phi^i \partial\phi^j}\,, \qquad c_{ijk} = \frac{\partial^3 \mathcal{F}}{\partial\phi^i \partial\phi^j \partial\phi^k}\,. \tag{2.2}$$

The IMS prepotential [33] of a pure 5d $\mathcal{N} = 1$ gauge theory with gauge group G is given by

$$\mathcal{F}_{\text{IMS}} = \frac{1}{2g_0^2} h_{ij}\phi^i\phi^j + \frac{k}{6} d_{ijk}\phi^i\phi^j\phi^k + \frac{1}{6}\sum_{\alpha\in\Phi_+} |\alpha\cdot\phi|^3\,, \tag{2.3}$$

where $h_{ij} = \text{Tr}\,(T_i T_j)$ and the $\alpha \in \Phi_+$ are the positive roots of $\mathfrak{g}$. For $G = SU(N)$, $N \geq 3$, the symmetric matrix $d_{ijk} = \frac{1}{2}\,\text{Tr}\,(T_i\,\{T_j, T_k\})$ is non-zero and k is the bare Chern-Simons level. We choose a Weyl wedge such that $\alpha\cdot\phi > 0$ for all α. To couple the theory to matter we add the term

$$\mathcal{F}_{\text{matter}} = \sum_{\boldsymbol{R}}\sum_{f=1}^{N_R} \mathcal{F}_f^{(\boldsymbol{R})}\,, \qquad \mathcal{F}_f^{(\boldsymbol{R})} = -\frac{1}{12}\sum_{a=1}^{\dim \boldsymbol{R}} |\lambda^a\cdot\phi - m_f|^3\,, \tag{2.4}$$

where $\boldsymbol{R}$ runs over the irreducible representations of G and the λ^a are the weights of $\boldsymbol{R}$. The matter content of such a theory consists of N_R hypermultiplets in the representation $\boldsymbol{R}$ with masses m_f. We will only be concerned with theories with gauge group $G = SU(N)$ or $G = Sp(N)$, coupled to antisymmetric and fundamental matter. These theories will be denoted by

$$G_k + N_{AS}\boldsymbol{AS} + N_F\boldsymbol{F}\,. \tag{2.5}$$

An important feature of the prepotential is its ability to describe the gauge theory in various phases. We see that the matter contribution (2.4) depends on the relative values of the Coulomb branch parameters ϕ_i and the flavour masses m_f. Together with the bare gauge coupling[1] $m_0 = \frac{1}{g_0^2}$ they form the extended Coulomb branch $\mathcal{K}$. Thus, the prepotential, and consequently the Lagrangian, depends on the position along $\mathcal{K}$. The SCFT sits at the origin of $\mathcal{K}$, where the prepotential vanishes.

[1] or multiple gauge couplings in the case of a quiver gauge theory

The classical flavour symmetry $G_{\rm F,cl}$ of a weakly coupled gauge theory is easy to determine. Given a theory with a single gauge group G, N_R hypermultiplets in representation $\boldsymbol{R}$ contribute as

$$\boldsymbol{R} \text{ complex } \Rightarrow U(N_R)\,, \qquad \boldsymbol{R} \text{ real } \Rightarrow Sp(N_R)\,, \qquad \boldsymbol{R} \text{ quaternionic } \Rightarrow SO(2N_R)\,. \tag{2.6}$$

For the theories in (2.5) this implies for some relevant choices of G

G	$SU(2)$	$SU(3)$	$SU(4)$	$SU(N \geq 5)$	$Sp(N \geq 2)$
$G_{\rm F,cl}$ for $\boldsymbol{F}$	$SO(2N_F)$	$U(N_F)$	$U(N_F)$	$U(N_F)$	$SO(2N_F)$
$G_{\rm F,cl}$ for $\boldsymbol{AS}$	–	–	$Sp(N_{AS})$	$U(N_{AS})$	$Sp(N_{AS})$

(2.7)

In a quiver gauge theory each bifundamental contributes an additional $U(1)$ to the classical flavour symmetry. Furthermore, each simple gauge group constituent has a topological flavour symmetry $U(1)_T$ with current

$$J_T = \frac{1}{8\pi^2} \star \mathrm{Tr}\,(dA \wedge dA)\ . \tag{2.8}$$

In the strongly coupled limit the flavour group is enhanced

$$G_{\rm F,cl} \times \prod_{I=1}^{n} U(1)_T^I \to G_{\rm F}\,, \tag{2.9}$$

where n is the number of simple gauge groups and the gauge rank is preserved.

We will be interested in explicitly integrating out matter. Consider a theory with a single gauge group and matter in representation $\boldsymbol{R}$ of mass m_f. Taking $m_f \to \pm\infty$[2] corresponds to decoupling the hypermultiplet. In this limit $\mathcal{F}_{\boldsymbol{R}}$ simplifies to

$$\lim_{m_f\to\pm\infty} \mathcal{F}_{\boldsymbol{R}} = \mp\frac{m_f^3}{12}\ \dim \boldsymbol{R} \mp \frac{m_f}{2} I_2(\boldsymbol{R})\ h_{ij}\phi^i\phi^j \pm \frac{1}{12} A(\boldsymbol{R})\ d_{ijk}\phi^i\phi^j\phi^k\,. \tag{2.10}$$

Here, the quantities I_2 and A are the second index and the triangle anomaly coefficient, respectively. They satisfy

$$I_2(\boldsymbol{R})\ h_{ij} = \sum_{a=1}^{\dim \boldsymbol{R}} \lambda_i^a \lambda_j^a\,, \qquad A(\boldsymbol{R})\ d_{ijk} = \sum_{a=1}^{\dim \boldsymbol{R}} \lambda_i^a \lambda_j^a \lambda_k^a\,, \tag{2.11}$$

[2]In fact it is sufficient to choose $|m_f|$ large enough such that all the terms in (2.4) have the same sign.

G	$\boldsymbol{R}$	I_2	A
$SU(N)$	$\boldsymbol{F}$	$\frac{1}{2}$	1
	$\boldsymbol{AS}$	$\frac{N-2}{2}$	$N-4$
$Sp(N)$	$\boldsymbol{F}$	$\frac{1}{2}$	–
	$\boldsymbol{AS}$	$N-1$	–

Table 2.1: Second index and triangle anomaly coefficient for various representations.

G	$SU(N)$					$Sp(N)$	
N_{AS}	0	1	1	2	2	0	1
N_F	$2N+4$	8	$N+6$	8	7	$2N+6$	8
k	0	$\frac{N}{2}$	0	0	$\frac{3}{2}$	–	

Table 2.2: List of assorted marginal 5d gauge theories

and only depend on $\boldsymbol{R}$ and G. For the gauge groups and representations of interest they are summarised in table 2.1. By comparison with (2.3) we see that integrating out a matter multiplet by taking its mass to $\pm\infty$ shifts the parameters

$$m_0 \to m_0 \mp m_f I_2(\boldsymbol{R})\,, \qquad k \to k \pm \frac{1}{2}A(\boldsymbol{R})\,. \tag{2.12}$$

Note that the constant shift in the prepotential is non-physical, whereas we should view the new shifted gauge coupling as physical.

Not all gauge theories have a 5d UV completion. For simple gauge groups the set of marginal theories was classified in [34, 54]. The UV completion of these marginal theories is a 6d (1,0) theory. However, each of their descendants, obtained by integrating out matter, leads to a 5d SCFT at strong coupling. The marginal theories of the form (2.5) considered in this thesis are summarised in table 2.2.

2.2 (p, q) 5-Brane-Webs and Monodromies

5d $\mathcal{N} = 1$ SCFTs can be realised in type IIB string theory in terms of webs of (p, q) 5- and 7-branes [24]. Consider type IIB string theory with axio-dilaton τ and a web of 5-branes extended along the $(x_0, \ldots, x_4)$-directions and at some angle θ in the (x_5, x_6)-plane. We adopt the convention that a (p, q) 5-brane is a bound state of p D5-branes and q NS5-branes. Rotations in the (x_7, x_8, x_9)-directions realise the $SU(2)_R$ R-symmetry of the 5d theory. Each 5-brane is a $\frac{1}{2}$-BPS object, preserving 16 supercharges. To be precise a single 5-brane imposes the condition [22]

$$\epsilon_2 = \Gamma_{01234} \left(\cos\theta \ \Gamma_5 + \sin\theta \ \Gamma_6\right) \left(\sin\beta \ \epsilon_1 + \cos\beta \ \epsilon_2\right) \tag{2.13}$$

on the supersymmetry parameters $\epsilon_{1,2}$ of type IIB, where

$$\tan\beta = \frac{\mathrm{Re}(p + q\tau)}{\mathrm{Im}(p + q\tau)} \,. \tag{2.14}$$

Additionally, a pure NS5-brane imposes

$$\epsilon_1 = -\Gamma_{01234} \left(\cos\theta \ \Gamma_5 + \sin\theta \ \Gamma_6\right) \epsilon_1 \,. \tag{2.15}$$

A general configuration of branes breaks supersymmetry completely. However, one can show that brane configurations satisfying

$$\tan\theta = \tan\beta \tag{2.16}$$

preserve eight supercharges. This condition implies that the angle of a (p, q) 5-brane in the (x_5, x_6)-direction is completely determined by (p, q) and the choice of τ. We can use the $SL(2, \mathbb{Z})$-invariance of type IIB to fix $\tau = i$, so that

$$\tan\theta = \frac{p}{q} \,. \tag{2.17}$$

All brane configurations related by a global $SL(2, \mathbb{Z})$ transformation are physically equivalent and all pictures are drawn at $\tau = i$. If there are no coincident branes the

most general web is engineered out of triple-intersections called junctions. At each junction, charge conservation implies

$$\sum_{i=1}^{3} \pm (p_i, q_i) = (0, 0) \ , \tag{2.18}$$

where the signs reflect the orientation of each brane with respect to the junction.

A generic brane-web contains both finite (internal) and semi-infinite (external) 5-branes. It is straightforward to read off the ranks of the gauge and flavour group of the 5d theory from the web [25], which correspond to the number of local and global deformations, respectively. A deformation of the brane-web leaves the type and relative position of the 5-branes invariant. Local deformations also leave the position of the external 5-branes invariant, whereas global deformations change them. The position of an external 5-brane is specified by a single coordinate, corresponding to one deformation for each semi-infinite 5-brane. However, there are three unphysical global deformations comprising two global translations in the (x_5, x_6)-plane and the position of one of the external 5-branes, which is fixed by supersymmetry.

Any semi-infinite (p, q) 5-brane can be made finite by letting it end on a corresponding (p, q) 7-brane, extended in the $(x_0, \ldots, x_4, x_7, x_8, x_9)$-directions. A 7-brane will be indicated by a circle and its (p, q)-charge is fixed by the angle of the 5-brane ending on it. The branch cut of a given (p, q) 7-brane will be taken to point away from the 5-brane, so as to not disrupt the 5-brane configuration. Furthermore, a (p, q) 7-brane can be translated along this direction without affecting the 5d theory.

Consider a brane-web with two external 5-branes ending on 7-branes whose branch cuts intersect. Going to the strong coupling point of the 5d theory corresponds to taking the length of the internal 5-branes to zero. If a brane-web contains monodromy cuts that cross, we must exchange the order of the corresponding 7-branes, preserving both the total monodromy and charge conservation, before taking the strong coupling limit. In the exchange, one 7-brane will change type because it crosses the branch cut of the other, whereas the type of the second 7-brane is preserved but the number of

5-branes that end on it changes to conserve charge. This is known as Hanany-Witten (HW) brane creation [22]. The branch cut of a (p,q) 7-brane induces a transformation

$$M_{p,q} = \begin{pmatrix} 1-pq & p^2 \\ -q^2 & 1+pq \end{pmatrix} . \tag{2.19}$$

The total monodromy is given by the counter-clockwise product of the $M_{p,q}$. Exchanging two 7-branes while preserving their total monodromy implies

$$M_{p_1,q_1} M_{p_2,q_2} = \begin{cases} M_{p_2,q_2} M_{p_1',q_1'} \,, & (p_1',q_1') = (p_1,q_1) + (p_1 q_2 - p_2 q_1)\,(p_2,q_2) \\ M_{p_2',q_2'} M_{p_1,q_1} \,, & (p_2',q_2') = (p_2,q_2) + (p_1 q_2 - p_2 q_1)\,(p_1,q_1) \end{cases} . \tag{2.20}$$

In order to guarantee charge conservation at the intersection, additional 5-branes are created when a 7-brane crosses a stack of 5-branes. The number of new 5-branes created depends on how many 5-branes are in the stack it crosses. In particular, exchanging two 7-branes as in the top line of (2.20), with N_1 5-branes ending on the first 7-brane and N_2 on the second, the number of new 5-branes created is

$$N_2' = N_2 + \Delta N_2 \,, \qquad \Delta N_2 = |p_1 q_2 - p_2 q_1|\, N_1 \,. \tag{2.21}$$

In general, the number of 5-branes that can end on a single 7-brane is constrained by the so-called s-rule. Given a web that satisfies the s-rule, performing HW moves conserves this property, i.e. it gives another consistent supersymmetric brane-web. The simplest formulation of the s-rule constrains the number of D5-branes n_{D5} that connect a single D7-brane and a stack of n_{NS5} NS5-branes to be $n_{\mathrm{D5}} \leq n_{\mathrm{NS5}}$. A brane-web is said to obey the s-rule if there exists a full resolution of the web, obtained by adding additional internal 5-branes, such that each junction locally obeys the s-rule [61]. The $SL(2,\mathbb{Z})$-invariant generalisation of the s-rule for a junction of three branes (p_i,q_i) is [1, 132–134]

$$\left| \det \begin{pmatrix} p_i & q_i \\ p_j & q_j \end{pmatrix} \right| \geq \gcd(p_k,q_k)^2 \,, \tag{2.22}$$

for every permutation (i,j,k) of $(1,2,3)$.

2.3 Magnetic Quivers and Hasse Diagrams

The moduli spaces of 5d SCFTs are parametrised by the vevs of scalar fields, either in the vector multiplet – the Coulomb branch (CB) – or the hypermultiplet – the Higgs branch (HB). One of the challenges has been to compute the Higgs branch from a geometric approach to 5d SCFTs. Unlike the CB in 5d, the HB receives quantum corrections from instantons.

In the 5-brane-webs, an alternative proposal was made that identifies the HB in 5d with the CB of a magnetic quiver (MQ), which is a 3d $\mathcal{N} = 4$ quiver gauge theory (and in the current context, with unitary gauge nodes). The conjecture in [73] is that the Coulomb branch of the magnetic quiver $\text{MQ}_{\mathcal{T}}$ associated to a theory $\mathcal{T}$ can be identified with the Higgs branch of the 5d SCFT

$$\text{CB}[\text{MQ}_{\mathcal{T}}] = \text{HB}[\mathcal{T}]\,. \tag{2.23}$$

Both of these spaces are hyper-Kähler cones, and the isomorphism is as such. The advantage however is that the CB of 3d $\mathcal{N} = 4$ theories is much better under control, using the monopole formula to compute their (refined) Hilbert series, see [83].

The method to compute the (unitary) magnetic quiver of a brane-web was developed in [73]. The idea is to divide the web into a (maximal) set of sub-webs that themselves are consistent, supersymmetric brane-webs. In type IIB this is justified by displacing these sub-webs along the (x_7, x_8, x_9)-directions, which make up the $SU(2)_R$ R-symmetry. Each different division into sub-webs produces a magnetic quiver and corresponds to a distinct component in the Higgs branch. Given a division into sub-webs, the magnetic quiver is computed as follows[3]

1. A sub-web corresponds to a $U(1)$ node. If there are m equivalent (i.e. identical and coincident) sub-webs this is enhanced to $U(m)$.

[3]In principle, there can also be adjoint matter associated to each node, governed by the self-intersection number. This possibility will play a very minor role in this thesis.

2. The number of bifundamental matter multiplets, i.e. intersections between the nodes, is determined by two contributions:

   (a) The stable intersection number is determined by regarding the 5-branes of the sub-webs as tropical curves, and infinitesimally displacing the curves. Then, in each point where 5-branes from the two sub-webs intersect there is a contribution to the stable intersection

   $$\left|\det \begin{pmatrix} p_1 & q_1 \\ p_2 & q_2 \end{pmatrix}\right| , \tag{2.24}$$

   where the intersecting branes are (p_1, q_1) and (p_2, q_2). The sum over these contributions is independent of the choice of displacement.

   (b) The second contribution comes from 7-branes. If two 5-branes belonging to different sub-webs end on opposite sides of a 7-brane, there is a contribution of $+1$, if they end on the same side, there is a contribution of -1.

Given a MQ with node multiplicities m_I and edge multiplicities k_{IJ}, we define the balance of a node as

$$\beta_I = -2m_I + \sum_{J \neq I} k_{IJ} m_J \, . \tag{2.25}$$

Naturally, there are different types of nodes,

$$\begin{aligned} &\beta_I = 0 \quad \text{balanced} \quad \circ \\ &\beta_I > 0 \quad \text{overbalanced} \quad \bullet \end{aligned} \tag{2.26}$$

which we indicate with different colours. Underbalanced nodes with $\beta_I < 0$ are not shown as discussed momentarily. A MQ with an underbalanced node is said to be "bad" or "ugly", see [23]. This means that there are BPS monopole operators violating or saturating the unitary bound respectively. For ugly quivers, it is known that one can use a Seiberg duality to flow to an SCFT, together with a set of free hypermultiplets. All magnetic quivers discussed in this paper are either good or ugly,

as they describe the Higgs branch of a physical SCFT, i.e. they always describe a hyper-Kähler cone. For ugly quivers we can use the following local Seiberg duality to balance the nodes:

$$U(n_I) + (2n_I - |\beta_I|)\boldsymbol{F} \longleftrightarrow U(n_I - |\beta_I|) + (2n_I - |\beta_I|)\boldsymbol{F} + |\beta_I|\,\boldsymbol{H}\,, \tag{2.27}$$

where $\boldsymbol{H}$ indicates free hypermultiplets and $\beta_I < 0$.[4] The process of repeatedly applying this duality always terminates for ugly quivers. We regard the endpoint of this process as the MQ of the theory and do not usually include the free hypermultiplets. Then, the balanced nodes form the Dynkin diagram of a finite Lie algebra of ADE type. In many cases this directly gives the non-abelian part of the enhanced flavour symmetry G_F of the theory. However, sometimes the flavour symmetry is larger than expected from the balanced nodes. To reliably compute the full flavour symmetry one must determine the Hasse diagram, which we discuss next.

The foliation structure of the hyper-Kähler cone (2.23) in terms of symplectic leaves, can be obtained combinatorically in terms of quiver subtractions [72], reviewed below. The partially ordered set of such leaves is the Hasse diagram. The elementary transverse slices of the Hasse diagram of the 5d Higgs branches for the theories in this thesis are closures of minimal nilpotent orbits $\mathfrak{g}$ or Kleinian singularities – see table 2.3, which includes their magnetic quivers [135, 136].

We can subtract a quivers Q^- from Q^+, if all their edge multiplicities k_{IJ} agree [5] and $m_I^+ \geq m_I^-$ for all nodes. The resulting quiver $Q = Q^+ - Q^-$ is defined as follows.

1. The node and edge multiplicities are $m_I = m_I^+ - m_I^-$ and $k_{IJ} = k_{IJ}^+$.

2. To rebalance we add an additional $U(1)$ node and connect it such that all remaining nodes retain the balance $\beta_I = \beta_I^+$.

[4] In [23] it was argued that this duality can only be applied for $\beta_I = -1$. However, evidence suggests that in the case of ugly quivers it also holds in general. For bad quivers the duality (2.27) can not be applied. Thus, in principle one first needs to check the dimensions of the monopole operators. It would indeed be interesting to derive the general duality from first principle.

[5] If Q^- has fewer nodes than Q^+ this condition is only required for the edges of Q^-.

The Hasse diagram is obtained by repeatedly subtracting symplectic leaves. Note that the quaternionic dimension of the Higgs branch (at a given point in the Hasse diagram) is given by

$$\dim_{\mathbb{H}}(\mathrm{HB}) = -1 + \sum_I m_I \,, \tag{2.28}$$

and the flavour symmetry is given by the lowest-lying leaves in the Hasse diagram.

Singularity	Magnetic quiver
$\mathfrak{a}_n$	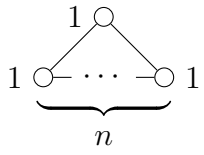
$\mathfrak{d}_n$	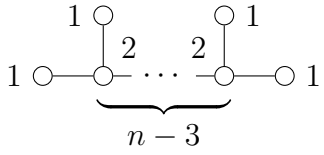
$\mathfrak{e}_6$	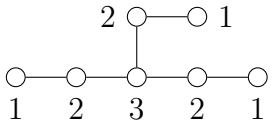
$\mathfrak{e}_7$	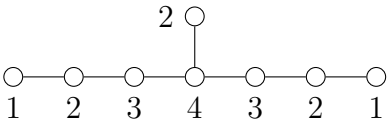
$\mathfrak{e}_8$	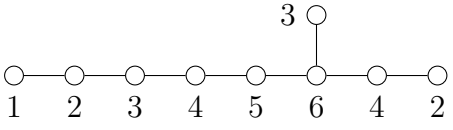
A_{N-1}	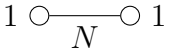

Table 2.3: Summary of the elementary transverse slices that can appear in the Hasse diagram of a symplectic variety defined by a unitary and simply laced magnetic quiver. For the first five lines, these are closures of minimal nilpotent orbits of type $\mathfrak{g}$. In the last line are the Kleinian singularities of type A_{N-1}. For each transverse slice, the second column gives a magnetic quiver.

Chapter 3

The Tropical Rain Forest

In this chapter we consider 5d SCFTs defined by a so-called generalised toric polygon (GTP) (or dot diagram) P introduced in [61]. We denote these theories by $\mathcal{T}_P$. The GTPs are lattice polygons, which generalise the concept of a toric fan for a Calabi-Yau three-fold. They map one-to-one to a 5-brane-web $\mathcal{W}_P$

$$P \quad \longleftrightarrow \quad \mathcal{W}_P \,, \tag{3.1}$$

which we discuss in detail in section 3.4. In the case when P is a toric polygon, we can associate an actual Calabi-Yau three-fold geometry X_P to it, and the dual web is associated to a tropical geometry [137].

The approach taken in this chapter makes use of the map in (3.1), which allows us to identify in the GTP P each of the steps in the construction of the magnetic quiver in the brane-web. In the brane-web picture $\mathcal{W}_P$ the map to the magnetic quiver is known from [73] and reviewed in section 2.3. It relies on a decomposition of the brane-web into sub-webs, each of them corresponding to a node, i.e. a gauge group, in the magnetic quiver. The edges, i.e. bifundamental matter, are determined from the intersections between these sub-webs in tropical geometry. To identify the direct map from P to $\mathrm{MQ}(\mathcal{T}_P)$, we proceed in two steps. In section 3.1 we define the GTPs and study the map (3.1). Based on this logic and on the understanding in the

brane-web, we propose an edge colouring of the GTP. This corresponds to a choice of refined Minkowski sum, i.e. a decomposition of the GTP. From this colouring we identify an algorithm to compute $\mathrm{MQ}(\mathcal{T}_P)$, where the intersection between two colours is computed from the mixed volume of two sub-polygons. Furthermore, we propose a method to directly determine the Hasse diagram of $\mathcal{T}_P$, based on the logic in [72, 75]. In short, the strategy is given by

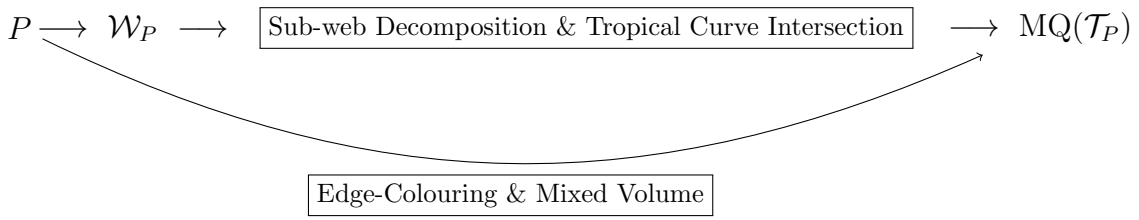

(3.2)

Although we propose a way to derive the MQ from P directly, a first principle derivation from geometry is of course missing. In fact for P not a toric, but a generalised toric polygon, it is thus far unknown what the associated canonical singularity is. Building this dictionary should now be strongly motivated, given the efficiency of how we can determine the MQs from P, using very simple combinatorial rules – which simplify not only the brane-web based analysis, but also connect to the known geometric constructions in toric geometry.

In section 3.3 we then apply this approach to SCFTs with a weakly coupled $SU(N)$ gauge theory description with antisymmetric and fundamental matter. We start by identifying all the GTPs for this class of submarginal theories. To this end we identify and apply the procedures necessary to transform a non-convex pre-GTP into a convex GTP. We also explain how to decouple matter which allows us to describe all possible descendants. From this we compute the magnetic quivers for this class of theories, using the prescription in section 3.2. Many of these results are summarised in appendix A.3.

3.1 Generalised Toric Polygons of 5d SCFTs

The concept of a generalised toric polygon was first introduced in [61] as a dual graph to a 5-brane-web with multiple 5-branes ending on a single 7-brane. This generalisation was motivated, as such diagrams furnish 5d SCFTs. In this section we properly define these objects and study their relationship to SCFTs that have a gauge theory description in the IR.

3.1.1 GTPs and Minkowski Sums

We define a generalised toric polygon P as a lattice polygon, i.e. in terms of a set of vertices $\boldsymbol{v}_i \in \mathbb{Z}^2$, and edges E_α, $\alpha = 1, \cdots, n_E$, which connect a subset of the vertices.[1] The GTP is the convex hull of the vertices and each vertex lies on at least one edge. The set of all vertices and edges will be denoted by

$$V_b = \{\boldsymbol{v}_i \in \mathbb{Z}^2\}\,, \qquad E = \cup_\alpha E_\alpha\,. \tag{3.3}$$

A subset of the edges are the external edges, which are the boundary of the GTP,

$$\partial P = \cup_\alpha E_\alpha^\partial \equiv E^\partial \subset E\,, \tag{3.4}$$

and likewise the complement of these in E are the internal edges, $E \backslash E^\partial \equiv E^{\text{in}}$.

The set of vertices is in general a subset of the set of points

$$V_b \subset E \cap \mathbb{Z}^2 \equiv V\,. \tag{3.5}$$

The set of points that are in the complement $V \backslash V_b \equiv V_w$, will sometimes be denoted by white dots/vertices and V denotes the complete set of vertices – black and white. The vertices along an edge E_α, will be labelled by $\boldsymbol{v}_{\alpha,i} \in V_b$, $i = 0, \ldots, b_\alpha + 1$. If a vertex is the boundary of an edge,

$$\partial E_\alpha = \boldsymbol{v}^{\text{ex}}_{\alpha,0} \cup \boldsymbol{v}^{\text{ex}}_{\alpha,b_\alpha+1}\,, \tag{3.6}$$

[1] A toric polygon, is a special case of this, where each lattice point on an edge is also a vertex. This is not necessarily the case for a GTP.

we refer to it as an extreme vertex. These are always the $\boldsymbol{v}_{\alpha,i}$ with $i = 0$ and $i = b_\alpha+1$. Note that extreme vertices cannot lie in the interior of any other edge and, in the absence of internal edges, must be part of the boundary of exactly two edges.

Given that an edge $E_\alpha = \overline{\boldsymbol{v}^{\text{ex}}_{\alpha,0}\boldsymbol{v}^{\text{ex}}_{\alpha,b_\alpha+1}}$ is a vector in $\mathbb{R}^2$ connecting two lattice points, it can be identified with a pair of integers. We call the greatest common divisor of this pair of integers

$$\lambda_\alpha = \text{gcd}(E_\alpha)\,, \tag{3.7}$$

where we note that this is $SL(2,\mathbb{Z})$-invariant. We then define the reduced vector

$$L_\alpha = \frac{E_\alpha}{\lambda_\alpha} \equiv (x_\alpha, y_\alpha)\,. \tag{3.8}$$

Furthermore, we define an orientation of the external edges by

$$\boldsymbol{v}^{\text{ex}}_{\alpha+1,0} = \boldsymbol{v}^{\text{ex}}_{\alpha,b_\alpha+1}\,, \tag{3.9}$$

where we understand the periodicity in the α-indices. Because of closedness of the boundary of P

$$0 = \sum_\alpha \lambda_\alpha L^\partial_\alpha\,, \tag{3.10}$$

where the L^∂_α are the line segments of the external edges and we take the sum with the orientation implied by (3.9).

Finally, we define a partition of λ_α in terms of the vertices along an external edge E^∂_α as

$$\lambda_\alpha = \sum_{i=1}^{b_\alpha+1} \mu_{\alpha,i}\,, \qquad \mu_{\alpha,i} L^\partial_\alpha = \overline{\boldsymbol{v}_{\alpha,i}\boldsymbol{v}_{\alpha,i-1}}\,, \tag{3.11}$$

with b_α the number of non-extreme vertices along E^∂_α. Note that for a toric polygon these partitions are always given by $\{1^{b_\alpha+1}\}$. We order the partition in descending magnitude

$$\mu_{\alpha,x} \geq \mu_{\alpha,x+1}\,, \tag{3.12}$$

where the index x is introduced as an ordered version of the index i. This ordered partition will also be referred to as $\{\mu_\alpha\}$. In the following we will make use of the

standard partial order pertaining to a set of integer partitions of an integer $N \geq 1$, called the dominance ordering.

Definition 1 (Dominance Ordering) *Let ρ and ρ' be two partitions of N, which means that they are sequences of integers satisfying*

$$N = \sum_{1\leq i} \rho_i = \sum_{1\leq i} \rho'_i \qquad \text{and} \qquad \rho_1 \geq \rho_2 \geq \cdots \geq 0\,, \quad \rho'_1 \geq \rho'_2 \geq \cdots \geq 0\,. \tag{3.13}$$

We say $\{\rho\} \geq \{\rho'\}$, if for all $j \geq 1$

$$\sum_{1\leq i\leq j} \rho_i \geq \sum_{1\leq i\leq j} \rho'_i\,, \tag{3.14}$$

i.e. the smallest partition is given by $\{1^N\}$, whereas the largest partition is $\{N\}$.

For a conventional toric polygon there exists a composition rule, the Minkowski sum, which is instrumental in analysing the deformations of a toric polygon [138, 139]. We give the definition of a Minkowski sum of two polygons below, as well as a generalisation that we introduce for GTPs, which we call the refined Minkowski sum. In section 3.2 we use this to define a notion of coloured GTPs, that underlie the construction of the magnetic quiver.

Definition 2 (Minkowski Sum) *A Minkowski sum of two polygons P_a and P_b is defined by*

$$P_a + P_b = \{\boldsymbol{v}_a + \boldsymbol{w}_b\}\,, \tag{3.15}$$

where $\boldsymbol{v}_a \in V_{P_a}$ and $\boldsymbol{w}_b \in V_{P_b}$ are the vertices of P_a and P_b.

Note that this definition does not distinguish between black and white vertices. This means that the Minkowski sum is not uniquely defined for a set of GTPs. We will thus introduce a refinement of the Minkowski sum, which can accommodate the presence of white dots in a GTP.

Definition 3 (Refined Minkowski Sum for GTPs) *Let P_a and P_b be GTPs. We define their refined Minkowski sum (or partition sum) as*

$$P_a \oplus P_b\,, \tag{3.16}$$

such that the edges agree with the ones of $P_a + P_b$, i.e. the ordinary Minkowski sum, and the partitions are

$$\mu_{\alpha,x}^{P_a \oplus P_b} = \mu_{\alpha,x}^{P_a} + \mu_{\alpha,x}^{P_b} \,. \tag{3.17}$$

This Minkowski sum uniquely determines the partition of all the edges of the resulting GTP. In other words, it imposes a unique configuration of black and white vertices along the edges (up to an irrelevant reordering) of the resulting GTP.

Finally, we review a well-known concept in tropical geometry, the mixed volume of a set of summands inside a polygon. The mixed volume is defined purely in terms of the edges of the summands and can be readily computed for any GTP. We will use the mixed volume in the following to construct the magnetic quiver.

Definition 4 (Mixed Volume) *Let P be a d-dimensional (refined) Minkowski sum*

$$P = \sum_{c=1}^{d} S^c \,. \tag{3.18}$$

Consider the object

$$P(\ell^c) = \sum_{c=1}^{d} \ell^c S^c \,, \tag{3.19}$$

where the $\ell^c \in \mathbb{R}$ are scaling parameters. Then, the volume of P is a formal polynomial in the ℓ^c of degree d, denoted by $vol_P(\ell^c)$. The mixed volume of d Minkowski summands inside P is given by the coefficient

$$MV(S^1, \ldots, S^d) = \left. vol_P(\ell^c) \right|_{\ell^1 \ldots \ell^d} \,. \tag{3.20}$$

Fact 1 (Mixed Volume for $d = 2$) *Let P be a (refined) Minkowski sum as above for $d = 2$. The mixed volume of two Minkowski summands is given by*

$$MV(S^1, S^2) = Area\left(S^1 + S^2\right) - Area\left(S^1\right) - Area\left(S^2\right) \,, \tag{3.21}$$

where we use the Euclidean metric to compute the areas.

Theory	Dot diagram
$SU(N)_k + N_F \boldsymbol{F}$	$\Big\{(0,0);(1,i)_{a\leq i\leq N_R+a};(0,N);$ $(-1,i)_{N-k-\frac{N_L-N_R}{2}-a\geq i\geq N-k-\frac{N_L+N_R}{2}-a}\Big\}$
$SU(2n)_k + 1\boldsymbol{AS} + N_F \boldsymbol{F}$	$\Big\{(0,-n);(1,i)_{k-\frac{N_F+2}{2}\leq i\leq k+\frac{N_F-2}{2}};$ $(0,n);(-1,n-1);(-n,0)\Big\}$
$SU(2n+1)_k + 1\boldsymbol{AS} + N_F \boldsymbol{F}$	$\Big\{(0,-n-1);(1,i)_{k-\frac{N_F+5}{2}\leq i\leq k+\frac{N_F-5}{2}};$ $(0,n);(-1,n);(-n-1,0)\Big\}$
$SU(2n)_k + 2\boldsymbol{AS} + N_F \boldsymbol{F}$	$\Big\{(0,-n);(1,-n);(n,n\ i)_{-1\leq i\leq N_R-1};$ $(0,n);(-1,n+k+\frac{N_L-N_R}{2});$ $(-n,n\ i)_{k+\frac{N_L-N_R}{2}+1\geq i\geq k-\frac{N_L+N_R}{2}+1}\Big\}$
$SU(2n+1)_k + 2\boldsymbol{AS} + N_F \boldsymbol{F}$	$\Big\{(0,-n-1);(n,-n-1);(n,n\ i)_{-1\leq i\leq N_R-1};$ $(0,n);(-n,n\ i)_{k+\frac{N_L-N_R}{2}+1\geq i\geq k-\frac{N_L+N_R}{2}+1};$ $(-n,n(k-\frac{N_L+N_R}{2}+1)-1)\Big\}$

Table 3.1: Construction of toric polygons for the theories studied in this chapter. a can take any integer value.

3.1.2 From Gauge Theory to GTP

As already mentioned a GTP describes a 5d gauge theory or SCFT by being the dual graph of the corresponding brane-web. In this section we present the GTPs of $SU(N)$ gauge theories with fundamental and antisymmetric matter that admit a UV completion. Our strategy is to start with the weakly coupled (p,q) 5-brane-webs which are summarised in appendix A.1. From this, we can easily determine the GTP of the gauge theory. These GTPs, represented by their set of black vertices V_b, are summarised in table 3.1. However, if the polygon is non-convex, it is not possible to remove the internal edge representing the gauge coupling. To enable this, we need to perform the GTP equivalent of the Hanany-Witten moves. Let us first fix the notation. We let P be a pre-GTP (pGTP), i.e. a GTP, where we relax the convexity requirement. For simplicity we ignore interior edges, such as rulings, for now but will return to this issue later. The pGTP is characterised by the list of its black vertices

$\boldsymbol{v}_i$ with $i \in \mathbb{Z}_{n_V}$, labelling them in counter clockwise order. Equivalently, P can be characterised by the list of vectors $[\boldsymbol{u}_i]_{i\in\mathbb{Z}_{n_V}}$ defined by

$$\boldsymbol{u}_i = \boldsymbol{v}_i - \boldsymbol{v}_{i-1}\,. \tag{3.22}$$

Note that such a list of vectors of $\mathbb{Z}^2$ defines a polygon only if they add up to zero. The polygon is convex if and only if two consecutive edges have direction vectors $\boldsymbol{u}_i$ and $\boldsymbol{u}_{i+1}$ forming a positively oriented basis of the plane. It is useful to introduce shorthand for the determinants and greatest common divisors

$$D_{i,j} = \det\left(\boldsymbol{u}_i, \boldsymbol{u}_j\right)\,, \qquad D_i = D_{i,i+1}\,, \qquad \mu_i = \gcd(\boldsymbol{u}_i)\,. \tag{3.23}$$

In other words,

$$P \text{ convex } \iff D_i \geq 0 \quad \forall i \in \mathbb{Z}_{n_V}\,. \tag{3.24}$$

Let

$$\mathfrak{C} := \{i \mid D_i < 0\} \tag{3.25}$$

be the set of labels which indicate the non-convexities of P. Clearly, the polygon is convex if and only if $\mathfrak{C} = \emptyset$.

Monodromies

In this section, we assume $\mathfrak{C} \neq \emptyset$, and our goal is to find a GTP, which is convex and physically equivalent to P. Inspired by the brane-web, we exhibit two basic, related operations which, upon being iterated in an appropriate way, can result in such a GTP.

1. Monodromy-preserving edge-moves

   Let $i \in \mathfrak{C}$. We define two operations on the polygon P, which affect the two

vectors $\boldsymbol{u}_i$ and $\boldsymbol{u}_{i+1}$ in the following way, leaving the other vectors unchanged:

$$\begin{aligned}\mathfrak{M}_i^+ \;:\; & [\dots,\boldsymbol{u}_{i-1},\boldsymbol{u}_i,\boldsymbol{u}_{i+1},\boldsymbol{u}_{i+2},\dots]\mapsto \\ & \left[\dots,\boldsymbol{u}_{i-1},\boldsymbol{u}_{i+1}\left(1-\frac{D_i}{\mu_{i+1}^2}\right),\boldsymbol{u}_i+\boldsymbol{u}_{i+1}\left(\frac{D_i}{\mu_{i+1}^2}\right),\boldsymbol{u}_{i+2},\dots\right]\end{aligned} \tag{3.26}$$

$$\begin{aligned}\mathfrak{M}_i^- \;:\; & [\dots,\boldsymbol{u}_{i-1},\boldsymbol{u}_i,\boldsymbol{u}_{i+1},\boldsymbol{u}_{i+2},\dots]\mapsto \\ & \left[\dots,\boldsymbol{u}_{i-1},\boldsymbol{u}_{i+1}+\boldsymbol{u}_i\left(\frac{D_i}{\mu_i^2}\right),\boldsymbol{u}_i\left(1-\frac{D_i}{\mu_i^2}\right),\boldsymbol{u}_{i+2},\dots\right]\end{aligned} \tag{3.27}$$

One can check that after having applied $\mathfrak{M}_i^\pm$, the polygon is convex at i, as

$$\det\left[\boldsymbol{u}_{i+1}\left(1-\frac{D_i}{\mu_{i+1}^2}\right),\boldsymbol{u}_i+\boldsymbol{u}_{i+1}\left(\frac{D_i}{\mu_{i+1}^2}\right)\right]=-D_i\left(1-\frac{D_i}{\mu_{i+1}^2}\right)>0\,, \tag{3.28}$$

and similarly for $\mathfrak{M}_i^-$. However, it is now possible that $i\pm1\in\mathfrak{C}$.

2. Pruning

Let $i\in\mathfrak{C}$. Let $k_\pm$ be the smallest positive integers such that

$$\begin{aligned}&D_{i+1,i+k_++1}>0 \quad\wedge\quad D_{i+1,i+k_++2}\le 0 \quad\wedge\quad i+1,\dots,i+k_+\notin\mathfrak{C}\\ &D_{i-k_-,i}>0 \quad\wedge\quad D_{i-k_--1,i}\le 0 \quad\wedge\quad i-1,\dots,i-k_-\notin\mathfrak{C}\,.\end{aligned} \tag{3.29}$$

If the respective integer $k_\pm$ exists we define the operations

$$\begin{aligned}\mathfrak{P}_i^+ \;:\; & \left[\dots,\boldsymbol{u}_i,\boldsymbol{u}_{i+1},\boldsymbol{u}_{i+2},\dots,\boldsymbol{u}_{i+k_++1},\boldsymbol{u}_{i+k_++2},\dots\right]\mapsto \\ & \left[\dots,\boldsymbol{u}_i,\boldsymbol{u}_{i+2}+\frac{D_{i+1,i+2}}{\mu_{i+1}^2}\boldsymbol{u}_{i+1},\dots,\boldsymbol{u}_{i+k_++1}+\frac{\left|D_{i+1,i+k_++1}\right|}{\mu_{i+1}^2}\boldsymbol{u}_{i+1},\right. \\ & \left.\boldsymbol{u}_{i+1}\left(1-\sum_{j=1}^{k_+}\frac{D_{i+1,i+j+1}}{\mu_{i+1}^2}\right),\boldsymbol{u}_{i+k_++2}\dots\right]\end{aligned} \tag{3.30}$$

$$\begin{aligned}\mathfrak{P}_i^- \;:\; & \left[\dots,\boldsymbol{u}_{i-k_--1},\boldsymbol{u}_{i-k_-},\dots,\boldsymbol{u}_{i-1},\boldsymbol{u}_i,\boldsymbol{u}_{i+1},\dots\right]\mapsto \\ & \left[\dots,\boldsymbol{u}_{i-k_--1},\boldsymbol{u}_i\left(1-\sum_{j=1}^{k_-}\frac{D_{i,i-j}}{\mu_i^2}\right),\boldsymbol{u}_{i-k_-}+\frac{D_{i,i-k_-}}{\mu_i^2}\boldsymbol{u}_i,\dots,\right. \\ & \left.\boldsymbol{u}_{i-1}+\frac{D_{i,i-1}}{\mu_i^2}\boldsymbol{u}_i,\boldsymbol{u}_{i+1}\dots\right]\,.\end{aligned} \tag{3.31}$$

This does not necessarily remove the non-convexity at i, but may increase D_i.

We can represent any monodromy- and charge-preserving transformation on P as a (finite) word using these operations as letters. We will present detailed examples in section 3.3 and appendix A.2.

Let us now consider internal edges, which in our context represent finite parameters along the extended Coulomb branch, i.e, gauge couplings m_0 or hypermultiplet masses m_f. Under an edge-move $\boldsymbol{u} \mapsto \mathfrak{M}_i^{\pm}\boldsymbol{u}$, the original internal edges are unchanged and $\boldsymbol{u}_i$ and $\boldsymbol{u}_{i+1}$ are added to the set, i.e. $\boldsymbol{u}_i$ and $\boldsymbol{u}_{i+1}$ become internal lines in the transformed polygon. We can also prune a polygon with internal edges, however, the transformation is very impractical to implement, and will therefore not be used in the following.

The Rank of a Theory

A very important property of a 5d gauge theory or SCFT is its rank. Similarly, we define the rank of a (p)GTP P as

$$r = r_0 - \frac{1}{2}\sum_{\alpha}\sum_{x=1}^{b_\alpha+1}\mu_{\alpha,x}\left(\mu_{\alpha,x}-1\right)\,, \tag{3.32}$$

where r_0 is the number of internal nodes of P. We can use Pick's theorem [140] to write this as

$$r_0 = A_P + 1 - \frac{1}{2}\sum_{\alpha}\lambda_\alpha\,, \tag{3.33}$$

where A_P is the area of P. Putting this together, and using (3.11), this gives

$$r = A_P + 1 - \frac{1}{2}\sum_{\alpha}\sum_{x=1}^{b_\alpha+1}\mu_{\alpha,x}^2\,. \tag{3.34}$$

We conjecture that this coincides with the gauge rank of the 5d gauge theory or SCFT that P represents. This is substantiated by agreement in all considered examples and the invariance of (3.34) under edge-moves and pruning. In this thesis we will only consider GTPs with $r \geq 0$, as polygons with negative rank can not describe physical SCFTs.

3.2 Higgs Branches for 5d SCFTs from Edge Colourings

We continue our analysis by presenting the direct construction of the MQ($\mathcal{T}_P$) from the GTP P in (3.2). We first provide criteria for a GTP (or a sub-polygon thereof) to satisfy the so-called s-rule, which in the dual brane-web ensures that the configuration preserves supersymmetry.

With this background, we then introduce the colouring of a GTP, which amounts to a refined Minkowski sum decomposition. Finally, we give a short algorithm that associates a tropical quiver (TQ) to each colouring of a given GTP. We conjecture that the tropical quiver can then be identified with the magnetic quiver characterising the 5d Higgs branch of the SCFT – and in cases when there are multiple cones of the Higgs branch, i.e. multiple colourings, the union of these tropical quivers comprises the full Higgs branch of the 5d SCFT.

3.2.1 The s-Rule

Not all GTPs give rise to a supersymmetric theory in 5d (unlike any convex toric polygon). It is possible for a GTP to have an insufficient distribution of vertices (in a sense, too many white dots). This is the GTP equivalent of a web configuration that is non-supersymmetric because it has too many 5-branes ending on a single 7-brane – this is referred to as a web that does not satisfy the s-rule. Determining whether a GTP satisfies the s-rule is a highly non-local problem. In [61] it was argued that a GTP P obeys the s-rule, if there exists a consistent resolution, i.e. a tessellation, of P into tiles. Here we generalise the definition of such a tile. We should add a word of caution regarding the s-rule. The rule argued for in [61] seems to not apply in general, in particular it is not invariant under $SL(2,\mathbb{Z})$ transformations. Instead, we use the proposed generalisation of the s-rule in (2.22).

Definition 5 (Tiles) *A tile T_R is a GTP such that*

1. *$E_\alpha = (E_1, E_2, E_3, E_4)$, where $L_4 = -L_2$ and $\lambda_2 \geq \lambda_4$ where we allow $\lambda_4 = 0$. Thus, T_R is either a trapezoid or a triangle.*

2. *The partitions are*

$$\{\mu_\alpha\} = \{\lambda_\alpha\}\,, \tag{3.35}$$

   i.e. T_R has no non-extreme vertices.

3. *Define the auxiliary GTP $\widetilde{T}_R$ with*

$$\widetilde{L}_\alpha = (L_1, L_2, L_3)\,, \qquad \widetilde{\lambda}_\alpha = (\lambda_1, \lambda_2 - \lambda_4, \lambda_3)\,, \qquad \{\widetilde{\mu}_\alpha\} = \{\widetilde{\lambda}_\alpha\}\,, \tag{3.36}$$

   such that T_R is the refined Minkowski sum of the triangle $\widetilde{T}_R$ and the line of length λ_4 along E_4. Then,

$$\widetilde{\lambda}_\alpha \widetilde{\lambda}_\beta \left|\det(\widetilde{L}_\alpha, \widetilde{L}_\beta)\right| \geq (\widetilde{\lambda}_\gamma)^2\,, \qquad \forall \alpha \neq \beta\,,\ \alpha \neq \gamma\,,\ \beta \neq \gamma\,. \tag{3.37}$$

With this general definition of a tile, we use the requirement of [61, 141] to determine whether a GTP respects the s-rule. We furthermore define concepts of minimality and irreducibility that are related to the s-rule, and which will be essential input for our definition of a colouring.

Definition 6 (s-Rule, Minimality and Irreducibility) *Let P be a GTP with edges E_α of length λ_α and partitions $\{\mu_\alpha\}$.*

1. *P is said to obey the s-rule, if P can, by the inclusion of internal edges, be resolved into resolution tiles.*[2]

2. *Let $\widetilde{P}$ be a GTP with edges E_α of length λ^α and partitions*

$$\{\widetilde{\mu}_\alpha\} > \{\mu_\alpha\}\,, \tag{3.38}$$

[2]Here we mean that the polygon can be tessellated by tiles by including internal edges.

i.e. $\widetilde{P}$ is obtained from P by removing vertices along the edges. P is said to obey the s-rule minimally (or we say that P itself is minimal) if $\widetilde{P}$ does not obey the s-rule for any choice of $\{\widetilde{\mu}_\alpha\}$.

3. *P is irreducible if there is no decomposition*

$$P = P_1 \oplus P_2 \,, \tag{3.39}$$

such that P_1 and P_2 obey the s-rule.

The idea is that, given any GTP as a starting point, one can always find a minimal GTP by removing vertices (i.e. converting black vertices into white ones) in the original polygon. A minimal polygon has the largest possible number of white dots, whilst still satisfying the s-rule, i.e. there is no possible way to remove another vertex from the GTP without breaking supersymmetry. On the other hand, a GTP is said to be irreducible if it cannot be further decomposed into a partition sum of two other polygons. It is possible for a GTP to be minimal but not irreducible, or irreducible but not minimal. In the following section, we will require both conditions to be met by the building blocks of the colouring. To avoid notational clutter, an irreducible GTP, that obeys the s-rule minimally is called an irreducible minimal polygon (IMP).

3.2.2 Colourings of GTPs

In this section we define the notion of a colouring of a GTP, which is the crucial step in determining the magnetic quiver. A colouring of a polygon is dual to a maximal subdivision of the 5-brane-web into consistent, supersymmetric sub-webs. The definition relies on the data of the polygon, as well as the generalised decomposition rule, which was introduced in section 3.1.1. Furthermore, an essential feature of the building blocks of the colouring is that they represent minimal supersymmetric configurations. This criterion is implemented by requiring irreducibility and minimality with respect to the s-rule (see section 3.2.1).

Algorithm 1 (Coloured Polygon) *Let P be a GTP (with no internal edges), with edge lengths λ_α. Let $\{\lambda_\alpha^c \in \mathbb{N}\}$ be a partition of the edge lengths, such that*

$$\sum_{c=1}^{n_c} \lambda_\alpha^c = \lambda_\alpha \,, \tag{3.40}$$

where n_c is the number of colours, and along each edge E_α of P, λ_α^c segments L_α are coloured by c. A partition defines a coloured GTP $(P, \{\lambda_\alpha^c\})$, if the following conditions are met:

1. *For each $c = 1, \ldots, n_c$ the associated line segments form a polygon, i.e.*

$$0 = \sum_\alpha \lambda_\alpha^c L_\alpha \,. \tag{3.41}$$

   We denote these colour sub-polygons by S^c.[3]

2. *Each S^c is a refined Minkowski sum of m^c times the same IMP T^c,*[4]

$$S^c = \underbrace{T^c \oplus \cdots \oplus T^c}_{m^c}, \tag{3.42}$$

   and we require that the IMPs used for different colours are distinct,

$$T^c \neq T^d \,, \qquad c \neq d \,. \tag{3.43}$$

3. *For each α,*

$$\{\mu_\alpha\} \leq \sum_{c=1}^{n_c} \{\mu_\alpha^c\} \,, \tag{3.44}$$

   where we use the dominance partial order of the partitions defined by (3.11) *for P and S^c respectively.*

We then write

$$P \leq \bigoplus_{c=1}^{n_c} S^c \,, \qquad P = S^1 + \cdots + S^{n_c} \,. \tag{3.45}$$

For strict inequality of the partitions in (3.44) *we also write $P < \bigoplus_{c=1}^{n_c} S^c$.*

[3] This also includes the case of two parallel lines.

[4] We assume that the rank of T^c is always non-negative.

In other words, we colour the edges of a GTP such that the edges pertaining to a single colour form a closed sub-polygon S^c. A closed sub-polygon must be made up of a number m^c of identical IMPs T^c. We require that no two distinct sub-polygons are comprised of the same IMP (in such a situation the two sub-polygons are identified and the resulting multiple of tiles m^c is the sum). The final condition essentially ensures that all the sub-polygons fit simultaneously into the GTP. The above conditions were derived by using the map from brane-web to GTP to identify the dual concept of a maximal subdivision of the web into sub-webs. The details of this map are explained in section 3.4.

In the convex toric case, our definition of a colouring exactly reduces to identifying the decomposition of a given polygon into Minkowski summands, which was shown in [138, 139] to parametrise the deformations of the geometry.

Fact 2 *For a convex toric polygon P, its colouring $(P, \{\lambda^c_\alpha\})$ defines a Minkowski sum decomposition*

$$P = S^1 + \cdots + S^{n_c}\,, \tag{3.46}$$

where the S^c are the sub-polygons, that are defined by the colouring $\{\lambda^c_\alpha\}$. Conversely, any Minkowski sum decomposition of P into S^c defines a colouring $\{\lambda^c_\alpha\}$, if the S^c are inequivalent, i.e. there is no $n \in \mathbb{Q}$ such that $S^c = nS^d$ for any c, d, and the decomposition is maximal, i.e. none of the sub-polygons can be further decomposed to a set of distinct sub-polygons (where two polygons that are related by scaling are not understood to be distinct).

Colour-Subdivided GTPs Before we show how to associate a quiver to a coloured GTP, we will explain how to graphically determine the mixed volume of definition 4, between two coloured subpolygons. To this end, we define a colour sub-division of a coloured GTP $(P, \{\lambda^c_\alpha\})$, in terms of uni-coloured polygons and bi-coloured parallelograms. The subdivision agrees with the colouring of the edges of P on the boundary,

and extends this to the interior. The mixed volume of two colour sub-polygons is dual to the tropical intersection of two sub-webs in the brane-web. In particular, two sub-webs can be interpreted as a pair of tropical curves whose intersection is determined by pulling apart the curves and adding up the intersections of individual 5-branes. The displacement of the tropical curves is exactly dual to the colour-subdivision of the coloured GTP.

Definition 7 (Colour-subdivided GTP) *A colour-subdivision of a GTP is a tiling of $(P, \{\lambda_\alpha^c\})$ by two types of polygons:*

1. *Parallelograms $G^{c_1c_2}$, where parallel edges have the same colour*

2. *Polygons G^c where all edges have the same colour*

such that as a set

$$P = \bigcup_{c_1,c_2} G^{c_1c_2} \cup \bigcup_{c} G^{c}\,, \tag{3.47}$$

with the subpolygons intersecting each other at most in edges. Furthermore, the colour subdivision agrees with the edge-colouring, i.e.

$$\partial\left(\bigcup_{c_1,c_2} G^{c_1c_2} \cup \bigcup_{c} G^{c}\right)\Bigg|_{E_\alpha} = \{\lambda_\alpha^c\}\,. \tag{3.48}$$

Due to the last requirement, a coloured polygon $(P, \{\lambda_\alpha^c\})$ determines a colour-subdivision of P, albeit not uniquely. Yet the sum of the area of all parallelograms $G^{c_1c_2}$ (that are bi-coloured in c_1 and c_2) is an invariant. For each pair c_1, c_2 we write this invariant

$$A^{c_1c_2} = \sum \mathrm{Area}(G^{c_1c_2})\,, \tag{3.49}$$

where the sum is over all parallelograms with colours c_1 and c_2, and we use the standard flat metric in $\mathbb{R}^2$ to compute the area. This area is exactly the mixed volume of the sub-polygons S^{c_1} and S^{c_2}.

Fact 3 (Colour-subdivided Polygons and the Mixed Volume) *Let $(P, \{\lambda_\alpha^c\})$ be a coloured GTP corresponding to a Minkowski sum $P = \sum_c S^c$. Then, for each choice of colour-subdivision*

$$A^{c_1 c_2} = MV(S^{c_1}, S^{c_2}) \,, \tag{3.50}$$

for all pairs c_1, c_2 [137].

3.2.3 Magnetic Quivers from Coloured GTPs

Associated to a coloured GTP we now define a quiver, which we refer to as the tropical quiver. If the GTP in question allows for more than a single consistent colouring, then each colouring gives rise to its own quiver. The tropical quiver will be identified with the magnetic quiver, i.e. the 3d $\mathcal{N} = 4$ theory, whose Coulomb branch is isomorphic to the Higgs branch of the 5d theory $\mathcal{T}_P$.

Definition 8 (Tropical Quiver) *The tropical quiver $TQ(P, \{\lambda_\alpha^c\})$ of a coloured GTP is given by a set of nodes with labels m_I, numbers of loops ℓ_I and symmetric intersections k_{IJ}. Given a coloured GTP $(P, \{\lambda_\alpha^c\})$ we define it as follows.*

1. *Colour nodes: Each colour maps to a node in the tropical quiver. The labels of the nodes are the m^c defined in* (3.42)*. In general, this is given by*

$$m^c = \gcd_\alpha \left(\lambda_\alpha^c\right) \,. \tag{3.51}$$

The intersections between the nodes of colour c_1 and c_2 are determined from two parts. The first is the mixed volume $MV(S^{c_1}, S^{c_2})$ of definition 4. The second contribution, which is negative, comes from configurations where an edge E_α is coloured in both colours, i.e. $\lambda_\alpha^{c_1}, \lambda_\alpha^{c_2} > 0$. Thus,

$$k^{c_1 c_2} = \frac{1}{m^{c_1} m^{c_2}} \left(MV(S^{c_1}, S^{c_2}) - \sum_\alpha \sum_{x=1}^{b_\alpha} \mu_{\alpha,x}^{c_1} \mu_{\alpha,x}^{c_2} \right) \,. \tag{3.52}$$

In particular, the self-intersection of a color node is given by

$$k^{cc} = \frac{1}{(m^c)^2}\left(2Area(S^c) - \sum_{\alpha}\sum_{x=1}^{b_\alpha}(\mu^c_{\alpha,x})^2\right) = 2r(T^c) - 2\,, \tag{3.53}$$

where r is the rank (3.34) *of the IMP T^c in* (3.42)*. This determines the number of loops on the c-colored node as*

$$\ell^c = 1 + \frac{k^{cc}}{2} = r(T^c)\,. \tag{3.54}$$

2. *Tails: There are additional nodes in the tropical quiver that are not associated to a colour. For each edge E_α, the tropical quiver contains a sequence of nodes of length b_α. The labels of these nodes are given by*

$$m_{\alpha,x} = \sum_{y=1}^{x}\left(-\mu_{\alpha,y} + \sum_{c=1}^{n_c}\mu^c_{\alpha,y}\right)\,, \tag{3.55}$$

where $x = 1, \dots b_\alpha$.[5] *Neighbouring nodes pertaining to the same edge are connected, i.e. the number of intersections between the tail nodes is*

$$k_{\alpha,x;\beta,y} = \delta_{\alpha,\beta}\ \delta_{|x-y|,1}\,. \tag{3.56}$$

The intersection between colour and tail nodes is given by

$$k^c_{\alpha,x} = \frac{1}{m^c}\left(\mu^c_{\alpha,x} - \mu^c_{\alpha,x+1}\right)\,, \tag{3.57}$$

and there are no loops

$$\ell_{\alpha,x} = 0\,. \tag{3.58}$$

Since each coloured subpolygon S^c, consisting of m^c IMPs, is dual to a sub-web of multiplicity m^c, we map it to a node in the tropical quiver with label m^c. The two contributions to the edges between colour nodes in the tropical quiver correspond to the "stable intersection number" and 7-brane contribution in the web. We refer the reader to section 3.4 for details on the GTP-to-brane-web map. The tail nodes

[5]Note that one can easily show that all $m_{\alpha,x}$ with $x > b_\alpha$ vanish identically.

are not realised in $(P, \{\lambda_\alpha^c\})$ as a coloured sub-polygon. The information needed to construct the tails is nonetheless contained in the coloured GTP, and is given above in terms of the data defined in the previous subsections.

The self-intersection k^{cc} of a coloured sub-polygon S^c is a measure of the amount of adjoint matter associated to the corresponding node, see also [82]. Specifically, the $U(m^c)$ ($m^c \neq 1$) node of the magnetic quiver is associated with ℓ^c adjoint matter multiplets, indicated by a loop attached to this node. For theories with a high number of flavours the appearance of adjoint matter is very rare and we will not encounter them in this thesis. However, some examples are discussed in [2].

The tropical quiver will be interpreted as defining a 3d $\mathcal{N} = 4$ quiver gauge theory: vertices $U(m_I)$ with ℓ_I adjoint matter multiplets, connected by k_{IJ} hypermultiplets. The key relation of this tropical quiver to the original 5d QFT, is via its Coulomb branch, which is a hyper-Kähler manifold, and is identified with the Higgs branch of the 5d QFT $\mathcal{T}_P$.

Conjecture 1 (Tropical and Magnetic Quivers) *Let P be a GTP, associated to a 5d SCFT $\mathcal{T}_P$. There is a bijection between the inequivalent colourings of P and the cones of the Higgs branch of $\mathcal{T}_P$; moreover, the tropical quiver associated to a colouring is identified with a magnetic quiver for the corresponding cone in the Higgs branch.*

3.2.4 Symplectic Leaves and Colourings with Internal Edges

Our discussion so far required the GTP to have no internal lines. In M-theory, such geometries correspond to 5d SCFTs – which are the main focus of our attention. In this section we generalise our approach to include GTPs with internal lines, which in the geometry are partial resolutions, and in 5d language correspond to opening up partial (extended) Coulomb branch directions. The motivation is two-fold: obviously if one would like to study weakly coupled 5d gauge theories, these have rulings, i.e.

internal edges. Secondly, and perhaps more importantly for the current endeavour of mapping out the Higgs branch, we require these to construct the Hasse diagram, i.e. the partially ordered set of symplectic leaves that comprise the Higgs branch, as a hyper-Kähler cone. The Higgsing is constructed by successively opening partial Coulomb branch directions. To construct the associated magnetic quivers after each Higgsing, we need to generalise the algorithm to GTPs with internal lines.

Colourings with Internal Edges

For a polygon with internal edges, the edge colouring has to be extended. The first step is to extend our algorithm 1. For polygons with internal edges, the s-rule only has to be obeyed on external edges (it is irrelevant to apply it to internal edges, given that these are dual to internal 5-branes which do not end on any 7-branes). A coloured subpolygon S^c needs to be divided completely by internal edges, so that all extreme vertices in S^c are part of at least two edges. We argue for this approach in the brane picture in section 3.4.1.

Algorithm 2 (Colouring for Polygons with Internal Edges) *Consider a GTP P with internal edges and denote the subpolygons by P_A, where $A \subset \alpha = \{1, \cdots, n_E\}$,*

$$E \cap P_A = \cup_{\alpha \in A} E_\alpha \,, \tag{3.59}$$

so the P_A do not have any internal edges.

A colouring for a GTP P with internal edges $E^{in} \neq \emptyset$ is a partition

$$\sum_{c=1}^{n_c} \lambda_\alpha^c = \lambda_\alpha \,. \tag{3.60}$$

For all c, the $\{\lambda_\alpha^c\}$ defines a refined Minkowski summand S^c of $P \leq S^1 \oplus \cdots \oplus S^{n_c}$ obeying the following rules:

1. *The S^c can be divided into subpolygons*

$$S^c = \bigcup S_A^c \,, \tag{3.61}$$

without internal lines.

2. *For all c and A*

$$S_A^c = \underbrace{T_A^c \oplus \cdots \oplus T_A^c}_{m_A^c}, \qquad T_A^c = \bigoplus_i T_A^i \,, \tag{3.62}$$

where each T_A^i is irreducible and obeys the s-rule minimally, for all external edges of P. We require that for $c \neq d$

$$T_A^c \neq T_A^d \,, \quad \forall A \,. \tag{3.63}$$

The multiplicity of S^c is given by

$$m^c = \gcd_A m_A^c \,. \tag{3.64}$$

3. *The partition is maximal, i.e. there is no subpartition*

$$S^{c_1} \leq S^{c_2} \oplus S^{c_3} \,, \tag{3.65}$$

such that the resulting colouring is valid.

Essentially, we can understand this algorithm as a generalisation of the algorithm 1 by extending the number of constraints imposed by the internal edges.

Hasse Diagram and Symplectic Leaves

The Higgs Branch of a 5d SCFT or gauge theory, has a foliation in terms of symplectic leaves, as reviewed in section 2.3. Starting from the magnetic quiver associated to the 5d QFT, the Hasse diagram can be obtained by successive quiver subtractions [72, 75, 76].

Here we provide a derivation in terms of the data of the coloured polygon $(P, \{\lambda_\alpha^c\})$, which characterise each cone of the Higgs branch of the theory $\mathcal{T}_P$. The full foliation structure is however in general interconnected.

The Hasse diagram is obtained by introducing successive partial resolutions into the GTP. In each step we start with a polygon P and find subtractions Δ_i that result in the next layer Q_i of the Hasse diagram – there can in general be multiple such subtractions:

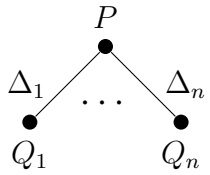

(3.66)

If at some point the GTPs Q_j along different branches agree, these nodes should be identified, leading to interconnections. This idea was first introduced in [75], where it was argued in the brane picture that the Higgs branch at specific points along the Coulomb branch reproduces the different layers in the Hasse diagram.

Definition 9 (Hasse diagram of a GTP) *Let P be a GTP, characterised by edges E_α with $\lambda_\alpha^{(P)}$ and $\mu_{\alpha,x}^{(P)}$. A transition in the Hasse diagram $P \xrightarrow{\Delta} Q$ is a set of internal edges E_β, which correspond to a partial resolution, with minimal line segments L_β of length ν_β, such that:*

1. *There is a GTP, Q, characterised by*

$$E_{(Q)}^{\partial} = E_{(P)}^{\partial}\,, \qquad E_{(Q)}^{in} = E_{(P)}^{in} \cup E_\beta\,, \qquad \lambda_\alpha^{(Q)} = \{\lambda_\alpha^{(P)}, \nu_\beta\}\,, \qquad \mu_{\alpha,x}^{(Q)} = \mu_{\alpha,x}^{(P)}\,. \tag{3.67}$$

2. *Q admits a colouring, such that there is a colour c^* with*

$$\nu_\beta^{c^*} = \nu_\beta \quad \forall \beta\,, \tag{3.68}$$

   with associated $\lambda_\alpha^{c^*}$ and $\mu_{\alpha,x}^{c^*}$.

3. *There is a GTP Δ characterised by*

$$E_{(\Delta)} = \{E_\alpha^{(P)} | \lambda_\alpha^{c^*} \neq 0\}\,, \qquad \lambda_\alpha^{(\Delta)} = \lambda_\alpha^{c^*}\,, \qquad \mu_{\alpha,x}^{(\Delta)} = \mu_{\alpha,x}^{c^*}\,, \tag{3.69}$$

   such that the magnetic quiver of Δ is a either the magnetic quiver of a Kleinian singularity or the closure of a minimal nilpotent orbit.

Note that the leaves that we allow here are those discussed in section 2.3. In case that a given GTP has symplectic leaves that go outside of this class, it would be interesting to see how these are realised in the GTP in terms of introducing internal lines. We are confident that any effect that occurs in the webs has a counterpart in our formulation in terms of the GTPs, including more general symplectic leaves.

A physical way to understand the transitions in the Hasse diagram is in terms of a Higgsing, or combinatorially in terms of quiver subtractions in the magnetic quiver [72]. Essentially, we replace the affine Dynkin diagram of an ADE algebra (or a Kleinian singularity) by a single $U(1)$ rebalancing node. The idea is that the newly introduced colour c^* represents the rebalancing node. Including the ν_β, S^{c^*} has magnetic quiver $U(1)$ but excluding them it would represent the ADE singularity. We argue about the details of this process in section 3.4.3, where we explain how it relates to a partial opening of a Coulomb branch and subsequent Higgsing.

Fact 4 *If $P \xrightarrow{\Delta} Q$ is a transition in a Hasse diagram, we can write P as a refined Minkowski sum*

$$P \leq \Delta \oplus S\,, \tag{3.70}$$

where S is another GTP, which need not be irreducible and could be empty. Conversely, such a Minkowski sum decomposition induces a transition in the Hasse diagram if

1. *The magnetic quiver of Δ is a symplectic singularity*
2. *There is an extension of Δ by internal lines ν_β to Δ_ν with $\lambda_\alpha^{(\Delta_\nu)} = \{\lambda_\alpha^{(\Delta)}, \nu_\beta\}$ such that the s-rule for Δ_ν is obeyed minimally on each external edge.*

Then, $Q \leq \Delta_\nu \oplus S$ with $\mu_{\alpha,x}^{(Q)} = \mu_{\alpha,x}^{(P)}$.

This implies that, should we find a Δ representing a symplectic singularity as a refined Minkowski summand of P, we can subtract the corresponding magnetic

quiver, provided that the magnetic quiver of Δ can be condensed to a $U(1)$ by the inclusion of internal lines.

3.3 Application: $SU(N)$ with AS and F Matter

For general $SU(N)$ with fundamental and anti-symmetric matter there are five marginal theories introduced in [34], see table 2.2. For each of them we consider the submarginal theory obtained by decoupling a single fundamental hypermultiplet. Furthermore, we consider the $SU(2)^m$ quiver theories without a dual SQCD description and the submarginal G_N-theories [3], whose descendants include the well-known T_N-theories [61, 87] in 5d. We give the GTP before and after edge-moves and compute the magnetic quiver for the SCFT. Decoupling further matter is discussed in section 3.3.2 and the magnetic quivers of the descendant trees are given in appendix A.3.

3.3.1 GTPs for Tree Tops

$\boldsymbol{SU(N)_{\frac{1}{2}} + (2N+3)F}$

First, we study the submarginal theory associated to the circle reduction of (D_{N+2}, D_{N+2})-conformal matter. This theory is the parent of all 5d SCFTs with an SQCD description in the IR. The polygon for $SU(N)_{\frac{1}{2}} + (2N+3)\boldsymbol{F}$ is given by

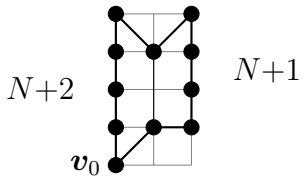

(3.71)

We draw the pGTP for $N = 2$, but the generalisation to any N is obtained by increasing the number of vertical edges as shown. The ruling indicating the $SU(N)$ gauge theory description is given by the thin internal line. Fixing $\boldsymbol{v}_0$ to be the lower

left corner the polygon can be represented by the vectors

$$\boldsymbol{u} = \left[(1,1),(1,0),\underbrace{(0,1)}_{N+1},(-1,-1),(-1,1),\underbrace{(0,-1)}_{N+2}\right] . \tag{3.72}$$

The edge-moves necessary to make this polygon convex were discussed in [73] in the web description, using pruning. An alternative choice, using only monodromy-preserving edge-moves, in our language is exemplified in detail in appendix A.2.1.

We show that the necessary sequence of transformations can be written as

$$\begin{aligned}\mathfrak{T} &= \mathfrak{M}_4^+ \cdots \mathfrak{M}_{N+4}^+ \mathfrak{M}_2^- \mathfrak{M}_1^+ \mathfrak{M}_3^+ \cdots \mathfrak{M}_{N+3}^+ \mathfrak{M}_{N+4}^- \\ \mathfrak{T}\boldsymbol{u} &= \left[(2,0),(N+2,2N+4),(0,N+3),(-N-4,-N-4),\underbrace{(0,-1)}_{2N+3}\right] .\end{aligned} \tag{3.73}$$

This leads to the convex GTP

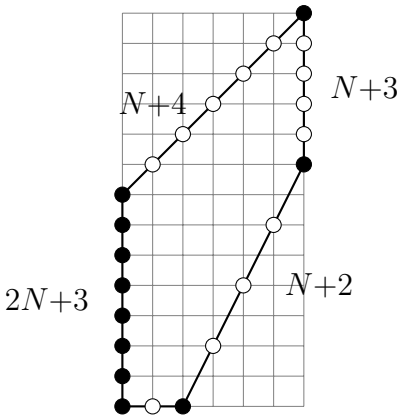

(3.74)

where we removed the internal lines to go to the SCFT limit.

In appendix A.2.2 we compute the magnetic quiver from this GTP. In this case there is a single colouring of (3.74), i.e. a single magnetic quiver. As is well-known, this is given by

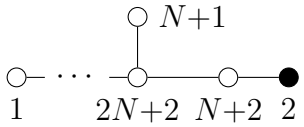

(3.75)

from which one can read off the $SO(4N+8)$ flavour symmetry.

$\boldsymbol{SU(N)_{\frac{N+1}{2}} + 1AS + 7F}$

Next, let us consider the higher rank E-string. Its descendants include the rank $r = (N-1)$ E_{N_F+1}-theories, which have two weakly coupled gauge theory descriptions.

$$SU(N)_{\frac{N+8-N_F}{2}} + 1\boldsymbol{AS} + N_F\boldsymbol{F} \quad \leftrightarrow \quad Sp(N-1) + 1\boldsymbol{AS} + N_F\boldsymbol{F}\,, \qquad N_F = 0,\ldots,7\,. \tag{3.76}$$

The submarginal theory has seven flavours and is known as the higher rank E_8-theory. Let us first consider the $Sp(N-1)$ description, which was discussed in [64, 142]. It turns out that the magnetic quiver is far easier to compute in this description. The polygons for the rank r E_8-theory before and after edge-moves are given by

$$\begin{aligned} \boldsymbol{u} &= \left[(r,r),(r,0),\underbrace{(0,r)}_{3},(-r,-r),(-r,r),\underbrace{(0,-r)}_{3},(0,-r+1),(0,-1)\right]\,, \\ \mathfrak{T}\boldsymbol{u} &= \left[(2r,0),(4r,8r),(0,5r),(-6r,-6r),\underbrace{(0,-r)}_{6},(0,-r+1),(0,-1)\right]\,, \end{aligned} \tag{3.77}$$

where we applied the same set of edge-moves as in (3.73), namely

$$\mathfrak{T} = \mathfrak{M}_4^+\mathfrak{M}_5^+\mathfrak{M}_6^+\mathfrak{M}_2^-\mathfrak{M}_1^+\mathfrak{M}_3^+\mathfrak{M}_4^+\mathfrak{M}_5^+\mathfrak{M}_6^-\,. \tag{3.78}$$

From this we deduce that the magnetic quiver for the rank $(N-1)$ E_8 theory is given by the affine Dynkin diagram of E_8, with each label multiplied by $(N-1)$, and an additional $U(1)$ node attached to the affine node, i.e.,

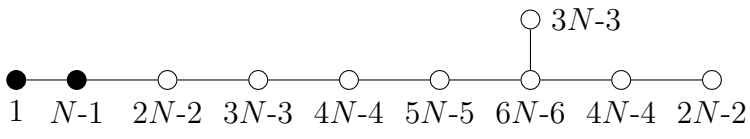

(3.79)

Indeed, this logic holds for all higher rank E_{N_F+1} theories, from which one reads off an $E_{N_F+1} \times U(1)$ flavour symmetry. However, for $N > 1$, the flavour symmetry is conjectured to enhance to $E_{N_F+1} \times SU(2)$. The appearance of this additional $SU(2)$ symmetry is somewhat mysterious both from the field theoretic and the geometric point of view.

Let us now discuss the $SU(N)$ description for which the brane-web was discussed in [34, 64]. In general these are constructed by the inclusion of $O7^-$-planes and differ qualitatively depending on whether N is even or odd. The corresponding polygons (before edge-moves) for the $SU(N)_{\frac{N+1}{2}} + 1\boldsymbol{AS} + 7\boldsymbol{F}$ are given by (drawn for $n = 3$)

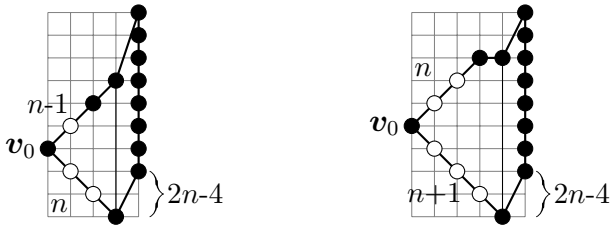

(3.80)

for $N = 2n$ even on the left and $N = 2n + 1$ odd on the right. These correspond to

$$N = 2n: \qquad \boldsymbol{u} = \left[(n,-n),(1,2n-4),\underbrace{(0,1)}_{7},(-1,-3),(-1,-1),(-n+1,-n+1)\right]$$

$$N = 2n+1: \qquad \boldsymbol{u} = \left[(n+1,-n-1),(1,2n-4),\underbrace{(0,1)}_{7},(-1,-2),(-1,0),(-n,-n)\right] \tag{3.81}$$

The necessary monodromy transformations are very difficult to obtain, as they depend non-trivially on N. However, one can show that these transformations exist [34] and, after the application of (2.27), lead to the same magnetic quiver (3.79) [2], further confirming the duality (3.76).

$\boldsymbol{SU(N)_{\frac{1}{2}} + 1AS + (N+5)F}$

The next submarginal SCFT has an $SU(N)_{\frac{1}{2}} + 1\boldsymbol{AS} + (N+5)\boldsymbol{F}$ description. Again, the pGTP depends on whether N is even or odd, so we will discuss them in turn.

The polygons before edge-moves are (drawn for $n = 3$)

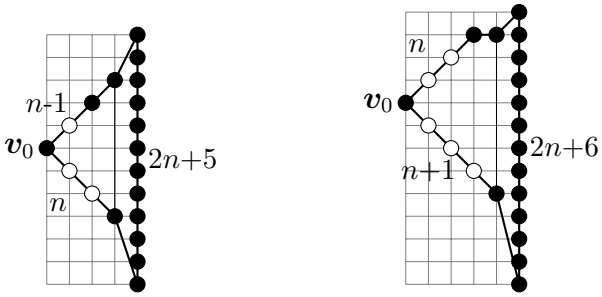

(3.82)

where $N = 2n$ and $N = 2n + 1$, respectively. The vectors of the polygons are

$$\begin{aligned} N = 2n: \qquad & \boldsymbol{u} = \Big[(n,-n),(1,-3),\underbrace{(0,1)}_{2n+5},(-1,-2),(-1,-1),(-n+1,-n+1)\Big] \\ N = 2n+1: \qquad & \boldsymbol{u} = \Big[(n+1,-n-1),(1,-4),\underbrace{(0,1)}_{2n+6},(-1,-1),(-1,0),(-n,-n)\Big] \end{aligned} \tag{3.83}$$

The sequences of edge-moves that make the polygons convex are given by

$$\begin{aligned} N = 2n: \qquad & \mathfrak{T} = \mathfrak{M}^-_{-1}\mathfrak{M}^-_0\mathfrak{M}^-_1\mathfrak{M}^+_{-1}\mathfrak{M}^-_{-2} \\ N = 2n+1: \qquad & \mathfrak{T} = \mathfrak{M}^-_{-2}\mathfrak{M}^-_{-3}\mathfrak{M}^-_0\mathfrak{M}^-_1 \end{aligned} \tag{3.84}$$

and the resulting GTPs are (drawn for $n = 3$)

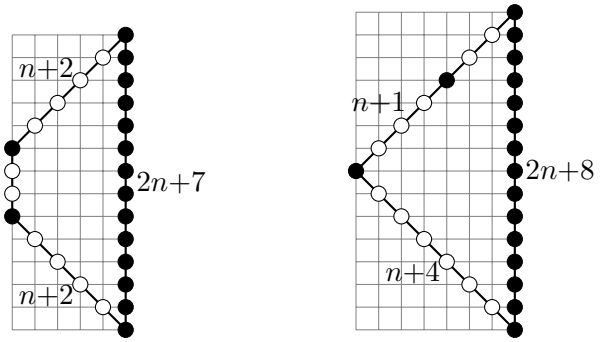

(3.85)

given by the vectors

$$\begin{aligned} N = 2n: \qquad & \mathfrak{T}\boldsymbol{u} = \Big[(n+2,-n-2),\underbrace{(0,1)}_{2n+7},(-n-2,-n-2),(0,-3)\Big] \\ N = 2n+1: \qquad & \mathfrak{T}\boldsymbol{u} = \Big[(n+4,-n-4),\underbrace{(0,1)}_{2n+8},(-3,-3),(-n-1,-n-1)\Big] \end{aligned} \tag{3.86}$$

From this we can compute the magnetic quivers for general N



(3.87)

for $N = 2n$ and $N = 2n + 1$, respectively. From the balanced nodes we see that generally the theory has flavour group $SU(N+7) \times U(1)$, which is enhanced for small N. Concretely, the symmetry enhances to $SU(12) \times SU(2)$ for $N = 5$ and to $SU(12)$ for $N = 4$. All of this is in agreement with the expected results [54].

$\boldsymbol{SU(N)_{\frac{1}{2}} + 2AS + 7F}$

Next, we are interested in the strongly coupled $SU(N)_{\frac{1}{2}} + 2\boldsymbol{AS} + 7\boldsymbol{F}$ theory. The brane-web for the gauge theory description was determined in [142] and dualises to the polygons (drawn for $n = 3$)

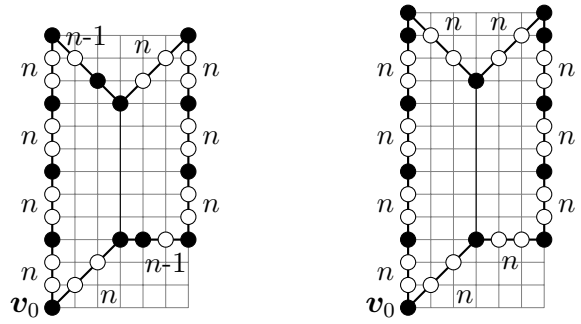

(3.88)

for $N = 2n$ and $N = 2n + 1$, respectively. The polygon vectors are

$$N = 2n: \qquad \boldsymbol{u} = \Big[(n,n),(1,0),(n-1,0),\underbrace{(0,n)}_{3},(-n,-n),$$
$$(-1,1),(-n+1,n-1),\underbrace{(0,-n)}_{4}\Big]$$

$$N = 2n+1: \qquad \boldsymbol{u} = \Big[(n,n),(n,0),\underbrace{(0,n)}_{3},(0,1),(-n,-n),(-n,n),(0,-1),\underbrace{(0,-n)}_{4}\Big] \tag{3.89}$$

For odd N the edge-moves are as for (3.73) but for even N they are different

$$\begin{aligned} N=2n: &\qquad \mathfrak{T}=\left(\mathfrak{M}_5^-\mathfrak{M}_6^-\mathfrak{M}_7^-\mathfrak{M}_8^-\right)\left(\mathfrak{M}_4^-\mathfrak{M}_5^-\mathfrak{M}_6^-\mathfrak{M}_7^-\right)\\ N=2n+1: &\qquad \mathfrak{T}=(\mathfrak{M}_4^+\cdots\mathfrak{M}_7^+)\mathfrak{M}_2^-\mathfrak{M}_1^+(\mathfrak{M}_3^+\cdots\mathfrak{M}_6^+)\mathfrak{M}_7^- \end{aligned} \tag{3.90}$$

This leads to the transformed vectors

$$\begin{aligned} N=2n: &\qquad \mathfrak{T}\boldsymbol{u}=\left[\underbrace{(1,0)}_{2},\underbrace{(n-1,0)}_{2},\underbrace{(n,0)}_{4},\underbrace{(0,2n)}_{3},\underbrace{(-3n,-3n)}_{2}\right]\\ N=2n+1: &\qquad \mathfrak{T}\boldsymbol{u}=\Big[(2n,0),(4n+1,8n+2),(0,5n+1),\\ &\qquad\qquad (-6n-1,-6n-1),\underbrace{(0,-n)}_{7},\underbrace{(0,-1)}_{2}\Big] \end{aligned} \tag{3.91}$$

The magnetic quiver computed from the GTP is

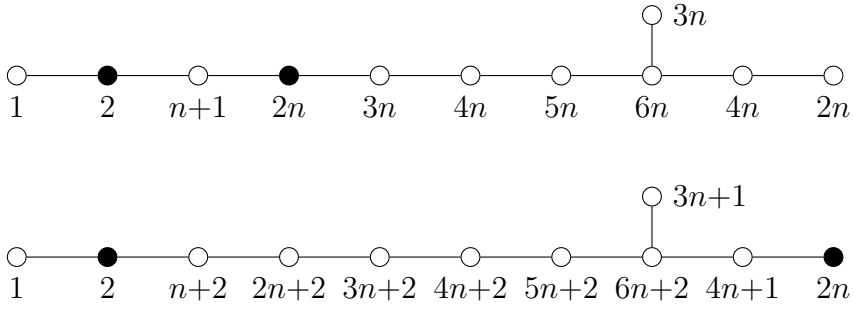

(3.92)

for $N=2n$ and $N=2n+1$ respectively. We see that the flavour symmetry coming from the balanced nodes depends on the parity of N. For N even it is $E_7\times SU(2)^2\times U(1)$ whereas for N odd it is $SO(16)\times SU(2)\times U(1)$. In both cases, the $U(1)$ is expected to enhance to $SU(2)$ and by studying the Hasse diagram we recognise a striking resemblance to the higher rank E-string. For $N=4$ the flavour symmetry seems to be enhanced to $E_7\times SU(4)$, where the $SU(4)$ is known to enhance further to $SO(7)$ [54, 143]. This can be confirmed by computing the Hilbert series of (3.92). Since the magnetic quiver is simply laced we do not expect to see the $\mathfrak{b}_3$ algebra in the Hasse diagram. However, by folding the magnetic quiver [144], this can be made explicit.

$SU(N)_2 + 2AS + 6F$

Finally, there is the strongly coupled $SU(N)_2 + 2\boldsymbol{AS} + 6\boldsymbol{F}$. Again, we have to distinguish between N even and odd. The weakly coupled pGTP is given by (drawn for $n = 3$)

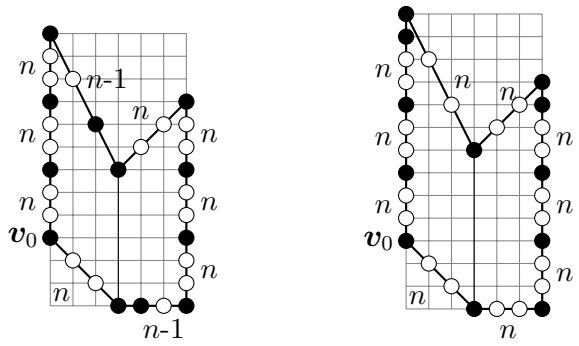

(3.93)

for $N = 2n$ and $N = 2n + 1$, respectively. The vectors of the polygons are

$$N = 2n: \qquad \boldsymbol{u} = \Big[(n,-n),(1,0),(n-1,0),\underbrace{(0,n)}_{3},(-n,-n),$$
$$(-1,2),(-n+1,2n-2),\underbrace{(0,-n)}_{3}\Big]$$
$$N = 2n+1: \quad \boldsymbol{u} = \Big[(n,-n),(n,0),\underbrace{(0,n)}_{3},(0,1),(-n,-n),(-n,2n),(0,-1),\underbrace{(0,-n)}_{3}\Big] \tag{3.94}$$

To make these polygons convex we apply the operations

$$\begin{aligned} N = 2n: &\qquad \mathfrak{T} = (\mathfrak{M}_4^-\mathfrak{M}_3^-)(\mathfrak{M}_2^+\mathfrak{M}_1^+)(\mathfrak{M}_4^-\cdots\mathfrak{M}_8^-)(\mathfrak{M}_3^-\cdots\mathfrak{M}_7^-) \\ N = 2n+1: &\qquad \mathfrak{T} = \mathfrak{M}_{11}^-(\mathfrak{M}_{10}^+\cdots\mathfrak{M}_2^+)\mathfrak{M}_1^-\mathfrak{M}_2^+(\mathfrak{M}_3^-\cdots\mathfrak{M}_7^-) \end{aligned} \tag{3.95}$$

leading to the transformed vectors

$$
\begin{aligned}
N=2n: \qquad & \mathfrak{T}\boldsymbol{u} = \Big[(4n,0),\underbrace{(0,3n)}_{3},(-4n,0),\underbrace{(0,-n)}_{3},\underbrace{(0,-n-1)}_{2},\underbrace{(0,-2n+1)}_{2}\Big] \\
N=2n+1: \qquad & \mathfrak{T}\boldsymbol{u} = \Big[(10n,-10n),\underbrace{(0,8n)}_{3},(0,7n+1),\underbrace{(-5n,-5n)}_{2}, \\
& \qquad (0,-4n),\underbrace{(0,-2n)}_{3},(0,-n-1)\Big]
\end{aligned}
\tag{3.96}
$$

We can then compute the magnetic quiver for $SU(N)_2 + 2\boldsymbol{AS} + 6\boldsymbol{F}$ using (2.27)

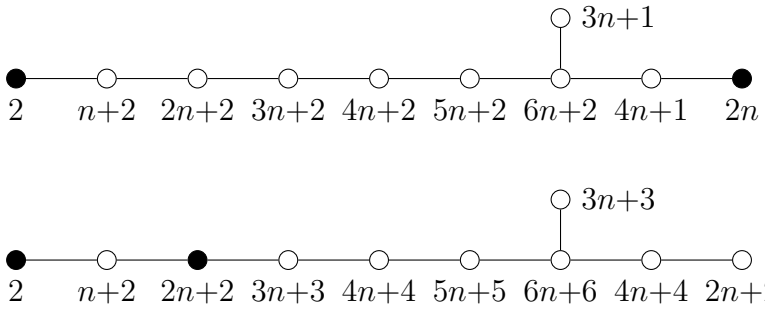

(3.97)

for $N = 2n$ and $N = 2n+1$, respectively. For N even and odd the visible flavour symmetry is $SO(16) \times U(1)$ and $E_7 \times SU(2) \times U(1)$, respectively. Again, the $U(1)$ is known to enhance to $SU(2)$. For low rank, the flavour symmetry is no longer simply laced. As explained after (3.92) this can be seen explicitly in the Hasse diagram and the Hilbert series. Concretely, we find $SO(18) \to SO(19)$ for $N = 4$ and $E_7 \times SU(3) \to E_7 \times G_2$ for $N = 5$.

$SU(2)$ Quivers without SQCD Duals

Most of the $[n_1] - SU(2)^m - [n_2]$ quiver gauge theories have a UV-dual SQCD description. For this reason, their UV brane-webs and associated UV-MQs are captured by the analysis in [73]. However, there is a subset of quiver theories that have a 5d UV fixed point, but that are not UV-dual to any other gauge theory. These are the $[n] - SU(2)^m - [0]_{\theta=0}$ theories, which must be treated separately.

For generic m the top descendant is the $[4]-SU(2)^m-[0]_{\theta=0}$ theory with polygon (drawn for $m=3$)

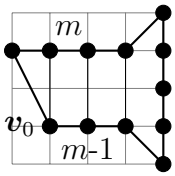

(3.98)

and corresponding vectors given by

$$\boldsymbol{u}=\left[\underbrace{(1,0)}_{m-1},(1,-1),\underbrace{(0,1)}_{4},(-1,-1),\underbrace{(-1,0)}_{m},(1,-2)\right]. \tag{3.99}$$

The non-convexities can be removed by the edge-moves

$$\begin{aligned}\mathfrak{T}&=(\mathfrak{M}_1^+\cdots\mathfrak{M}_{m-2}^+\mathfrak{M}_{m-1}^+)(\mathfrak{M}_{2m+4}^-\cdots\mathfrak{M}_{m+6}^-\mathfrak{M}_{m+5}^-)\,,\\ \mathfrak{T}\boldsymbol{u}&=\left[(m,-m),\underbrace{(0,1)}_{2m+3},(-m-1,-m-1),(1,-2)\right],\end{aligned} \tag{3.100}$$

producing a GTP given by (drawn for $m=3$)

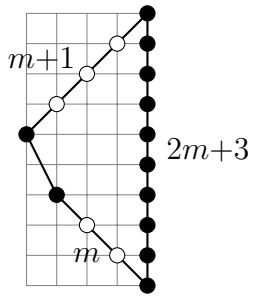

(3.101)

The MQ computed from this GTP, showing the $SO(4m+6)$ flavour symmetry, is

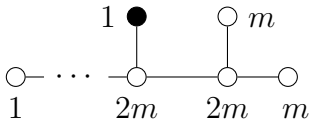

(3.102)

In the case of rank $m=2$, there is an additional quiver theory with no SQCD dual, that descends from the E-string, namely $[5]-SU(2)-SU(2)_0$ with polygon

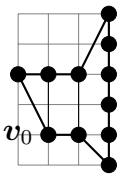

(3.103)

and vectors

$$\boldsymbol{u} = \left[(1,0),(1,-1),\underbrace{(0,1)}_{5},(-1,-2),\underbrace{(-1,0)}_{2},(1,-2)\right] . \tag{3.104}$$

We can remove the non-convexities by

$$\begin{aligned}\mathfrak{T} &= (\mathfrak{M}_4^+\cdots\mathfrak{M}_8^+\mathfrak{M}_9^+)(\mathfrak{M}_3^-\cdots\mathfrak{M}_6^-\mathfrak{M}_7^-)(\mathfrak{M}_6^+\cdots\mathfrak{M}_3^+\mathfrak{M}_2^+)(\mathfrak{M}_3^-\cdots\mathfrak{M}_7^-\mathfrak{M}_8^-)\mathfrak{M}_1^+ ,\\ \mathfrak{T}\boldsymbol{u} &= \left[\underbrace{(2,-2)}_{2},(14,42),(-37,0),\underbrace{(3,-6)}_{6},(1,-2)\right] ,\end{aligned} \tag{3.105}$$

leading to the magnetic quiver

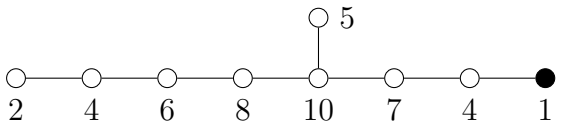

(3.106)

with flavour symmetry E_8.

G_N: Ancestors of T_N

In [142] it was discussed, that there is a submarginal quiver theory given by

$$[N+2]-SU(N-1)_0-\cdots-SU(2)-[2]\,, \tag{3.107}$$

whose strongly coupling limit we denote by G_N. By decoupling two flavour multiplets, one on each side of the quiver, we arrive at the quiver description of T_N [145]. The pGTP of the weakly coupled G_N is given by

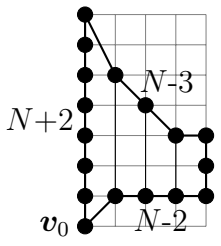

(3.108)

drawn for $N=5$, corresponding to the vectors

$$\boldsymbol{u} = \left[(1,1),\underbrace{(1,0)}_{N-2},\underbrace{(0,1)}_{2},(-1,0),\underbrace{(-1,1)}_{N-3},(-1,2),\underbrace{(0,-1)}_{N+2}\right] \tag{3.109}$$

We can remove the non-convexity by applying

$$\begin{aligned}\mathfrak{T} &= (\mathfrak{M}^+_{N+4}\cdots\mathfrak{M}^+_{2N})(\mathfrak{M}^+_{N+3}\cdots\mathfrak{M}^+_{2N-1})(\mathfrak{M}^+_{N+2}\cdots\mathfrak{M}^+_{2N-2})(\mathfrak{M}^+_{-N-1}\cdots\mathfrak{M}^+_{N-2})\\ &\quad \mathfrak{M}^-_{N-1}\mathfrak{M}^-_{N}\mathfrak{M}^-_{N+1}(\mathfrak{M}^+_{N+2}\cdots\mathfrak{M}^+_{2N-3})\mathfrak{M}^-_{2N-2}\mathfrak{P}^-_1\\ \mathfrak{T}\boldsymbol{u} &= \Bigg[\underbrace{(1,0)}_{N-2},\underbrace{(N-2,0)}_{2},(-2N+4,2N+4),(-3N+5,-3N+5),\\ &\quad (5N-9,-5N+9),(N-2,0),\underbrace{(1,0)}_{2N+2}\Bigg]\end{aligned} \tag{3.110}$$

After applying (2.27) this leads to the magnetic quiver

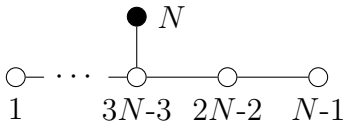

(3.111)

from which we can read off the $SU(3N)$ flavour symmetry.

3.3.2 Decoupling of Matter

5d SCFTs can be related by decoupling matter hypermultiplets. In the context of geometric models realised as singular Calabi-Yau spaces, this is achieved by flop transitions, which take matter curves of normal bundle degree $(-1,-1)$ and flop them out of the compact surfaces, that realise the Cartans of the gauge group. In this way in 5d, one can construct decoupling trees, which start with a marginal theory, which itself UV completes in 6d, and apply decoupling limits [43]. Applied in the context of toric models, these flops have a simple realisation: the $(-1,-1)$ curves are particular curves, which are connections of an internal vertex (compact divisors) to an external one – subject to the normal bundle condition. Here we will extend this to pGTPs and GTPs.

The first important point to note is that the decoupling in the pGTP is straight forward, as we will explain in this section. We can trace the decoupling process

through the monodromy transformations, which map the pGTP to a convex GTP. However, we do not find a simple decoupling rule on GTPs: the main complication is that applying the decoupling to a GTP usually results in a pGTP, i.e. convexity is not retained in this process. We will therefore construct our decoupling trees before applying the monodromies, and then map them to GTPs afterwards.

There are several cases of interest to consider: those that are purely made of black dots, convex or not, and those that do not have such a representation, e.g. the situation with AS matter. We now discuss decoupling in all these instances.

Decoupling Fundamental Matter

Let us first recall briefly the toric situation. In this case a hypermultiplet curve is decoupled by a flop, which contracts the curve and flops it outside of the compact surfaces – in practice this means that one of the external vertices (corresponding to a non-compact divisor) is no longer connected to an internal vertex.

Similarly for the case of pGTPs a fundamental matter multiplet will correspond locally to a curve connecting an internal to an external corner vertex. Decoupling this we follow the same procedure as in the toric diagram (even though of course the geometric analogy does not exist here). Depending on where we perform this flop the mass given to the hypermultiplet is either positive or negative. Depending on this choice, the Chern-Simons level of the resulting theory is shifted by $\pm\frac{1}{2}$, see (2.12). An example is shown on the right of figure 3.1.

Decoupling Anti-Symmetric Matter

We can also decouple the antisymmetric matter. This occurs e.g. for the higher rank E-strings, which then connect to SQCD theories without AS matter. It is particularly interesting to keep track of the Chern-Simons level in the process. Starting e.g. from

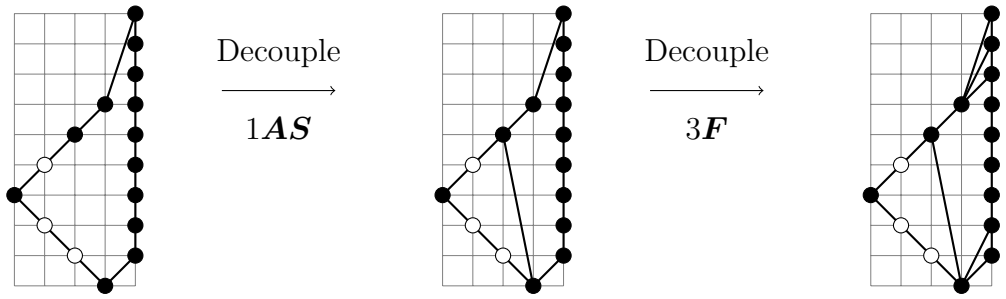

Figure 3.1: Example of decoupling matter. We start from $SU(2n)_n + 1\boldsymbol{AS} + 8\boldsymbol{F}$ and after decoupling an antisymmetric we obtain $SU(2n)_{2n-2} + 8\boldsymbol{F}$. We then decouple three fundamentals (one with positive and two with negative mass) to reach $SU(2n)_{2n-\frac{5}{2}} + 5\boldsymbol{F}$.

the $SU(2n)_0 + 1\mathbf{AS}$, the decoupling of the **AS** hyper is given by (drawn for $n = 4$)

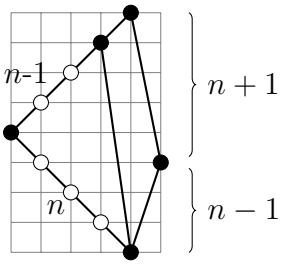

(3.112)

After decoupling, we obtain a polygon corresponding to pure $SU(2n)_{n-2}$. Therefore the **AS** hyper contributes to $(n-2)$ units of Chern-Simons level in $SU(2n)$ theories, in agreement with (2.12). We see that the decoupling is obtained by connecting two extremal vertices, while preserving the gauge theory description. One can also decouple several hypermultiplets at the same time using the same procedure. This is illustrated in figure 3.1.

3.4 Derivation from the Tropics

We now turn to deriving the rules that we propose in the previous sections. The origin is in tropical geometry, or in physics language, the (p, q) 5-brane-webs. The precise relation to tropical geometry is only strictly known in the case when the GTP is toric, and generalising this to non-toric GTPs would be very interesting indeed. These are

dual to the generalised toric polygons, and in this context some progress was recently made in extracting the Higgs branch using magnetic quivers and Hasse diagrams. In this section, we give a precise dictionary between these concepts in the webs, and the data that we introduced in the GTP, and thereby provide a derivation of the rules set out in sections 3.1 and 3.2. We summarise the most important features in table 3.2.

3.4.1 Sub-web Decomposition to Coloured Polygon

The most important identification is between a GTP and brane-web. First, recall that a (p, q) 5-brane-web is made up of connecting (p, q) 5-branes, where we distinguish between external branes (which end on corresponding (p, q) 7-branes) and internal branes (which only connect to other (p, q) 5-branes). Given a web, the corresponding GTP is its dual graph. As such, a set of n_5 (p, q) 5-branes maps to a line in the GTP, that is perpendicular to the branes, i.e. to an edge E_α with the properties

$$L_\alpha = (-q, p)\,, \qquad \lambda_\alpha = n_5\,. \tag{3.113}$$

This holds both for internal and external branes. Note that charge conservation in the web ensures closedness of the GTP. A stack of n_5 external 5-branes, which end on n_7 7-branes gives rise to an external edge in the GTP with $n_7 + 1$ vertices along it, i.e.

$$b_\alpha = n_7 - 1\,. \tag{3.114}$$

Such a web configuration naturally defines a partition of n_5 into the number of 5-branes ending on each 7-brane, which is exactly given by the $\mu_{\alpha,x}$. Note that from the L_α and $\mu_{\alpha,x}$ we can infer the positions of the vertices $\boldsymbol{v}_i$, up to equivalent configurations, as follows. Choosing an initial position for $\boldsymbol{v}^{\text{ex}}_{\alpha,0}$ we take any reordered set of $\mu_{\alpha,x}$, which we call $\mu_{\alpha,i}$. All such reorderings are equivalent. The positions of the

black vertices are then defined inductively by

$$\boldsymbol{v}_{\alpha,i+1} = \boldsymbol{v}_{\alpha,i} + \mu_{\alpha,i+1} L_\alpha \,. \tag{3.115}$$

Furthermore, for neighbouring edges E_α and $E_{\alpha+1}$ we have

$$\partial E_\alpha \cap \partial E_{\alpha+1} = \boldsymbol{v}^{\text{ex}}_{\alpha,b_\alpha+1} = \boldsymbol{v}^{\text{ex}}_{\alpha+1,0} \,. \tag{3.116}$$

The brane-web thus induces the vertices V_b of the corresponding GTP.

Monodromy-preserving edge-moves in the brane-web were reviewed in section 2.2. It is straightforward to translate the rules in (2.20) and (2.21) into GTP language to obtain (3.26). Similarly, we can think of pruning. We can take a (p, q) 7-brane in the brane-web, on which n_5 5-branes end, and push it through the entire web, turning it into a $(-p, -q)$ 7-brane. This operation needs to preserve both the total monodromy and charge conservation. The first condition is ensured by changing the branch cut of each of the passed 7-branes. The second condition fixes the number of $(-p, -q)$ 5-branes ending on the moved $(-p, -q)$ 7-brane. This can be done in either direction around the web. By explicit computation we arrive at the results in section 3.1.2.

To extract the magnetic quiver, the brane-web is divided into sub-webs that are themselves consistent brane-webs. There can be multiple (maximal) divisions into sub-webs, which are identified with different cones of the Higgs branch. Here, we will only consider a single division. We distinguish between two kinds of sub-webs, which are those that are associated to colours in the GTP, and those that are not but which give rise to tails in the tropical quiver.

For now we will focus on the first class of sub-webs W^c, which contain 5-branes that end on distinct types of 7-branes. Each W^c is mapped to a coloured sub-polygon S^c, as specified in definition 1. An edge segment is part of S^c if the corresponding 5-brane is contained in W^c, defining the partition of λ_α into λ^c_α for each edge. The refined Minkowski sum of two sub-polygons $S^{c_1} \oplus S^{c_2}$ is understood as combining two sub-webs W^{c_1} and W^{c_2}, where we identify the 7-branes involved in the W^c.

Definition 1 contains certain conditions for a colouring of a GTP to be valid, which have their origin in the brane-web:

1. Each sub-web W^c gives rise to a sub-polygon S^c because charge conservation in the brane-web ensures closedness in the GTP.

2. A sub-web W^c has a multiplicity, i.e. it consists of m^c identical minimal webs W^c_{min}.

3. The s-rule states that the number of D5-branes that may connect a single D7-brane and a stack of NS5-branes is less or equal to the number of NS5-branes in the stack. Let us consider a minimal web W^c_{min}. It obeys the s-rule if there is a full resolution such that each intersection obeys the s-rule locally. This idea was advanced in [61] from which the introduction of tiles follows. An $SL(2,\mathbb{Z})$-invariant formulation has been discussed in [1, 141] and is given by (2.22)

A comment on internal edges Let us briefly comment on the case where a GTP has internal edges, which is the subject of section 3.2.4. This corresponds to a brane-web containing internal 5-branes, i.e. 5-branes that connect two 5-brane junctions (rather than ending on a 7-brane). Such a set of internal 5-branes necessarily pertains to a collection of sub-webs $\{W^c\}$. There is no obstruction to taking the length of the internal 5-branes to be large, i.e. the webs connected by the internal 5-branes are independent of each other, apart from a matching condition along the internal 5-branes, and must obey the s-rule locally. This is the reason the s-rule should be applied separately to each S^c_A, as detailed in section 3.2.4.

3.4.2 Magnetic Quivers

What we have seen so far is that a coloured GTP contains the same data as the sub-web decomposition of the dual web. We will now argue for the derivation of the

tropical quiver from the GTP data, as explained in section 3.2.3, starting from the brane-web.

Each sub-web W^c corresponds to a node in the magnetic quiver, labelled by the multiplicity m^c of the sub-web. The sub-webs are mapped to colourings, or coloured subpolygons S^c, in the GTP. To each colour we thus associate a node in the tropical quiver with label $m^c = \mathrm{gcd}_\alpha(\lambda^c_\alpha)$.

The intersections between the colour nodes are computed as follows. Consider the colour-subdivision of the GTP. The area $A^{c_1c_2}$ corresponds to the stable intersection (SI) between the sub-webs W^{c_1} and W^{c_2} in tropical geometry [73]. Recall, that the SI is defined by infinitesimally displacing the two minimal sub-webs and computing the intersection

$$\mathrm{SI} = \sum \left| \det \begin{pmatrix} p^{c_1} & q^{c_1} \\ p^{c_2} & q^{c_2} \end{pmatrix} \right| , \tag{3.117}$$

where the sum goes over all intersections and the (p^c, q^c) are normalised by a factor of m^c. Now consider the parallelograms $G^{c_1c_2}$ in the colour sub-divided polygon, with the two sides characterised by $\lambda^{c_1}_\alpha L_\alpha$ and $\lambda^{c_2}_\beta L_\beta$. The Euclidean area of $G^{c_1c_2}$ is then given by

$$\mathrm{Area}(G^{c_1c_2}) = \lambda^{c_1}_\alpha \lambda^{c_2}_\beta \left|\det\left(L_\alpha, L_\beta\right)\right| = \lambda^{c_1}_\alpha \lambda^{c_2}_\beta \left| \det \begin{pmatrix} q^{c_1} & -p^{c_1} \\ q^{c_2} & -p^{c_2} \end{pmatrix} \right| , \tag{3.118}$$

because of (3.113). However, here the (p^c, q^c) are normalised to be coprime, so, by the inclusion of the λ^c, this agrees with the SI in (3.117).

There is an additional contribution to the intersection between two sub-webs, W^{c_1} and W^{c_2}, which is the effective number of 7-branes on which they both end. To see this contribution in the GTP consider a single edge E_α, corresponding to a tail of (p, q) 5- and 7-branes, all of the same p and q, in the brane-web. Recall that the number of 7-branes that an edge E_α gives rise to is $n_7 = b_\alpha + 1$, and the intermediate segments (which are stacks of 5-branes in the web) are labelled by x. Consider the 7-brane

between segments $(x-1)$ and x. The number of 5-branes in colour c on either side differ by $\mu^c_{\alpha,x}$, by definition. The sum over all 7-branes yields the second contribution to the intersection between W^{c_1} and W^{c_2}. However, we need to divide by the product of the multiplicities of the two sub-webs to obtain the effective intersection in the magnetic quiver, given by $-\frac{1}{m^{c_1}m^{c_2}}\sum_{x=1}^{b_\alpha}\mu^{c_1}_{\alpha,x}\mu^{c_2}_{\alpha,x}$. Together with the SI contribution (3.118) this gives the number of edges (3.52) between nodes in the tropical quiver associated to the two colours c_1 and c_2.

Furthermore, we can determine the number of 5-branes in a tail, which do not belong to any of the W^c. These sub-webs $W_{\alpha,x}$, spanning the segment x between 7-branes in a tail labelled by α, do not appear as sub-polygons in the GTP. Nonetheless, they do give rise to additional nodes in the magnetic quiver, and their presence can be detected in the GTP. Their multiplicities $m_{\alpha,x}$ are given by the total number of 5-branes along a segment x in the tail α, minus the number of 5-branes in that segment that belong to a W^c. The former is the total number of 5-branes protruding from the internal web in this direction, λ_α, minus the number of 5-branes that have ended on a 7-brane further up the tail, $\sum_{y=1}^{x}\mu_{\alpha,y}$. The computation of the latter is the same but restricted to a colouring c.[6] Hence, the multiplicities of the sub-webs $W_{\alpha,x}$, in terms of GTP data, combine to (3.55). These sub-webs give rise to the additional tail nodes in the magnetic quiver with labels $m_{\alpha,x}$. They are connected to their nearest neighbours by a single edge, since the only contribution to the intersection between $W_{\alpha,x}$ and $W_{\alpha,x+1}$ comes from ending on opposite sides of the same 7-brane.

Finally, we determine the number of edges between colour nodes and tail nodes in the tropical quiver. Consider a tail segment x made up of $m_{\alpha,x}$ 5-branes between two 7-branes. The number of 5-branes in colour c ending on these two 7-branes is given by $\mu^c_{\alpha,x}$ and $\mu^c_{\alpha,x+1}$ respectively. Each time the number of c-coloured 5-branes ending on the 7-branes on either side of a segment differs, the corresponding tail

[6] By some abuse of notation we say $\mu^c_{\alpha,y}=0$ if y is larger than the length of the partition $\mu^c_{\alpha,x}$.

node is connected to the c-colour node. Thus, the intersection, after accounting for multiplicity, is given by (3.57).

3.4.3 Hasse Diagrams

Now, let us turn to the computation of the Hasse diagrams in section 3.2.4. Recall that given a magnetic quiver of a theory, a transition in the Hasse diagram corresponds to the quiver subtraction of a symplectic leaf. Here, those are either the affine Dynkin diagram of an ADE Lie algebra $\mathfrak{g}$ corresponding to the magnetic quiver of the closure of a minimal nilpotent orbit, or a Kleinian singularity – these are summarised in table 2.3. It was argued in [75, 76] that this process can be translated into the language of brane-webs as follows. Consider a brane-web W_P, corresponding to a theory with some original magnetic quiver. A quiver subtraction by a symplectic leaf [7] $\mathfrak{g}$ corresponds to turning on certain Coulomb branch parameters of the theory, i.e. the introduction of internal 5-branes in the brane-web, resulting in a new brane-web W_Q. The Coulomb branch parameters must be turned on in such a way that, in a maximal sub-division of W_Q, all the newly introduced 5-branes belong to the same sub-web W_{Δ_ν}. At the origin of its extended Coulomb branch (we could call this brane-web W_Δ in parallel with the notation in section 3.2.4), the magnetic quiver of this sub-web is the affine Dynkin diagram of $\mathfrak{g}$. By going into the Coulomb branch of this sub-theory, the associated Higgs branch reduces as $\mathfrak{g} \to \mathfrak{u}(1)$. In the magnetic quiver this corresponds to a quiver subtraction with subsequent rebalancing with a $\mathfrak{u}(1)$ node.

Now, we can further translate this into the language of GTPs. Turning on Coulomb branch parameters corresponds to a partial resolution of the GTP P, i.e. the introduction of dual internal edges E_β of length ν_β, which results in a new GTP Q. The internal 5-branes forming the sub-web W_{Δ_ν}, corresponding to a colour-subpolygon Δ_ν in Q, which includes the internal edges. To describe the Higgs branch

[7] We assume for notational simplicity that the singularity is of ADE type, the logic holds in the Kleinian case.

(p,q) 5-Brane-web/Tropics	Generalised toric polygon
n_5 coincident (p,q) 5-branes	Edge E_α with $L_\alpha = (-q,p)$ and $\lambda_\alpha = n_5$
External and internal 5-branes	External edges E^∂ and internal edges E^{in}
n_5 5-branes subsequently ending on n_7 7-branes	Partition $\mu_{\alpha,x}$ of length $b_\alpha = n_7 - 1$
Compact and non-compact faces	Black vertices V_b
Division into sub-webs	Colouring
Internal sub-web W^c	Coloured subdiagram S^c
Partition of coincident 5-branes into sub-webs	$\lambda_\alpha = \sum \lambda_\alpha^c$
Multiplicity of W^c	m^c
s-rule, # branes of W^c ending on each 7-brane	$\mu_{\alpha,x}^c$
Stable intersection	Mixed volume $MV(S^{c_1}, S^{c_2})$
Multiplicities of sub-webs between 7-branes	$m_{\alpha,x}$
5-brane displacement that is quiver subtraction	Transition $P \xrightarrow{\Delta} Q$
Coulomb branch parameters	Partial resolution ν_β

Table 3.2: Dictionary between brane-webs/tropics and coloured GTPs: sub-webs, magnetic quivers and Hasse diagrams.

at a generic point on the extended Coulomb branch, the magnetic quiver of Δ_ν should be a single $U(1)$ node. However, at the origin of the extended Coulomb branch, i.e. in the absence of the E_β where the GTP is Δ, the magnetic quiver is the affine Dynkin diagram of $\mathfrak{g}$.

Part II

Three Dimensions

Chapter 4

Background in Three Dimensions

4.1 $T[M_3]$ and the 3d-3d Correspondence

At the centre of this second part is the idea of reducing the 6d $\mathcal{N} = (2, 0)$ theory of Lie type $\mathfrak{g}$ on a three-cycle M_3 to obtain a three-dimensional gauge theory denoted by $T[M_3, \mathfrak{g}]$. We are interested in preserving supersymmetry, which is achieved by performing a topological twist. This corresponds to turning on a background value for the $Sp(4)_R$ R-symmetry of the 6d (2,0) theory, to cancel the non-trivial spin connection of M_3.

We will usually restrict to $\mathfrak{g} = A_{N-1}$ for which there is a geometric interpretation in terms of N coincident M5-branes wrapping a supersymmetric three-cycle inside M-theory. The 6d Lorentz symmetry is broken to

$$SO(1,5)_L \to SO(1,2)_L \times \underline{SO(3)_M}\,, \tag{4.1}$$

where $SO(3)_M$ is the holonomy of M_3. A general M_3 does not admit any covariantly constant spinors and supersymmetry is not preserved in 3d. To perform the topological twist we identify

$$SU(2)_{\text{twist}} = \text{diag}(SO(3)_M, SU(2))\,, \qquad SU(2) \subset Sp(4)_R\,, \tag{4.2}$$

such that there are covariantly constant spinors under the twisted holonomy, i.e. singlets under $SU(2)_{\text{twist}}$. There are two choices for $SU(2)$ in (4.2), which correspond to the two different calibrated three-cycles, see table 1.2.

1. First, M_3 can be a special Lagrangian inside a CY_3. For our purposes it suffices to consider the local model

$$\text{CY}_3 \cong T^*M_3, \tag{4.3}$$

i.e. the normal bundle of M_3 agrees with its cotangent bundle. The R-symmetry splits as

$$Sp(4)_R \to \underline{SU(2)_R} \times U(1)_R\,, \tag{4.4}$$

where the $SU(2)_R$ represents the fibres of T^*M_3 and is naturally identified with $SO(3)_M$ as in (4.2). This topological twist

$$\begin{gathered} SO(1,5)_L \times Sp(4)_R \to SO(1,2)_L \times SU(2)_{\text{twist}} \times U(1)_R \\ (\mathbf{4},\mathbf{4}) \mapsto \underline{(\mathbf{2},\mathbf{1})_{\pm\frac{1}{2}}} \oplus (\mathbf{2},\mathbf{3})_{\pm\frac{1}{2}} \end{gathered} \tag{4.5}$$

preserves four supercharges, transforming under the $U(1)_R$ R-symmetry, which corresponds to 3d $\mathcal{N}=2$. This twist will be relevant in chapter 5.

2. The second choice is for M_3 to be an associative three-cycle inside a seven-manifold X_7 of holonomy G_2. The local model is

$$(V \otimes \mathbb{S}) \hookrightarrow X_7 \to M_3\,, \tag{4.6}$$

where $\mathbb{S}$ is the spin bundle and V is a rank two $SU(2)$ bundle. Some important properties of G_2-manifolds are collected in appendix B.5. The R-symmetry splits as

$$Sp(4)_R \to SU(2)_\ell \times \underline{SU(2)_r}\,, \tag{4.7}$$

where the two copies of $SU(2)$ correspond to the two parts of the normal bundle

in (4.6). Under this twist

$$\begin{aligned} SO(1,5)_L \times Sp(4)_R &\to SO(1,2)_L \times SU(2)_{\text{twist}} \times SU(2)_\ell \\ (\mathbf{4},\mathbf{4}) &\mapsto \underline{(\mathbf{2},\mathbf{1},\mathbf{1})} \oplus (\mathbf{2},\mathbf{3},\mathbf{1}) \oplus (\mathbf{2},\mathbf{2},\mathbf{2}) \end{aligned} \tag{4.8}$$

there are two supercharges invariant under $SU(2)_{\text{twist}}$, corresponding to 3d $\mathcal{N} = 1$. The $SU(2)_\ell$, associated to V in (4.6), remains as a global symmetry. The resulting theory is denoted by $T_{\mathcal{N}=1}[M_3, \mathfrak{g}]$ and its dependence on the geometry (4.6) is discussed in chapter 6.

There is no Lagrangian description of the 6d (2,0) theory for general $\mathfrak{g}$. This implies that it is difficult to explicitly determine the theories $T[M_3, \mathfrak{g}]$. The only exception is $\mathfrak{g} = \mathfrak{u}(1)$, where the 6d (2,0) theory consists of a free tensor multiplet. Nevertheless, we can extract information about the $T[M_3, \mathfrak{g}]$ by computing physical observables, i.e. partition functions on a manifold W_3. Geometrically, this corresponds to M5-branes on

$$M_6 = M_3 \times W_3 \,. \tag{4.9}$$

Since the 6d (2,0) theory is superconformal, we can reverse the order of reduction, i.e. first reduce along W_3, together with a topological twist along M_3. This yields a topological field theory on M_3 which depends on the choice of W_3. The 3d-3d correspondence then states

$$\mathcal{Z}_{W_3}(T[M_3, \mathfrak{g}]) = Z_{\text{TFT},\mathfrak{g}}(M_3) \,, \tag{4.10}$$

i.e. the W_3-partition function of $T[M_3]$ agrees with the M_3-partition function of the corresponding TFT. Here, we will primarily be concerned with $W_3 = T^3$, in which case the observable is the Witten index [146]

$$\mathcal{Z}_{T^3} = \text{Tr}(-1)^{\text{F}} \,, \tag{4.11}$$

where F is the fermion number and the trace goes over the vacua of the theory. Another choice for W_3 is the three-sphere S^3, or more general the Lens space $L(k,1)$,

which we primarily discuss in section 6.3. For this choices the relevant TFTs are summarised in table 4.1. Filling the table for $\mathcal{N} = 1$ is an essential part of chapter 6.

	$W_3 = T^3$	$W_3 = L(k, 1)$
$\mathcal{N} = 2$	cx. BF-model	cx. Chern-Simons at level k
$\mathcal{N} = 1$	BFH-model	Chern-Simons-Dirac at level k

Table 4.1: TFTs obtained from 6d (2,0) on W_3 with a topological twist on M_3

4.2 Higher-Form Symmetries

In this section we briefly review higher-form, or q-form, symmetries of QFTs in general [111] and in 3d gauge theories in particular.

4.2.1 Higher-Form Symmetries in QFTs

A q-form symmetry with group Γ in a d-dimensional QFT can be described by a set of topological charge operators, $U_\gamma[\sigma]$, which are labelled by an element $\gamma \in \Gamma$ and a $(d - q - 1)$-dimensional submanifold σ in spacetime, on which the operator is supported. The fusion of two charge operators obeys the group law, i.e.,

$$U_\gamma[\sigma]\ U_{\gamma'}[\sigma] \cong U_{\gamma\gamma'}[\sigma]\,. \tag{4.12}$$

In addition, the operator may have non-trivial commutation relations with a physical q-dimensional extended operator $\mathcal{O}$, which we then say is charged under the q-form symmetry. For example, if we work in the Hilbert space picture on a spacetime $M_{d-1} \times \mathbb{R}$, we have the commutation relations

$$\left[\ U_\gamma[\sigma]\ ,\ \mathcal{O}[\rho]\ \right]\ =\ R_{\mathcal{O}}(\gamma)^{\rho\cap\sigma} \cdot \mathcal{O}[\rho]\,, \tag{4.13}$$

where $R_{\mathcal{O}}$ is the representation of Γ in which $\mathcal{O}$ transforms, and $\rho\cap\sigma$ is the intersection number of ρ and σ in M_{d-1}. Higher-form symmetries are a generalisation of ordinary

global symmetries, which correspond to the case $q = 0$, where the charged operators are local. For $q > 0$, it can be shown that Γ must be abelian.

When $q = \frac{d-1}{2}$, the charge operators have the same dimension as the charged operators, and so they may themselves be charged under the symmetry. When this happens we say that the symmetry has an 't Hooft anomaly, which is an obstruction to gauging it.[1] When the symmetry is non-anomalous, the expectation value of a set of charge operators depends only on the cycle $\widetilde{\omega} \in H_{d-q-1}(M_d, \Gamma)$ determined by the choice of σ and γ of the operators. By Poincaré duality, this is the same as a choice of cocycle, $\omega \in H^{q+1}(M_d, \Gamma)$, and we may equivalently interpret this as computing the partition function in the presence of a background $(q+1)$-form gauge field, labelled by ω, and define

$$\mathcal{Z}_{M_d}[\omega] = \langle U[\widetilde{\omega}] \rangle_{M_d} \,. \tag{4.14}$$

This gives a refinement of the ordinary partition function, which keeps track of the response of the system to sources for the higher-form symmetry.

When a higher-form symmetry is non-anomalous, we may gauge it to obtain a new theory. This means we promote the background $(q+1)$-form gauge field to be dynamical, and so the partition function of the gauged theory is given by summing over all such background gauge fields. It is natural to also introduce a coupling to a new background gauge field, and define

$$\widehat{\mathcal{Z}}_{M_d}[\widehat{\omega}] = \frac{1}{|H^{q+1}(M_d, \Gamma)|^{1/2}} \sum_{\omega \in H^{q+1}(M_d, \Gamma)} e^{i \int_{M_d} \omega \cup \widehat{\omega}} \mathcal{Z}[\omega] \,, \tag{4.15}$$

where $\widehat{\omega} \in H^{d-q-1}(M_d, \widehat{\Gamma})$, $\widehat{\Gamma}$ is the Pontryagin dual group,

$$\widehat{\Gamma} = \mathrm{Hom}(\Gamma, U(1)) \,, \tag{4.16}$$

and $e^{i \int_{M_d} \omega \cup \widehat{\omega}} \in U(1)$ is the natural pairing. This may be interpreted as the partition function of a theory with a $(d-q-2)$-form symmetry with group $\widehat{\Gamma}$, which we call

[1] This follows because the charge operators should be trivial in the gauged theory, but this is not compatible with the non-trivial commutation relations in the presence of an anomaly.

the dual symmetry. Repeating this gauging operation brings us back to the original theory. More generally, we may gauge a subgroup of Γ or include an additional local action for the background gauge fields, which leads to more general versions of the theory.

An important set of examples that will arise below are the electric and magnetic symmetries of a gauge theory. Given a theory with gauge group G with centre Z_G, if a subgroup Γ of Z_G does not act on the charged matter of the theory, the theory admits a 1-form Γ symmetry, called the electric symmetry. The charged operators are Wilson loop operators, which transform according to the action of Γ on the representation of the Wilson loop. The partition function in the background of a 2-form gauge field is given by

$$\mathcal{Z}_G[\omega] = \sum_{P|w_2(P)=\omega} \mathcal{Z}_P \,, \qquad \omega \in H^2(M_d, \Gamma) \,, \tag{4.17}$$

where $\mathcal{Z}_P$ is the contribution to the partition function from a principal G/Γ-bundle P over spacetime, and we sum over all principal bundles with a specified value for their second Stiefel-Whitney class, $w_2(P) \in H^2(M_d, \Gamma)$, which measures the obstruction to lifting a G/Γ-bundle to a G-bundle. Then the G/Γ theory is simply given by gauging this symmetry, i.e. summing over all G/Γ-bundles as in (4.15). The G/Γ theory naturally comes with a $(d-3)$-form $\widehat{\Gamma}$ symmetry which we call the magnetic symmetry. The charged $(d-3)$-dimensional operators are the 't Hooft loops.

4.2.2 1-Form Symmetries in 3d Gauge Theories

Let us now review some general features of 1-form electric symmetries in 3d gauge theories, which will arise in the study of $T[M_3]$.

Recall that $d = 3$ is the case where a 1-form symmetry may have an 't Hooft anomaly, and such anomalies turn out to arise from Chern-Simons terms for the gauge groups. To describe these anomalies more carefully, we follow [147]. Consider a 3d gauge theory with gauge and flavour groups, G_g and G_f, which we take to be

simply connected. However, there may in general be some subgroup Γ of the centre of these groups which does not act on the matter content. Then in principle, we might try to couple the system to a $(G_g \times G_f)/\Gamma$ bundle. However, anomalies may cause this observable to be ill-defined.

To see this, let us exhibit the 3d spacetime as the boundary of a 4d manifold, and extend the gauge fields into the bulk. Then the 3d theory may include Chern-Simons terms for the gauge and flavour symmetries, which we assume are properly quantised for $G_g \times G_f$ connections. However, they may not be well-defined for $(G_g \times G_f)/\Gamma$ connections. To cure this, we include appropriate 4d topological terms, such that the combined 3d-4d system is well-defined. Thus we obtain an action

$$S_{\text{anom}} = \int_{M_4} c(A)\,, \tag{4.18}$$

where c is some characteristic class of a 4d $(G_g \times G_f)/\Gamma$ gauge bundle. We refer to this as the anomaly polynomial. If we consider two different ways of extending the 3d system into the 4d bulk, the difference is given by the integral of the anomaly polynomial over a closed four-manifold. This characterises the extent to which the 3d partition function is not uniquely defined. While this is not necessarily a problem for the flavour symmetries, the theory must be well-defined with respect to the gauge connection, and so we demand that the anomaly polynomial is trivial for any allowed choice of gauge bundles.

Below, we will be mostly interested in theories with $SU(2)^n$ gauge and $SU(2)^m$ flavour symmetry. The centre is ${\mathbb{Z}_2}^n \oplus {\mathbb{Z}_2}^m$, and let us suppose that it acts trivially on the matter. Let us further include Chern-Simons levels k_i and K_j for the gauge and flavour fields, respectively. The necessary anomaly polynomial is

$$c(A) = \pi\left(\sum_{i=1}^{n} k_i \frac{\mathcal{P}(w_2^{(i)})}{2} + \sum_{j=1}^{m} K_j \frac{\mathcal{P}(w_2^{(j)})}{2} \right). \tag{4.19}$$

Here w_2 is the second Stiefel-Whitney class, valued in $H^2(M_4, \mathbb{Z}_2)$, and

$$\mathcal{P}: \quad H^2(M_4, \mathbb{Z}_2) \to H^4(M_4, \mathbb{Z}_4) \tag{4.20}$$

is the Pontryagin square operation, which satisfies $\mathcal{P}(w) = w^2 \pmod 2$. On a spin manifold, where the intersection form is even, $\mathcal{P}/2$ is well-defined as an element of $H^4(M_4, \mathbb{Z}_2)$.

For example, consider the T_2 trinion theory, given by an $\mathcal{N} = 2$ chiral multiplet transforming in the trifundamental representation of an $SU(2)^3$ flavour symmetry. In order to act trivially on the matter the Stiefel-Whitney classes of the three groups must satisfy

$$w_2^{(1)} + w_2^{(2)} + w_2^{(3)} = 0\,. \tag{4.21}$$

Now we gauge one of the $SU(2)$ symmetries, say the third, with a level k CS term, and we also include level $K_{1,2}$ CS terms for the remaining flavour symmetries. After imposing (4.21) the anomaly polynomial in this case is

$$c(A) = \pi\left((k+K_1)\frac{\mathcal{P}(w_2^{(1)})}{2} + (k+K_2)\frac{\mathcal{P}(w_2^{(2)})}{2} - k\; w_2^{(1)} \cup w_2^{(2)}\right), \tag{4.22}$$

independent of the dynamical gauge field.

In general, given a theory with ${\mathbb{Z}_N}^n$ 1-form symmetry, we may encode the anomalies in a symmetric $n \times n$ matrix, $\mathcal{A}_{ij}$, with entries valued in $\mathbb{Z}_N$, such that the anomaly polynomial is given by

$$S_{\text{anom}} = \frac{2\pi}{N}\int_{M_4}\left(\sum_{i=1}^{n}\mathcal{A}_{ii}\frac{\mathcal{P}(w_2^i)}{2} + \sum_{i<j}\mathcal{A}_{ij}w_2^i \cup w_2^j\right). \tag{4.23}$$

Then one finds that non-anomalous symmetries are labelled by a vector $\gamma = (\gamma_1, ..., \gamma_n) \in {\mathbb{Z}_N}^n$ such that

$$\gamma\mathcal{A}\gamma = 0 \pmod N\,. \tag{4.24}$$

More generally, for a subgroup Λ of the set of 1-form symmetries to be non-anomalous, we impose also that all mixed anomalies vanish, i.e.,

$$\gamma\mathcal{A}\gamma' = 0 \pmod N, \quad \gamma, \gamma' \in \Lambda\,. \tag{4.25}$$

Note that when $\mathcal{A}$ is trivial, every subgroup is non-anomalous. In this case we refer to the group Γ as being "anomaly-free."

Chapter 5

Higher-Form Symmetries, Bethe Vacua and the 3d-3d Correspondence

In this chapter we are concerned with the 3d-3d correspondence for $\mathcal{N} = 2$ theories, relating the Witten index of the theory $T[M_3]$ to complex flat connections on M_3. More precisely, we study the sensitivity of the correspondence to the higher-form symmetry of $T[M_3]$. We unveil that the theory $T[M_3]$ is not fully specified by the manifold M_3, but requires additional topological data, which translates into the residual 0- and 1-form symmetry of the 3d theory. We therefore propose a refined definition of the theories, specifying this data

$$T[M_3, \mathfrak{g}, H]\,, \qquad H \leq \widehat{\Upsilon} \equiv H^2(M_3, Z_{\widetilde{G}})\,, \tag{5.1}$$

where $Z_{\widetilde{G}}$ is the centre of the simply connected group $\widetilde{G}$ with Lie algebra $\mathfrak{g}$. One of the main interests of this chapter is to develop a thorough definition of the theories $T[M_3, \mathfrak{g}, H]$ in (5.1) for M_3 a Seifert manifold.

In the process we point out new features related to the global structure of the gauge groups and higher-form symmetries of these theories, as well as the explicit

computation of the Witten index. The approach we take in sections 5.1 and 5.2 is as follows:

1. The Seifert manifolds we consider (which have Betti number $b_1 = 0$) can be cut along disjoint embedded tori into degree k circle fibre bundles over S^2s with boundary. This allows us to assign to each Seifert manifold M_3 a graph Ω as follows. Each fibration is represented by a vertex, dressed by the degree k. These are connected by edges representing gluing along boundary tori by S-transformations, which exchange the cycles of the boundary tori. From the graph we define theories $\widehat{T}[\Omega, G]$ using the building blocks

$$\text{vertex}_k: \quad \mathcal{N}=2 \; G_k \text{ CS theory} \qquad\qquad \text{edge}: \quad T(G) \; S\text{-wall theory}\,, \tag{5.2}$$

   where $T(G)$ was defined in [23]. In addition to (5.2) we need to couple the theory to $\mathcal{N}=2$ adjoint scalar multiplets.

2. The graph Ω representing M_3 is not unique. Instead, it represents a four-manifold M_4 with boundary M_3. There are various operations that leave M_3 topologically invariant but change Ω. We can check that $\widehat{T}[\Omega, G]$ is only invariant under these operations up to decoupled topological sectors [148]. Inspired by [149], we propose that we can decouple these topological factors on which the physical 1-form symmetry acts trivially.

3. We denote the theory obtained in this way by $T[M_3, \mathfrak{g}, 1]$. It has no discrete 0-form symmetry and a global anomaly-free 1-form symmetry with group $H^1(M_3, Z_{\widetilde{G}})$. Any of its subgroups can be gauged such that the new 0-form symmetry is H, giving a theory we denote by $T[M_3, \mathfrak{g}, H]$.

Having established a Lagrangian description for $T[M_3, \mathfrak{g}, H]$, we can exploit the Bethe/gauge correspondence to compute the Witten index. The twisted superpotential of $\widehat{T}[\Omega, G]$ is obtained from its quiver description and leads to the Bethe

Theory	Definition
$\widehat{T}[\Omega, G]$	Quiver theory for Seifert manifold M_3 associated to a graph Ω. If $G = G^\vee$, then $\widehat{T}[\Omega, G] = T[M_3, G]$.
$T[M_3, \mathfrak{g}]$	Theory obtained by decoupling topological sectors from $\widehat{T}[\Omega, G]$ Independent of four-manifold.
$T[M_3, \mathfrak{g}, H]$	$T[M_3, \mathfrak{g}]$ with a gauged 1-form symmetry, H is resulting 0-form symmetry $T[M_3, \mathfrak{g}] = T[M_3, \mathfrak{g}, 1]$

Table 5.1: Summary of the theories defined in this chapter

equations, whose solutions determine the "Bethe vacua", forming a special subsector in the Hilbert space of $\widehat{T}[\Omega, G]$ on T^2. With this method we can in principle compute this Hilbert space for any choice of Ω and G. In section 5.3 we do this explicitly for $G = SU(2)$ and various Seifert manifolds.

As mentioned above, this Hilbert space is unphysical as it depends explicitly on the choice of graph, Ω. However, we outline a procedure to decouple the topological sector by projecting out certain vacua. To do this, we must understand how the 1-form symmetry of the theory acts on the space of Bethe vacua. We characterise this action in detail, and in particular derive the factorisation of the Hilbert space into two decoupled sectors, one physical and one purely topological, such that the Hilbert space of the $T[M_3, \mathfrak{g}]$ is given by the former. This yields the Witten index of $T[M_3, \mathfrak{g}]$. We then further refine the Hilbert space into eigenspaces under the action of the 1-form symmetry of $T[M_3, \mathfrak{g}]$, and we refer to the trace in the various sectors as the refined Witten index. We can then compute the Witten index for all choices of H in $T[M_3, \mathfrak{g}, H]$. For some simple examples we can confirm that this observable detects the choice of H and so the theories in (5.1) are physically distinct.

The choice of H also affects the topological field theory side of the 3d-3d correspondence. In our setup, we expect that the Witten index of $T[M_3, \mathfrak{g}, H]$ counts complex flat connections on M_3. As described in section 5.4, we find that the refined Witten index of $T[M_3, \mathfrak{g}]$ in a sector of fixed 1-form symmetry charges maps to the

number of flat $\widetilde{G}^{\mathbb{C}}$ connections on M_3 with prescribed values for their second Stiefel-Whitney class and behaviour under large gauge transformations. We confirm this refined correspondence in various examples.

5.1 $\widehat{T}[\Omega, G]$ from Graphs

In this section we begin our study of the theories $T[M_3]$ obtained by compactification of the 6d $(2,0)$ theory on a Seifert manifold M_3. We introduce the quiver description of the resulting 3d theories, and its dualities. In particular, as we describe below, we may associate a graph to a decomposition of a three dimensional Seifert manifold along disjoint embedded tori, and this graph directly determines the quiver gauge theory.

We first treat the global structure of the gauge group in a naive way by taking the gauge group to be G for every node in the quiver gauge theories below. As we will see, this prescription means that the quiver theories we associate to the graph Ω are not, in general, the theories $T[M_3]$ obtained by compactification, but rather some closely related theories we define as

$$\widehat{T}[\Omega, G]\,. \tag{5.3}$$

When G is equal to its Langlands dual $G^\vee$ (i.e., the lattice of weights of G is self-dual), then we may define

$$T[M_3, G] = \widehat{T}[\Omega, G]\,, \tag{5.4}$$

where Ω is any graph decomposition of M_3. However, in general, two graphs, Ω and Ω', which give rise to the same three-manifold do not give the same 3d theory. In section 5.2 we will describe how to pass from the theory $\widehat{T}[\Omega, G]$ to the more physical $T[M_3, \mathfrak{g}, H]$ theories, which involves a more careful treatment of the global structure of the gauge groups.

5.1.1 Graphs for Seifert Manifolds

The class of geometries M_3 that we will consider here are Seifert manifolds (see e.g. [150]), which are circle bundles over a Riemann surface $\Sigma_{g,r}$ of genus g with r marked points

$$\pi : \; S^1 \hookrightarrow M_3 \to \Sigma_{g,r} \,. \tag{5.5}$$

The fibration is specified by the Seifert data

$$M_3 \cong [d; g; (p_i, q_i)] \,, \quad i = 1, \ldots, r \,, \tag{5.6}$$

where $(d, q_i) \in \mathbb{Z}$ and $p_i \in \mathbb{Z}_+$. Furthermore, p_i and q_i are coprime. Away from the punctures, M_3 is a smooth degree d circle fibration over Σ_g. The exceptional fibres are located above the marked points. Around each puncture, excise a tubular neighbourhood which together with the fibre forms a solid torus, $S^1 \times D^2$. On each of these boundaries we attach a mapping class torus, i.e., a T^2 fibered over an interval $x_3 \in [0, L]$. We view the torus as a complex manifold with complex structure τ and $SL(2,\mathbb{Z})$ action $\tau \to (r\tau + p)/(s\tau + q)$, where[1]

$$\varphi_{p,q} = \begin{pmatrix} r & p \\ s & q \end{pmatrix} = T^{k_1} S T^{k_2} \ldots S T^{k_n} \in SL(2,\mathbb{Z}) \,, \tag{5.7}$$

and r, s encode the framing, i.e., the choice of trivialisation of the tangent bundle. The integers k_j are given by the continued fraction

$$\frac{p}{q} = k_1 - \cfrac{1}{k_2 - \cfrac{1}{\ldots - \cfrac{1}{k_n}}} \equiv [k_1, \ldots, k_n] \,. \tag{5.8}$$

This representation ensures that the $(0,1)$-cycle at $x_3 = 0$ is identified with the (p,q)-cycle at $x_3 = L$. Here and in the following we denote the A- and B-cycle of the boundary of a solid torus as the S^1 and the ∂D^2 respectively and denote general

[1] The explicit representation for the generators S and T of $SL(2,\mathbb{Z})$ and the central element $C = S^2 = (ST)^3$ is $S = \begin{pmatrix} 0 & -1 \\ 1 & 0 \end{pmatrix}$, $T = \begin{pmatrix} 1 & 1 \\ 0 & 1 \end{pmatrix}$ and $C = \begin{pmatrix} -1 & 0 \\ 0 & -1 \end{pmatrix}$.

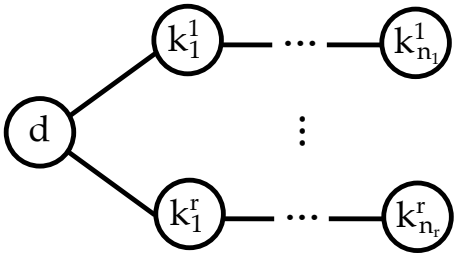

Figure 5.1: Plumbing graph for Seifert manifolds with r special fibres. For $r = 3$ this graph corresponds to the Seifert quivers in the text. We consider $g = 0$ for the central node. This also gives the quiver for the theory $\widehat{T}[\Omega_{[d;0,[k_1^i,\cdots,k_{n_i}^i]]}, G]$.

cycles in the (A, B)-basis. To close the boundary we then glue back in a solid torus. We represent a Seifert manifold by its plumbing graph, shown in figure 5.1, where the Seifert data is encoded in the continued fractions p_i/q_i given by (5.8). This plumbing graph defines a four-manifold with the Seifert manifold as its boundary. The concept extends more generally to graph manifolds, see e.g. [151], which we will not discuss in this thesis. In general there is a choice of genus for the central node, which we take to be $g = 0$ in the following. There are redundancies in the definition of the Seifert data which leave the M_3 invariant and only affect the ambient four-manifold. We will discuss these identities and their implications on the graph shortly.

The simplest class of examples are the Lens spaces, $M_3 = L(p, q)$, which are obtained by gluing two solid tori, $(S^1 \times D^2)_\pm$, identifying the $(0, 1)_+$ cycle with the $(p, q)_-$ cycle. This is known as the Heegaard splitting of the Lens space, see e.g. [152,153]. We can easily see that this definition corresponds to Seifert manifolds with $g = 0$ and $r \leq 2$. First consider $r = 0$, i.e. M_3 is a degree d circle fibration over S^2. This is a definition of $L(d, 1)$ in terms of a generalisation of the Hopf fibration. We thus assign to $L(d, 1)$ the element $\varphi_{d,1} = T^d$. Now add a puncture with exceptional fibre (p_1, q_1). Excising the tubular neighbourhood of the puncture leaves us with a circle fibration over the disk. We now glue this to the solid torus as explained above. After the gluing we obtain

$$\varphi_{[d;0;(p_1,q_1)]} = T^d S \varphi_{p_1,q_1} = \varphi_{dp_1-q_1,p_1} \quad \Rightarrow \quad [d; 0; (p_1, q_1)] \cong L(dp_1 - q_1, p_1)\,. \tag{5.9}$$

The generalisation to two exceptional fibres is obvious. By exchanging the two fibres one can see that $L(p,q) \cong L(p, q^{-1} \mod p)$.

Introducing a third marked point fundamentally changes the geometry and the resulting Seifert manifold is no longer a Lens space (for generic (p_i, q_i)). The description in terms of a linear chain of S and T in $SL(2,\mathbb{Z})$ breaks down but we will present a natural way to couple the central node to three fibres when discussing the quiver description in section 5.1.2. In what follows, we will be concerned with $g = 0$, and will label the vertices only by k. We are primarily concerned with Seifert manifolds of positive curvature which are summarised in appendix B.1.

The continued fraction presentation of p/q in (5.8) is not unique, which implies a non-uniqueness of the Seifert data or, equivalently, the ambient four-manifold. These relations are summarised in figure 5.2:

i) $[k_1, \ldots, k_n] \cong [k_1, \ldots, k_n + 1, 1]$:

This corresponds to adding a factor of TST on the right hand side of $\varphi_{p,q}$. This leaves (p_i, q_i) invariant but affects the framing of the manifold and corresponds to taking the connected sum of M_3 with an S^3. We can also attach this to the central node, adding a new fibre with $p_{r+1}, q_{r+1} = (1,1)$, while increasing the degree by one. Thus,

$$[d; g; (p_i, q_i)] \cong [d+1; g; (p_i, q_i), (1,1)]\,. \tag{5.10}$$

ii) $[k_1, \ldots, k_j, \ldots, k_n] \cong [k_1, \ldots, k_j - k, 0, k, \ldots, k_n]$ for any k:

This corresponds to including a factor of $S^2 = C$. This sends $(p,q) \to (-p,-q)$ leaving p/q invariant.

iii) $[k_1, \ldots, k_j, k_{j+1}, \ldots, k_n] \cong [k_1, \ldots, k_j - 1, -1, k_{j+1} - 1, \ldots, k_n]$:

This follows from including a factor of $(TS)^{-3} = C$. Inserting this element between the central node and a fibre decreases the degree by one and acts on

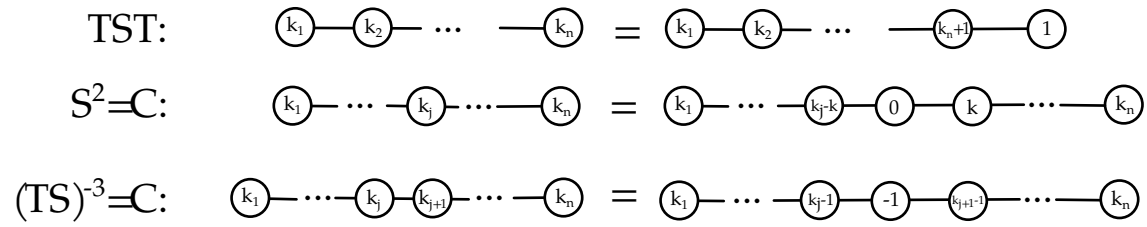

Figure 5.2: The relations TST, S^2 and $(TS)^{-3}$ acting on the plumbing data associated to the three-manifold.

the fibre element as $\varphi_{p,q} \to \varphi_{p,q-p}$. This generalises to

$$[d; g; (p_i, q_i)] \cong [d + \sum_{i=1}^{r} m_i; g; (p_i, q_i + m_i p_i)] \,, \tag{5.11}$$

for any choice of $m_i \in \mathbb{Z}$.

Before moving on, we note that an efficient way to characterise the graph Ω, associated to a Seifert manifold, is by its linking matrix, which we denote by Q. Its entries are defined as

$$Q_{ij} = \begin{cases} k_i & \text{if } i = j \\ -1 & \text{if } i \text{ connected to } j \text{ by } S \\ 0 & \text{else} \end{cases} \,. \tag{5.12}$$

Here the choice of taking off-diagonal terms to be -1 is a convention, but will be useful in the definition of $T[M_3]$ below.

5.1.2 $\widehat{T}[\Omega, G]$

We now define the theories $\widehat{T}[\Omega, G]$, which will be the building blocks for all the physical theories that we consider in later sections. It is useful to define this theory in terms of boundary conditions of $\mathcal{N} = 2^*$ gauge theory with gauge group G that preserve a $U(1)_t$ flavour symmetry. For the $\mathcal{N} = 2$ twist, the construction in terms of boundary conditions has been extensively studied, see e.g. [23, 93, 103, 154–158], which we briefly summarise below. For example, the Lens spaces can be constructed

from the Heegaard splitting with one-punctured torus boundaries. This corresponds to the 4d $\mathcal{N}=2^*$ theories on an interval with $\frac{1}{2}$-BPS boundary conditions. In this picture, the puncture on the boundary torus induces a network of line defects in M_3, which correspond to the circle actions in the Seifert fibration (5.5).

Boundary Conditions for 4d $\mathcal{N}=4$ SYM The basic building blocks can be constructed from the $\frac{1}{2}$-BPS equations of the mass deformed 4d $\mathcal{N}=2^*$ G gauge theory on the half-space $x_3 \in [0,\infty)$, as studied in [158]. The bosonic degrees of freedom of the 4d theory can be decomposed into that of an $\mathcal{N}=2$ vector multiplet and a hypermultiplet in the adjoint representation, $(A_\mu,\ \phi)$ and $(X,\ Y)$. In the $\mathcal{N}=2$ language, the theory has a $U(1)_t$ global symmetry, under which the complex scalars (ϕ, X, Y) have charges $(0, 1, -1)$ respectively.

The basic boundary conditions that can be used to build a $\widehat{T}[\Omega, G]$ theory are

$$\begin{aligned} &|N_+\rangle: \quad D_3X=0\ ,\ Y=0\ ,\ N\ , && |N_-\rangle: \quad D_3Y=0\ ,\ X=0\ ,\ N\ , \\ &|\mathcal{V}_+\rangle: \quad D_3Y=0\ ,\ X=0\ ,\ D(\mathcal{V})\ , && |\mathcal{V}_-\rangle: \quad D_3X=0\ ,\ Y=0\ ,\ D(\mathcal{V})\ , \end{aligned} \tag{5.13}$$

where N and $D(\mathcal{V})$ denote the Neumann and Dirichlet boundary conditions for the vector multiplet respectively

$$\begin{aligned} N: &\qquad F^{3\mu}=0\,, \quad D_3\,\mathrm{Re}\,\phi=0\,, \quad \mathrm{Im}\,\phi=0 \\ D(\mathcal{V}): &\qquad F^{\mu\nu}=0\,, \quad D_3\,\mathrm{Im}\,\phi=0\,, \quad \mathrm{Re}\,\phi=a\,, \end{aligned} \tag{5.14}$$

where the Dirichlet boundary condition depends on the choice of background 3d $\mathcal{N}=2$ vector multiplet $\mathcal{V}$ whose lowest component is a. For the Neumann boundary condition, the vector multiplet $\mathcal{V}$ remains dynamical.

The overlaps between these boundary conditions can be obtained by studying the low energy limit of the 4d $\mathcal{N}=2^*$ theory on an interval with two boundary conditions. First of all, one can check

$$\langle N_\pm | N_\pm \rangle = \int_{\mathcal{V}} d\mathcal{V}\ \mathrm{adj}_\pm(\mathcal{V})\ , \tag{5.15}$$

where we integrate over the dynamical 3d $\mathcal{N}=2$ vector multiplet $\mathcal{V}$. In addition to this, we have the $\mathcal{N}=2$ chiral multiplet valued in the adjoint representation with $U(1)_t$ charge ± 1, which we denote by $\mathrm{adj}_{\pm}(\mathcal{V})$. If both types of adjoints are present in the theory, the pair can be integrated out in the low-energy effective theory, which leads to the relation

$$\mathrm{adj}_{+}(\mathcal{V})\mathrm{adj}_{-}(\mathcal{V}) = 1\,. \tag{5.16}$$

We also need the following relations

$$\langle \mathcal{V}_{\pm}|\mathcal{V}_{\pm}\rangle = \mathrm{adj}_{\mp}(\mathcal{V})\ ,\quad \langle \mathcal{V}_{\pm}|N_{\pm}\rangle = 1\ ,\quad \langle \mathcal{V}_{\pm}|N_{\mp}\rangle = \mathrm{adj}_{\mp}(\mathcal{V})\ , \tag{5.17}$$

which are straightforward to check by studying the propagating degrees of freedom between the overlaps.

For each T^2 boundary with a puncture, we specify a choice of polarisation, which corresponds to the A- and B-cycle of the torus. The gauge symmetry G of the 4d theory is associated to the A-cycles of the tous and the holonomy around the A- and B- cycle correspond to the Wilson and 't Hooft loop expectation values of the gauge theory, respectively.

A class of boundary conditions for the $\mathcal{N}=4$ theory are provided by the compactification of the 6d $(2,0)$ theory on a three-manifold with a torus boundary, where the polarisation data is specified. The simplest example is the solid torus, $M_3 = D^2 \times S^1$, where the S^1 is the A-cycle. In this case, we claim that the theory corresponds to the 4d theory with the Neumann boundary condition $|N_+\rangle$ assigned [158].

Seifert manifolds with exceptional fibres can be obtained from the surgery procedure discussed in section 5.1.1. The surgery around each marked point corresponds to an operation inserting a mapping torus between two boundary tori, which implements an $SL(2,\mathbb{Z})$ transformation (5.7). The puncture associated to the $U(1)_t$ symmetry defines a line defect connecting two torus boundaries. When we glue them with another building block of the three-manifold, the polarisation data should be

identified. Each mapping torus corresponds to an $SL(2,\mathbb{Z})$ interface in the 4d gauge theory, which defines an operator acting on the space of boundary conditions (5.13). We now list the operators and the associated boundary conditions for the building blocks:

1. The mapping cylinder implementing the T operation corresponds to adding a background $\mathcal{N}=2$ Chern-Simons level to the theory

$$T^k = \int_{\mathcal{V}} |\mathcal{V}_+\rangle\langle\mathcal{V}_+| \text{ adj}_+(\mathcal{V}) \; e^{-k \text{ CS}(\mathcal{V})} \; , \tag{5.18}$$

where the last factor denotes an $\mathcal{N}=2$ CS theory at level k. Similarly, we can describe it in terms of the multiplet $\mathcal{V}_-$. For $k=0$ this corresponds to the identity operator.

2. The S operation corresponds to the $T(G)$ theory defined in [155], which has $G\times G^\vee$ flavour symmetry

$$S = \int_{\mathcal{V},\mathcal{V}'} |\mathcal{V}_-\rangle \; T(G)(\mathcal{V}_-,\mathcal{V}'_+) \; \langle\mathcal{V}'_+| \; . \tag{5.19}$$

Using the relation $\langle\mathcal{V}'_+| = \text{adj}_-(\mathcal{V}') \; \langle\mathcal{V}'_-|$, we can write the expression more symmetrically in the two background gauge fields as

$$\begin{aligned} S &= \int_{\mathcal{V},\mathcal{V}'} |\mathcal{V}_-\rangle \; T(G)(\mathcal{V}_-,\mathcal{V}'_+) \; \text{adj}_-(\mathcal{V}') \; \langle\mathcal{V}'_-| \\ &= \int_{\mathcal{V},\mathcal{V}'} |\mathcal{V}_-\rangle \; FT(G)(\mathcal{V}_-,\mathcal{V}'_+) \; \langle\mathcal{V}'_-| \; , \end{aligned} \tag{5.20}$$

where $FT(G)$ is the so-called "flipped" $T(G)$ theory defined by adding an adjoint field in one of the flavour symmetries [159].

3. Finally, let us consider the building blocks with more than two torus boundaries. We claim that $\Sigma_{0,r}\times S^1$ with the A-cycle along the S^1 identifies all the global symmetries associated to the r punctures. For the three-punctured sphere, we have

$$\int_{\mathcal{V}} |\mathcal{V}_+\rangle|\mathcal{V}_+\rangle|\mathcal{V}_+\rangle \text{ adj}_+(\mathcal{V}) \; , \tag{5.21}$$

which can be equivalently expressed in terms of the multiplet $\mathcal{V}_-$.

Definition of $\widehat{T}[\Omega, G]$ A description of $\widehat{T}[\Omega, G]$ can be obtained by a combination of the above building blocks according to the surgery procedure discussed in section 5.1.1.

We start with the plumbing graph Ω of a Seifert manifold M_3, from which we construct $\widehat{T}[\Omega, G]$ in the following way:[2]

1. To each vertex, labelled by k and g, we assign an $\mathcal{N} = 2$ gauge multiplet at Chern-Simons level k together with an $\mathcal{N} = 2$ adjoint chiral multiplet, to which we assign $U(1)_t$ charge $+1$. We also couple this to a set of g $\mathcal{N} = 4$ adjoint hypermultiplets [157, 160], although we will mostly consider the case $g = 0$. This vertex has r boundaries along which it is glued to neighboring vertices. To each of these boundaries we assign a $|\mathcal{V}_+\rangle$.

2. To each edge we assign the S-transformation (5.20), i.e., the $T(G)$ theory. More precisely, it is convenient to use the second line of (5.20) to write this more symmetrically using the $FT(G)$ theory, which is the $T(G)$ theory with one flavour symmetry coupled to an adjoint chiral multiplet of negative $U(1)_t$ charge. To the two flavour groups we assign $|\mathcal{V}_-\rangle$ and $|\mathcal{V}'_-\rangle$ respectively.

3. We glue these building blocks using the overlap $\langle \mathcal{V}_+ | \mathcal{V}'_- \rangle = \delta(\mathcal{V}, \mathcal{V}')$.

In this paper we use the following depiction of the quivers for the $\widehat{T}[\Omega, G]$, where we henceforth assume $g = 0$ for all vertices:

gauge field $\mathcal{V}$ at CS level k	round node dressed with k
flavour group	square node
$\mathrm{adj}_\pm(\mathcal{V})$	node dressed with upward/downward arc
$T(G)(\mathcal{V}_-, \mathcal{V}'_+)$	line with a downward and an upward arc
$FT(G)$	line with two downward arcs

(5.22)

[2]Here we specify the action of the $U(1)_t$ symmetry, which is related to the geometrical $U(1)$ isometry of Seifert manifolds.



Figure 5.3: Quiver description of Lens space quiver $\widehat{T}[\Omega_{[k_1,k_2]},G]$, where $p/q = k_1 - 1/k_2$ and the dictionary in (5.22) is used. On the left we use the $T(G)$ theory, and on the right the $FT(G)$ theory, which is related by flipping an adjoint field. This flipping operation can be represented pictorially by contracting an upward arc on a node and an adjacent downward arc on an edge to leave an upward arc on the edge. Further equivalent descriptions of this theory are shown in figure 5.4 below.

Examples We now consider some examples of Seifert quivers. The simplest non-trivial example is the graph $\Omega_{[k_1,k_2]}$ of the Lens space $L(p,q)$ with $\frac{p}{q} = k_1 - \frac{1}{k_2}$. It consists of two vertices with labels k_j and $g=0$, connected by an edge and therefore

$$\begin{aligned}\widehat{T}[\Omega_{[k_1,k_2]},G] = \int_{\mathcal{V}^{1,2,3,4}} e^{-k_1\ \mathrm{CS}(\mathcal{V}^1)}\ \mathrm{adj}_+(\mathcal{V}^1)\ \underbrace{\langle \mathcal{V}^1_+|\mathcal{V}^2_-\rangle}_{\delta(\mathcal{V}^1,\mathcal{V}^2)}\ T(G)(\mathcal{V}^2_-,\mathcal{V}^3_+) \\ \mathrm{adj}_-(\mathcal{V}^3)\ \underbrace{\langle \mathcal{V}^3_-|\mathcal{V}^4_+\rangle}_{\delta(\mathcal{V}^3,\mathcal{V}^4)}\ \mathrm{adj}_+(\mathcal{V}^4)\ e^{-k_2\ \mathrm{CS}(\mathcal{V}^4)}\,.\end{aligned} \tag{5.23}$$

Using the delta functions we can integrate out $\mathcal{V}^2$ and $\mathcal{V}^3$ after which two adjoints with opposite charge cancel. After these simplifications

$$\widehat{T}[\Omega_{[k_1,k_2]},G] = \int_{\mathcal{V}^{1,4}} e^{-k_1\mathrm{CS}(\mathcal{V}^1)}\ \mathrm{adj}_+(\mathcal{V}^1)\ T(G)(\mathcal{V}^1_-,\mathcal{V}^4_+)\ e^{-k_2\mathrm{CS}(\mathcal{V}^4)}\,. \tag{5.24}$$

This theory is depicted in figure 5.3, illustrating the conventions of (5.22). More generally, we can write the corresponding quiver for $\Omega_{[k_1,\cdots,k_n]}$ as n CS-theories at levels k_j coupled by $T(G)$ theories, with a single adjoint scalar coupled to the left-most node.

For Seifert manifolds with three or more exceptional fibres, i.e., $M_3 \cong [d;0;(p_i,q_i)]$, we label the graph by $\Omega_{[d;0,[k^i_1,\cdots,k^i_{n_i}]]}$, depicted in figure 5.1. We identify the degree d with a central T^d coupled to r linear quivers. More generally we understand a node labelled by $\frac{p_i}{q_i} = [k^i_1,\ldots,k^i_{n_i}]$ as being the same as the linear quiver representing the Lens space $L(p_i,q_i)$ [91], where we take the left-most node as a G flavour symmetry. Then, applying the rules above, one finds that $\widehat{T}[\Omega_{[d;0,[k^i_1,\cdots,k^i_{n_i}]]},G]$ is obtained by

gauging these common flavour symmetries with level d CS term and a single adjoint chiral multiplet of $U(1)_t$ charge $+1$.

5.1.3 Symmetries and Dualities of $\widehat{T}[\Omega, G]$

The non-uniqueness of the Seifert data discussed in section 5.1.1, should map to dualities of the theories $\widehat{T}[\Omega, G]$. However, we will see below that for non-self-dual G, the $SL(2,\mathbb{Z})$ actions and equivalence relations of three-manifolds discussed in section 5.1.1 hold only up to a decoupled topological sector at the level of the $\widehat{T}[\Omega, G]$ theory, indicating an undesired dependence on the decomposition graph Ω. We will discuss how to cure this problem in the following sections. We now summarise the dualities:

i) $[k_1, \ldots, k_n] \cong [k_1, \ldots, k_n + 1, 1]$:

The equivalence of the quiver under this operation was discussed in [91,103,161]. In the case of the $G = U(N)$ theory, this is related to the following duality of [162]

$$U(N)_{k=1} \; + \; \text{adjoint chiral} \quad \leftrightarrow \quad N \text{ free chirals} \; . \tag{5.25}$$

We discuss this relation and the role of this duality in more detail in the $N = 2$ case below. For $G = SU(N)$, we use instead the following duality, a special case of which is the duality appetiser of [163]

$$SU(N)_1 \; + \; \text{adjoint chiral} \quad \leftrightarrow \quad (N-1 \text{ free chirals}) \otimes (\text{top. } U(1)_N \text{ CS theory}) \; . \tag{5.26}$$

The duality implies the relation[3]:

$$[k_1, ..., k_n + 1, 1] \text{ quiver} \quad \leftrightarrow \quad ([k_1, ..., k_n] \text{ quiver}) \otimes (\text{top. } U(1)_N \text{ CS theory}) \; . \tag{5.27}$$

Note the presence of the decoupled topological sector, which is directly related to the fact that $SU(N)$ is not self-dual. This sector will play an important role

[3]This holds up to a relative gravitational CS term which does not affect our discussion.

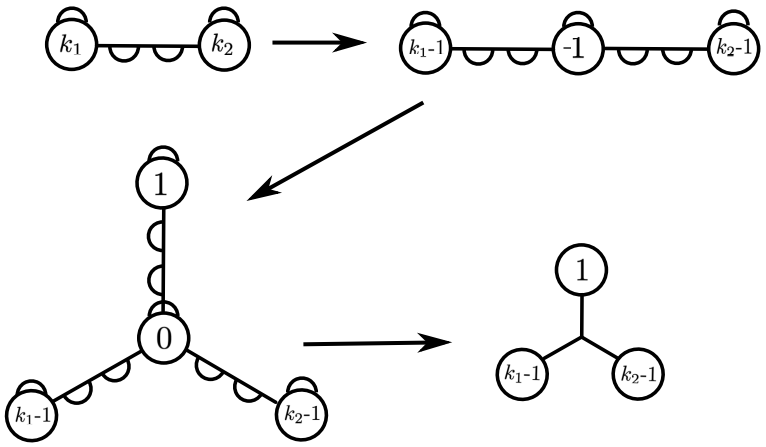

Figure 5.4: Sequence of moves leading to the duality between the $FT(G)$ theory and a trinion theory with one G symmetry gauged with level 1 CS term. In the last step with use the star-shaped quiver description of the trinion of [160].

in what follows.

ii) $[k_1, \ldots, k_i, \ldots, k_n] \cong [k_1, \ldots, k_i - k, 0, k, \ldots, k_n]$:

This corresponds to two factors of $T(G)$ coupled at a common node and gauged at level zero. However, since we take the gauge field in G (rather than $G^\vee$) this operation adds a topological factor, which for $G = SU(N)$ is $(U(1)_N)^2$.

iii) $[k_1, \ldots, k_i, k_{i+1}, \ldots, k_n] \cong [k_1, \ldots, k_i - 1, -1, k_{i+1} - 1, \ldots, k_n]$:

For $G = SU(N)$, we claim that the $SL(2,\mathbb{Z})$ relation $(TS)^3 = C$ holds only up to the decoupled topological $U(1)_N$ CS theory, as in the relation i) discussed above. Let us consider the case $n = 2$ and $i = 1$ without loss of generality. This implies the duality

$$[k_1, k_2] \text{ quiver} \quad \leftrightarrow \quad ([k_1 - 1, -1, k_2 - 1] \text{ quiver}) \otimes (\text{top. } U(1)_N \text{ CS theory})\,. \tag{5.28}$$

Using the relation (5.27) for the theory on the right hand side, we find that this theory precisely corresponds to the trinion theory with the three flavour symmetries gauged at levels $(k_1 - 1, k_2 - 1, 1)$ respectively.

In fact, we may make a stronger statement. Rather than taking these nodes with

level k_1 and k_2 CS terms as gauge symmetries, we may retain them as flavour symmetries. Then, in the former case, we obtain the T_N theory with one of its G flavour symmetries gauged with a level 1 CS term, while in the latter case we obtain the $T(G)$ theory, or more precisely, the flipped theory, $FT(G)$. Both have $G \times G$ flavour symmetry. We also notice that the levels of the CS terms are shifted by one in the latter description, which we may attribute to relative contact terms appearing in the duality. In summary, this yields the following duality

$$\begin{aligned} & T_G \text{ trinion theory with one flavour symmetry gauged at level 1} \\ \leftrightarrow\ & FT(G) \text{ with level 1 contact terms for } G \times G \text{ flavour symmetry} \end{aligned} \tag{5.29}$$

This observation was also made in [164] for $G = SU(N)$ and is illustrated in figure 5.4.

5.1.4 $T(SU(2))$

Let us illustrate some of the properties discussed in the previous subsection in more detail in the special cases $G = SU(2)$, and also point out some additional subtleties that arise.

To start, let us briefly recall some relevant features of the $T(SU(2))$ theory. The usual description of the $T(SU(2))$ theory is as a 3d $\mathcal{N} = 4$ $U(1)$ gauge theory with $N_f = 2$ hypermultiplets. This theory has $SU(2)_F \times SU(2)_J$ flavour symmetry, the former acting manifestly on the hypermultiplets, and the latter being an infrared enhancement of the $U(1)_J$ symmetry visible in the UV gauge theory Lagrangian. This is the theory living on a domain wall interpolating between S-dual instances of the 4d $\mathcal{N} = 4$ $SU(2)$ SYM theory, with each bulk theory coupling to one of the $SU(2)$ flavour symmetries of the domain wall, as discussed in [23].

Now let us consider the relation i) above in the case of $G = SU(2)$. Consider a linear quiver associated to the RHS of this relation: this ends with an S-wall, followed

by an $SU(2)$ gauge node with a CS level 1. Let us take the latter $SU(2)$ symmetry to couple to the $SU(2)_F$ symmetry of the $T(SU(2))$ theory, and let us denote the gauge symmetry of $T(SU(2))$ as $U(1)_g$. Thus the $SU(2)_F$ node has a single fundamental flavour, also charged under $U(1)_g$, and CS level 1. Then this theory has a dual description [165, 166] as a single chiral multiplet, and importantly, a level 2 contact term for the $U(1)_g$ symmetry. Therefore, this part of the quiver is replaced by a singlet chiral multiplet along with a $U(1)_g$ level 2 topological CS theory, leading to

$$\begin{aligned} G = SU(2): \quad & [k_1, ..., k_n + 1, 1] \text{ quiver} \\ \leftrightarrow \quad & ([k_1, ..., k_n] \text{ quiver}) \otimes (\text{top. } U(1)_2 \text{ CS theory}) \,, \end{aligned} \tag{5.30}$$

and so the relation only holds up to a decoupled topological sector, as noted above. A special case of this, noted in [161], is the case $n = 0$, where this relation formally gives the "duality appetiser" of [163], which indeed contains such a decoupled $U(1)_2$ topological sector.

Next consider the relation iii). Recall this follows from the duality of the T_G theory with one G flavour symmetry gauged at level 1 and the $T(G)$ theory. In general, the T_G theory is non-Lagrangian, and so this duality is not of immediate practical use. However, for the case of $G = SU(2)$ the T_2 theory is simply a free bifundamental hypermultiplet. Thus, we arrive at the duality[4]

$$\begin{aligned} & 3d\, \mathcal{N} = 4\, U(1) \text{ with } N_f = 2 \text{ hypermultiplets} \\ \leftrightarrow \quad & SU(2)_{k=1} \text{ with } N_f = 2 \text{ hypermultiplets with level } -1 \text{ contact terms} \\ & \text{for } SU(2) \times SU(2) \cong SO(4) \text{ symmetry} \,. \end{aligned} \tag{5.31}$$

This duality was noticed earlier in [167], and also discussed in [164]. Importantly, note that in this dual description, the $SU(2) \times SU(2)$ symmetry is manifest in the Lagrangian, unlike in the usual description of $T(SU(2))$. This observation makes this

[4]More precisely, the relation between the two theories involves a "flipping" of one of the $SU(2)$ flavour symmetries, and so the theory appearing on the LHS should be thought of as the $FT(SU(2))$ theory of [159].

description of $T(SU(2))$ more convenient for constructing Lagrangians for general Seifert manifold theories, and it will play an important role in what follows.

5.2 $T[M_3, \mathfrak{g}, H]$ and Higher-Form Symmetries

In this section we define the theories obtained by compactification of the 6d $\mathcal{N} = (2, 0)$ theory of type $\mathfrak{g}$ on a three-manifold M_3. What will emerge from this section is that to fully define the theory, we must specify, in addition to the gauge algebra and three-manifold, a subgroup H of the cohomology group $H^2(M_3, Z_{\widetilde{G}})$, and so we will actually define theories

$$T[M_3, \mathfrak{g}, H]\,, \quad H \leq H^2(M_3, Z_{\widetilde{G}})\,. \tag{5.32}$$

Here $Z_{\widetilde{G}}$ is the centre of the simply connected Lie group $\widetilde{G}$ with Lie algebra $\mathfrak{g}$. For ease of notation, we will often refer to $T[M_3, \mathfrak{g}, H = 1]$ simply as $T[M_3, \mathfrak{g}]$.

For M_3 a Seifert manifold, the theories $T[M_3, \mathfrak{g}, H]$ can be naturally defined in terms of the theories, $\widehat{T}[\Omega, \widetilde{G}]$, constructed in the previous section, where Ω is a graph associated to M_3. To describe the procedure of obtaining the former theory from the latter, it turns out to be natural to use the language of higher-form symmetries, reviewed in section 4.2. In particular, the theories $T[M_3, \mathfrak{g}, H]$ in general have several interesting higher-form symmetries, and the theories corresponding to different subgroups H can be obtained from each other by gauging these symmetries in a suitable way. This structure can be traced to a higher-form symmetry present already in the 6d theory, and in particular, to its nature as a relative QFT.

5.2.1 6d theory as a Relative QFT

Let us first review some properties of the 6d theory relevant to the compactification to 3d, which we consider in the next subsection. The role of discrete topological data in compactifications of the 6d $\mathcal{N} = (2, 0)$ theory has been discussed extensively in the

literature; see, for example, [29, 112, 168–171].

First we recall that the 6d $\mathcal{N} = (2, 0)$ theory is a relative QFT, meaning it is not well-defined by itself, but naturally lives on the boundary of a 7d topological theory, which can be described by a Wu-Chern-Simons (WCS) theory [29,168,169,172]. Then the notion of a partition function is replaced by a partition vector, which is an element of the Hilbert space of this TQFT.

In more detail, let us first consider the A_{N-1} type 6d $\mathcal{N} = (2, 0)$ SCFT. Then, roughly speaking, the WCS theory can be thought of as a level N 3-form Chern-Simons theory, and has 3d Wilson surface operators $\mathcal{O}_\omega$, supported on 3-cycles $\omega \in H_3(M_7, \mathbb{Z}_N)$. These may be thought of as charge operators for a 3-form symmetry of the Chern-Simons theory, with group $\mathbb{Z}_N$. This symmetry has an 't Hooft anomaly, i.e. the charge operators do not commute. Rather, when we consider the theory on a spacetime $M_6 \times \mathbb{R}$, they obey the appropriate version of (4.13), specifically

$$\mathcal{O}_\omega \mathcal{O}_{\omega'} = e^{\frac{2\pi i}{N}\omega\cap\omega'} \mathcal{O}_{\omega'} \mathcal{O}_\omega, \qquad \omega, \omega' \in H_3(M_6, \mathbb{Z}_N)\,. \tag{5.33}$$

To describe the Hilbert space of the TQFT on M_6 we first must choose a polarisation of $H_3(M_6, \mathbb{Z}_N)$, which is a maximal isotropic subgroup Λ, i.e. with $\lambda \cap \lambda' = 0$ for all $\lambda, \lambda' \in \Lambda$. Let us assume that we can write

$$H_3(M_6, \mathbb{Z}_N) \cong \Lambda \oplus \widetilde{\Lambda}\,, \tag{5.34}$$

where it follows that $\widetilde{\Lambda}$ is also maximal isotropic. Then we pick a basis in which the operators, $\mathcal{O}_{\widetilde{\lambda}}$, $\widetilde{\lambda} \in \widetilde{\Lambda}$, are diagonal. Namely, one can find a unique vector $|0\rangle$, which is fixed by all $\mathcal{O}_{\widetilde{\lambda}}$, and for $\lambda \in \Lambda$ we define states

$$|\lambda\rangle \equiv \mathcal{O}_\lambda |0\rangle, \quad \lambda \in \Lambda\,. \tag{5.35}$$

Then one can check that

$$\mathcal{O}_\lambda |\lambda'\rangle = |\lambda + \lambda'\rangle, \quad \mathcal{O}_{\widetilde{\lambda}} |\lambda\rangle = e^{\frac{2\pi i}{N}\lambda\cap\widetilde{\lambda}} |\lambda\rangle\,, \quad \lambda, \lambda' \in \Lambda,\ \widetilde{\lambda} \in \widetilde{\Lambda}\,, \tag{5.36}$$

and so these states form a basis for the Hilbert space of the 7d theory. The choice of polarisation picks out a corresponding basis of the Hilbert space as above. E.g., if we had chosen $\widetilde{\Lambda}$ rather than Λ, the basis states would be related by a discrete Fourier transform. Note that a choice of polarisation will typically break some of the diffeomorphism symmetry of M_6.

For other ADE Lie algebras $\mathfrak{g}$, we expect a similar description, where in general the polarisation is determined by a decomposition

$$H_3(M_6, Z_{\widetilde{G}}) \cong \Lambda \oplus \widetilde{\Lambda}\,, \tag{5.37}$$

where $Z_{\widetilde{G}}$ is the centre of $\widetilde{G}$, the simply connected Lie group with Lie algebra $\mathfrak{g}$.

After picking the polarisation, we may write the partition vector of the 6d $\mathcal{N} = (2,0)$ theory on M_6 in the corresponding basis as

$$\left|\mathcal{Z}^{M_6}\right\rangle = \sum_{\lambda\in\Lambda} \mathcal{Z}^{M_6}_{\lambda} |\lambda\rangle\,. \tag{5.38}$$

We refer to $\mathcal{Z}^{M_6}_{\lambda}$, $\lambda \in \Lambda$, as the components of the partition vector. We emphasise that they depend not only on λ, but also on the choice of polarisation, Λ.

Abelian Case In addition to the simple Lie algebras considered above, we may define the 6d $\mathcal{N} = (2,0)$ theory in the case $\mathfrak{g} = \mathfrak{u}(1)$, where it corresponds to a free $\mathcal{N} = (2,0)$ tensor multiplet. Although this theory is free, there are still several subtleties that arise, as discussed, e.g., in [168, 173].

To fully define the theory we must specify a periodicity, $N \in \mathbb{Z}_{>0}$, and rather than a partition function, the observables on a spacetime M_6 are given by conformal blocks or a partition vector, as we saw in the ADE case above, namely

$$\mathcal{Z}_{\lambda}\,, \qquad \lambda \in \Lambda \subset H_3(M_6, \mathbb{Z}_N)\,. \tag{5.39}$$

These may also be understood as vectors in the Hilbert space of a 7d TQFT on M_6, a 3-form version of the Chern-Simons theory. In particular, for $N > 1$, the theory is not an ordinary QFT, but a relative QFT, as we saw in the ADE case above.

We note for later reference that the self-dual 2-form with periodicity N has a $U(1)$ 2-form symmetry [111], whose charge operators are

$$U_\alpha[\Sigma_3] = e^{2\pi i\alpha \int_{\Sigma_3} H}\,, \tag{5.40}$$

where $H = dB$ is the self-dual 3-form field strength. This symmetry has an 't Hooft anomaly, which implies that when we place the U_α operator on a manifold with boundary, $\partial\Sigma_3 = \Sigma_2$, this configuration has a non-trivial 2-form charge supported on Σ_2. We will return to the consequences of this statement below.

Self-dual G Let $\mathfrak{g}$ be a semi-simple, simply-laced Lie algebra, and suppose we can find a subgroup, L, of $Z_{\widetilde{G}}$, such that $L \cong Z_{\widetilde{G}}/L$. In this case, the group $G \equiv \widetilde{G}/L$, is isomorphic to its Langlands dual group, and we call such groups "self-dual." Some examples are $SO(2N) = \mathrm{Spin}(2N)/\mathbb{Z}_2$, $(SU(N) \times SU(N))/\mathbb{Z}_N$, and $SU(N^2)/\mathbb{Z}_N$. For such G, there is a corresponding choice of polarisation of the 6d theory, which is[5]

$$\Lambda_G \equiv H^3(M_6, L) \subset H^3(M_6, Z_{\widetilde{G}})\,. \tag{5.41}$$

One can check that this is a maximal isotropic subgroup. Note that this choice does not break any diffeomorphism symmetry of M_6, and so we may naturally interpret these observables as partition functions of an ordinary QFT. Specifically, since the partition function is labelled by an element in $H^3(M_6, L)$, we see that this theory has a 2-form symmetry with group L. We may naturally refer to the 6d theory of type $\mathfrak{g}$ with the polarisation Λ_G as the "6d $\mathcal{N} = (2,0)$ theory of type G," which is an ordinary rather than relative QFT. We emphasise this terminology only makes sense for G self-dual.

Similar considerations apply in the non-semi-simple case. For example, $G = U(1)$ is self-dual, and we saw above that the $N = 1$ case of this theory is indeed an ordinary QFT. More generally, we may define the "6d $\mathcal{N} = (2,0)$ theory of type $U(N)$" as

[5]For convenience, we sometimes specify the polarisation in terms of the cohomology, rather than homology, which is equivalent by Poincaré duality.

follows. We start with the tensor product of the theory of type $\mathfrak{g} = \mathfrak{su}(N)$, along with the $\mathfrak{u}(1)$ theory with periodicity N. These are separately relative QFTs, and so we must choose a maximal isotropic subgroup of

$$H^3(M_6, \mathbb{Z}_N) \oplus H^3(M_6, \mathbb{Z}_N) \cong H^3(M_6, \mathbb{Z}_N \oplus \mathbb{Z}_N)\,. \tag{5.42}$$

However, as above, a natural choice of polarisation that preserves diffeomorphism symmetry is given by

$$\Lambda \cong H^3(M_6, \mathbb{Z}_N^{\text{diag}}) \subset H^3(M_6, \mathbb{Z}_N \oplus \mathbb{Z}_N)\,. \tag{5.43}$$

This gives rise to an ordinary 6d QFT, which is acted on by a $\mathbb{Z}_N$ 2-form symmetry. In fact, this $\mathbb{Z}_N$ sits inside a larger $U(1)$ 2-form symmetry coming from the $\mathfrak{u}(1)$ factor, as in (5.40). This theory corresponds to the low energy theory of N M5-branes, without decoupling the centre of mass motion.

In the above cases, the reduction to 5d gives rise to the 5d $\mathcal{N} = 2$ SYM theory with gauge group G, which has both 1-form and 2-form symmetries with group Z_G.

5.2.2 Compactification on M_3

In this subsection we describe some general features of the compactification of the 6d theory on M_3, which follow from properties of the 6d theory described above.[6] In this context, we are interested in the case where M_6 is a product manifold of the form

$$M_6 = M_3 \times W_3\,, \tag{5.44}$$

which describes a 3d theory, $T[M_3, \mathfrak{g}]$, on the spacetime W_3. As we will see in a moment, additional data is necessary to fully specify the theory. We will mainly be interested in $W_3 = T^3$ and from now on assume that W_3 has no torsion. Then, the

[6]Similar global considerations in the 3d-3d correspondence were discussed in [170]. See also [171] for related discussions in the 4d-2d correspondence.

universal coefficient version of the Künneth theorem states that for the $Z_{\widetilde{G}}$-valued cohomology

$$H^3(M_3 \times W_3, Z_{\widetilde{G}}) \cong Z_{\widetilde{G}} \oplus A \oplus B \oplus Z_{\widetilde{G}}\,, \tag{5.45}$$

with the notation

$$\begin{aligned} A &= \left(H^1(M_3, Z_{\widetilde{G}}) \otimes_{Z_{\widetilde{G}}} H^2(W_3, Z_{\widetilde{G}})\right) \cong H^2(W_3, \Upsilon) \\ B &= \left(H^2(M_3, Z_{\widetilde{G}}) \otimes_{Z_{\widetilde{G}}} H^1(W_3, Z_{\widetilde{G}})\right) \cong H^1(W_3, \widehat{\Upsilon})\,, \end{aligned} \tag{5.46}$$

where we have used the universal coefficient theorem to rewrite these groups, and have also defined

$$\Upsilon \equiv H^1(M_3, Z_{\widetilde{G}}), \quad \widehat{\Upsilon} \equiv H^2(M_3, Z_{\widetilde{G}})\,, \tag{5.47}$$

which are naturally Pontryagin dual.

We now have to make a choice of polarisation.[7] One possibility is to pick the A-polarisation. In this case, the observables of the theory will be labelled by an element of $H^2(W_3, \Upsilon)$. This naturally suggests that this 3d theory has a 1-form symmetry with group Υ. Another choice is the B-polarisation, in which case the observables are labelled by an element of $H^1(W_3, \widehat{\Upsilon})$, which gives a theory with 0-form $\widehat{\Upsilon}$ symmetry. We should interpret these choices as leading to different versions of the $T[M_3, \mathfrak{g}]$ theories.

More generally, we may choose a subgroup

$$H \leq \widehat{\Upsilon}\,, \tag{5.48}$$

and correspondingly define

$$\Upsilon_H = \{x \in \Upsilon \mid \chi(x) = 1, \ \ \forall \chi \in H\} \subset \Upsilon\,. \tag{5.49}$$

Then we may take our polarisation, Λ, to correspond to a subgroup

$$\Lambda = H^1(W_3, H) \oplus H^2(W_3, \Upsilon_H)\,. \tag{5.50}$$

[7] We may always choose the polarisation to include one of the $Z_{\widetilde{G}}$ factors in (5.45), and ignore these factors from now on, as they do not depend on the topology in an interesting way.

Here the A and B polarisations above correspond to $H = 1$ and $H = \widehat{\Upsilon}$, respectively. These give rise to a general class of polarisations preserving the diffeomorphism symmetry of W_3, which is natural in the context of defining a 3d QFT.

Thus we find there is not a unique theory $T[M_3, \mathfrak{g}]$, but rather, different choices corresponding to the choice of H above. We define the theory

$$T[M_3, \mathfrak{g}, H] \tag{5.51}$$

to be the 3d theory corresponding to the compactification of the type $\mathfrak{g}$ 6d $\mathcal{N} = (2, 0)$ theory with the polarisation labelled by H above. We see that the observables are labelled by

$$H^1(W_3, H) \oplus H^2(W_3, \Upsilon_H)\,, \tag{5.52}$$

which we may interpret as corresponding to symmetries

$$\text{0-form symmetry:} \qquad \Gamma_0 = H \qquad\qquad \text{1-form symmetry:} \qquad \Gamma_1 = \Upsilon_H\,.$$

5.2.3 $T[M_3, \mathfrak{g}, H]$ for M_3 a Seifert Manifold

Let us turn to an explicit description of the $T[M_3, \mathfrak{g}, H]$ in the case of M_3 a Seifert manifold. Here we will use the theories $\widehat{T}[\Omega, G]$ defined in the previous section, but we will see that, in general, some additional operations are necessary to produce the $T[M_3, \mathfrak{g}, H]$ theory.

Abelian Case Let us start in the abelian case, and consider the reduction of the 6d theory of type $\mathfrak{u}(1)$. Recall we must also choose the periodicity, N, and we first consider the case $N = 1$ which gives rise to an ordinary QFT in 6d, which we refer to as the $U(1)$ theory. Then we denote the 3d theory obtained by compactification of this theory on M_3, with the appropriate twist, as

$$T[M_3, U(1)]\,. \tag{5.53}$$

We focus on the case of M_3 a Seifert manifold, for which we take a particular graph decomposition, Ω. This graph gives a prescription for forming M_3 by gluing simple pieces along boundary tori by S and T transformations. Then, as discussed in [91], the theory may be built by iteratively applying the S and T operations of Witten [148], or more precisely, their supersymmetric completions. Namely, we assign a $U(1)$ gauge multiplet to each node in the graph associated to M_3, a level k_i CS term for the gauge group in the ith node, where k_i is the label of the node, and an off-diagonal CS term to two nodes connected by an S-gluing. In summary, this results in

$$S = \frac{1}{4\pi}\int Q_{ij} A_i \wedge dA_j + \cdots \,, \tag{5.54}$$

where Q_{ij} is the linking matrix, defined in (5.12), and the dots denote additional fields in the vector multiplet, which we suppress. This is precisely the description of $\widehat{T}[\Omega, U(1)]$ given in the previous section, where we recall the duality wall theory, $T(U(1))$, is simply a mixed BF-term for a $U(1) \times U(1)$ flavour symmetry. Thus we have, in this case

$$T[M_3, U(1)] \equiv \widehat{T}[\Omega, U(1)] \,. \tag{5.55}$$

As a consistency check, we must verify that this theory is independent of the choice of graph decomposition Ω of M_3. This is almost true, but there is a slight subtlety, which is that the $SL(2,\mathbb{Z})$ operations used above do not quite close onto a representation of $SL(2,\mathbb{Z})$, but rather form a projective representation, as noted in [148, 158]. For example, the $(ST)^3$ operation does not completely leave the theory invariant, but introduces a tensor factor with an invertible TQFT, the $U(1)_1$ CS theory, and correspondingly the partition function is not invariant, but incurs a phase. This can be attributed to a gravitational anomaly of the 6d theory. We will work modulo such invertible TQFTs in what follows.

More generally, we may consider the theory,

$$T[M_3, \mathfrak{u}(1)_N] \,, \tag{5.56}$$

obtained by the compactification of the free tensor multiplet with periodicity N. The case above corresponds to $N = 1$, and more generally, we claim we should now consider the action

$$S_{\widehat{T}[\Omega,U(1)_N]} = \frac{1}{4\pi}\int N\, Q_{ij} A_i \wedge dA_j + \cdots \tag{5.57}$$

Let us denote this theory by $\widehat{T}[\Omega, U(1)_N]$, as we have not yet checked independence on Ω. Indeed, once again we find that the $SL(2,\mathbb{Z})$ relations are not satisfied on the nose, but now the discrepancy is more severe. For example, the $(ST)^3$ relation now introduces a tensor factor of the $U(1)_N$ CS theory, which is not invertible. This means the partition function is multiplied by a more complicated factor than the phase above, and even the Hilbert space of the theory will in general be modified. Thus the theory $\widehat{T}[\Omega, U(1)_N]$ is not independent of the graph decomposition of M_3, and so is not yet equal to the theory $T[M_3, \mathfrak{u}(1)_N]$. We will see below that a similar issue arise in the ADE case, and will describe the resolution in that context.

Self-dual G The case $G = U(1)$ above is a special case of the more general situation where G is self dual. Then, as discussed in section 5.2.1, there is a natural choice of polarisation which preserves all diffeomorphism symmetry of the spacetime, M_6, and may naturally be interpreted as an ordinary QFT, which we call the 6d theory with group G. Then we claim that, in this case, compactification on M_3 gives a theory

$$T[M_3, G] \equiv \widehat{T}[\Omega, G]\,. \tag{5.58}$$

In particular, this is independent of the choice of graph decomposition of M_3. Indeed, one can check that, in the self-dual case, the $SL(2,\mathbb{Z})$ relations discussed in section 5.1.3 are satisfied on the nose (or at least up to invertible TQFTs).

The higher-form symmetry of this 3d theory may be inferred by dimensional re-

duction of the 2-form Z_G-symmetry of the 6d theory, and the theory has

$$\begin{aligned} &\text{0-form symmetry:} \quad \Gamma_0 = H^2(M_3, Z_G) \\ &\text{1-form symmetry:} \quad \Gamma_1 = H^1(M_3, Z_G)\,. \end{aligned} \tag{5.59}$$

In the case of $G = U(N)$, the 1-form symmetry has a contribution from the $U(1)$ sector, and is given as above by $\Gamma_1 = H^2(M_3, \mathbb{Z})$. However, due to the periodicity of the $U(1)$ theory being N, the anomaly form is now N times the linking form. Then one can check that the non-anomalous subgroup is given as in (5.59) with $Z_G \to \mathbb{Z}_N$. In the language of section 5.2.2, this theory corresponds to

$$T[M_3, \mathfrak{g}, H] \quad \text{with} \quad H = H^2(M_3, L) \leq H^2(M_3, Z_{\widetilde{G}})\,, \tag{5.60}$$

where we recall L is defined by $G = \widetilde{G}/L$.

General $\mathfrak{g}$ Let us now consider the general case. As described in section 5.2.2, on general grounds, we expect the theories, $T[M_3, \mathfrak{g}, H]$, obtained by compactification to be labelled by a subgroup

$$H \leq \widehat{\Upsilon} \equiv H^2(M_3, Z_{\widetilde{G}}) \tag{5.61}$$

and to have 0-form symmetry H and 1-form symmetry Υ_H.

Let us first describe the case $T[M_3, \mathfrak{g}, 1]$, which we denote by $T[M_3, \mathfrak{g}]$ for short. Here our naive guess might be

$$T[M_3, \mathfrak{g}, 1] \stackrel{?}{=} \widehat{T}[\Omega, \widetilde{G}]\,, \tag{5.62}$$

where we recall $\widetilde{G}$ is the simply connected group with Lie algebra $\mathfrak{g}$, and Ω is some graph decomposition of M_3. However, one basic problem we run into is that this theory is not independent of the graph. Indeed, as observed in section 5.1.4, for $\mathfrak{g} = \mathfrak{su}(2)$, the theory can pick up decoupled tensor factors of topological theories upon operations on Ω which preserve the topology of M_3. In order to find a definition of $T[M_3, \mathfrak{g}]$ which depends only on M_3, we must somehow eliminate these decoupled topological sectors.

First, let us review the result of [149], which states that, for a 3d TQFT $\mathcal{T}$ with anomalous 1-form symmetry Γ, one finds that the theory factorises

$$\mathcal{T} = \mathcal{T}' \otimes \mathcal{T}_{\Gamma,\mathcal{A}}\,, \tag{5.63}$$

where

$$\mathcal{T}_{\Gamma,\mathcal{A}} \equiv \text{minimal TQFT with } \Gamma \text{ symmetry with anomaly } \mathcal{A}\,. \tag{5.64}$$

One way to isolate the sector $\mathcal{T}'$ is by coupling to another topological theory, $\mathcal{T}_{\Gamma,-\mathcal{A}}$, which has the opposite anomaly, and gauging the non-anomalous diagonal subgroup

$$(\mathcal{T} \otimes \mathcal{T}_{\Gamma,-\mathcal{A}})/\Gamma \;=\; \mathcal{T}' \otimes (\mathcal{T}_{\Gamma,\mathcal{A}} \otimes \mathcal{T}_{\Gamma,-\mathcal{A}})/\Gamma \;\cong\; \mathcal{T}'\,. \tag{5.65}$$

We conjecture that a similar decoupling takes place in the theories $\widehat{T}[\Omega,\widetilde{G}]$. Namely, we conjecture that we may write

$$\widehat{T}[\Omega,\widetilde{G}] \cong T[M_3,\mathfrak{g}] \otimes \mathcal{T}_{\Gamma/Z,\mathcal{A}}\,. \tag{5.66}$$

Here Γ is the 1-form symmetry of $\widehat{T}[\Omega,\widetilde{G}]$, with centre Z, so that Γ/Z is the anomalous part. We conjecture that this anomalous symmetry acts only on a decoupled topological sector, and the physical theory, $T[M_3,\mathfrak{g}]$, appears as a subsector. Then one way to isolate the latter is as in (5.65), namely

$$T[M_3,\mathfrak{g}] \cong (\widehat{T}[\Omega,\widetilde{G}] \otimes \mathcal{T}_{\Gamma/Z,-\mathcal{A}})/(\Gamma/Z)\,. \tag{5.67}$$

However, any procedure which eliminates this decoupled sector will lead to an equivalent result. For example, this can sometimes be achieved by gauging a suitable subgroup of the symmetry Γ in the $\widehat{T}$ theory, as we will see in examples below.

It would of course be desirable to find a first principle derivation of the conjecture (5.66). However, let us mention several pieces of evidence in favour of it. First note that with this assumption, the dependence on the graph, Ω, due to the appearance of decoupled sectors, as discussed in section 5.1.3, is cured. Namely, as we will describe

in more detail below, such sectors contribute only to $\mathcal{T}_{\Gamma/Z,\mathcal{A}}$, and so will be removed in (5.67).

One tempting interpretation of this decoupling is as follows. Recall from section 5.1.1 that the graph Ω, can naturally be interpreted as describing a plumbed four-manifold M_4, bounded by M_3. Then there are operations which preserve M_3, but modify M_4 by taking a connected sum with $\mathbb{P}^2$. Now, as we saw above, the 6d theory naturally lives on the boundary of a 7d TQFT, and so the compactification of the 6d theory on M_3 can be interpreted as being accompanied by a compactification of the 7d theory on M_4. Then the compactification of the 7d theory on these connected $\mathbb{P}^2$ summands will lead to tensor factors with decoupled topological sectors, precisely as we observed above. The decoupling procedure can then be understood as removing the dependence on the auxiliary four-manifold to obtain a theory $T[M_3]$, which depends intrinsically on M_3.

One can check that the anomalous part of the 1-form symmetry can be taken to act only on a decoupled tensor factor of the Hilbert space of the theory on T^2. Then we claim that the Hilbert space of the theory $T[M_3, \mathfrak{g}]$ has an anomaly-free 1-form symmetry, and the procedure above is defined so as to isolate this factor. We will see this explicitly when we study the T^2-vacua of these theories in the next section. Finally, we will see in section 5.4 that this decoupling arises naturally when we study the topological side of the 3d-3d correspondence, and is necessary to achieve a precise matching to the counting of flat connections.

An important feature of this procedure is that it removes the anomalous 1-form symmetry, but does not modify the central subgroup, Z. In particular, we claim

$$\begin{aligned} \text{1-form symmetry of } T[M_3, \mathfrak{g}] &= \text{centre of 1-form symmetry of } \widehat{T}[\Omega, \widetilde{G}] \\ &\cong \Upsilon = H^1(M_3, Z_{\widetilde{G}})\,, \end{aligned} \tag{5.68}$$

which is the expected 1-form symmetry for this theory from the discussion in section 5.2.2. We will see this explicitly in examples below.

Finally, to define the more general theories $T[M_3, \mathfrak{g}, H]$, we must gauge a subgroup of the Υ 1-form symmetry isomorphic to H

$$T[M_3, \mathfrak{g}, H] \equiv T[M_3, \mathfrak{g}, 1]/H\,. \tag{5.69}$$

This will leave a theory with 1-form symmetry Υ_H and a new 0-form symmetry H, as expected. This gauging of a 1-form symmetry is precisely the same as changing the polarisation of the 6d theory.

5.2.4 Examples

Let us consider some examples of how this 1-form symmetry structure arises in $T[M_3, \mathfrak{su}(N)]$. While this is applicable to general M_3, here and below we focus on the case of M_3 a Seifert manifold, and moreover a rational homology sphere, and we use the Lagrangians discussed in section 5.1.2.

Lens Space Quiver We start with the case of the Lens space, $M_3 = L(p, q)$. Then,

$$H^1(L(p,q), \mathbb{Z}_N) \cong H^2(L(p,q), \mathbb{Z}_N) \cong \mathbb{Z}_{(N,p)}\,, \tag{5.70}$$

where (N, p) denotes the greatest common divisor. Thus, we expect that if $(N, p) \neq 1$ there are multiple versions of the theory, e.g., one with 1-form $\mathbb{Z}_{(N,p)}$ symmetry and no 0-form symmetry, and one with 0-form $\mathbb{Z}_{(N,p)}$ symmetry and no 1-form symmetry, and that we may pass between these two theories by gauging these symmetries. On the other hand, when $(N, p) = 1$, there is no such symmetry, and correspondingly only one choice of theory.

$\boldsymbol{T[L(p,1)], \mathfrak{su}(N)]}$ Let us first consider the case of $L(p, 1)$. Then we may take the decomposition graph, $\Omega_{[p]}$, to have a single node with label p, and so $\widehat{T}[\Omega_{[p]}, SU(N)]$ is given by

$$\widehat{T}[\Omega_{[p]}, SU(N)] = SU(N)_p \;+\; \text{adjoint scalar}\,. \tag{5.71}$$

This theory has a $\mathbb{Z}_N$ 1-form symmetry, however, due to the Chern-Simons term, it has an 't Hooft anomaly with coefficient p, and so only a $Z = \mathbb{Z}_{(N,p)}$ subgroup is non-anomalous. Comparing to (5.70), we see we may identify this with

$$Z = H^1(L(p,1), \mathbb{Z}_N) \cong \mathbb{Z}_{(N,p)}\,, \tag{5.72}$$

as expected from (5.68).

In the case where p is a multiple of N, there is no remaining anomalous symmetry, and we simply have

$$N|p \;:\quad T[L(p,1), \mathfrak{su}(N)] = SU(N)_p \;+\; \text{adjoint scalar}\,. \tag{5.73}$$

More generally, we must also decouple the anomalous part of the symmetry, which is contained in the quotient, $\Gamma/Z = \mathbb{Z}_N/\mathbb{Z}_{(p,N)} \cong \mathbb{Z}_d$, where $d \equiv N/(N,p)$. For example, consider the case where $(N,p) = 1$, so that $d = N$. Then, to accomplish this, we must couple to the theory $\mathcal{T}_{\mathbb{Z}_N}$ with a $\mathbb{Z}_N$ 1-form symmetry of maximal anomaly, which in the present case may be taken as

$$\mathcal{T}_{\mathbb{Z}_N} = U(1)_N \text{ Chern-Simons theory}\,. \tag{5.74}$$

Thus, the prescription in (5.67) tells us we should define

$$T[L(p,1), \mathfrak{su}(N)] \equiv \Big((SU(N)_p \;+\; \text{adjoint scalar}) \otimes U(1)_{-N} \Big)/\mathbb{Z}_N\,. \tag{5.75}$$

This defines the theory corresponding to the subgroup $H = 1$. When $(N,p) = 1$, this is the only choice, but more generally, let us choose some integer k that divides (N,p). Then the theory has an anomaly-free 1-form $\mathbb{Z}_k$ symmetry which we may gauge. This then defines the theory

$$T[L(p,1), \mathfrak{su}(N), \mathbb{Z}_k] \cong T[L(p,1), \mathfrak{su}(N)]/\mathbb{Z}_k\,, \tag{5.76}$$

and this theory has a 0-form $\mathbb{Z}_k$ symmetry. We may gauge any of the non-anomalous $\mathbb{Z}_k$ symmetries so there might be various choices of global structure. The simplest

example is $N = 2$. Then, if p is even we may gauge a 1-form $\mathbb{Z}_2$ symmetry passing over to gauge group $SO(3)$. If p is odd this is not possible and only the $SU(2)$ version exists.

An important special case is the theory $T[S^3, \mathfrak{su}(N)]$. Recall that $S^3 = L(1,1)$ so in this case, we have

$$\widehat{T}[\Omega_{[1]}, SU(N)] = SU(N)_1 \ + \ \text{adjoint scalar}\,. \tag{5.77}$$

From (5.26), this theory is dual to $(N-1)$ free chiral multiplets tensored with a $U(1)_N$ topological sector. This is precisely the decoupling behavior conjectured in (5.66), providing an explicit example where this conjecture holds. Then applying the decoupling procedure above, we find

$$T[S^3, \mathfrak{su}(N)] \cong \ (N-1) \text{ free chiral multiplets}\,. \tag{5.78}$$

It is important that this theory has only a single BPS state in order for the number of such states to be a topological invariant of general M_3. Namely, for any such M_3 we can take a connected sum with S^3, which tensors $T[M_3]$ with a copy of $T[S^3]$, and for this to leave the number of BPS states invariant, the latter should have only one BPS state. Note this is only true after performing the decoupling procedure above.

$\boldsymbol{T[L(p,q)], \mathfrak{su}(N)]}$ For more general $L(p,q)$, we use the linear graph, $\Omega_{[k_1,\cdots,k_n]}$, associated to the continued fraction expansion, $[k_1, ..., k_n]$, of $\frac{p}{q}$, as described in section 5.1. Then $\widehat{T}[\Omega_{[k_1,\cdots,k_n]}, SU(N)]$ is given by a sequence of $SU(N)$ gauge groups with level k_i Chern-Simons terms, and connected by copies of the $T(SU(N))$ theory. However, as noted above, this linear quiver theory is not quite the theory $T[L(p,q), \mathfrak{su}(N)]$ itself, as it contains an additional decoupled topological sector that must be removed.

From the general considerations above, we expect that the $T[L(p,q), \mathfrak{su}(N)]$ theory has a 1-form symmetry group isomorphic to

$$\Upsilon = H^1(L(p,q), \mathbb{Z}_N) = \mathbb{Z}_{(N,p)}\,. \tag{5.79}$$

To identify this symmetry, we need to determine the anomaly matrix $\mathcal{A}$, using the discussion in section 4.2.2. Clearly, by comparing (4.19) and (4.23) the diagonal terms of the anomaly matrix are given by the Chern-Simons levels $\mathcal{A}_{ii} = k_i$. Furthermore, it is known that the anomaly polynomial of the $T(SU(N))$ theory is given by [170]

$$S_{\text{anom}}^{T(SU(N))} = -\frac{2\pi}{N}\int_{M_4} w_2^{(1)} \cup w_2^{(2)}\,. \tag{5.80}$$

This can be verified in the dual trinion description by generalising (4.22) with $k = -K_1 = -K_2 = 1$ to general N. Thus, the anomaly matrix agrees with the linking matrix (5.12), i.e.,

$$\mathcal{A} = \begin{pmatrix} k_1 & -1 & 0 & \cdots & & 0 \\ -1 & k_2 & -1 & & & \\ 0 & -1 & k_3 & & & \\ \vdots & & & \ddots & & \vdots \\ & & & & k_{n-1} & -1 \\ 0 & & & \cdots & -1 & k_n \end{pmatrix} \mod N\,. \tag{5.81}$$

Thus this theory has a $\Gamma = {\mathbb{Z}_N}^n$ 1-form symmetry. However, many of these symmetries are anomalous, and we are interested in the non-anomalous subgroup, Z. This can be identified as the kernel of $\mathcal{A}$ acting on Γ. One may compute that

$$\det \mathcal{A} = p \mod N\,. \tag{5.82}$$

This implies that the anomaly matrix has a (unique, up to scalar multiplication) null-vector δ precisely when the RHS of (5.79) is non-trivial. We call δ the central element, and in general it generates the central subgroup $Z \cong \mathbb{Z}_{(N,p)}$. Thus we have identified the expected 1-form symmetry in (5.79).

Next let us discuss the remaining, anomalous 1-form symmetry. For simplicity, we consider the case of N prime. Then, since $\Gamma \cong {\mathbb{Z}_N}^n$ is freely generated, we find that it splits into a direct sum of the centre Z and the anomalous part Γ/Z

$$\Gamma = {\mathbb{Z}_N}^n \cong Z \oplus (\Gamma/Z)\,, \tag{5.83}$$

where

$$Z = \begin{cases} \mathbb{Z}_N & N|p \\ 1 & \text{else} \end{cases}, \qquad \Gamma/Z = \begin{cases} {\mathbb{Z}_N}^{n-1} & N|p \\ {\mathbb{Z}_N}^{n} & \text{else} \end{cases}. \tag{5.84}$$

To decouple the anomalous (Γ/Z) 1-form symmetry and obtain the $T[L(p,q),\mathfrak{su}(N)]$ theory, following (5.67) we define

$$T[L(p,q),\mathfrak{su}(N)] \equiv (\widehat{T}[\Omega, SU(N)] \otimes \mathcal{T}_{\Gamma/Z,-\mathcal{A}})/(\Gamma/Z)\,. \tag{5.85}$$

For example, if $\mathcal{A}$ can be diagonalised over $\mathbb{Z}_N$, then we may take $\mathcal{T}_{\Gamma/Z,-\mathcal{A}}$ to equal $\text{rank}(\Gamma/Z)$ copies of the $U(1)_{-N}$ CS theory.

The theory obtained after this procedure retains the expected anomaly-free $Z \cong \Upsilon = H^1(L(p,q),\mathbb{Z}_N)$ 1-form symmetry, and we claim this is the theory obtained by compactification of the 6d theory on $L(p,q)$. One may then obtain $T[L(p,q),\mathfrak{su}(N),H]$ for $H \leq \Upsilon$ by gauging non-anomalous subgroups, as above.

Seifert Quivers Next we look at more general quivers associated to Seifert manifolds. For simplicity, we focus on the gauge algebra $\mathfrak{g} = \mathfrak{su}(2)$, which already reveals much of the interesting structure. We also restrict ourselves to graphs $\Omega_{(k_i)}$ with intersection matrix

$$Q = \begin{pmatrix} 0 & -1 & -1 & -1 \\ -1 & k_1 & 0 & 0 \\ -1 & 0 & k_2 & 0 \\ -1 & 0 & 0 & k_3 \end{pmatrix}, \tag{5.86}$$

with the k_i chosen to correspond to the manifolds S^3/Γ_{ADE} in (B.8). If any $k_i = 1$, M_3 is a Lens space, which were discussed in the previous section, so we will consider $k_i = (2,-2,n-2)$ for D_n and $k_i = (3,-2,m-3)$ for E_m. The theory $\widehat{T}[\Omega_{(k_i)}, SU(2)]$ has a $\Gamma = {\mathbb{Z}_2}^4$ 1-form symmetry, which in the notation of (5.83) splits as

$$\Gamma \cong Z \oplus (\Gamma/Z)\,, \qquad Z = H^1(M_3,\mathbb{Z}_2)\,, \tag{5.87}$$

depending on the choice of M_3. Concretely,

$$H^1(S^3/\Gamma_{D_n},\mathbb{Z}_2)=\begin{cases}\mathbb{Z}_2\times\mathbb{Z}_2 & n \text{ even}\\ \mathbb{Z}_2 & n \text{ odd}\end{cases},\qquad H^1(S^3/\Gamma_{E_m},\mathbb{Z}_2)=\begin{cases}1 & m \text{ even}\\ \mathbb{Z}_2 & m \text{ odd}\end{cases}. \tag{5.88}$$

We then define $T[S^3/\Gamma_{DE},\mathfrak{g}]$ in analogy to (5.85).

Let us now focus on the D_n case. The kernel of the anomaly matrix $\mathcal{A}_n$[8] has dimension two if n is even and dimension one if n is odd, in agreement with (5.88). For n odd the 1-form symmetry of $T[S^3/\Gamma_{D_n},\mathfrak{su}(2)]$ is generated by $\delta^1=(0,0,1,1)$. Gauging this symmetry gives us the theory $T[S^3/\Gamma_{D_n},\mathfrak{su}(2),\mathbb{Z}_2^{(1)}]$. For n even there is an additional $\mathbb{Z}_2$ 1-form symmetry generated by $\delta^2=(0,1,0,1)$. Thus there are multiple choices for H, namely

$$\begin{aligned}&T[S^3/\Gamma_{D_n},\mathfrak{su}(2),\mathbb{Z}_2^{(i)}]\,,\quad i=1,2,3\\ &T[S^3/\Gamma_{D_n},\mathfrak{su}(2),\mathbb{Z}_2\times\mathbb{Z}_2]\,,\end{aligned} \tag{5.89}$$

where $\mathbb{Z}_2^{(3)}$ is the diagonal subgroup generated by $\delta^3=\delta^1+\delta^2$. The E_m case does not unveil any additional structure with E_7 being equivalent to D_n with n odd and for E_m, m even, there is no 1-form symmetry.

5.2.5 Geometric Interpretation of Global Structure

Here we comment on a geometric picture for the 1-form symmetry above in terms of a compactification of the 6d theory. Let us first focus on the case $M_3=L(p,1)$ for simplicity, where we found a non-anomalous $\mathbb{Z}_N$ 1-form symmetry generated by δ if $p=0 \mod N$. Recall the possible 1-form symmetry group operators on W_3 are constructed by first picking a 1-cocycle on M_3, or equivalently a 2-cycle, with $\mathbb{Z}_N$ coefficients. We may describe this explicitly using the Heegaard decomposition of $L(p,1)$, as shown in figure 5.5. Here we show the 2-cycle in red on the left solid torus,

[8]Recall that this is given by $\mathcal{A}=Q \mod 2$.

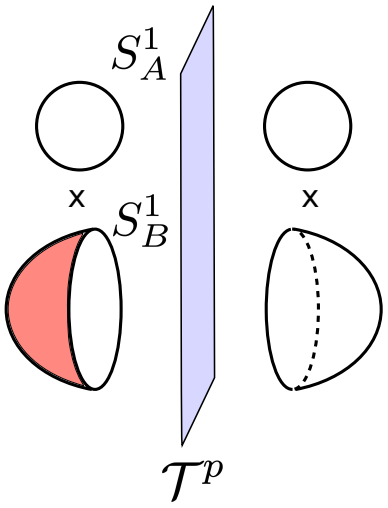

Figure 5.5: Heegaard decomposition of $L(p,1)$, where the two solid tori are glued with a T^p transformation. In red is shown the 2 cycle with $\mathbb{Z}_N$ coefficients. For this to be consistently extended to the right side, we must have $p = 0 \mod N$, which reflects the fact that the homology group is non-trivial only in this case.

which we take to generate a $\mathbb{Z}_N$ 2-chain on the left hand side. At the boundary, we have labelled the two cycles of the torus by S^1_A and S^1_B. We see the 1-cycle wrapped by the 2-cycle as it crosses the boundary is $(0,1)$ in the (A,B) basis. Upon passing through the T^p transformation, this will now wrap the cycle $(p,1) = T^p(0,1)$. Then for this to be contractible on the right side, so that we can consistently close the 2-cycle, we see that we must impose $p = 0 \mod N$. This is the geometric origin of the fact that the $\mathbb{Z}_N$ homology is equal to $\mathbb{Z}_N$ only in this case. Then this maps precisely to the generator of the $\mathbb{Z}_N$ 1-form symmetry that is present in $T[L(p,1), \mathfrak{su}(N)]$ in this case.

Let us now consider a more general Lens space. Recall from the previous subsection that, in this case, the 1-form symmetry is $\mathbb{Z}_N$ when p is a multiple of N, and is generated by an element δ inside the ${\mathbb{Z}_N}^n$ 1-form symmetry of the linear quiver theory, $\widehat{T}[\Omega_{[k_1,\cdots,k_n]}, SU(N)]$. Explicitly, the components of δ are

$$\delta = (p_1, ..., p_n) \ , \tag{5.90}$$

where we have defined

$$p_j = \det(\mathcal{A}_j), \quad j = 0, ..., n, \quad \mathcal{A}_j = j \times j \text{ upper left submatrix of } \mathcal{A}\,. \tag{5.91}$$

We have

$$p_0 = 1, \quad p_1 = k_1, \quad p_2 = k_1 k_2 - 1, \quad \cdots, \quad p_{n-1} = q, \quad p_n = p\,. \tag{5.92}$$

In figure 5.6 we have drawn the analogue of figure 5.5 for a more general Lens space corresponding to gluing by an $SL(2,\mathbb{Z})$ element

$$\varphi_{p,q} = T^{k_1} S T^{k_2} .... S T^{k_n}\,. \tag{5.93}$$

As above, we start with the 2-cycle wrapping the disk inside the solid torus on the left. We call this the generating 2-cycle. The intermediate segments in the diagram have the form of an interval times a torus, which we label as $S^1_A \times S^1_B$ as above, and the 2-cycle will lie along this interval, and wrap some cycle of the torus. In fact the cycle wrapped after the ith wall is given in the (A, B) basis by

$$\begin{pmatrix} p_i \\ q_i \end{pmatrix} \equiv \begin{pmatrix} p_i \\ p_{i-1} \end{pmatrix}\,, \tag{5.94}$$

where the p_i are defined in (5.92). Here $L(p_i, q_i)$ is the space we would obtain if we were to cap off after the ith step.

Note that in each segment, we are compactifying the 6d theory on a torus times an interval, which leads to the 4d $\mathfrak{su}(N)$ $\mathcal{N} = 4$ theory on an interval. Moreover, the cycles of the torus Poincaré dual to the polarisation Λ determine the global form of the $\mathfrak{s}u(N)$ theory we obtain in 4d [112, 174]. Let us give a quick review. Given a Lie algebra $\mathfrak{su}(N)$ we can characterise the global structure of the gauge group in a phase of the 4d $\mathcal{N} = 4$ by the allowed line operators. They are characterised by two integers

$$(z_e, z_m) \in \mathbb{Z}_N \times \mathbb{Z}_N\,, \tag{5.95}$$

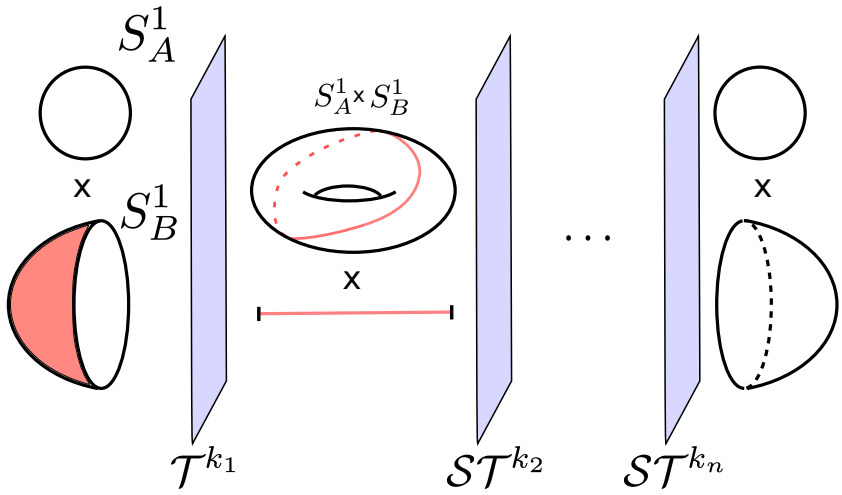

Figure 5.6: Heegaard decomposition of $L(p,q)$ for linear quiver, where the two solid tori are glued with an $SL(2,\mathbb{Z})$ transformation.

where with $(1,0)$ and $(0,1)$ we label the minimal Wilson and 't Hooft lines, respectively. Then, the charge lattice of a gauge group G is spanned by the allowed line operator charges. For N prime the structure is particularly simple. For $G = SU(N)$ only the Wilson lines are allowed, i.e., the charge lattice is generated by $(1,0)$. On the other hand, there are N different ways to define the $\mathbb{Z}_N$ quotients. The charge lattice of $G = PSU(N)_n$ is generated by the dyonic line $(n,1)$. Here, $n = 0,\ldots,N-1$ denotes the different choices of gauge groups. An $SL(2,\mathbb{Z})$ transformation acts on the line operators as

$$T:\ (z_e,z_m)\to(z_e+z_m,z_m)\,,\qquad S:\ (z_e,z_m)\to(z_m,-z_e)\,. \tag{5.96}$$

From this prescription we can determine how the T and S transformations change the gauge group in the related phases. If N is prime they simply act as

$$\begin{aligned} T:&\quad SU(N)\to SU(N) && PSU(N)_n\to PSU(N)_{n+1}\\ S:&\quad SU(N)\leftrightarrow PSU(N)_0 && PSU(N)_n\leftrightarrow PSU(N)_{1/n}\,. \end{aligned} \tag{5.97}$$

For N not prime this is more involved as we have to also take into account the phases where a subgroup of $\mathbb{Z}_N$ is gauged. The precise prescription can be found in [174].

If we look at the transformation behavior of (5.96) we see that it agrees with the

geometric behavior of (p_i, q_i), i.e.,

$$T: \ \frac{p}{q} \to \frac{p+q}{q}\,, \qquad S: \ \frac{p}{q} \to \frac{q}{-p}\,. \tag{5.98}$$

It is thus intuitive to identify the values (p_i, q_i), labelling the generating 2-cycle at some point in the Heegaard splitting, with the gauge group of the 4d $\mathcal{N} = 4$ theory on the respective interval. In order to make sense of this we have to assign the value $(0, 1)$, i.e., gauge group $PSU(N)_0$, to the generating 2-cycle on the left cap of the Heegaard splitting. The condition $p = 0$ ensures that the gauge group on the right cap is also $PSU(N)_0$, i.e., the cycle is contractible. Let us for example consider $\mathfrak{g} = \mathfrak{su}(2)$. Then, the three choices of gauge groups are

(p_i, q_i)	$(1,0)$	$(0,1)$	$(1,1)$
G	$SU(2)$	$SO(3)_+$	$SO(3)_-$

(5.99)

In order to obtain the $H = \mathbb{Z}_2$ version of the theory we now have to gauge all the nodes where the gauge group is $SO(3)$. In order for this to be globally consistent, we have to end up with an $SO(3)_+$ gauge group on the right cap, i.e., $p = 0$. We can easily generalise this to any prime N.

More generally, for N not prime, we can define any other $H = \mathbb{Z}_k$ version, where k divides N, provided k is a multiple of (N, p). To this end we assign the charge vector $(0, \frac{N}{k})$ to $(SU(N)/\mathbb{Z}_k)_0$, i.e., we let the generating 2-cycle wrap the disk $\frac{N}{k}$ times. Then, we can go through the Heegaard splitting as before, but at each step the charges are multiples of $\frac{N}{k}$ and thus non-anomalous.

5.3 Bethe Vacua for $T[M_3, \mathfrak{g}]$

In this section we study the set of supersymmetric vacua of the theory $T[M_3, \mathfrak{g}]$ for M_3 a Seifert manifold with $g = 0$. This provides a detailed test of several of the general features described above. In the next section, we compare the number of vacua to

the expectation from the 3d-3d correspondence, which maps this observable to the counting of certain flat connections on M_3, and find agreement.

We will focus on the cases of $\mathfrak{g} = \mathfrak{u}(1)$ and $\mathfrak{su}(2)$. For the latter we will use the Bethe ansatz equation approach to studying supersymmetric vacua of 3d $\mathcal{N} = 2$ gauge theories of [106], which we briefly review in section 5.3.2.

5.3.1 Abelian Case

The theory with $G = U(1)$ is free and has featured in [91]. As discussed in section 5.2.3 the theory is independent of the specific choice of graph Ω for M_3, so we can immediately define $T[M_3, U(1)]$. The bosonic Lagrangian is determined by the linking matrix of M_3

$$\mathcal{L}_{\text{CS}} = \frac{1}{4\pi} \sum_{i,j=1}^{n} Q_{ij} \; A_i \wedge dA_j \,, \tag{5.100}$$

as well as a set of adjoint scalars. Since the centre of mass field is massless there is a flat direction and the index is ill-defined. This can be remedied by removing this mode and defining the index of $T[M_3, U(1)]$ as the number of vacua of (5.100). This modified index is computed by consecutively integrating out the gauge fields and equals

$$I(T[M_3, U(1)]) = |\det(Q_{ij})| \,. \tag{5.101}$$

For the case of a Seifert manifold $M_3 = [d; 0; (p_i, q_i)]$, the number of vacua is

$$I(T[M_3, U(1)]) = \left| \left(\sum_{i=1}^{r} \frac{q_i}{p_i} - d \right) \prod_{i=1}^{r} p_i \right| \,. \tag{5.102}$$

For the manifolds discussed in this chapter this simplifies to

$$I(T[L(p,q), U(1)]) = p \,, \quad I(T[M^{\text{Prism}}_{p_3,q_3}, U(1)]) = 4|q_3| \,, \quad I(T[S^3/\Gamma_{E_m}, U(1)]) = (9-m) \,. \tag{5.103}$$

5.3.2 Twisted Superpotentials and Coulomb Branch Vacua

To compute the vacua for non-abelian gauge groups, we will use the framework developed in [106], i.e. we compute the vacua using the twisted superpotential and counting the solutions to the resulting Bethe equations.

Let us consider a 3d $\mathcal{N} = 2$ gauge theory of gauge group G on $\mathbb{R}^2 \times S^1$. The dynamics of the Coulomb branch is governed by the twisted superpotential, $\mathcal{W}(u, m)$, where u is the Coulomb branch variable

$$u = i\beta(\sigma + ia_0) \in \mathfrak{t}^{\mathbb{C}}/\Lambda_{\text{co-char}} \ , \tag{5.104}$$

where $\mathfrak{t}^{\mathbb{C}}$ is the complexified Cartan subalgebra, and β is the radius of the S^1. Here a_0 is the holonomy of the abelianised gauge field along the S^1

$$\frac{1}{2\pi}\oint_{S^1} A = a_0 \ , \tag{5.105}$$

and σ is the abelianised constant real scalar field in the vector multiplet. Similarly, $m = i\beta(\sigma_F + ia_{0,F})$ is a flavour group variable. Let us define T as the maximal torus of G and $\mathfrak{t}$ as the Cartan subalgebra. Then the lattice $\Lambda_{\text{co-char}}$ is the co-character lattice of G defined as the kernel of the exponential map

$$\exp : \mathfrak{t} \to T \ . \tag{5.106}$$

The large gauge transformation along S^1 is defined by

$$u \to u + \lambda \ , \tag{5.107}$$

where λ is an element in the lattice $\Lambda_{\text{co-char}}$.

The twisted superpotential receives a contribution from the classical CS level as well as the chiral multiplets of the theory. For gauge group $SU(2)$ we review the explicit structure of the twisted superpotential in detail in appendix B.2. To simplify the notation we use

$$x = e^{2\pi i u}, \quad z = e^{2\pi i \zeta} \ , \quad y = e^{2\pi i m} \ , \quad t = e^{2\pi i \tau} \ , \tag{5.108}$$

where t is the fugacity for the distinguished flavour symmetry in $\mathcal{N}=4$ theories, which corresponds to the $\mathcal{N}=2^*$ mass. If G contains a $U(1)$ factor, we turn on the FI parameter ζ for the associated topological symmetry.

For convenience we define the flux operators

$$\Pi_a = \exp\left(2\pi i \frac{\partial \mathcal{W}(u,m)}{\partial u_a}\right) , \qquad \Pi_\alpha = \exp\left(2\pi i \frac{\partial \mathcal{W}(u,m)}{\partial m_\alpha}\right) , \tag{5.109}$$

for the gauge and flavour symmetry, respectively. The Coulomb branch vacua are described by the solutions to the Bethe equations [106]

$$\mathcal{S}_{\text{BE}} = \{u_a \mid \Pi_a = 1 \ , \forall a = 1, \cdots \text{rank}(G), \quad w(u) \neq u, \forall w \in W_G\} / W_G \ , \tag{5.110}$$

where W_G is the Weyl group. Note that we removed the solutions which are fixed under the Weyl group action, which we call degenerate vacua.

5.3.3 Bethe Vacua for $\widehat{T}[\Omega, SU(2)]$ and $T[M_3, U(2)]$

Before constructing the theories $T[M_3, \mathfrak{g}, H]$ in general, we study the unphysical theory $\widehat{T}[\Omega, G]$, defined in section 5.1, focusing on Ω the graph of a Seifert manifold M_3 and $G = SU(2)$. This theory is defined by taking the Seifert quiver, connecting $SU(2)$ gauge nodes with level k_i CS-terms and $T(SU(2))$ S-walls and taking all gauge groups as $SU(2)$. A refinement including other choices of gauged 1-form symmetries will be the topic of section 5.3.4.

The $\widehat{T}[\Omega, SU(2)]$ theories are also used to construct the theories $T[M_3, U(2)]$. As discussed in section 5.2.1, we can define $T[M_3, U(2)]$ as a tensor product of the two decoupled theories

$$\widehat{T}[\Omega, SU(2)] \quad \text{and} \quad \widehat{T}[\Omega, U(1)_2] \, . \tag{5.111}$$

For each gauge node, we identify a non-anomalous $\mathbb{Z}_2$ subgroup of the 1-form symmetry, and gauge it to replace the gauge group at this node by $(U(1) \times SU(2))/\mathbb{Z}_2 \cong U(2)$.[9]

[9]Note this is the same description one obtains from the quiver $\widehat{T}[\Omega, U(2)]$, as follows from the

The $\Omega_{[k]}$ Theory As a simple example, let us first consider $\widehat{T}[\Omega_{[k]}, SU(2)]$, which can be described as the $\mathcal{N} = 2^*$ Chern-Simons theory at level k. The twisted superpotential for the $\mathcal{N} = 2^*$ CS theory is given by

$$\mathcal{W}_{T^k}^{\mathcal{N}=2^*} = k\mathcal{W}_{\rm CS}(u) + \mathcal{W}_{\rm adj}(u,\tau) \ , \tag{5.113}$$

see (B.16) and (B.17), such that the Coulomb branch vacua are determined as solutions to the Bethe equations

$$\Pi \equiv \exp\left(2\pi i \frac{\partial \mathcal{W}_{T^k}^{\mathcal{N}=2^*}}{\partial u}\right) = x^{2k}\left(\frac{x^2 - t^{-2}}{1 - x^2 t^{-2}}\right)^2 = 1 \, . \tag{5.114}$$

It is convenient to split this into two polynomial equations

$$\Pi^{1/2} = x^k \frac{x^2 - t^{-2}}{x^2 t^{-2} - 1} = \pm 1 \, . \tag{5.115}$$

Since the Weyl symmetry acts as

$$x \to x^{-1} \ , \tag{5.116}$$

the solutions at $x = \pm 1$ are degenerate vacua. When k is even, we have $k+2$ solutions from each sign of the equation (5.115). The degenerate vacua are contained in the solution for the bottom sign. Therefore we have $2k + 2$ regular solutions paired by the Weyl symmetry. The number of Coulomb branch vacua are $k + 1$. When k is odd, we have $k + 1$ regular vacua from each sign, paired by the Weyl symmetry.[10]

The Linear Quivers $\Omega_{[k_1,\cdots,k_n]}$ The graph for a general Lens space $L(p, q)$ is linear and we denote it by $\Omega_{[k_1,\cdots,k_n]}$. The corresponding quiver is shown in figure 5.7. To simplify the computation, we recall the duality (5.31) which relates the $T(SU(2))$ theory to the trinion T_2.[11]

---

more general fact that

$$U(N)_k = \frac{SU(N)_k \times U(1)_{Nk}}{\mathbb{Z}_N} \, . \tag{5.112}$$

Then, $T(U(N))$ can essentially be regarded as a tensor product of $T(SU(N))$ and $T(U(1))$ with level N BF coupling, with an additional operation to account for the $\mathbb{Z}_N$ quotient.

[10] A similar calculation was considered in [110]; see footnote 18 below for the relation between these computations.

[11] We should note that this also allows us to write a standard Lagrangian for these theories, which is not true using the usual $T(SU(2))$, as the $SU(2)$ is not manifest.

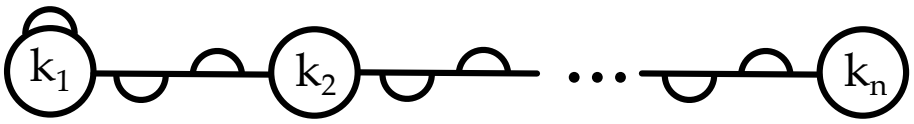

Figure 5.7: Quiver corresponding to $\Omega_{[k_1,\cdots,k_n]}$

In appendix B.2 we study the Bethe equations for the theories $\widehat{T}[\Omega_{[k_1,\cdots,k_n]}, SU(2)]$. These correspond to coupled polynomial equations, which can be solved using Gröbner basis techniques. By studying several examples up to length $n = 4$, we have found evidence for the following conjectural number of vacua for a general linear quiver

$$I(\widehat{T}[\Omega_{[k_1,\cdots,k_n]}, SU(2)]) = 2^{n-1}(p+1)\,. \tag{5.117}$$

It would be interesting to derive this formula analytically, but we leave this to future work.

Since $\widehat{T}[\Omega, U(1)_2]$ is the abelian Chern-Simons theory of section 5.3.1 with each Chern-Simons level multiplied by 2, the number of vacua is $|\det(2Q_{ij})| = 2^n p$. Putting this together, the tensor product in (5.111) has

$$I(\widehat{T}[\Omega, SU(2)] \;\otimes\; \widehat{T}[\Omega, U(1)_2]) = 2^{2n-1}p(p+1)\,. \tag{5.118}$$

Finally, we must implement the 1-form gauging. Each $\mathbb{Z}_2$ gauging reduces the number of vacua by a factor of four, consisting of a factor of $|\mathbb{Z}_2|$ for each of the two cycles in the T^2 we put the theory on. Thus, we find

$$I(T[L(p,q), U(2)]) = \frac{1}{2}p(p+1)\,. \tag{5.119}$$

Note this result no longer depends on the choice of Ω, in agreement with the logic in section 5.2.1.

Seifert Quivers For general Seifert manifolds the counting of vacua becomes computationally difficult. However for a subclass we are able to perform the analysis explictly. These are Seifert manifolds, which have base S^2 and three special fibres,

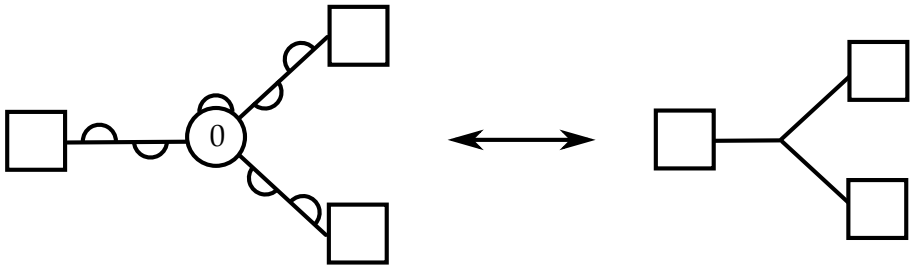

Figure 5.8: Duality to trinion theory: Three copies of $T(SU(N)) \cong T_N$

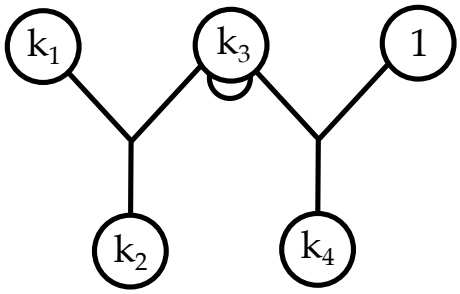

Figure 5.9: Quiver for two coupled trinions and an adjoint at the central node indicated by the arc. We denote this quiver by $\Omega_{(k_1,k_2,k_3,k_4,1)}$.

and are discussed in appendix B.1 and summarised in table 5.2. We can simplify the quiver using the trinion theory T_N, using the following duality: couple three copies of $T(SU(N))$ by identifying one of their flavour groups each and gauging it at Chern-Simons level zero, together with an adjoint scalar. This theory is dual to the trinion theory [160]. This means that if the degree in the Seifert data vanishes, we can write the quiver using the trinion description, as in figure 5.8. The vanishing of the degree can always be assumed using (5.10) and (5.11). Then, the graph $\Omega_{(k_i)}$[12] for the Seifert manifolds that we are interested in is given by figure 5.9. In order to guarantee that this corresponds to a Seifert manifold we have to impose $k_5 = 1$.

The graphs in figure 5.9 describe the Lens spaces $L(p,q)$, Prism manifolds $M^{\text{Prism}}_{p,q}$ and S^3/Γ_{E_m}. In each case we can compute the number of vacua $I(\widehat{T}[\Omega_{(k_i)}, SU(2)])$. Then, taking the abelian index in (5.102) and the $\mathbb{Z}_2$ gauging into account, we can

[12]For linear quivers we used the subscript $[k_1, \cdots, k_n]$. For the nonlinear quivers we usually indicate the CS-levels, depending on the associated graph.

M_3	k_i	$I(\widehat{T}[\Omega_{(k_i)}, SU(2)])$	$I(T[M_3, U(2)])$
$L(p,q)$, $\frac{p}{q} = [\widetilde{k}_1, \widetilde{k}_2, \widetilde{k}_3]$	(1,$\widetilde{k}_1$-1,$\widetilde{k}_2$-1,$\widetilde{k}_3$-1,1)	$4(p+1)$	$\binom{p+1}{2}$
$M^{\text{Prism}}_{p,q}$, $\frac{p}{q} = [\widetilde{k}_1, \widetilde{k}_2]$	(-2,2,$\widetilde{k}_1$-1,$\widetilde{k}_2$-1,1)	$2(p+1+8q)$	$q(p+1+8q)$
S^3/Γ_{E_m}	(-2,3,m-3,0,1)	24	$3(9-m)$

Table 5.2: Quiver data and vacuum count for various Seifert manifolds for $G = U(2)$

compute the physical Witten indices

$$I(T[M_3, U(2)]) = \frac{I(\widehat{T}[\Omega_{(k_i)}, SU(2)])\ I(T[M_3, U(1)])}{2^3}\,. \tag{5.120}$$

We summarise the results in table 5.2.

5.3.4 Bethe Vacua for $T[M_3, \mathfrak{su}(2), H]$

In this section we construct the physical theories $T[M_3, \mathfrak{su}(2), H]$ from $\widehat{T}[\Omega, SU(2)]$ and count the number of vacua. Recall that the unphysical theory $\widehat{T}$ is obtained by gauging all nodes of a graph Ω corresponding to the manifold M_3 at gauge group $SU(2)$. However, as discussed in section 5.2.4 the theory has anomalous $\mathbb{Z}_2$ 1-form symmetries associated to decoupled topological sectors, which need to be eliminated to obtain the physical theories.

The $\boldsymbol{\Omega_{[k]}}$ Theory First, consider the case $M_3 = L(k,1)$ using the minimal graph with a single node. The Bethe equation is

$$\Pi = x^{2k}\left(\frac{x^2t^2-1}{x^2-t^2}\right)^2\,, \tag{5.121}$$

where $x = e^{2\pi i u}$, which has $k+1$ solutions, after accounting for the Weyl symmetry $u \to -u$. These form the Hilbert space of $\widehat{T}[\Omega_{[k]}, SU(2)]$. To obtain the physical Witten index we need to decouple the topological sector. From the prescription in

section 5.2.4 we can deduce that

$$T[L(k,1),\mathfrak{su}(2)] = \begin{cases} \widehat{T}[\Omega_{[k]},SU(2)] & k \text{ even} \\ \left(\widehat{T}[\Omega_{[k]},SU(2)]\otimes U(1)_{-2}\right)/\mathbb{Z}_2 & k \text{ odd} \end{cases} . \tag{5.122}$$

For k even, the counting of vacua is therefore the same as above, while for k odd, the decoupling procedure removes a tensor factor of dimension 2, so that

$$I(T[L(k,1),\mathfrak{su}(2)]) = \begin{cases} k+1 & k \text{ even} \\ \frac{k+1}{2} & k \text{ odd} \end{cases} . \tag{5.123}$$

The above correspond to the $T[L(k,1),\mathfrak{su}(2),H=1]$ theories. When k is even, we may also consider the case $H=\mathbb{Z}_2$, which is obtained by gauging the non-anomalous $\mathbb{Z}_2$ 1-form symmetry of this theory. Thus, it will be important to understand how the 1-form symmetries act on the Bethe vacua of these 3d $\mathcal{N}=2$ theories. As discussed in appendix B.3, the space of T^2 vacua is naturally acted on by two 1-form charge operators, $U_{A,B}$, wrapping the two cycles of the torus. The action of these charge operators on the Bethe vacua is discussed in appendix B.3. In the present case, we find these operators act on the Bethe vacua as[13]

$$U_A|\widehat{u}\rangle = \widehat{x}^k\frac{\widehat{x}^2t^2-1}{\widehat{x}^2-t^2}|\widehat{u}\rangle\,, \qquad U_B|\widehat{u}\rangle = |\widehat{u}+\frac{1}{2}\rangle\,. \tag{5.124}$$

Note that in general, $U_AU_B=(-1)^kU_BU_A$, so for k even this symmetry is indeed non-anomalous. The irreducible representations are then 1-dimensional, and the Hilbert space decomposes into

$$\mathcal{H}\to\bigoplus_{\epsilon_A,\epsilon_B=\pm1}\mathcal{H}_{\epsilon_A\epsilon_B}\,, \tag{5.125}$$

with the $\epsilon_{A,B}$ the eigenvalues under $U_{A,B}$. We will be interested in the space of Bethe vacua V, which is a subspace of the full Hilbert space, that also decomposes as $V_{\epsilon_A\epsilon_B}$ under the 1-form charge operators wrapping the A and B cycles of the torus

$$V\to V_{++}\oplus V_{+-}\oplus V_{-+}\oplus V_{--}\,. \tag{5.126}$$

[13]The overall sign of U_A can be fixed by modular invariance.

We define

$$v_{\epsilon_A\epsilon_B} = \mathrm{Tr}_{\mathcal{H}_{\epsilon_A\epsilon_B}}(-1)^F = \mathrm{dim}V_{\epsilon_A\epsilon_B}\,, \tag{5.127}$$

which we refer to as the refined Witten index. Gauging the $\mathbb{Z}_2$ symmetry then amounts to projecting onto the V_{++} subspace, and including the twisted sectors, as discussed around (B.28). To analyze the decomposition (5.126) it is useful to split the common eigenbasis of the U into

$$|\widehat{v}_j^{\pm}\rangle = \frac{1}{\sqrt{2}}\left(|\widehat{u}_j\rangle \pm |\widehat{u}_j + \frac{1}{2}\rangle\right),\ j = 1, \dots \frac{k}{2}\,, \qquad |\widehat{u}^{B\text{-inv.}}\rangle = |\frac{1}{4}\rangle\,, \tag{5.128}$$

where $|\widehat{u}^{B\text{-inv.}}\rangle$ is invariant under U_B after using the Weyl-symmetry. Clearly

$$U_B|\widehat{v}_j^{\pm}\rangle = \pm|\widehat{v}_j^{\pm}\rangle\,, \qquad U_A|\widehat{u}^{B\text{-inv.}}\rangle = (-1)^{\frac{k}{2}}|\widehat{u}^{B\text{-inv.}}\rangle\,. \tag{5.129}$$

To determine v_{++} we still need to find the action of U_A on the $|\widehat{v}_j^{\pm}\rangle$. Alternatively, to count the solutions we can directly solve the equation $U_A = \pm 1$, and one finds the result always satisfies

$$v_{+-} = v_{-+}\,. \tag{5.130}$$

Physically, this corresponds to modular invariance along the T^2, obtained by exchanging A- and B-cycle.[14] Combining (5.129) and (5.130) we can show that the contribution to the Witten index from the untwisted sectors is

$$I_{\text{untwisted}}(T[L(k,1),\mathfrak{su}(2),\mathbb{Z}_2]) = v_{++} = \left\lfloor \frac{k}{4} \right\rfloor + 1\,. \tag{5.131}$$

To account for the twisted sectors, we note, as reviewed in appendix B.3 that these are associated to fixed points of the U_B operators. In the present case, there is a single such state[15], at $\widehat{u} = \frac{1}{4}$, and so we find

$$I(T[L(k,1),\mathfrak{su}(2),\mathbb{Z}_2]) = \left\lfloor \frac{k}{4} \right\rfloor + 2\,. \tag{5.132}$$

[14]In the following we will always assume that this is guaranteed to give analytic arguments. However, in all examples modular invariance can also be checked explicitly by evaluating U_A on the vacua.

[15]Note, that the sign of U_A in the twisted sector is again determined by modular invariance, and may differ from the one in the untwisted sector.

General Linear Quivers Next, consider the general linear quiver $\Omega_{[k_1,\cdots,k_n]}$ of length n, corresponding to $M_3 = L(p,q)$. The theory $\widehat{T}[\Omega_{[k_1,\cdots,k_n]}, SU(2)]$ has n 1-form symmetries, with anomaly matrix given by (5.81). This matrix has $\det(\mathcal{A}) = p$, and admits a single null vector if and only if p is even. The set of Bethe vacua on T^2 for a theory acted on by such a 1-form symmetry has the form,

$$\widehat{V} = V \otimes R^{\otimes m}\,, \qquad m = \begin{cases} n-1 & p \text{ even} \\ n & p \text{ odd} \end{cases}\,, \tag{5.133}$$

where R is a two dimensional representation of an anomalous $\mathbb{Z}_2$ 1-form symmetry. As noted in (5.117), we find

$$I(\widehat{T}[\Omega_{[k_1,\cdots,k_n]}, SU(2)]) = 2^{n-1}(p+1)\,, \tag{5.134}$$

and so we deduce that

$$I(T[L(p,q), \mathfrak{su}(2)]) = \dim(V) = \begin{cases} p+1 & p \text{ even} \\ \frac{p+1}{2} & p \text{ odd} \end{cases}\,, \tag{5.135}$$

agreeing with the expected q-independent result (5.123).

When p is even we may gauge an additional $\mathbb{Z}_2^{(\delta)}$ 1-form symmetry generated by δ, the central element in (5.90). This amounts to projecting onto the V_{++} eigenspace and by studying a few low n cases explicitly we find

$$I_{\text{untwisted}}(T[L(p,q), \mathfrak{su}(2), \mathbb{Z}_2^{(\delta)}]) = \left\lfloor \frac{p}{4} \right\rfloor + 1\,, \tag{5.136}$$

generalising (5.131). Additionally, we find that there is always a single twisted sector state, and so the answer for the full Witten index is

$$I(T[L(p,q), \mathfrak{su}(2), \mathbb{Z}_2^{(\delta)}]) = \left\lfloor \frac{p}{4} \right\rfloor + 2\,. \tag{5.137}$$

Gauged Trinion As a final example consider the manifolds S^3/Γ_{ADE} also discussed in section 5.2.4 and appendix B.1. Recall that the Seifert data can be written as

$$S^3/\Gamma_{ADE} \cong [0; 0; (k_1, 1), (k_2, 1), (k_3, 1)]\,, \tag{5.138}$$

with the k_i given by:

1. $(k_1, k_2, 1)$ for the Lens space with $\frac{p}{q} = [k_1 + 1, k_2 + 1]$

2. $(-2, 2, n-2)$ for S^3/Γ_{D_n}

3. $(-2, 3, m-3)$ for S^3/Γ_{E_m}.

The $\widehat{T}[\Omega_{(k_i)}, SU(2)]$ theory is the gauged trinion theory: a trifundamental chiral multiplet of $SU(2)$ with the three $SU(2)$ flavour symmetries gauged at levels k_1, k_2, k_3, and the three Bethe equations are given by

$$\Pi_i = x_i^{2k_i} \frac{(x_i x_j x_k - t)(x_i x_j - x_k t)(x_i x_k - x_j t)(x_i - x_j x_k t)}{(x_i x_j x_k t - 1)(x_i x_j t - x_k)(x_i x_k t - x_j)(x_i t - x_j x_k)}, \qquad i, j, k = 1, 2, 3\,, \tag{5.139}$$

defined in a cyclic way. Using Gröbner basis techniques we find that the number of solutions is given by[16]

$$\begin{aligned} I(\widehat{T}[\Omega_{(k_i)}, SU(2)]) &= (k_1+1)(k_2+1)(k_3+1) && \text{if } k_i \geq 0 \\ I(\widehat{T}[\Omega_{(k_i)}, SU(2)]) &= (k_1+1)(k_2+1)(-k_3+1) - 4k_1k_2 && \text{if } k_{1,2} \geq 0,\ k_3 \leq -2\,, \end{aligned} \tag{5.140}$$

after accounting for the Weyl symmetry.

To find the Witten index of $T[M_3, \mathfrak{su}(2)]$ we need to decouple the topological sector. If not all k_i are even, we can specify k_3 odd. Since only $k_i \mod 2$ is relevant for the anomalies, the decoupling of the topological sector is analogous to the Lens space, using the duality in figure 5.4. This case was discussed above. If all the k_i are even no decoupling is necessary. Putting this together we find

M_3	$L(p,q)$	S^3/Γ_{D_n}	S^3/Γ_{E_m}
$I(M_3, \mathfrak{su}(2)])$	$p+1$ p even	$n+7$ n even	3 m even
	$\frac{p+1}{2}$ p odd	$\frac{n+7}{2}$ n odd	6 m odd

(5.141)

[16] All other possibilities can be obtained by permutation of the k_i and parity symmetry.

The Hilbert space spanned by these vacua splits into the eigenspaces of the charge operators $U_{A,B}^{\delta^j}$

$$V \to \bigoplus_{\epsilon^j_{A,B}=\pm 1} V_{\epsilon_A^1\epsilon_B^1\cdots\epsilon_A^r\epsilon_B^r}\,, \qquad r = \mathrm{rk}\left(H^1(M_3,\mathbb{Z}_2)\right)\,, \tag{5.142}$$

where the δ^j generate the $\mathbb{Z}_2^r$ 1-form symmetry. Let us now study this explicitly. If two of the k_i, say k_1 and k_2, are even then the theory has a physical non-anomalous $\mathbb{Z}_2$ 1-form symmetry, as argued for in section 5.2.4. Thus, the theory has a 1-form symmetry generated by $\delta = (1,1,0)$. The charge operators act as, see (B.23),

$$\begin{aligned} U_A^\delta|\widehat{u}_1,\widehat{u}_2,\widehat{u}_3\rangle &= (\Pi_1\Pi_2)^{1/2}\,|\widehat{u}_1,\widehat{u}_2,\widehat{u}_3\rangle = \widehat{x}_1^{k_1}\widehat{x}_2^{k_2}\frac{(\widehat{x}_1\widehat{x}_2\widehat{x}_3-t)(\widehat{x}_1\widehat{x}_2-\widehat{x}_3 t)}{(\widehat{x}_3-\widehat{x}_1\widehat{x}_2 t)(1-\widehat{x}_1\widehat{x}_2\widehat{x}_3 t)}|\widehat{u}_1,\widehat{u}_2,\widehat{u}_3\rangle \\ U_B^\delta|\widehat{u}_1,\widehat{u}_2,\widehat{u}_3\rangle &= |\widehat{u}_1+\frac{1}{2},\widehat{u}_2+\frac{1}{2},\widehat{u}_3\rangle\,. \end{aligned} \tag{5.143}$$

We proceed as for the T^k theory and determine the solutions fixed under U_B^δ, which are given by

$$|\widehat{u}^{B\text{-inv.}}\rangle^j = |\frac{1}{4},\frac{1}{4},\widehat{u}_3^j\rangle\,. \tag{5.144}$$

By plugging in these solutions into the Bethe equations (5.139) we find that they reduce to

$$\Pi_{1,2} = 1\,, \qquad \Pi_3 = x_3^{2k_3}\left(\frac{x_3^2-t^2}{x_3^2t^2-1}\right)^2\,. \tag{5.145}$$

This is nothing but the T^{k_3} theory with an adjoint and thus has $|k_3|+1$ vacua.[17] These B-invariant vacua obey

$$U_A^\delta|\widehat{u}^{B\text{-inv.}}\rangle^j = (-1)^{\frac{k_1+k_2}{2}}|\widehat{u}^{B\text{-inv.}}\rangle^j\,, \qquad j=1,\ldots \begin{cases} |k_3|+1 & k_3 \text{ even} \\ \frac{|k_3|+1}{2} & k_3 \text{ odd} \end{cases}\,. \tag{5.146}$$

As before, the remaining vacua $|\widehat{v}^\pm\rangle$ split into pairs with eigenvalues ± 1 under U_B. Modular invariance fixes the dimension of the subspaces with $\epsilon_{A,B} = \pm 1$. We can repeat this for all choices of δ^j, $j = 1,\cdots,r$ to determine the refined Witten index

$$v_{\epsilon_A^1\epsilon_B^1\cdots\epsilon_A^r\epsilon_B^r} = \dim V_{\epsilon_A^1\epsilon_B^1\cdots\epsilon_A^r\epsilon_B^r}\,. \tag{5.147}$$

[17] This is the number of vacua before the decoupling so only half of them are physical if k_3 is odd.

The following discussion depends heavily on the rank of the maximal 1-form symmetry, $\Upsilon = \mathbb{Z}_2^r$:

1. Lens spaces $L(p,q)$, with p odd, and $S^3/\Gamma_{E_{m\text{ even}}}$ have no 1-form symmetry, i.e., $r = 0$. This means there is no further decomposition of V.

2. The manifolds $L(p,q)$, with p even, $S^3/\Gamma_{D_{n\text{ odd}}}$ and S^3/Γ_{E_7} have $r = 1$. We can study the dimension of the eigenspaces $V_{\epsilon_A\epsilon_B}$ which are summarised in table 5.3.[18] Recall that modular invariance implies $v_{+-} = v_{-+}$.

S^3/Γ_{ADE}, $r=1$	$\dim V$	v_{++}	v_{+-}	v_{--}
A_{p-1}, $p = 0 \mod 4$	$p+1$	$\frac{p}{4}+1$	$\frac{p}{4}$	$\frac{p}{4}$
A_{p-1}, $p = 2 \mod 4$	$p+1$	$\frac{p+2}{4}$	$\frac{p+2}{4}$	$\frac{p-2}{4}$
D_n, n odd	$\frac{n+7}{2}$	$\frac{n+1}{2}$	1	1
E_7	6	2	2	0

Table 5.3: Dimensions of the eigenspaces $V_{\epsilon_A\epsilon_B}$ for $\Upsilon = \mathbb{Z}_2$

Gauging the 1-form symmetry projects onto the subspace V_{++}, which yields the number of vacua in the untwisted sector. In addition, one finds the following contribution from the twisted sectors, which we recall are associated to the fixed points of U_B. We summarise the results in table 5.4.

M_3	untwisted sector	twisted sector	total index
$L(p,q)$, p even	$\left\lfloor \frac{p}{4} \right\rfloor + 1$	1	$\left\lfloor \frac{p}{4} \right\rfloor + 2$
S^3/Γ_{D_n}, n odd	$\frac{n+1}{2}$	$\frac{n-1}{2}$	n
S^3/Γ_{E_7}	2	2	4

Table 5.4: Indices of $T[M_3, \mathfrak{su}(2), \mathbb{Z}_2^{(\delta)}]$

[18] In [110], the number of Bethe vacua for the $\mathcal{N} = 2$ $SU(2)$ CS_k theory with one adjoint chiral multiplet was computed and compared to the number of flat $SU(2)$-connections on the Lens space. In our notation, their counting corresponds to the number of Bethe vacua for the $T[L(p,1), \mathfrak{su}(2), 1]$ theory with $\epsilon_A = 1$. We will see in section 5.4 that this prescription indeed agrees with the refined 3d-3d correspondence we propose.

3. The remaining case is $S^3/\Gamma_{D_n \text{ even}}$ with $r = 2$. As discussed in section 5.2.4 there are three choices of non-anomalous 1-form symmetries

$$\delta^1 = (0,1,1)\,, \quad \delta^2 = (1,0,1)\,, \quad \delta^3 = (1,1,0)\,, \tag{5.148}$$

where we take the first cohomology to be generated by δ^1 and δ^2.[19] We note the quiver has a symmetry which means that we can exchange the two $\mathbb{Z}_2$s, i.e.,

$$v_{\epsilon^1_A \epsilon^1_B \epsilon^2_A \epsilon^2_B} = v_{\epsilon^2_A \epsilon^2_B \epsilon^1_A \epsilon^1_B}\,. \tag{5.149}$$

Together with modular invariance we only need to specify the dimensions in table 5.5.

S^3/Γ_{ADE}, $r=2$	v_{++++}	v_{+++-}	v_{+-+-}	v_{+--+}	v_{++--}	v_{+---}	v_{----}
D_n, $n = 0 \mod 4$	$\frac{n}{4}+1$	1	$\frac{n}{4}$	0	1	0	$\frac{n}{4}$
D_n, $n = 2 \mod 4$	$\frac{n+2}{4}$	1	$\frac{n+2}{4}$	1	0	0	$\frac{n-2}{4}$

Table 5.5: Dimensions of the eigenspaces $V_{\epsilon^1_A \epsilon^1_B \epsilon^2_A \epsilon^2_B}$ for $\Upsilon = \mathbb{Z}_2^{(1)} \times \mathbb{Z}_2^{(2)}$. In both cases $\dim V = n + 7$.

To gauge, say, $\mathbb{Z}_2^{(1)}$ we need to project onto the subspace with $\epsilon^1_{A,B} = +1$. On the other hand, to gauge $\mathbb{Z}_2^{(3)}$, generated by $\delta^3 = \delta^1 + \delta^2$, we project onto $\epsilon^1_A \epsilon^2_A = +1 = \epsilon^1_B \epsilon^2_B$. Finally, we can gauge the full $\mathbb{Z}_2 \times \mathbb{Z}_2$ 1-form symmetry, projecting onto V_{++++}. The number of vacua in the untwisted and twisted sector respectively and the resulting indices for the different choices of H are summarised in tables 5.6 and 5.7.

H	untwisted sector	twisted sector	refined index
$\mathbb{Z}_2^{(1,2)}$	$\frac{n}{4}+4$	3	$\frac{n}{4}+7$
$\mathbb{Z}_2^{(3)}$	$n+1$	$n-1$	$2n$
$\mathbb{Z}_2 \times \mathbb{Z}_2$	$\frac{n}{4}+1$	$\frac{n}{4}+2$	$\frac{n}{2}+3$

Table 5.6: Refined index of $T[D_n, \mathfrak{su}(2), H]$ for $n = 0 \mod 4$

[19] Note that we need to specify this choice because the charge operators act in a distinct way.

H	untwisted sector	twisted sector	refined index
$\mathbb{Z}_2^{(1,2)}$	$\frac{n+2}{4}+2$	3	$\frac{n+2}{4}+5$
$\mathbb{Z}_2^{(3)}$	$n+1$	$n-1$	$2n$
$\mathbb{Z}_2\times\mathbb{Z}_2$	$\frac{n+2}{4}$	$\frac{n+2}{4}+2$	$\frac{n}{2}+3$

Table 5.7: Refined index of $T[D_n,\mathfrak{su}(2),H]$ for $n=2 \mod 4$

5.4 Flat Connections on M_3 and the 3d-3d Correspondence

In this section we use the results for the refined Witten index of the previous section to test the 3d-3d correspondence [93]. This correspondence predicts that the Witten index of the theory $T_{\mathcal{N}=2}[M_3,\mathfrak{g}]$ counts the flat $\mathfrak{g}^{\mathbb{C}}$ connections on the 3-manifold M_3, which has been extensively studied in the literature [110,156,157,175–177]. However, a more careful consideration of the global structure of the gauge group leads to a refinement of this statement.

The Witten index, or T^3 partition function, counts the number of BPS ground states in the Hilbert space of the $T[M_3,\mathfrak{g}]$ theory on $T^2\times\mathbb{R}$. This space is equivalently the Hilbert space of the 6d theory of type $\mathfrak{g}$ on $M_3\times T^2\times\mathbb{R}$. Compactifying in the opposite order, we see it is also the Hilbert space of a 4d $\mathcal{N}=4$ SYM theory with Lie algebra $\mathfrak{g}$ on $M_3\times\mathbb{R}$, where we take the GL topological twist along M_3 [91,178]. Now, the vacua for the $\mathcal{N}=4$ theory with gauge group G on this space can be identified with flat $G^{\mathbb{C}}$ connections on M_3 [178], and so one expects a relation between these flat connections and the T^2 vacua of the $T[M_3,\mathfrak{g}]$ theory. However, as we have seen above, the global form of the gauge group of the SYM theory depends on the choice of polarisation of the 6d theory, and this will determine the precise observable in $T[M_3,\mathfrak{g}]$ we must consider.

In the case of self-dual G, the Witten index of $T[M_3,G]$ simply counts the number of flat $G^{\mathbb{C}}$ connections on M_3. However, in the general case, we find the following

correspondence. Recall that the T^2 Hilbert space of the $T[M_3, \mathfrak{g}]$ theory is acted on by an anomaly-free 1-form symmetry with group $\Upsilon = H^1(M_3, Z_{\widetilde{G}})$. Then we may refine the Hilbert space into eigenspaces of the two 1-form operators, U_A^γ and U_B^γ, wrapping the two cycles of the torus

$$V \to \bigoplus_{\chi_{A,B} \in H^2(M_3, Z_{\widetilde{G}})} V_{\chi_A, \chi_B} \,, \qquad v_{\chi_A,\chi_B} \equiv \dim V_{\chi_A,\chi_B} \,. \tag{5.150}$$

On the other hand, we consider flat $\widetilde{G}^{\mathbb{C}}$ connections on M_3. More precisely, in addition to ordinary $\widetilde{G}^{\mathbb{C}}$ connections, we may consider connections which are not strictly $\widetilde{G}^{\mathbb{C}}$ connections, but rather connections for the quotient group, $\widetilde{G}^{\mathbb{C}}/Z_{\widetilde{G}}$. These may be classified according to their second Stiefel-Whitney class, $\omega \in H^2(M_3, Z_{\widetilde{G}})$, which measures the obstruction to lifting these to well-defined $\widetilde{G}^{\mathbb{C}}$ connections. In addition, the connections are acted on by large gauge transformations (LGTs), which are determined by elements of $H^1(M_3, Z_{\widetilde{G}})$. We may refine the flat connections into eigenspaces of these LGTs,[20] which are labelled by $\chi_{\mathrm{LGT}} \in H^2(M_3, Z_{\widetilde{G}})$. Then we claim[21]

$$\#\{\text{flat } \widetilde{G}^{\mathbb{C}}/Z_{\widetilde{G}} \text{ conn. } A \text{ with } w_2(A) = \omega \text{ and } \chi_{\mathrm{LGT}}\} = v_{\omega, \chi_{\mathrm{LGT}}} \,. \tag{5.151}$$

This formula can be obtained by comparing the 4d $\mathcal{N} = 4$ theory on $M_3 \times S^1_t$ and the $T[M_3]$ on $T^2 \times S^1_t$, where S^1_t is a distinguished time cycle [4]. We will test this conjecture in explicit examples below. One interesting feature of this formula is that modular invariance of the torus exchanges the two arguments on the RHS. This implies that the geometric quantity on the LHS also exhibits this symmetry under exchange of ω and χ_{LGT}, which is not obvious, but which we will verify in examples. This can also be understood as a consequence of S-duality of the 4d $\mathcal{N} = 4$ SYM theory.

[20] More formally, we may consider the vector space with basis given by the flat connections, on which the LGTs act linearly, and refine this space into eigenspaces of this action.

[21] More precisely, this formula holds as stated when the moduli space of flat connections is zero-dimensional, which is the case for the homology spheres we consider in this section. In general, we expect a generalisation in terms of a suitably defined Euler characteristic on the moduli space of flat connections on M_3.

5.4.1 Example: $T[M_3, U(N)]$

Let us first consider the choice of polarisation of the 6d theory associated to a self-dual group G. As described in section 5.2.3, this gives rise to an ordinary (rather than relative) QFT in six dimensions. In this case, the compactification to 3d gives the $T[M_3, G]$ theory, while the compactification on T^2 to 4d gives the $\mathcal{N} = 4$ SYM theory with gauge group G. Thus we expect that the Witten index of this theory counts the flat $G^{\mathbb{C}}$ connections on M_3. This correspondence in the case of G self-dual has been observed and checked in various examples, e.g., in [91, 110, 175].

First, we observe that in the case $G = U(1)$ on a general rational homology sphere M_3, the number of vacua of $T[M_3, U(1)]$ is the order of $H^1(M_3, \mathbb{Z})$. This is the same as the number of $U(1)^{\mathbb{C}} = \mathbb{C}^\times$ flat connections on M_3, as also mentioned in section 5.3.1, demonstrating the formula in this simple example.

Next consider the case of $G = U(N)$, so that $G^{\mathbb{C}} = GL(N, \mathbb{C})$. The theory $T[L(p, 1), U(N)]$ is the 3d $\mathcal{N} = 2$ $U(N)$ theory with level p Chern-Simons term and an adjoint chiral multiplet. The number of vacua is [91]

$$I(T[L(p,1), U(N)]) = \binom{N+p-1}{N} . \tag{5.152}$$

On the other hand, as shown in appendix B.4.1, this is also the number of flat $GL(N, \mathbb{C})$ connections on $L(p, 1)$.

For more general Seifert M_3, we may use the quiver Lagrangians and computations of the previous section in the case of $G = U(2)$. In section 5.3.3, we found

$$I(T[S^3/\Gamma_{D_n}, U(2)]) = n + 7 , \qquad I(T[S^3/\Gamma_{E_m}, U(2)]) = 3(9 - m) . \tag{5.153}$$

In appendix B.4.1 we find the same result for the number of flat $GL(2, \mathbb{C})$ connections on these spaces.

5.4.2 Example: $T[L(p,1),\mathfrak{su}(N)]$

Let us consider the theory associated to the Lens space, $L(p,1)$, which is a theory with $\mathfrak{su}(N)$ Lie algebra and level p CS term and an adjoint chiral multiplet. We focus on the case of N prime for simplicity. Then there are two cases to consider.

$GCD(N,p)=1$ From (5.152) we can deduce that

$$I(T[L(p,1),\mathfrak{su}(N)]) = \frac{1}{N}\binom{N+p-1}{N-1}. \tag{5.154}$$

Note that in this case, since $H^2(L(p,1),\mathbb{Z}_N)=1$, the formula (5.151) predicts that the Witten index of this theory should directly count the flat $PSL(N,\mathbb{C})$ connections on $L(p,1)$, and in this case, these are the same as $SL(N,\mathbb{C})$ connections. The latter are given by representations

$$\phi: \quad \pi_1(L(p,1)) \cong \mathbb{Z}_p \;\to\; SL(N,\mathbb{C}), \tag{5.155}$$

modulo $SL(N,\mathbb{C})$ transformation. Without loss of generality, we may take these representations to be diagonal, with generator given by

$$\mathrm{diag}\left(e^{\frac{2\pi i m_1}{p}}, e^{\frac{2\pi i m_2}{p}}, \cdots, e^{\frac{2\pi i m_N}{p}}\right), \qquad \sum_{i=1}^{N} m_i = 0 \mod p, \tag{5.156}$$

considered up to permutations. An arbitrary choice of $\{m_i\}$ may have a non-zero sum modulo p, however shifting $m_i \to m_i+1$ shifts this sum by N, and so precisely one element in the orbit under this $\mathbb{Z}_p$ action will have sum zero. Thus we have

$$\#\{\text{flat } SL(N,\mathbb{C}) \text{ conn. on } L(p,1)\} \;=\; \frac{1}{p}\binom{N+p-1}{N}, \tag{5.157}$$

which equals (5.154).

$GCD(N,p)=N$ Recall that $T[L(p,1),\mathfrak{su}(N)] = \widehat{T}[\Omega_{[p]}, SU(N)]$ is the $SU(N)_p$ theory. This has an anomaly-free 1-form symmetry, and so the Hilbert space decomposes as

$$V = \bigoplus_{\chi_A,\chi_B\in\mathbb{Z}_N} V_{\chi_A\chi_B}, \tag{5.158}$$

where χ_A, χ_B run over the characters of $\mathbb{Z}_N$. This is a generalisation of (5.126) with the prescription that

$$\epsilon_{A,B} = \exp\left(\frac{2\pi i \chi_{A,B}}{N}\right) . \tag{5.159}$$

Let us consider $N = 2$ for simplicity. Then the dimensions of the $V_{\chi_A \chi_B}$ are summarised in table 5.3 in terms of $\epsilon_{A,B}$. Let us compare to the flat connections on $L(p,1)$, using the formula (5.151). Let us check this by counting the flat $PSL'(2,\mathbb{C})$ connections explicitly. These are given by homomorphisms from $\pi_1(L(p,1)) \cong \mathbb{Z}_p$ into $PSL(2,\mathbb{C})$, but considered only up to conjugation by $SL(2,\mathbb{C})$. Without loss of generality we may write the image of the generator of $\mathbb{Z}_p$ as $\mathrm{diag}(\alpha, \alpha^{-1})$, (written as an $SL(2,\mathbb{C})$ matrix), where

$$\alpha^p = \pm 1, \quad \alpha \sim \alpha^{-1} , \tag{5.160}$$

where we identify by Weyl symmetry. We can classify the connections according to their class in $H^2(L(p,1),\mathbb{Z}_2) = \mathbb{Z}_2$, which in this case is determined by $\alpha^p \in \{\pm 1\}$. These solutions are also acted on by LGTs, which act as multiplication by the $\mathbb{Z}_2$ centre of $SL(2,\mathbb{C})$, and take

$$\alpha \to -\alpha . \tag{5.161}$$

All the solutions therefore come in pairs, $\pm\alpha$, except for the solution $\alpha = i$, which is Weyl-equivalent to $-\alpha$.

Now if we project onto the LGT-invariant solutions, which is the same as considering $PSL(2,\mathbb{C})$ connections with $w_2 = \omega$, we find

ω	0	1
$L(p,q)\,,\ p = 0 \mod 4$	$\frac{p}{4} + 1$	$\frac{p}{4}$
$L(p,q)\,,\ p = 2 \mod 4$	$\frac{p+2}{4}$	$\frac{p+2}{4}$

(5.162)

From (5.151), map to the sectors in table 5.3 with $\chi_B = 0$, along with $\chi_A = \omega$, and one verifies that these precisely match. On the other hand, for each pair $(\alpha, -\alpha)$ with

$\alpha \neq i$, we can also construct an antisymmetric formal linear combination of solutions with $\chi_{LGT} = 1$. Thus in this we sector find a similar counting, but now with the contribution of $\alpha = i$ removed. Thus, the number of flat $PSL'(2,\mathbb{C})$ connections with $w_2 = \omega$ and $\chi_{LGT} = 1$ is given by

ω	0	1
$L(p,q)\,,\ p = 0 \mod 4$	$\frac{p}{4}$	$\frac{p}{4}$
$L(p,q)\,,\ p = 2 \mod 4$	$\frac{p+2}{4}$	$\frac{p-2}{4}$

(5.163)

One can check this matches the remaining entries in table 5.3, with $\chi_B = 1$.

One interesting feature of this calculation is that modular invariance of the field theory implies a relation between the Stiefel-Whitney class and LGT behaviour of the flat $PSL'(2,\mathbb{C})$ connections. We are not aware of a simple derivation of this fact.

5.4.3 Example: Gauged Trinion

As a final example, we consider the theory associated to the S^3/Γ_{DE} discussed in section 5.3.4. Note that the analysis for $L(p,q)$ is independent of q and is thus covered by section 5.4.2. We again focus on $N = 2$, where the results for the vacuum counting, refined by 1-form charges, are summarised in tables 5.3 and 5.5.

Let us compare this to the flat connection counting, which is reviewed in appendix B.4.2. The Seifert data of a Seifert manifold with three exceptional fibres fixes its fundamental group (B.34). In the general case the number of $PSL(2,\mathbb{C})$ representations is given by (B.40) and their Stiefel-Whitney classes can be computed explicitly. We find for the flat $PSL(2,\mathbb{C})$ connections with $w_2 = \omega \in H^2(M_3,\mathbb{Z}_2)$

ω	(0,0)	(1,0)	(0,1)	(1,1)
$D_n\,,\ n = 0 \mod 4$	$\frac{n}{4}+1$	1	1	$\frac{n}{4}$
$D_n\,,\ n = 2 \mod 4$	$\frac{n+2}{4}$	1	1	$\frac{n+2}{4}$

ω	0	1
$D_n\,,\ n$ odd	$\frac{n+1}{2}$	1
E_7	2	2

(5.164)

For E_6 and E_8 there is no distinction of the connections in terms of SW classes.

To compare this to the field theory, we recall that the $PSL(2,\mathbb{C})$ connections correspond to the $PSL'(2,\mathbb{C})$ connections with $\chi_{LGT} = 0$. Then we may compare the entries above to the relevant entries in tables 5.3 and 5.5 with $\chi_B = 0$. For example, for D_n with $n = 0 \pmod 4$, we see $v_{++++} = \frac{n}{4}$, agreeing with the $\omega = (0,0)$ entry above, and one may similarly compare the remaining entries.

We can also check the flat connections with non-trivial χ_{LGT}. Let us analyze the case of S^3/Γ_{D_n} for n even. Then one can classify them under Stiefel-Whitney class, ω, and χ_{LGT}. Let us describe this explicitly in the case $n = 4$. Here there is one trivial connection, three other reducible connections, and one irreducible connection. The trivial connection is acted on freely by LGTs, and so contributes states with $\omega = (0,0)$ and all four values of χ_{LGT}. Each of the other reducible connections is fixed by by one LGT. e.g., the connection with $\omega = (1,0)$ is fixed by the LGT corresponding to $(0,1)$, and so this contributes states with $\chi_{LGT} = (0,0)$ and $(1,0)$, and similarly for the others. Finally, the irreducible connection is fixed by all LGTs, and so only contributes a state with $\chi_{LGT} = (0,0)$. We summarise the results for general even n in table 5.8. One can verify that this precisely matches with the refinement of the supersymmetric vacua of $T[S^3/\Gamma_{D_n}, \mathfrak{su}(2)]$ in table 5.5. Moreover, one can see explicitly the symmetry under reflection in the diagonal, which is implied by modular invariance on the field theory side.

χ_{LGT} \ ω	$(0,0)$	$(1,0)$	$(0,1)$	$(1,1)$
$(0,0)$	$\frac{n}{4}+1$	1	1	$\frac{n-4}{4}+1$
$(1,0)$	1	1	0	0
$(0,1)$	1	0	1	0
$(1,1)$	$\frac{n-4}{4}+1$	0	0	$\frac{n-4}{4}+1$

$n = 0 \pmod 4$

χ_{LGT} \ ω	$(0,0)$	$(1,0)$	$(0,1)$	$(1,1)$
$(0,0)$	$\frac{n-2}{4}+1$	1	1	$\frac{n-2}{4}+1$
$(1,0)$	1	0	1	0
$(0,1)$	1	1	0	0
$(1,1)$	$\frac{n-2}{4}+1$	0	0	$\frac{n-6}{4}+1$

$n = 2 \pmod 4$

Table 5.8: Counting of flat $PSL'(2,\mathbb{C})$ connections on S^3/Γ_{D_n} refined by Stiefel-Whitney class, ω, and χ_{LGT}, for $n = 0 \pmod 4$ on the top and $n = 2 \pmod 4$ below. Here we show the contribution from the trivial connection in blue, the other reducible connections in green, and the irreducible connections in red.

Chapter 6

An $\mathcal{N} = 1$ 3d-3d Correspondence

In this chapter we turn to the topological twist in (4.7) preserving 3d $\mathcal{N} = 1$ supersymmetry. Geometrically, this corresponds to a reduction of the 6d (2,0) theory on an associative three-cycle M_3, embedded into a manifold of holonomy G_2, see appendix B.5. This reduction defines a theory $T_{\mathcal{N}=1}[M_3]$. As in the previous chapter we are primarily concerned with computing the Witten index $I_{T^3}\left(T_{\mathcal{N}=1}[M_3]\right)$ of these theories. We determine the 3d topological field theory, whose partition function on M_3 we conjecture to compute the Witten index of the $T_{\mathcal{N}=1}[M_3]$ theory: first we dimensionally reduce the 6d (2,0) theory on T^3 to 3d $\mathcal{N} = 8$ SYM, which is then topologically twisted along M_3 to preserve two scalar supercharges. This results in a super-**BF**-model coupled to a **H**ypermultiplet, denoted by BFH-model in the following, and we propose the following identification of observables

$$I_{T^3}\left(T_{\mathcal{N}=1}[M_3]\right) = Z_{\mathrm{BFH}}(M_3)\,, \tag{6.1}$$

where Z denotes the partition function of the BFH-model on M_3 – see figure 6.1.

The partition function of the BFH-model is computed in terms of the Euler characteristic of the moduli space of solutions to the BPS equations. These take the form

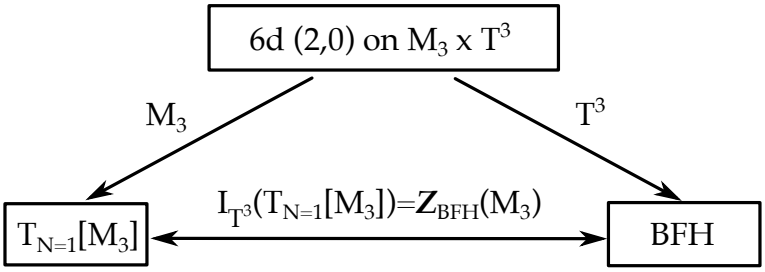

Figure 6.1: The setup for the $\mathcal{N} = 1$ 3d–3d correspondence is the 6d (2,0) theory on $M_3 \times T^3$. The topologically twisted reduction along M_3 preserves 3d $\mathcal{N} = 1$ and geometrically corresponds to an embedding of M_3 as an associative three-cycle in a G_2-holonomy manifold. The correspondence states that the Witten index of the resulting theory $T_{\mathcal{N}=1}[M_3]$ can alternatively be computed from the partition function on M_3 of a topological twist of the T^3-reduction of the 6d theory, a BF-theory coupled to a spinorial hypermultiplet (BFH).

of a generalised set of 3d Seiberg-Witten equations on M_3 for the pair $(A, \phi^{\alpha\hat{\alpha}})$

$$(\mathrm{gSW}_{M_3}): \qquad \begin{aligned} (\not{\mathcal{D}}\phi)^{\alpha\hat{\alpha}} &= 0 \\ \varepsilon_{abc}F^{bc} - \frac{i}{2}[\phi_{\alpha\hat{\alpha}}, (\sigma_a)^{\alpha}{}_{\beta}\phi^{\beta\hat{\alpha}}] &= 0\,. \end{aligned} \tag{6.2}$$

Here $\phi^{\alpha\hat{\alpha}}$ is a section of the normal bundle of the associative cycle, i.e. a section of the spin bundle twisted with an $SU(2)$-bundle V, and A is a gauge connection with field strength F. Furthermore, $\not{\mathcal{D}}$ is the twisted Dirac operator of the covariant derivative $\mathcal{D}$, with respect to A, the $SU(2)$-connection $\mathfrak{A}$ on V, and the spin connection on M_3.

To substantiate the conjectured correspondence (6.1), several checks are performed in the course of this chapter:

1. In the abelian case, the theory $T_{\mathcal{N}=1}[M_3, U(1)]$ and its Witten index can be computed explicitly by dimensional reduction of the 6d abelian (2,0) tensor multiplet. On the topological field theory side the BPS equations decouple into flat $U(1)$-connections and twisted harmonic spinors, and the partition function can be computed to verify (6.1).

2. For non-abelian theories, we specialise the three-cycle M_3 to a Lens space $L(p, q)$ with the standard metric (which does not admit twisted harmonic spinors).

In this case we propose an explicit description of a mass-deformation of the theory $T_{\mathcal{N}=1}[L(p,q)]$, based on the results of the previous chapter. For gauge algebra $\mathfrak{g} = \mathfrak{su}(2)$ we compute the refined Witten index and match it to the flat connections on $L(p,q)$.

In the final section 6.3 we consider a less explored observable for 3d $\mathcal{N} = 1$ theories, the S^3-partition function. We nevertheless propose a variant of the 3d–3d correspondence for this observable, by determining the topological field theory, whose partition function on M_3 computes the S^3-partition function of $T_{\mathcal{N}=1}[M_3]$ theory. The strategy is again to start with the 6d (2,0) theory and dimensionally reduce on S^3 in a suitable conformal supergravity background. We find that the topological theory is a Chern-Simons-Dirac (CSD) theory, i.e. real Chern-Simons gauge theory at level 1 coupled to a twisted harmonic spinor ϕ, whose equations of motion are precisely the generalised Seiberg-Witten equations (6.2). This leads us to conjecture

$$Z_{S^3}\left(T_{\mathcal{N}=1}[M_3, G]\right) = \mathcal{Z}_{\mathrm{CSD}_{\mathbb{R}},G}(M_3)\,. \tag{6.3}$$

Furthermore, we discuss the generalisation to CSD level k, which corresponds to the partition function on the Lens space $L(k,1)$.

6.1 $T_{\mathcal{N}=1}[M_3]$

6.1.1 $T_{\mathcal{N}=1}[M_3, U(1)]$

We start by deriving the 3d $\mathcal{N} = 1$ theory $T_{\mathcal{N}=1}[M_3, U(1)]$ from a topological twist of the 6d $\mathcal{N} = (2,0)$ theory, which geometrically corresponds to a single M5-brane wrapped on an associative three-cycle M_3 in a G_2-holonomy manifold. We reduce the equations of motion of the 6d abelian tensor multiplet to the ones of the 3d theory $T_{\mathcal{N}=1}[M_3, U(1)]$, and compute the Witten index for this theory for general M_3.

We consider the reduction of the 6d abelian tensor multiplet [179], consisting of five scalars $\Phi^{\underline{\hat{m}\hat{n}}}$, a self-dual three-form $H = dB$, and fermions $\varrho^{\underline{\alpha\hat{m}}}$ satisfying a symplectic-Majorana-Weyl condition. A summary of our conventions can be found in appendix B.8.[1] Under the topological twist (4.8) these become

$$\begin{aligned} SO(1,5)_L \times Sp(4)_R \quad &\to \quad SO(1,2)_L \times SU(2)_{\text{twist}} \times SU(2)_\ell \\ \Phi^{\underline{\hat{m}\hat{n}}}: \quad (\mathbf{1},\mathbf{5}) \quad &\to \quad (\mathbf{1},\mathbf{2},\mathbf{2}) \oplus (\mathbf{1},\mathbf{1},\mathbf{1}) \equiv (\phi^{\alpha\hat{\alpha}}, \varphi) \\ H_{\underline{abc}}: \ (\mathbf{10},\mathbf{1}) \quad &\to \quad (\mathbf{1},\mathbf{1},\mathbf{1}) \oplus (\mathbf{3},\mathbf{3},\mathbf{1}) \equiv (h, H_{axy}) \\ \varrho^{\underline{\alpha\hat{m}}}: \quad (\bar{\mathbf{4}},\mathbf{4}) \quad &\to \quad (\mathbf{2},\mathbf{2},\mathbf{2}) \oplus (\mathbf{2},\mathbf{1},\mathbf{1}) \oplus (\mathbf{2},\mathbf{3},\mathbf{1}) \equiv (\rho^{\sigma\alpha\hat{\alpha}}, \lambda^\sigma, \xi_a^\sigma)\,. \end{aligned} \tag{6.4}$$

A key point to observe here is that from the 6d scalars we obtain a field $\phi^{\alpha\hat{\alpha}}$ transforming as a spinor under both the twisted Lorentz $SU(2)_{\text{twist}}$ and the remnant flavour symmetry $SU(2)_\ell$. We therefore identify the $SU(2)_\ell$ with the $SU(2)$-bundle V in (B.43), which makes $\phi^{\alpha\hat{\alpha}}$ a section of the normal bundle N_{M_3}.

In appendix B.6 we carry out the reduction explicitly and show $T_{\mathcal{N}=1}[M_3, U(1)]$ to be a supersymmetric Chern-Simons theory with free scalar multiplets. The spectrum of $T_{\mathcal{N}=1}[M_3, U(1)]$ depends on the first integral homology of M_3

$$H_1(M_3, \mathbb{Z}) \cong \mathbb{Z}^{b_1(M_3)} \oplus \mathbb{Z}_{p_1} \oplus \cdots \oplus \mathbb{Z}_{p_r}\,, \tag{6.5}$$

as well as the number of twisted harmonic spinors $d_{\not{D}}(M_3, g)$ on M_3 and consists of the following free 3d $\mathcal{N} = 1$ multiplets:

1. A single scalar multiplet $\{\varphi, \lambda^\sigma, h\}$. If we view $T_{\mathcal{N}=1}[M_3, U(1)]$ as a domain wall in the 4d $\mathcal{N} = 1$ bulk theory, obtained by compactifying M-theory on the G_2-holonomy manifold, this multiplet describes the centre of mass.

2. $b_1(M_3)$ massless scalar multiplets $\{\alpha, \xi^\sigma\}^I$ coming from the free part of the first homology group of M_3.

[1] We use the convention of non-hatted indices and hatted indices to denote Lorentz and R-symmetry indices, respectively.

3. $d_{\not D}(M_3, g)$ massless scalar multiplets $\{\phi, \rho^\sigma\}^i$ which describe the deformations of the associative three-cycle M_3 inside the G_2-holonomy manifold. These explicitly depend on the G_2-holonomy metric g restricted to the associative cycle M_3.

4. A set of r massive gauge multiplets $\{A, \xi^\sigma\}^m$ whose masses are generated by Chern-Simons terms at levels p_m. Each multiplet is induced by a factor in the torsion part of the first homology group (6.5) of M_3 .

This gives the dictionary between the field content of $T_{\mathcal{N}=1}[M_3, U(1)]$ and the geometry of the associative three-cycle M_3.

The observable for the proposed 3d–3d correspondence (6.1) is the T^3-partition function, or Witten index, of $T_{\mathcal{N}=1}[M_3]$ and for $\mathcal{N} = 1$ theories is the most natural and well-explored observable to consider.

The key geometric input from M_3 are its first Betti number $b_1(M_3)$, the torsion numbers p_m in (6.5) and the number $d_{\not D}(M_3, g)$ of zero-modes of the twisted Dirac operator, with g being the metric arising from the restriction of the G_2-metric onto M_3. Since the abelian theory is non-interacting the multiplets decouple and the vacua can be written as tensor products. Thus, the Witten index is a product with the following contributions:

1. Independent of the details of the compact M_3 the theory includes a free scalar multiplet consisting of a bosonic and a fermionic state. Thus, the ground states always come in pairs with opposite fermion number and the full Witten index vanishes. Since this does not yield any information about the associative three-cycle we will exclude this centre of mass multiplet from the computation of $I' = \mathrm{Tr}'(-1)^F$ in the same fashion as in [123] and in section 5.3.1.

2. There are $b_1(M_3)+d_{\not D}(M_3, g)$ scalar multiplets, and as argued above, the Witten index of a free scalar multiplet vanishes. Thus, the Witten index vanishes unless

$b_1(M_3) = d_{\not D}(M_3, g) = 0$. It is believed, [115,180], that generic associative three-cycles have no deformation space, i.e. $d_{\not D}(M_3, g) = 0$. For many examples, such as three-spheres and simple modifications thereof, furthermore $b_1(M_3) = 0$.

3. The final piece is the set of r vector multiplets with Chern-Simons self-interactions at levels p_m given by the torsion numbers (6.5). For a single $U(1)$ gauge field with Chern-Simons level k the Witten index is k [181]. Since the r gauge fields are independent of each other the total contribution of this sector is $I_{\text{CS}} = \prod_{m=1}^{r} p_m$.

The total Witten index I', excluding the centre of mass contribution, is thus given by

$$I'(b_1(M_3), d_{\not D}(M_3, g), p_m) = \begin{cases} \prod_{m=1}^{r} p_m & \text{if } b_1(M_3) = d_{\not D}(M_3, g) = 0 \\ 0 & \text{else}\,. \end{cases} \tag{6.6}$$

Thus the Witten index is non-zero if and only if M_3 has trivial first rational homology ($b_1(M_3) = 0$) and a vanishing obstruction space ($d_{\not D}(M_3, g) = 0$, see the discussion in appendix B.5). These manifolds are known as unobstructed rational homology three-spheres.[2] Under smooth deformations of the metric of the G_2-holonomy manifold, or equivalently the associative three-form, this index is discontinuous, whenever the kernel of $\not D$ is non-vanishing. There is no guarantee that the index is invariant after passing through these loci, as the deformation space of an obstructed associative three-cycle can be singular. This phenomenon is known as wall-crossing.

6.1.2 Non-abelian Generalisation

Ideally, at this point we would provide a derivation of the non-abelian theories $T_{\mathcal{N}=1}[M_3, U(N)]$ for general, compact three-manifolds. However since the non-abelian 6d theory is unknown this is hard to come by. Thus, a precise dictionary between the

[2]Note that if $M_3 = S^3$ the index is one although there are no non-trivial cycles. This can be seen by an explicit reduction, where the Hopf fibre induces a Chern-Simons term at level one. This is consistent with (6.6) as I' reduces to the empty product.

associative submanifolds and the non-abelian theories in general is beyond the scope of this work. However, we provide two alternate ways to obtain some information about the non-abelian generalisations. One approach is to first reduce from 6d to 5d on a circle and study the 5d SYM theory on M_3. This results in a 2d sigma-model with $(1,1)$ supersymmetry, whose target space is the moduli space of the gSW equations (6.2). The alternative is to use a specialisation of M_3, when the reduction is known, such as for M_3 a Lens space. More generally one can consider circle-fibrations and use methods as in [101] to compute the dimensional reduction in those cases. We leave this for future work and focus here on the Lens spaces.

Circle Reduction to 2d $\mathcal{N} = (1,1)$ Sigma-Model To further understand the non-abelian theories, without specialising the three-manifold, we first dimensionally reduce the 6d theory to 5d, and consider the non-abelian 5d SYM theory on M_3. This will not immediately reveal the $T_{\mathcal{N}=1}[M_3]$ theory, however we will be able to generalise our results to the non-abelian version of this theory dimensionally reduced on a circle to a 2d $\mathcal{N} = (1,1)$ sigma-model. The target of this sigma-model is the moduli space of a particular generalisation of 3d Seiberg-Witten equations. The setup is sketched in figure 6.2.

The circle reduction of the 6d $\mathcal{N} = (2,0)$ theory results in 5d $\mathcal{N} = 2$ SYM, i.e. the worldvolume theory of D4-branes in type IIA string theory, which is known for any gauge algebra. We can then reduce further on M_3, which encodes information about the circle reduction of $T_{\mathcal{N}=1}[M_3]$ to two dimensions. Consider the topological twist (4.7), which is unaltered by the reduction to 5d. The twist of the 5d $\mathcal{N} = 2$ vector yields gauge fields A_b on M_3 and $A_\pm$ on $\mathbb{R}^{1,1}$ respectively. The decomposition of the spinor and scalar sectors is similar to (6.4). This preserves two supercharges of opposite chirality corresponding to 2d $\mathcal{N} = (1,1)$. In order to put this theory on a general associative M_3 the Dirac operator has to be covariantised with respect

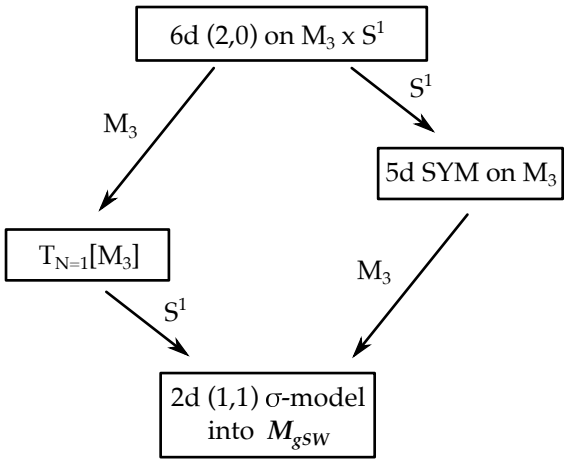

Figure 6.2: To study the non-abelian theory we consider first the dimensional reduction to 5d SYM and then the reduction on M_3 to 2d. This corresponds to the circle-reduction of $T_{\mathcal{N}=1}[M_3]$ to a 2d $\mathcal{N}=(1,1)$ sigma-model, whose target space are the generalised Seiberg-Witten equations (gSW) in (6.7).

to the spin connection on M_3 as well as the $SU(2)_V$ connection $\mathfrak{A}$ as discussed in appendix B.6.[3] To dimensionally reduce on M_3 we introduce a length scale s of the three-manifold and consider the theory in the limit $s \to 0$. To this end we rescale the fields and coordinates on M_3 to make their s-dependence explicit. The reduction proceeds by solving the BPS equations, which are the most divergent terms in the s-expansion of the supersymmetry variations

$$\begin{aligned} \varepsilon_{abc}F^{bc} - \frac{i}{2}[\phi_{\alpha\hat{\alpha}}, \phi^{\beta\hat{\alpha}}](\sigma_a)^{\alpha}{}_{\beta} &= 0 \\ (\not{D}\phi)^{\alpha\hat{\alpha}} &= 0 \\ D_a\varphi = [\varphi, \phi^{\alpha\hat{\alpha}}] &= 0\,. \end{aligned} \tag{6.7}$$

The first two BPS equations are the generalised Seiberg-Witten equations (6.2). For field configurations satisfying (6.7) the leading order terms in 5d vanish and the action is minimised. The reduction to two dimensions is performed in a standard way and leads to a 2d $\mathcal{N}=(1,1)$ sigma model into the moduli space of solutions to (6.7).

[3]Note that this introduces a mass term for the $\phi^{\alpha\hat{\alpha}}$ proportional to the Ricci scalar $\mathcal{R}(M_3)$ as well as a term involving the field strength $\mathfrak{F}$ of $\mathfrak{A}$. These terms arise naturally by requiring invariance under the covariantised supersymmetry transformations. This is discussed in greater detail in section 6.3.

To consider the 2d $\mathcal{N}=(1,1)$ sigma model on T^2 one needs to choose boundary conditions for the fermions. As described in [182], choosing Ramond boundary conditions for both positive and negative chirality fermions corresponds to computing the Witten index, which is equivalent to the Euler characteristic of the moduli space of solutions to (6.7). As will be discussed in section 6.2.1, the topologically twisted theory on the other side of the $\mathcal{N}=1$ 3d–3d correspondence computes the Euler characeristic of the moduli space of gSW equations, i.e. solutions to (6.7) with $\varphi=0$.

Specialising M_3: $T_{\mathcal{N}=1}[L(p,q)]$ Another approach to obtaining further insight into the non-abelian generalisations is to consider special cases of three-cycles M_3. In fact one of the most common associative cycles in known compact G_2-manifolds are three-spheres or simple modifications thereof – see e.g. the twisted connected sum constructions in [116–118], where associatives are either S^3 or diffeomorphic to $S^2\times S^1$.

It is thus useful to consider specialisations of the three-cycles M_3 and determine the non-abelian theories using special properties of the geometries. In particular we focus on Lens spaces $L(p,q)$ which for example appear as associative three-cycles in the G_2-manifolds

$$X_7=(\mathbb{R}^4\times S^3)/\mathbb{Z}_p\,, \tag{6.8}$$

considered in [123]. We now propose a method to describe the (mass-deformed) $T_{\mathcal{N}=1}[L(p,q)]$ as a quiver theory, similar to the discussion in section 5.1. From this we compute the refined Witten index for $\mathfrak{g}=\mathfrak{su}(2)$.

Let us first consider the case $q=1$. The reduction of the 6d $\mathcal{N}=(2,0)$ theory along the fibre direction yields 5d $\mathcal{N}=2$ SYM in the presence of p units of graviphoton flux. This theory possesses a Lagrangian description for general gauge group G and the subsequent reduction on S^2 can be performed explicitly. This yields a 3d SYM theory with a Chern-Simons term at level p coupled to an adjoint scalar multiplet.

The bosonic part of the action is given by

$$S = \frac{1}{g^2}\int d^3x \,\mathrm{Tr}\left(-\frac{1}{2}F_{ij}F^{ij} + \frac{1}{2}D_i\varphi D^i\varphi\right) + \frac{p}{4\pi}\int \mathrm{CS}(A)\,, \tag{6.9}$$

where the scale of the gauge coupling is given by the radius of the Lens space $g^{-2} \sim r$. It is known that the associated 3d $\mathcal{N}=1$ theory has an $\mathcal{N}=2$ enhancement point in the space of mass parameters. Tuning the scalar mass to

$$m_{\mathcal{N}=2} = -\frac{pg^2}{4\pi}\,, \tag{6.10}$$

yields a pure $\mathcal{N}=2$ G_k CS-theory. The mass deformation from $m=0$ to $m_{\mathcal{N}=2}$ preserves the number of vacua [183]. Thus, at the enhancement point, we can define and count Bethe vacua of $\widehat{T}_{\mathcal{N}=1}[\Omega_{[p]}, G]$, which can be described as an $\mathcal{N}=2$ quiver consisting of a single gauged node at Chern-Simons level p. We will return to this computation below.

We conjecture that we can similarly define a more general $\mathcal{N}=2$ quiver which computes the number of vacua of the $\mathcal{N}=1$ theory for general $\frac{p}{q} = [k_1, \cdots, k_n]$. This can be done by taking each T^{k_i} theory, enhancing it to $\mathcal{N}=2$ supersymmetry and coupling them together with the $T(G)$ theory. This quiver description can also be obtained from a procedure similar to section 5.1.2, with the adjoint multiplets $\mathrm{adj}(\mathcal{V}_\pm)$ removed from all the basic building blocks and gluing rules. The quiver for $\widehat{T}_{\mathcal{N}=1}[\Omega_{[k_1,\cdots,k_n]}, G]$ is then given in figure 6.3. It is obtained from the quiver in figure 5.7 by removing the adjoint attached to the left-most node. It would be interesting to show that this is indeed the same as the prescription that is obtained from the direct dimensional reduction on $L(p,q)$ with the $\mathcal{N}=1$ twist with a mass deformation. This prescription is supported by the vacuum count and the compatibility with the dualities of section 5.1.3, which also apply to these quivers. The physical theory $T_{\mathcal{N}=1}[L(p,q), \mathfrak{g}]$ is then obtained by decoupling various topological sectors, precisely as in the discussion in section 5.2.4 for the $\mathcal{N}=2$ case.

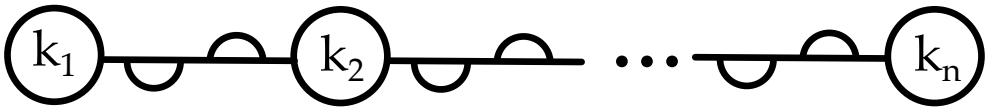

Figure 6.3: Quiver of the $\mathcal{N}=2$ enhancement point of $\widehat{T}_{\mathcal{N}=1}[\Omega_{[k_1,\cdots,k_n]}, G]$

For $G = U(N)$ the Witten index was computed in [104, 123] to be

$$I_{T^3}(T_{\mathcal{N}=1}[L(p,q), U(N)]) = \binom{p}{N}, \tag{6.11}$$

which allows us to also check our proposal for $N = 2$. To compute this one uses the fact that the vacua of the Chern-Simons theory (6.9) are given by flat $U(N)$-connections. This moduli space consists of a set of points, each representing an N-dimensional representation of the fundamental group $\pi_1(L(p,q)) = \mathbb{Z}_p$, and the Witten index is given by the sum over all such points. The abelian flat connections are in one-to-one correspondence with the irreducible representations of $\mathbb{Z}_p$, and can be represented by the p nodes on the associated affine Dynkin diagram for A_{p-1} [184]. The generalisation to flat $U(N)$-connections follows by considering the number of ways in which N-dimensional representations of $\mathbb{Z}_p$ can be built from the 1-dimensional irreducible representations, which is given by (6.11). In section 6.2.1 we shall show that in this case the $\mathcal{N}=1$ 3d–3d correspondence holds by determining the partition function of the BFH-model.

Bethe Vacua for $T_{\mathcal{N}=1}[L(p,q), \mathfrak{su}(2), H]$ To check this proposed description of the quivers we now compute the number of vacua for $M_3 = L(p,q)$ and $\mathfrak{g} = \mathfrak{su}(2)$. As in section 5.3.3 we first determine the number of vacua of $\widehat{T}_{\mathcal{N}=1}[\Omega_{[k_1,\cdots,k_n]}, SU(2)]$. The simplest case is the single node T^k, where the Bethe equation is

$$\Pi(x) = x^{2k}\,. \tag{6.12}$$

The solutions are $\widehat{u}_j = \frac{j}{2k}$, with $j = 0, \ldots, 2k-1$, with the $\mathbb{Z}_2$ Weyl symmetry acting as $\widehat{u}_j \to \widehat{u}_{-j}$. Except for the two degenerate solutions $\widehat{u}_0, \widehat{u}_k$ they appear in Weyl

pairs, so

$$I(\widehat{T}_{\mathcal{N}=1}[\Omega_{[k]}, SU(2)]) = k-1\,. \tag{6.13}$$

The anomaly is exactly as for the $\mathcal{N}=2$ case in section 5.3.4, so

$$I(T_{\mathcal{N}=1}[L(k,1),\mathfrak{su}(2)]) = \begin{cases} k-1 & k \text{ even} \\ \frac{k-1}{2} & k \text{ odd} \end{cases}. \tag{6.14}$$

If k is even we can gauge the $\mathbb{Z}_2$ 1-form symmetry of this theory. Since the Bethe vacua are known explicitly we can do this by hand. The Hilbert space is spanned by the physical vacua $|\widehat{u}_j\rangle$, $j=1,\ldots,k-1$ and the two generators of the 1-form symmetry (B.23) act as[4]

$$U_A|\widehat{u}_j\rangle = (-1)^{j+1}|\widehat{u}_j\rangle\,, \qquad U_B|\widehat{u}_j\rangle = |\widehat{u}_{k-j}\rangle\,. \tag{6.15}$$

Thus, the common eigenvectors of the U are $|\widehat{u}_{k/2}\rangle$ and $|\widehat{v}_j^{\pm}\rangle = \frac{1}{\sqrt{2}}\left(|\widehat{u}_j\rangle \pm |\widehat{u}_{k-j}\rangle\right)$, $j=1,\ldots,\frac{k}{2}-1$. The eigenvalues of the U are given by

$$(U_A,U_B)\,|\widehat{u}_{k/2}\rangle = \left((-1)^{\frac{k}{2}+1},+1\right)|\widehat{u}_{k/2}\rangle\,, \qquad (U_A,U_B)\,|\widehat{v}_j^{\pm}\rangle = \left((-1)^{j+1},\pm 1\right)|\widehat{v}_j^{\pm}\rangle\,. \tag{6.16}$$

From this we easily see that the subspace with eigenvalues $(1,1)$ has dimension $\left\lceil \frac{k}{4} \right\rceil$.

We can explicitly check this structure for general linear quivers. This is analogous to the $\mathcal{N}=2$ theories discussed in section 5.3. We find

$$I(\widehat{T}_{\mathcal{N}=1}[\Omega_{[k_1,\cdots,k_n]}, SU(2)]) = 2^{n-1}(p-1)\,, \tag{6.17}$$

from which we can deduce that

$$\begin{aligned} I(T_{\mathcal{N}=1}[L(p,q),SU(2)]) &= \begin{cases} p-1 & p \text{ even} \\ \frac{p-1}{2} & p \text{ odd} \end{cases}, \\ I(T_{\mathcal{N}=1}[L(p,q),U(2)]) &= \binom{p}{2}, \end{aligned} \tag{6.18}$$

[4]The overall sign of U_A is fixed by modular invariance.

the latter in agreement with (6.11). Furthermore, we can gauge the $\mathbb{Z}_2$ 1-form symmetry if p is even. Doing this explicitly for small values of n and p we find

$$I_{\text{untwisted}}(T_{\mathcal{N}=1}[L(p,q),\mathfrak{su}(2),\mathbb{Z}_2]) = \left\lceil \frac{p}{4} \right\rceil \,. \tag{6.19}$$

As in the $\mathcal{N}=2$ case, there is also a single vacuum in the twisted sector, leading to

$$I(T_{\mathcal{N}=1}[L(p,q),\mathfrak{su}(2),\mathbb{Z}_2]) = \left\lceil \frac{p}{4} \right\rceil + 1 \,. \tag{6.20}$$

The interesting point to note here is that the Bethe vacua counting is – as expected, although it is not manifest – independent of q. It would be interesting to extend this to higher rank and, more general, non-linear quivers and to test the $\mathcal{N}=1$ 3d-3d correspondence for these theories.

6.2 The BFH Model

We now turn to the topological field theory side of the correspondence, i.e. the right hand side of figure 6.1, whose partition function is conjectured to compute the Witten index of the 3d $T_{\mathcal{N}=1}[M_3]$ theory. The TQFT can be obtained from the T^3-reduction of the 6d (2,0) theory, to a maximally supersymmetric 3d theory, which we then topologically twist along M_3 in the same fashion as in section 6.1.1. Following the correspondence (6.1) the partition function of this topological theory computes the Witten index $I_{T^3}(T_{\mathcal{N}=1}[M_3])$ of the 3d $\mathcal{N}=1$ theory, and we verify this in examples.

6.2.1 Topological Twist of 3d $\mathcal{N}=8$ SYM

The reduction of the 6d $\mathcal{N}=(2,0)$ theory on T^3 yields maximally supersymmetric 3d $\mathcal{N}=8$ SYM theory on M_3. The topological twist preserves two scalar supercharges $Q^{\dot{\sigma}}$. The field content of the theory and its transformation behaviour under the

$SU(2)_{\text{twist}} \times SU(2)_\ell \times SU(2)_I$ symmetry is given by

A_a	$\varsigma_{\dot{a}}$	$\phi_{\alpha\hat{\alpha}}$	$\xi_a^{\dot{\sigma}}$	$\lambda^{\dot{\sigma}}$	$\rho^{\dot{\sigma}}_{\alpha\hat{\alpha}}$
$(\mathbf{3},\mathbf{1},\mathbf{1})$	$(\mathbf{1},\mathbf{1},\mathbf{3})$	$(\mathbf{2},\mathbf{2},\mathbf{1})$	$(\mathbf{3},\mathbf{1},\mathbf{2})$	$(\mathbf{1},\mathbf{1},\mathbf{2})$	$(\mathbf{2},\mathbf{2},\mathbf{2})$

(6.21)

Here, the hatted and dotted indices denote the representations under the internal symmetries $SU(2)_\ell$ and $SU(2)_I$, respectively. The 3d topological action is given by the 3d super-BF-model [185, 186] coupled to a spinorial hypermultiplet, which first appeared in [187]. In addition, we will gauge the $SU(2)_\ell$ flavour symmetry, which is identified with the bundle V in (B.43), to ensure that M_3 is embedded as an associative three-cycle.

Inspired by the description in [187] we find that the reduction of the supersymmetry variations can be written in an off-shell form with the introduction of two auxiliary fields, B_a and $W^{\alpha\hat{\alpha}}$,

$$
\begin{aligned}
Q^{\dot{\sigma}} A_a &= \frac{1}{2}\xi_a^{\dot{\sigma}}\,, & Q^{\dot{\sigma}}\varsigma^{\dot{a}} &= -\frac{1}{2}(\sigma^{\dot{a}})^{\dot{\sigma}}{}_{\dot{\tau}}\lambda^{\dot{\tau}} \\
Q^{\dot{\sigma}}\phi^{\alpha\hat{\alpha}} &= \frac{1}{2}\rho^{\dot{\sigma}\alpha\hat{\alpha}}\,, & Q^{\dot{\sigma}}\lambda^{\dot{\tau}} &= -\frac{i}{2}\varepsilon_{\dot{a}\dot{b}\dot{c}}(\sigma^{\dot{a}})^{\dot{\sigma}\dot{\tau}}[\varsigma^{\dot{b}},\varsigma^{\dot{c}}] \\
Q^{\dot{\sigma}}\xi_a^{\dot{\tau}} &= (\sigma^{\dot{a}})^{\dot{\sigma}\dot{\tau}} D_a\varsigma_{\dot{a}} + \varepsilon^{\dot{\sigma}\dot{\tau}} B_a & Q^{\dot{\sigma}}\rho^{\dot{\tau}\alpha\hat{\alpha}} &= -[(\sigma^{\dot{a}})^{\dot{\sigma}\dot{\tau}}\varsigma_{\dot{a}},\phi^{\alpha\hat{\alpha}}] + \varepsilon^{\dot{\sigma}\dot{\tau}} W^{\alpha\hat{\alpha}} \\
Q^{\dot{\sigma}} B_a &= -\frac{1}{2}D_a\lambda^{\dot{\sigma}} - \frac{1}{2}(\sigma^{\dot{a}})^{\dot{\sigma}}{}_{\dot{\tau}}[\varsigma_{\dot{a}},\xi_a^{\dot{\tau}}]\,, & Q^{\dot{\sigma}} W^{\alpha\hat{\alpha}} &= \frac{1}{2}[\lambda^{\dot{\sigma}},\phi^{\alpha\hat{\alpha}}] - \frac{1}{2}(\sigma^{\dot{a}})^{\dot{\sigma}}{}_{\dot{\tau}}[\varsigma_{\dot{a}},\rho^{\dot{\tau}\alpha\hat{\alpha}}]\,.
\end{aligned}
\tag{6.22}
$$

The supersymmetry algebra closes up to gauge transformations induced by the $\varsigma_{\dot{a}}$

$$
\{Q^{\dot{\sigma}}, Q^{\dot{\tau}}\} = -(\sigma^{\dot{a}})^{\dot{\sigma}\dot{\tau}}\delta_I(\varsigma_{\dot{a}})\,, \tag{6.23}
$$

where the gauge transformation acts as $\delta_I(\varsigma_{\dot{a}})A_b = -D_b\varsigma_{\dot{a}}$ and $\delta_I(\varsigma_{\dot{a}}) = [\varsigma_{\dot{a}},\cdot]$ on all other fields. The action invariant under this set of supersymmetry transformations

has a BF-type coupling and is given by

$$\begin{aligned}S_{\text{BFH}} = \frac{1}{e^2}\int d^3x\,\text{Tr}\,\Big[&-B^a\left(B_a - \varepsilon_{abc}F^{bc} + \frac{i}{2}[\phi_{\alpha\hat{\alpha}},(\sigma_a)^{\alpha}{}_{\beta}\phi^{\beta\hat{\alpha}}]\right)\\ &-\frac{1}{2}W_{\alpha\hat{\alpha}}\left(W^{\alpha\hat{\alpha}} - 2i\not{D}^{\alpha}{}_{\beta}\phi^{\beta\hat{\alpha}}\right) + \frac{1}{2}[\varsigma_{\dot{a}},\varsigma_{\dot{b}}][\varsigma^{\dot{a}},\varsigma^{\dot{b}}] + D_a\varsigma_{\dot{a}}D^a\varsigma^{\dot{a}}\\ &+\frac{1}{2}[\varsigma_{\dot{a}},\phi_{\alpha\hat{\alpha}}][\varsigma^{\dot{a}},\phi^{\alpha\hat{\alpha}}] + \xi_{a\dot{\sigma}}D^a\lambda^{\dot{\sigma}} + \frac{1}{2}\varepsilon^{abc}\xi_{a\dot{\sigma}}D_b\xi_c^{\dot{\sigma}}\\ &+\frac{i}{4}\rho_{\dot{\sigma}\alpha\hat{\alpha}}\not{D}^{\alpha}{}_{\beta}\rho^{\dot{\sigma}\beta\hat{\alpha}} + \frac{1}{4}\rho_{\dot{\sigma}\alpha\hat{\alpha}}(\sigma^{\dot{a}})^{\dot{\sigma}}{}_{\dot{\tau}}[\varsigma_{\dot{a}},\rho^{\dot{\tau}\alpha\hat{\alpha}}] + \frac{1}{2}\xi_{a\dot{\sigma}}(\sigma^{\dot{a}})^{\dot{\sigma}}{}_{\dot{\tau}}[\varsigma_{\dot{a}},\xi^{a\dot{\tau}}]\\ &+\frac{1}{2}\lambda_{\dot{\sigma}}(\sigma^{\dot{a}})^{\dot{\sigma}}{}_{\dot{\tau}}[\varsigma_{\dot{a}},\lambda^{\dot{\tau}}] + \frac{1}{2}\rho_{\dot{\sigma}\alpha\hat{\alpha}}[\phi^{\alpha\hat{\alpha}},\lambda^{\dot{\sigma}}] - \frac{i}{2}\xi_{a\dot{\sigma}}[\rho^{\dot{\sigma}}_{\alpha\hat{\alpha}},(\sigma^a)^{\alpha}{}_{\beta}\phi^{\beta\hat{\alpha}}]\Big]\,,\end{aligned} \tag{6.24}$$

which can be written in a Q-exact form

$$S_{\text{BFH}} = \frac{1}{2e^2}\varepsilon_{\dot{\sigma}\dot{\tau}}Q^{\dot{\sigma}}Q^{\dot{\tau}}V_{\text{BFH}}\,, \tag{6.25}$$

where

$$\begin{aligned}V_{\text{BFH}} = \int d^3x\,\text{Tr}\,\Big(&2\varepsilon^{abc}(A_a\partial_bA_c + \frac{2}{3}A_aA_bA_c) + \frac{1}{2}(\xi_{a\dot{\sigma}}\xi^{a\dot{\sigma}} - \lambda_{\dot{\sigma}}\lambda^{\dot{\sigma}})\\ &+ i\phi_{\alpha\hat{\alpha}}(\sigma^a)^{\alpha}{}_{\beta}D_a\phi^{\beta\hat{\alpha}} + \frac{1}{4}\rho_{\dot{\sigma}\alpha\hat{\alpha}}\rho^{\dot{\sigma}\alpha\hat{\alpha}}\Big)\,.\end{aligned} \tag{6.26}$$

We identify the gauge coupling constant e as

$$\frac{1}{e^2} = \frac{v_{T^2}}{8\pi^2 r}\,, \tag{6.27}$$

where v_{T^2} is the T^2-volume and r is the radius of the M-theory circle. Note that the radii of the three circles enter the gauge coupling differently, as we first reduce to 5d, where the fields are rescaled by the corresponding radius r to ensure canonical scaling dimension.[5]

The auxiliary fields can be integrated out to give

$$\begin{aligned}B_a &= \frac{1}{2}\left(\varepsilon_{abc}F^{bc} - \frac{i}{2}[\phi_{\alpha\hat{\alpha}},\phi^{\beta\hat{\alpha}}](\sigma_a)^{\alpha}{}_{\beta}\right)\\ W^{\alpha\hat{\alpha}} &= i\not{D}^{\alpha}{}_{\beta}\phi^{\beta\hat{\alpha}}\,,\end{aligned} \tag{6.28}$$

[5]This is very similar to the arguments in the geometric interpretation of S-duality in $4d$ $\mathcal{N}=4$ SYM obtained by a T^2-reduction of the $6d$ $\mathcal{N}=(2,0)$ theory.

such that the bosonic action can be written as

$$S_{\text{BFH}}|_{\text{bosonic}} = \frac{1}{e^2}\int d^3x\,\text{Tr}\left(\frac{1}{2}F_{ab}F^{ab} + \frac{1}{2}[\varsigma_{\dot{a}},\varsigma_{\dot{b}}][\varsigma^{\dot{a}},\varsigma^{\dot{b}}] + D_a\varsigma_{\dot{a}}D^a\varsigma^{\dot{a}} - \frac{1}{2}\phi_{\alpha\hat{\alpha}}(\not{D}^2\phi)^{\alpha\hat{\alpha}} + \frac{1}{2}[\varsigma_{\dot{a}},\phi_{\alpha\hat{\alpha}}][\varsigma^{\dot{a}},\phi^{\alpha\hat{\alpha}}] + \frac{1}{8}[\phi_{\alpha\hat{\alpha}},\phi_{\beta\hat{\beta}}][\phi^{\alpha\hat{\alpha}},\phi^{\beta\hat{\beta}}]\right). \tag{6.29}$$

Note that the above derivation holds for curved M_3 by covariantising the derivatives with respect to the spin connection on M_3 and the connection $\mathfrak{A}$ of the $SU(2)$ bundle V. Indeed, the energy momentum tensor T_{ab}, the variation of S_{BFH} with respect to the metric on M_3, can be written in a Q-exact form. The BFH-model is therefore topological in the sense of Witten, however this does not forbid the observables to exhibit wall-crossing. As will be discussed in section 6.2.2, the partition function of the BFH-model, under the proposed correspondence (6.1), is expected to undergo wall-crossing for metrics admitting twisted harmonic spinors. We can understand this as the moduli space of vacua becoming singular due to the obstructions discussed in section B.5.

The BFH-model (6.24) preserves two topological supercharges and the partition function is expected to compute the Euler characteristic of some moduli space [188, 189].[6] For the case of the supersymmetric BF-model, where the spinorial hypermultiplet is absent, it was shown in [185] that for gauge group $SU(2)$ and $M_3 = S^3$ the partition function computes the Casson invariant. For general three-manifolds the partition function computes the Euler characteristic of the moduli space of flat connections [191], which was conjectured to be the generalisation of the Casson invariant to arbitrary three-manifolds. For the BFH-model (6.24) we expect the associated moduli space to be the moduli space of solutions to the generalised Seiberg-Witten equations (6.2), which minimises the action (6.29) for $D_a\varsigma_{\dot{a}} = [\varsigma_{\dot{a}},\phi^{\alpha\hat{\alpha}}] = 0$. The partition function of this topological theory is then, under the $\mathcal{N} = 1$ 3d–3d corre-

[6]For the Euler characteristic to be well-defined the moduli space needs to be compact. This was shown to be the case for the 3d abelian Seiberg-Witten equations coupled to n spinors transforming under an $SU(n)$-bundle in [190]. To our knowledge the compactification of the moduli space of 3d non-abelian Seiberg-Witten equations has not been studied.

spondence, conjectured to match the T^3-partition function of the $T_{\mathcal{N}=1}[M_3]$ theory.

Indeed, for the simple case of Lens spaces $L(p,q)$ considered in section 6.1.2 there are no twisted harmonic spinors for the standard metric and the gSW equations reduce to flat $U(N)$-connections. Thus, the partition function of the BFH model reduces to the Euler characteristic of the moduli space of flat connections. Since the moduli space of flat connections for Lens spaces consists of a set of points, the counting of flat connections computed in section 6.1.2 to determine the vacua of the theory $T_{\mathcal{N}=1}[L(p,q)]$ corresponds to the Euler characteristic of the moduli space. We thus find that the partition function of the BFH-model for Lens spaces is given by

$$Z_{\mathrm{BFH},U(N)}(L(p,q)) = \chi(\mathcal{M}_{\mathrm{flat},U(N)}) = \binom{p}{N} \,, \tag{6.30}$$

and matches with the Witten index of $T_{\mathcal{N}=1}[L(p,q),U(N)]$ in (6.11).

6.2.2 The Abelian BFH-Model

Let us look at the abelian case more closely, where we are able to perform concrete computations and comparisons. The action of the abelian BFH-model is minimised by solutions to the now decoupled equations

$$F_{ab} = 0\,, \qquad (\not{\mathcal{D}}\phi)^{\alpha\hat{\alpha}} = 0\,, \qquad \partial_a\varphi = 0\,. \tag{6.31}$$

This implies that the moduli space splits into a tensor product where the individual pieces relate to one of the equations in (6.31). The solutions to the last equation are constant scalars on M_3, which we identify with the centre of mass mode introduced in section 6.1.1. The two remaining contributions correspond to flat $U(1)$-connections and twisted harmonic spinors on M_3, respectively. It is discussed in appendix B.6 that the moduli space of flat $U(1)$-connections has two independent contributions coming from the free and torsion part of the first homology group (6.5) respectively. For the free part the moduli space is given by a $b_1(M_3)$-dimensional torus. The torsion part

$\mathcal{M}_{\mathcal{T}}$ of the moduli space is a finite set of $\prod_{m=1}^{r} p_m$ points, where the p_m are the torsion numbers. Finally, the elements of the moduli space $\mathcal{H}_{\not{\mathcal{D}}}$ of twisted harmonic spinors on M_3 are locally described by the sections of the normal bundle $N_{M_3} = \mathbb{S} \otimes V$, which is the space of deformations of the associative.

The full moduli space of solutions to (6.31), neglecting the centre of mass contribution, is thus given by

$$\mathcal{M}_{U(1)} = T^{b_1(M_3)} \times \mathcal{M}_{\mathcal{T}} \times \mathcal{H}_{\not{\mathcal{D}}} \,. \tag{6.32}$$

Under the 3d–3d correspondence the T^3-partition function of $T_{\mathcal{N}=1}[M_3, U(1)]$ is equivalent to the partition function of the abelian BFH-model which is computed by the Euler characteristic of the moduli space (6.32),

$$Z_{\mathrm{BFH}}(M_3) = \chi\left(\mathcal{M}_{U(1)}\right) = \chi\left(T^{b_1(M_3)}\right) \chi\left(\mathcal{M}_{\mathcal{T}}\right) \chi\left(\mathcal{H}_{\not{\mathcal{D}}}\right) \,. \tag{6.33}$$

For generic metrics on M_3 no solutions for twisted harmonic spinors exist besides the trivial solution $\phi^{\alpha\hat{\alpha}} = 0$. In that case the partition function computes the Euler characteristic of the moduli space of flat $U(1)$-connections on M_3, which is given by

$$Z_{\mathrm{BFH}}(M_3) = \begin{cases} \prod_{m=1}^{r} p_m & b_1(M_3) = 0 \\ 0 & \text{else} \end{cases} \,. \tag{6.34}$$

For the case of $d_{\not{\mathcal{D}}}(M_3, g) = 0$ this result is in agreement with the Witten index computed in section 6.1.1. In order to recover the full Witten index, i.e. including $d_{\not{\mathcal{D}}}(M_3, g) \neq 0$, one needs to prove that the index $Z_{\mathrm{BFH}}(M_3)$ vanishes unless $b_1(M_3) = d_{\not{\mathcal{D}}}(M_3, g) = 0$. However, the moduli space of twisted harmonic spinors is not necessarily smooth and compact for $d_{\not{\mathcal{D}}}(M_3, g) \geq 0$, and these cases require a more careful treatment of how the partition function is defined in terms of integrals over the moduli space. For cases when the moduli space $\mathcal{H}_{\not{\mathcal{D}}}$ is compact we conjecture via the $\mathcal{N} = 1$ 3d–3d correspondence that

$$\chi(\mathcal{H}_{\not{\mathcal{D}}}) = 0 \qquad \text{for} \;\; d_{\not{\mathcal{D}}}(M_3, g) \neq 0 \,. \tag{6.35}$$

This has the consequence that the partition function of the abelian theory is not completely invariant under metric deformations, but can jump, whenever the metric deforms to allow for harmonic spinors. Although this is not explicitly verified in the non-abelian case we expect this type of wall-crossing to persist in the more general case as well.

6.3 S^3-Partition Function and Chern-Simons-Dirac Theory

In this section we will discuss a much less explored observable for 3d $\mathcal{N}=1$ theories, the S^3-partition function.[7] Much progress in computing this observable has been made for $\mathcal{N}=2$ thanks to localisation results, however these seem to be not applicable in the minimal supersymmetric situation. Nevertheless there is a well-defined question as to what a 3d–3d correspondence for this case would look like, i.e. what constitutes the topological field theory whose partition function on M_3 computes the S^3-partition function of $T_{\mathcal{N}=1}[M_3]$. For 3d $\mathcal{N}=2$ this topological theory is the complex Chern-Simons theory. In this section we will argue that for $\mathcal{N}=1$ the topological theory is real Chern-Simons gauge theory at level $k=1$ coupled to a twisted harmonic spinor. The equations of motion of this theory are precisely the generalised Seiberg-Witten equations in (6.2). We thus propose that the S^3-partition function of $T_{\mathcal{N}=1}[M_3, G]$ is computed by

$$Z_{S^3}(T_{\mathcal{N}=1}[M_3, G]) = \mathcal{Z}_{\mathrm{CSD}_{\mathbb{R},\mathrm{G}}}(M_3)\,. \tag{6.36}$$

The derivation of this proceeds by considering M5-branes on S^3 in a conformal supergravity background that preserves $\mathcal{N}=1$ supersymmetry. The circle-reduction along the fibre of the Hopf fibration $S^1 \hookrightarrow S^3 \to S^2$ gives 5d SYM on S^2 with radius

[7] Note that there is no refinement regarding the higher-form symmetries because the first and second cohomology groups of S^3 are trivial with respect to any group.

$R_{S^2} = \frac{r}{2}$, where r is the radius of the Hopf circle. For the $\mathcal{N} = 2$ preserving background this reduction from 5d to 3d after non-abelianisation was carried out in [101]. Due to the non-trivial geometry of the S^2 it is necessary to couple to conformal supergravity [100, 192]. We determine the values of the background fields by solving the Killing spinor equations. The coupling to supergravity then leads to additional mass terms and interactions.

6.3.1 Supergravity Background for 5d SYM

The 6d (2,0) theory on $M_3 \times S^3$ can be described in terms of a supergravity background of 5d SYM on $M_3 \times S^2$, that is obtained after dimensional reduction along the Hopf-fibre. Here M_3 will be as before, an associative three-cycle in a G_2-manifold. The metric of the background for 5d SYM is

$$ds^2_{5d} = \frac{r^2}{4}(d\theta^2 + \sin^2\theta d\phi^2) + dx_a dx^a\,, \tag{6.37}$$

where (θ, ϕ) are the spherical polar coordinates. As the Hopf fibration is non-trivial, there is a non-vanishing graviphoton $C = \cos^2\frac{\theta}{2}d\phi$, in 5d with field strength $G = dC$ proportional to the volume form of the S^2.

We begin with the 5d $\mathcal{N} = 2$ SYM coupled to background supergravity, which was derived in [100, 193]. The topological twists in 5d and 6d are very similar, and the 5d $\mathcal{N} = 2$ vector multiplet reduces as

$$\begin{aligned}
SO(5)_L \times Sp(4)_R \quad &\to \quad U(1)_L \times SU(2)_{\text{twist}} \times SU(2)_\ell \\
A: \quad (\mathbf{5},\mathbf{1}) \quad &\to \quad (\mathbf{1},\mathbf{1})_\pm \oplus (\mathbf{3},\mathbf{1})_0 \equiv (A_x, A_b) \\
\rho: \quad (\mathbf{4},\mathbf{4}) \quad &\to \quad (\mathbf{1},\mathbf{1})_{\pm\frac{1}{2}} \oplus (\mathbf{3},\mathbf{1})_{\pm\frac{1}{2}} \oplus (\mathbf{2},\mathbf{2})_{\pm\frac{1}{2}} \equiv (\lambda^\mu, \xi^\mu_a, \rho^{\mu\alpha\hat{\alpha}}) \\
\Phi: \quad (\mathbf{1},\mathbf{5}) \quad &\to \quad (\mathbf{1},\mathbf{1})_0 \oplus (\mathbf{2},\mathbf{2})_0 \equiv (\varphi, \phi^{\alpha\hat{\alpha}})\,,
\end{aligned} \tag{6.38}$$

where $x = 1, 2$ and $\mu = 1, 2$ are the vector and spinor index along the S^2. As before, $a = 1, 2, 3$ and $\alpha = 1, 2$ are the vector and spinor indices along the twisted M_3 and $\hat{\alpha}$ is the $SU(2)_\ell$ spinor index.

The derivation of the supergravity background is summarised in appendix B.7. We find that there is a one parameter family of supergravity solutions, labelled by a real parameter v, which preserve two scalar supercharges ϵ^μ, satisfying

$$\left(\sigma_3 \not{\mathcal{D}}_{S^2}\right)^\mu{}_\nu \epsilon^\nu = -\epsilon^\mu \,, \tag{6.39}$$

where $\left(\not{\mathcal{D}}_{S^2}\right)^\mu{}_\nu$ is the Dirac operator on the S^2.

6.3.2 5d SYM on $M_3 \times S^2$

By plugging in the solutions for the supergravity background into the 5d $\mathcal{N} = 2$ action and supersymmetry variations we find a consistent theory on $M_3 \times S^2$ for each choice of the parameter v. It features as the prefactor of a spinorial kinetic term for the field $\phi^{\alpha\hat{\alpha}}$ of the form

$$\mathcal{L}_v \sim v \; \phi_{\alpha\hat{\alpha}} (\not{\mathcal{D}}\phi)^{\alpha\hat{\alpha}} \,, \tag{6.40}$$

where $\not{\mathcal{D}}$ is the (twisted) Dirac-operator on M_3. To preserve supersymmetry we also need to add mass terms for the bosonic fields φ and $\phi^{\alpha\hat{\alpha}}$ and their superpartners. We

then find the action

$$
\begin{aligned}
S &= \frac{r}{32\pi^2}\int_{M_3\times S^2}\sqrt{|g|}\;d^3x\;\sin\theta\;d\theta\;d\phi\,(\mathcal{L}_A+\mathcal{L}_\Phi+\mathcal{L}_\rho+\mathcal{L}_{\rm int})\\
\mathcal{L}_A &= \mathrm{Tr}\left(\frac{1}{2}F_{ab}F^{ab}+\frac{4}{r^2}F_{xa}F^{xa}+\frac{8}{r^4}F_{xy}F^{xy}+\frac{2i}{r}\;\mathrm{CS}(A)\right)\\
\mathcal{L}_\Phi &= \mathrm{Tr}\left(\mathcal{D}_a\varphi\mathcal{D}^a\varphi-\frac{1}{2}\phi_{\alpha\hat\alpha}(\not{\mathcal{D}}^2\phi)^{\alpha\hat\alpha}-\frac{i}{4}\varepsilon_{abc}F^{ab}[\phi_{\alpha\hat\alpha},\phi^{\beta\hat\alpha}](\sigma^c)^\alpha{}_\beta\right.\\
&\qquad -\frac{v}{2r}\phi_{\alpha\hat\alpha}(\not{\mathcal{D}}\phi)^{\alpha\hat\alpha}+\frac{4}{r^2}\mathcal{D}_x\varphi\mathcal{D}^x\varphi+\frac{2}{r^2}\mathcal{D}_x\phi_{\alpha\hat\alpha}\mathcal{D}^x\phi^{\alpha\hat\alpha}\\
&\qquad \left.-\frac{8(1-v)}{r^3}\varepsilon^{xy}F_{xy}\varphi+\frac{4(1-v)}{r^2}\varphi^2+\frac{(2+v)(2-v)}{8r^2}\phi_{\alpha\hat\alpha}\phi^{\alpha\hat\alpha}\right)\\
\mathcal{L}_\rho &= \mathrm{Tr}\left(-\xi_{a\mu}(\sigma_3)^\mu{}_\nu\mathcal{D}^a\lambda^\nu-\frac{1}{2}\varepsilon_{abc}\xi^a_\mu(\sigma_3)^\mu{}_\nu\mathcal{D}^b\xi^{c\nu}+\frac{i}{4}\rho_{\mu\alpha\hat\alpha}(\sigma_3)^\mu{}_\nu(\not{\mathcal{D}}_{M_3}\rho)^{\nu\alpha\hat\alpha}\right.\\
&\qquad +\frac{i}{r}\lambda_\mu\not{\mathcal{D}}_{S^2}{}^\mu{}_\nu\lambda^\nu+\frac{i}{r}\xi_{a\mu}\not{\mathcal{D}}_{S^2}{}^\mu{}_\nu\xi^{a\nu}+\frac{i}{2r}\rho_{\mu\alpha\hat\alpha}\not{\mathcal{D}}_{S^2}{}^\mu{}_\nu\rho^{\nu\alpha\hat\alpha}\\
&\qquad \left.-\frac{iv}{r}\lambda_\mu(\sigma_3)^\mu{}_\nu\lambda^\nu-\frac{i(2-v)}{8r}\rho_{\mu\alpha\hat\alpha}(\sigma_3)^\mu{}_\nu\rho^{\nu\alpha\hat\alpha}\right)\\
\mathcal{L}_{\rm int} &= \mathrm{Tr}\left(-\frac{1}{2}\lambda_\mu[\varphi,\lambda^\mu]-\frac{1}{2}\xi_{a\mu}[\varphi,\xi^{a\mu}]+\frac{1}{4}\rho_{\mu\alpha\hat\alpha}[\varphi,\rho^{\mu\alpha\hat\alpha}]-\frac{1}{2}\lambda_\mu[\rho^\mu_{\alpha\hat\alpha},\phi^{\alpha\hat\alpha}]\right.\\
&\qquad \left.+\frac{i}{2}\xi_{a\mu}[\rho^\mu_{\alpha\hat\alpha},\phi^{\beta\hat\alpha}](\sigma^a)^\alpha{}_\beta+\frac{1}{2}[\varphi,\phi_{\alpha\hat\alpha}][\varphi,\phi^{\alpha\hat\alpha}]+\frac{1}{8}[\phi_{\alpha\hat\alpha},\phi_{\beta\hat\beta}][\phi^{\alpha\hat\alpha},\phi^{\beta\hat\beta}]\right),
\end{aligned}
\tag{6.41}
$$

where $\mathrm{CS}(A)$ is the Chern-Simons functional on M_3. This action is invariant under the supersymmetry variations

$$
\begin{aligned}
\delta A_b &= -\frac{1}{2}\epsilon_\mu(\sigma_3)^\mu{}_\nu\xi^\nu_b\,, & \delta A_x &= -\frac{ir}{4}\epsilon_\mu(\sigma_x)^\mu{}_\nu\lambda^\nu\\
\delta\varphi &= \frac{1}{2}\epsilon_\mu\lambda^\mu\,, & \delta\phi^{\alpha\hat\alpha} &= -\frac{1}{2}\epsilon_\mu\rho^{\mu\alpha\hat\alpha}\\
\delta\lambda^\mu &= -\frac{2i}{r}\varphi(\sigma_3)^\mu{}_\nu\epsilon^\nu+\frac{2i}{r}\mathcal{D}_x\varphi(\sigma^x)^\mu{}_\nu\epsilon^\nu+\frac{2i}{r^2}F_{xy}\varepsilon^{xy}(\sigma_3)^\mu{}_\nu\epsilon^\nu\\
\delta\xi^\mu_a &= -\frac{1}{2}\varepsilon_{abc}F^{bc}\epsilon^\mu-\mathcal{D}_a\varphi(\sigma_3)^\mu{}_\nu\epsilon^\nu-\frac{2i}{r}F_{xa}(\sigma_3\sigma^x)^\mu{}_\nu\epsilon^\nu+\frac{i}{4}[\phi_{\alpha\hat\alpha},(\sigma_a)^\alpha{}_\beta\phi^{\beta\hat\alpha}]\epsilon^\mu\\
\delta\rho^{\mu\alpha\hat\alpha} &= i\frac{(2-v)}{2r}\phi^{\alpha\hat\alpha}(\sigma_3)^\mu{}_\nu\epsilon^\nu-i(\sigma_a)^\alpha{}_\beta\mathcal{D}^a\phi^{\beta\hat\alpha}(\sigma_3)^\mu{}_\nu\epsilon^\nu\\
&\quad -\frac{2i}{r}\mathcal{D}_x\phi^{\alpha\hat\alpha}(\sigma^x)^\mu{}_\nu\epsilon^\nu+[\varphi,\phi^{\alpha\hat\alpha}]\epsilon^\mu\,.
\end{aligned}
\tag{6.42}
$$

after imposing (6.39) on the supersymmetry parameter.

6.3.3 Reduction to Chern-Simons-Dirac Theory

The reduction of the action and supersymmetry variations proceeds by expanding the fields in terms of spherical harmonics on S^2. For the gauge fields we first note that S^2 does not admit any non-trivial one-forms and therefore there are no zero modes for the gauge field A_x. However, we need to integrate out F_{xy} which sets it to

$$F_{xy} = \frac{r}{2}(1-v)\ \varphi\ \varepsilon_{xy}\,, \tag{6.43}$$

leading to an additional mass term for φ. Taking the zero mode of A_b on the sphere leads to the 3d action

$$S_A = \frac{1}{4\pi}\int d^3x\,\mathrm{Tr}\left(\frac{r}{2}F\wedge\star F + i\mathrm{CS}(A)\right)\,, \tag{6.44}$$

where all higher modes become massive and decouple. In the limit $r\to 0$ the Yang-Mills term is suppressed and we obtain real Chern-Simons theory at level $k=1$. Depending on the choice of v this is coupled to additional fields. For a generic choice for v the theory reduces to real Chern-Simons theory. However it is clear that if the 3d–3d correspondence is to hold, the topological theory has to be sensitive to the twisted harmonic spinors ϕ on M_3. Even for the abelian theory it is clear that non-trivial $d_{\not{\mathcal{D}}}(M_3,g)$ will result in additional scalar multiplets that contribute to the sphere partition function. This motivates us to consider the case $v=2$, where the twisted harmonic spinor and its superpartner become massless. It would indeed be very nice to have another first principle way to fix v from the reduction in the supergravity background.

For this choice, the mode of $\phi^{\alpha\hat{\alpha}}$ that is constant along the S^2 becomes massless in 3d and the reduction of its kinetic term is straightforward

$$S_\phi^{v=2} = \frac{1}{8\pi}\int d^3x\,\mathrm{Tr}\left(-\frac{r}{2}\phi_{\alpha\hat{\alpha}}(\not{\mathcal{D}}^2\phi)^{\alpha\hat{\alpha}} - \phi_{\alpha\hat{\alpha}}(\not{\mathcal{D}}\phi)^{\alpha\hat{\alpha}}\right)\,. \tag{6.45}$$

Crucially, the spinorial kinetic term is leading in the limit $r\to 0$. The massless field content is completed by spinors λ and scalars φ. Since the kinetic term of λ couples

to ξ in (6.41) the massive modes ξ^a have to be integrated out correctly. The same procedure was also used in [101]. Crucially, the kinetic terms of the λ become bosonic and scale with r. The same naturally happens for the kinetic terms of the scalars φ. Here, we will only consider terms at leading order in r, so these fields do not receive a kinetic term.[8] Nevertheless, they still appear in the action to order $\mathcal{O}(r^0)$ in the form of non-vanishing Yukawa couplings. However, these fields do not couple to the gauge field or the bispinor and are thus non-dynamical. This interaction term therefore vanishes on-shell. At leading order in r we are left with the action

$$S^{v=2} = \frac{i}{4\pi}\int d^3x\,\mathrm{Tr}\left(\mathrm{CS}(A) + \frac{i}{2}\phi_{\alpha\hat{\alpha}}(\not{\mathcal{D}}\phi)^{\alpha\hat{\alpha}}\right)\,. \tag{6.46}$$

This theory is non-abelian Chern-Simons theory coupled to twisted harmonic spinors, i.e. non-abelian Chern-Simons-Dirac theory. The equations of motion are given by the generalised Seiberg-Witten equations

$$(\not{\mathcal{D}}\phi)^{\alpha\hat{\alpha}} = 0\,, \qquad \varepsilon_{abc}F^{bc} - \frac{i}{2}[\phi_{\alpha\hat{\alpha}}, (\sigma_a)^{\alpha}{}_{\beta}\phi^{\beta\hat{\alpha}}] = 0\,, \tag{6.47}$$

that have already appeared at various points throughout this chapter.

6.3.4 Generalisation to $L(k,1)$

In the preceding sections we have determined the reduction of the 6d $\mathcal{N} = (2,0)$ theory on a three-sphere. There is a straightforward generalisation to Lens spaces $L(k,1)$ which we can write as a Hopf fibration $S^1 \hookrightarrow L(k,1) \to S^2$, where the radii of the spheres are given by

$$R_{S^1} = \frac{r}{k}\,, \qquad R_{S^2} = \frac{r}{2}\,. \tag{6.48}$$

The length scale r is chosen to have the same interpretation as in the previous discussion, such that for $k = 1$ the setup reduces to $L(1,1) = S^3$. The metric of the

[8] In [101] the corresponding fields are interpreted as ghosts responsible for gauge fixing. In the case at hand this interpretation is rather unclear.

Lens space is given by

$$ds^2 = \left(\frac{r}{2}\right)^2 \left(d\theta^2 + \sin^2\theta \; d\phi^2\right) + \left(\frac{r}{k}\right)^2 (kC + d\psi)^2 \,, \tag{6.49}$$

where C is the graviphoton and ψ is the coordinate on the fibre. One can then repeat the reduction of the 6d $\mathcal{N} = (2,0)$ along the fibre in [100] for general k. From the metric (6.49) we find that the dilaton $g_{\psi\psi}^{-1/2} = \frac{k}{r}$ gets rescaled by k and we can interpret the resulting 5d theory as $\mathcal{N} = 2$ SYM coupled to k units of graviphoton flux.

The rescaling of the dilaton by k has the effect of rescaling the entire 5d action as

$$S_k = k \; S_{k=1} \,, \tag{6.50}$$

where $S_{k=1}$ is the action in (6.41). The 5d supersymmetry variations and Killing spinor equations in [100] are unchanged since they only depend on the invariant combination $G \; g_{\psi\psi}^{1/2}$. This rescaling does not affect the subsequent reduction on the S^2 and we can thus conclude that the reduction on the Lens space yields the same one-parameter family of theories, now with Chern-Simons level k. Choosing $v = 2$ we obtain

$$S_k^{v=2} = \frac{ik}{4\pi} \int d^3x \, \mathrm{Tr} \left(\mathrm{CS}(A) + \frac{i}{2} \phi_{\alpha\hat{\alpha}} (\not{\mathcal{D}}\phi)^{\alpha\hat{\alpha}} \right) \,, \tag{6.51}$$

i.e. Chern-Simons-Dirac theory at level k. This generalises our proposed correspondence (6.3) to

$$Z_{L(k,1)}(T_{\mathcal{N}=1}[M_3, G]) = \mathcal{Z}_{\mathrm{CSD}_k, G}(M_3) \,. \tag{6.52}$$

Chapter 7

Conclusion and Outlook

In this thesis we have discussed two related but yet distinct topics. The goal of this concluding chapter is to bring our different results together and point to some possible future research.

In part I we were primarily concerned with 5d $\mathcal{N} = 1$ SCFTs. Starting with (p, q) 5-brane-webs we associated to them a generalised toric polygon whose primary role in this thesis was as an efficient description of the SCFT. We proposed an algorithm to compute the magnetic quiver, and thus the Higgs branch, directly in the GTP and successfully tested this procedure in a variety of examples. In the ideal case we would identify the Calabi-Yau manifold which corresponds to the GTP. Of course, this is no simple task, as there is no geometric interpretation of unoccupied lattice sites in toric geometry. Nevertheless, a proper dictionary would allow for a complete understanding of the Higgs branch of 5d SCFTs directly in the geometry. Another possible route concerns the applicability of the algorithm to compute the magnetic quiver from a GTP. In practice it is hard to check whether a polygon obeys the s-rule, i.e. is supersymmetric — the Mathematica programme attached to [1] relies on a simplified rule. Thus, it would be immensely beneficial to find a more efficient method to check the s-rule for a given polygon, or equivalently for a (p, q) 5-brane-web.

In part II we looked at the 3d-3d correspondence. In chapter 5 we proposed a refinement of the correspondence, due to the presence of higher-form symmetries. We

properly defined the 3d $\mathcal{N} = 2$ theories $T[M_3]$, for M_3 a Seifert manifold, paying special attention to the global structure of the gauge group. For various examples we computed the Witten index for gauge algebra $\mathfrak{su}(2)$, by counting Bethe vacua. These results were compared to certain flat connections on M_3, verifying the proposed correspondence. A pressing question is whether this construction is adaptable to more general three-manifolds. Our logic relies on the existence of a $U(1)_t$ flavour symmetry, which corresponds to a $U(1)$ isometry of M_3. Another possible generalisation is the analysis of other observables, especially the partition functions on manifolds with torsion.

In chapter 6 we proposed 3d-3d correspondences for the Witten index and the S^3-partition function of 3d $\mathcal{N} = 1$ theories. We discussed details of the $T_{\mathcal{N}=1}[M_3]$ theories and related them to the geometry of associative three-cycles. Finally, we tested the correspondences in some simple examples. Several details of this setup require further attention. First of all, the relevant equations for this correspondence, the generalised Seiberg-Witten equations, are not well-studied. On general manifolds very little is known about their solutions, so the correspondence is difficult to check. However, they provide an excellent opportunity to study associative three-cycles and their embedding into G_2-manifolds. Another interesting question is whether it is possible to study these 3d $\mathcal{N} = 1$ theories by mimicking the construction of chapter 5. To this end it is necessary to study which boundary conditions of the 4d $\mathcal{N} = 4$ theory [23, 154, 155, 194–198] correspond to the geometric construction.

One of the properties of 5d SCFTs we discussed in this thesis is their flavour or zero-form symmetry. Recently, it was found that these theories can also exhibit a discrete one-form symmetry [199–202]. These were shown to be invariant under RG-flow and consistent with dualities. However, one-form symmetries only occur in theories with a limited amount of matter. Notably, these results were found from a geometric point of view, looking at the M-theory compactification on a Calabi-Yau manifold. If

the geometry is toric, the one-form symmetry can be easily obtained from the toric diagram. An obvious question is how these methods transfer to general GTPs, that do not immediately correspond to Calabi-Yau manifolds. In addition, this analysis could function as a clarification of the geometric interpretation of general GTPs. A related question is whether higher-form symmetries can be directly computed in the (p, q) 5-brane-web. In principle, we would expect the brane-web to include string modes, invariant under the RG-flow and dualities, that generate this one-form symmetry. However, it is unclear which modes could be responsible for this.

Another interesting question is whether 3d-3d correspondences also exist for 6d SCFTs with $\mathcal{N} = (1, 0)$ supersymmetry. These are harder to handle than the 6d (2,0) theory since usually the field content is not known. However, some theories, like the conformal matter theories [38], are reasonably well-understood. Flux compactifications of such 6d (1,0) SCFTs were already considered on Riemann surfaces to 4d $\mathcal{N} = 1$ [89, 203–207] and Kähler four-cycles to 2d $\mathcal{N} = (0, 1)$ theories [171]. Similarly, one can consider the compactification on a special Lagrangian three-cycle, resulting in a 3d $\mathcal{N} = 1$ theory. However, a common strategy in even dimensions is the analysis of anomaly polynomials which is not an option in 3d. An alternative way to make progress is to consider three-manifolds with circle fibres and study the compactification of 5d SCFTs on a Riemann surface.

As presented, this work includes a multitude of important results on various aspects of supersymmetric gauge theories and superconformal field theories. Undoubtedly, they lend themselves as basis for further research in a wide range of different directions. We are convinced that this thesis provides a further piece of the puzzle that is understanding string theory.

Appendix A

Appendices to Part I

A.1 Brane-Webs for $SU(N)$ Gauge Theories

In this appendix we collect various existing results in the literature, regarding the (p,q) 5-brane-webs of $SU(N)$ gauge theories with antisymmetric and fundamental matter. These were discussed in a variety of papers [54,64,68,142]. We will use these results to construct the corresponding GTPs summarised in table 3.1. This discussion is ordered by the number of antisymmetric hypermultiplets, N_{AS}. First, for $N_{AS} = 0$ the theories are SQCDs. The brane-web for the $SU(N)_k + N_F \boldsymbol{F}$ is given by[1]

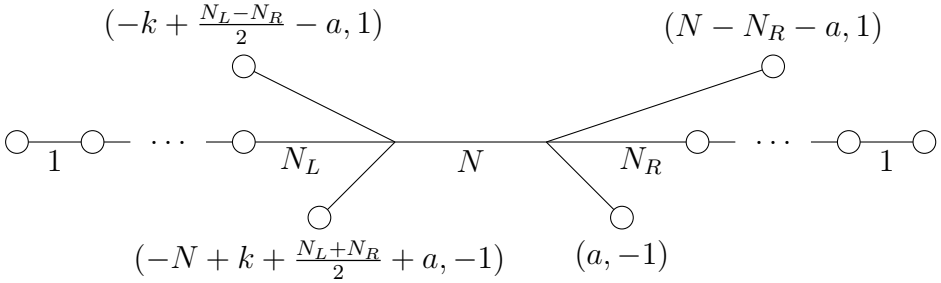

(A.1)

If not stated otherwise, the same number of D5-branes end on each of the D7-branes and unlabelled 5-branes have multiplicity one. There are apparently two free parameters. First, we can choose the number of D7-branes on the left and on the right

[1]The drawing is for parameters $(N, k, N_L, N_R, a) = (N, \frac{1}{2}, N-3, N-4, 1)$

respectively, where

$$N_L + N_R = N_F \,. \tag{A.2}$$

Secondly, there is an overall $SL(2,\mathbb{Z})$ transformation with $\phi = T^n$, that leaves the D7-branes invariant.[2] This freedom is parametrised by a. However, the resulting theory is in fact invariant under both these operations. Thus, we can choose $N_L - N_R$ and a to simplify the setup. In the following, we will always use an appropriate choice of $SL(2,\mathbb{Z})$-frame.

Next, consider the case with a single antisymmetric $N_{AS} = 1$. It was found that the web can be written in terms of a (resolved) $O7^-$-plane and depends on whether N is even or odd. Concretely, the web is[3]

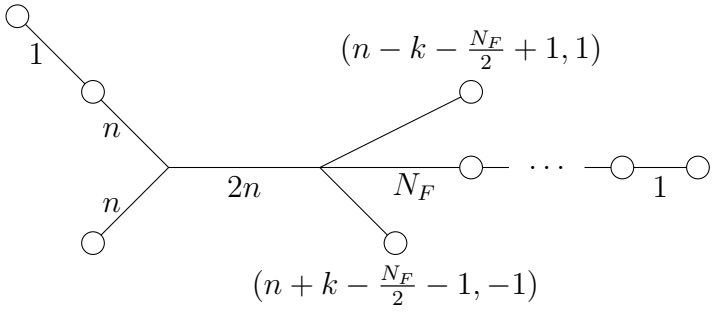

(A.3)

for even $N = 2n$ and

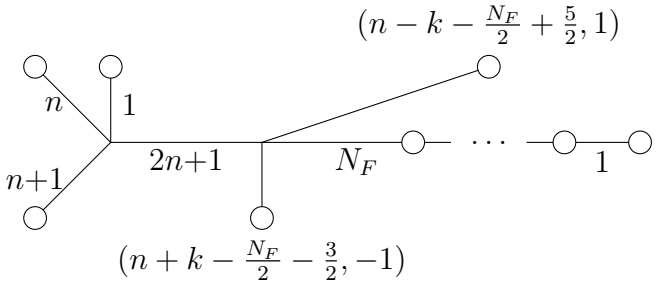

(A.4)

for odd $N = 2n+1$. In both cases we choose to have antisymmetric and fundamental matter on different sides, i.e. $N_L = 0$, but this is not strictly necessary.

[2] In fact, we could also choose any other $SL(2,\mathbb{Z})$-transformation.

[3] Both drawings are for parameters $(N, k, N_F) = (N, \frac{1}{2}, N-3)$

Finally, there are theories with $N_{AS} = 2$. Again, they depend on the parity of N and are given by[4]

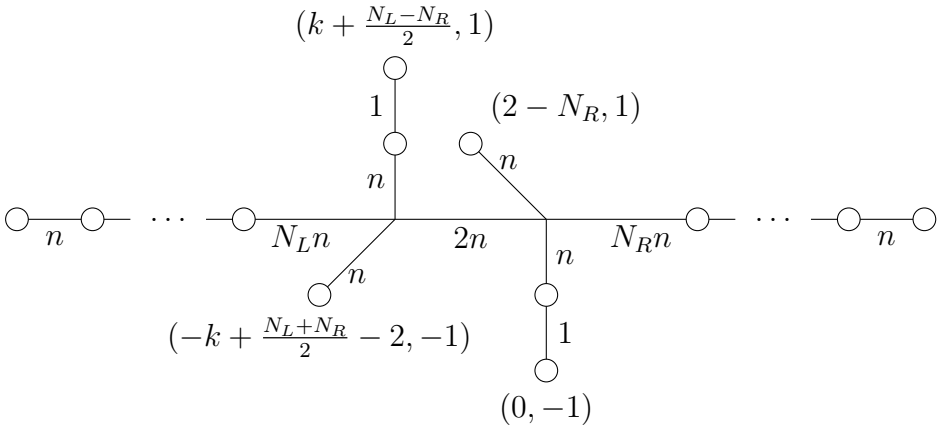

(A.5)

for even $N = 2n$ and

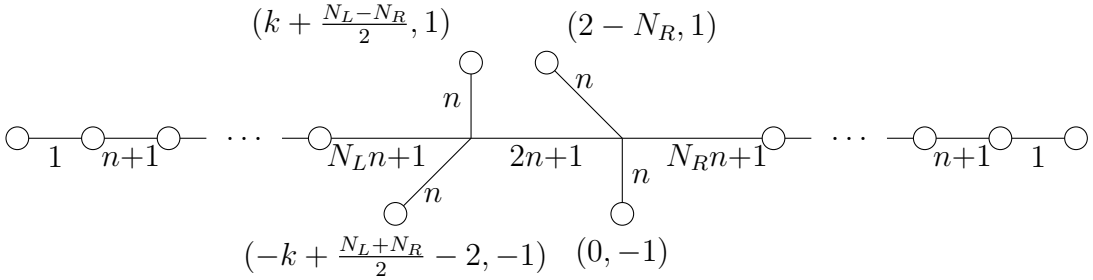

(A.6)

for odd $N = 2n + 1$.

A.2 Detailed Analysis of the Submarginal SQCD

In this appendix we provide a full analysis of the $SU(N)_{\frac{1}{2}} + 1\boldsymbol{AS} + (2N{+}3)\boldsymbol{F}$ starting with the non-convex pGTP (3.71), drawn for $N = 2$

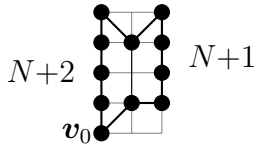

(A.7)

[4]Both drawings are for parameters $(N, k, N_L, N_R) = (N, 1, 1, 3)$

A.2.1 Monodromy Moves

We now present how to determine the convex GTP (3.74) from (A.7). Recall, that the polygon is represented by

$$\boldsymbol{u} = \left[(1,1),(1,0),\underbrace{(0,1)}_{N+1},(-1,-1),(-1,1),\underbrace{(0,-1)}_{N+2}\right] . \tag{A.8}$$

The non-convex edges are $\mathfrak{C} = \{1, N+4\}$. First, let us perform an edge-move $\mathfrak{M}^-_{N+4}$. Using the rules laid out in (3.26), the polygon becomes

$$\boldsymbol{u} \mapsto \mathfrak{M}^-_{N+4}\boldsymbol{u} = \left[(1,1),(1,0),\underbrace{(0,1)}_{N+1},(1,3),(-3,-3),\underbrace{(0,-1)}_{N+2}\right] , \quad N+2 \quad N+1 \quad \boldsymbol{v}_0 \tag{A.9}$$

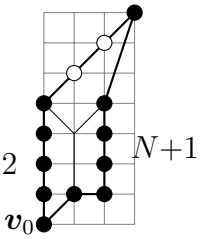

As we can see there are now white vertices, because in the resulting polygon $\mathfrak{M}^-_{N+4}\boldsymbol{u}$ we have $\mu_{N+5} = 3$. Next, we move the $(1,3)$ edge through all the $(0,1)$ edges by applying $\mathfrak{M}^+_3 \ldots \mathfrak{M}^+_{N+3}$. Then, the vectors are given by

$$\mathfrak{T}\boldsymbol{u} = \left[(1,1),(1,0),(N+2,3N+6),\underbrace{(-1,-2)}_{N+1},(-3,-3),\underbrace{(0,-1)}_{N+2}\right] . \tag{A.10}$$

Now, we remove the non-convexity at $i = 1$. We apply the edge-move $\mathfrak{M}^+_1$ which yields the vectors

$$\mathfrak{T}\boldsymbol{u} = \left[(2,0),(0,1),(N+2,3N+6),\underbrace{(-1,-2)}_{N+1},(-3,-3),\underbrace{(0,-1)}_{N+2}\right] , \tag{A.11}$$

and subsequently apply the operation $\mathfrak{M}^-_2$ to arrive at

$$\mathfrak{T}\boldsymbol{u} = \left[(2,0),(N+2,2N+4),(0,N+3),\underbrace{(-1,-2)}_{N+1},(-3,-3),\underbrace{(0,-1)}_{N+2}\right] . \tag{A.12}$$

The series of polygons, obtained after each of the previous steps, is given by

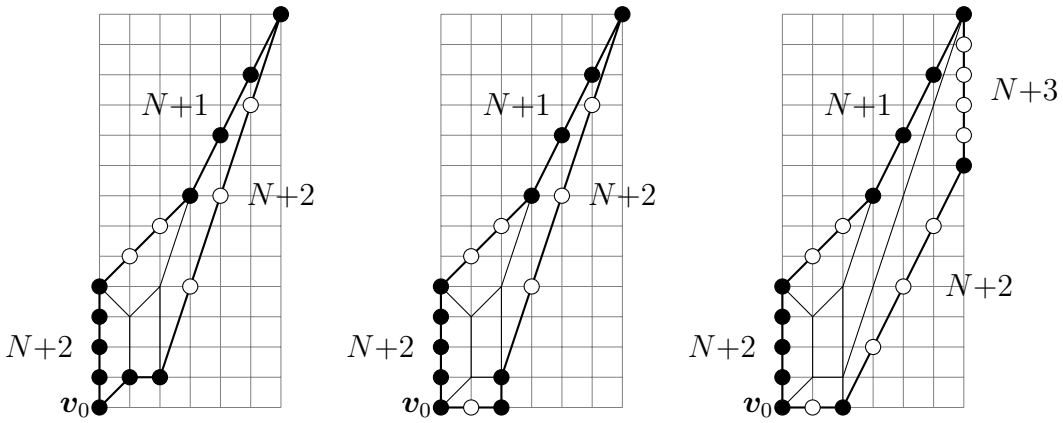

(A.13)

Finally, we move the $(-3,-3)$ edge through the $(-1,-2)$ edges, and obtain the vectors

$$\mathfrak{T}\boldsymbol{u} = \left[(2,0),(N+2,2N+4),(0,N+3),(-N-4,-N-4),\underbrace{(0,-1)}_{2N+3}\right], \tag{A.14}$$

where we have written the entire sequence of transformations in a compact form as

$$\mathfrak{T} = \mathfrak{M}_4^+ \ldots \mathfrak{M}_{N+4}^+ \mathfrak{M}_2^- \mathfrak{M}_1^+ \mathfrak{M}_3^+ \cdots \mathfrak{M}_{N+3}^+ \mathfrak{M}_{N+4}^- . \tag{A.15}$$

The convex GTP is

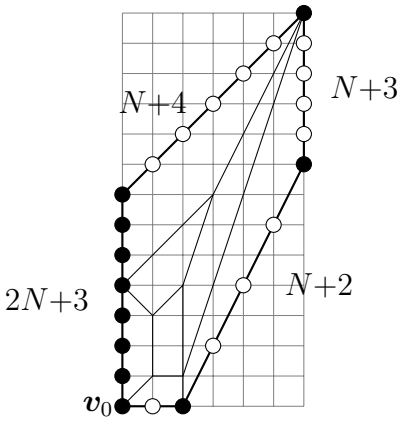

(A.16)

A.2.2 Magnetic Quiver

SCFT

We can now compute the magnetic quiver. Let us start with the SCFT, obtained by removing the internal edges. The data of the GTP, which we call P, as defined in

section 3.1.1, is given by

$$E_\alpha = ((2,0),(N+2,2N+4),(0,N+3),(-N-4,-N-4),(0,-2N-3))\,,$$
$$L_\alpha = ((1,0),(1,2),(0,1),(-1,-1),(0,-1))\,, \quad \lambda_\alpha = (2,N+2,N+3,N+4,2N+3) \tag{A.17}$$

From the distribution of black and white vertices we can read off

$$b_\alpha = (0,0,0,0,2N+2)\,, \qquad \mu_{\alpha,x} = \left(\{2\},\{N+2\},\{N+3\},\{N+4\},\{1^{2N+3}\}\right)\,. \tag{A.18}$$

The only possible colouring with its subdivision is given by

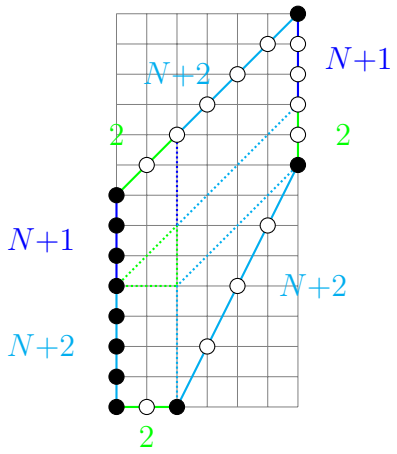

(A.19)

Thus, the refined Minkowski sum decomposition of P is given by

$$P < \ (N+2)\times \ \oplus \ 2\times \ \oplus \ (N+1)\times \tag{A.20}$$

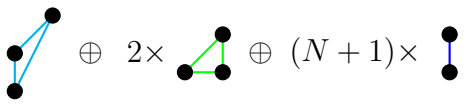

with the partitions and multiplicities of these colourings being

$$\begin{aligned} \mu^c_{\alpha x} &= (-,\{N+2\},-,\{N+2\},\{N+2\})\,, & m^c &= N+2 \\ \mu^g_{\alpha x} &= (\{2\},-,\{2\},\{2\},-)\,, & m^g &= 2 \\ \mu^b_{\alpha x} &= (-,-,\{N+1\},-,\{N+1\})\,, & m^b &= N+1\,. \end{aligned} \tag{A.21}$$

Clearly, all the summands in (A.20) are irreducible and obey the s-rule minimally (up to multiplicity). From the colour-subdivision we see that the mixed volumes are

$$A^{cg} = 4(N+2)\,, \quad A^{cb} = (N+1)(N+2)\,, \quad A^{gb} = 2(N+1)\,, \tag{A.22}$$

and from (A.21) and (A.22) we can compute the intersections between the colour nodes using (3.52)

$$k^{cg} = 1\,, \quad k^{cb} = 0\,, \quad k^{gb} = 0\,. \tag{A.23}$$

Now, let's turn to the additional nodes, which only appear at edge E_5. The node labels and their connections to the colour nodes can be read off from the $\mu_{\alpha,x}$ and $\mu^c_{\alpha,x}$ in (A.17) and (A.21)

$$m_{5,x} = (2N+2, \ldots, 1)\,, \qquad k^c_{5,1} = 1\,, \quad k^b_{5,1} = 1 \tag{A.24}$$

and all others vanishing. Putting all this together the magnetic quiver is given by

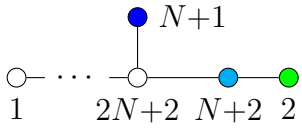

(A.25)

where we depicted the nodes according to the colouring of P.

Gauge Theory

Let us now include the internal edges, from which we can compute the magnetic quiver of the weakly coupled gauge theory description. There is one colouring, given by

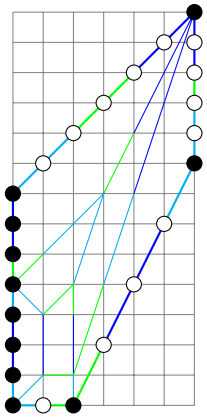

(A.26)

Here, the blue sub-web has multiplicity $m^b = N$, whereas the other ones have multiplicity $m^g = m^c = 1$. As expected, the resulting magnetic quiver is given by

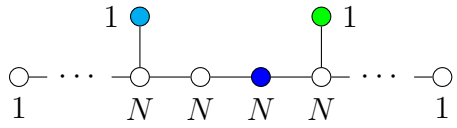

(A.27)

A.3 Tables of Magnetic Quivers

In this appendix we tabulate some of the magnetic quivers for SCFTs with a weakly coupled description of the form $SU(N)_k + N_{AS}\boldsymbol{AS} + N_F\boldsymbol{F}$ for $N > 3$[5] with sufficiently many flavours. A more exhaustive set of tables can be found in [2].[6] We will group them first depending on $N_{AS} = 0, 1, 2$ and possibly the parity of their rank. Each table is then structured in terms of

$$\Delta_\pm = \pm k - N + \frac{1}{2}\sum_{\boldsymbol{R}} N_{\boldsymbol{R}}\,|A(\boldsymbol{R})| = \pm k + \frac{N_F}{2} + \frac{N_{AS}}{2}\,|N-4| - N\,. \tag{A.28}$$

Without loss of generality we consider $k \geq 0$, i.e. $\Delta_+ \geq \Delta_-$. We will see that theories with the same Δ_+ or Δ_- have similar properties. Furthermore, we give the flavour symmetry, which might be further enhanced for low rank [2, 53, 208]. Finally, we consider the theories of the form $[n_1] - SU(2)^m - [n_2]$ with $n_2 = 0$ and $\theta = 0$, labelled by n_1 in table A.6. The remaining theories of this form have an SQCD dual with $\Delta_\pm = (n_1 - 2, n_2 - 2)$.

[5] Recall that for $N = 2$ and $N = 3$ the $\boldsymbol{AS}$ representation corresponds to the trivial and anti-fundamental representation respectively.

[6] There, we consider theories with even fewer flavours and include the descendants of the higher rank E-string.

$\Delta_\pm$	2	1	0	-1
2	Marginal	–	–	–
1	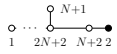 $\mathfrak{d}_{2N+4}$	 $\mathfrak{a}_{2N+3}$	–	–
0	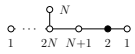 $\mathfrak{d}_{2N+2} \oplus \mathfrak{a}_1$	 $\mathfrak{a}_{2N+1} \oplus \mathfrak{a}_1$	 $\mathfrak{a}_{2N-1} \oplus \mathfrak{a}_1^2$	–
−1	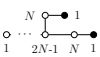 $\mathfrak{d}_{2N+1} \oplus \mathfrak{u}_1$	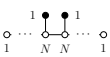 $\mathfrak{a}_{2N} \oplus \mathfrak{u}_1$	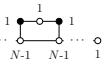 $\mathfrak{a}_{2N-2} \oplus \mathfrak{a}_1 \oplus \mathfrak{u}_1$	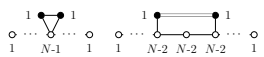 $\mathfrak{a}_{2N-3} \oplus \mathfrak{u}_1^2$
−2	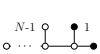 $\mathfrak{d}_{2N} \oplus \mathfrak{u}_1$	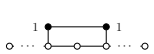 $\mathfrak{a}_{2N-1} \oplus \mathfrak{u}_1$	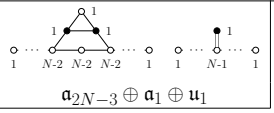 $\mathfrak{a}_{2N-3} \oplus \mathfrak{a}_1 \oplus \mathfrak{u}_1$	
−3	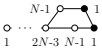 $\mathfrak{d}_{2N-1} \oplus \mathfrak{u}_1$	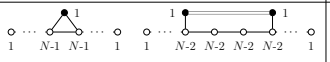 $\mathfrak{a}_{2N-2} \oplus \mathfrak{u}_1$		
−4	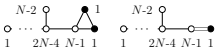 $\mathfrak{d}_{2N-2} \oplus \mathfrak{u}_1$			

Table A.1: UV-MQs for descendants of $SU(N)_0 + (2N+4)\boldsymbol{F}$ with $N_F \geq (2N-2)$, $k = \frac{1}{2}(\Delta_+ - \Delta_-)$, $N_F = (\Delta_+ + \Delta_- + 2N)$

$\Delta_\pm$	1	0	-1	-2
1	Marginal	–	–	–
0	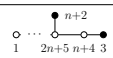 $\mathfrak{a}_{2n+6} \oplus \mathfrak{u}_1$	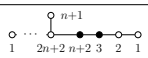 $\mathfrak{a}_{2n+3} \oplus \mathfrak{a}_2 \oplus \mathfrak{u}_1$	–	–
−1	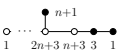 $\mathfrak{a}_{2n+4} \oplus \mathfrak{u}_1^2$	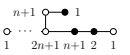 $\mathfrak{a}_{2n+2} \oplus \mathfrak{a}_1 \oplus \mathfrak{u}_1^2$	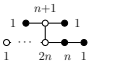 $\mathfrak{a}_{2n+1} \oplus \mathfrak{u}_1^3$	–
−2	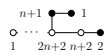 $\mathfrak{a}_{2n+3} \oplus \mathfrak{u}_1^2$	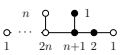 $\mathfrak{a}_{2n+1} \oplus \mathfrak{a}_1 \oplus \mathfrak{u}_1^2$	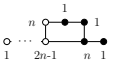 $\mathfrak{a}_{2n} \oplus \mathfrak{u}_1^3$	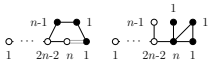 $\mathfrak{a}_{2n-1} \oplus \mathfrak{u}_1^3$
−3	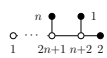 $\mathfrak{a}_{2n+2} \oplus \mathfrak{u}_1^2$	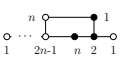 $\mathfrak{a}_{2n} \oplus \mathfrak{a}_1 \oplus \mathfrak{u}_1^2$	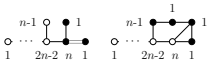 $\mathfrak{a}_{2n-1} \oplus \mathfrak{u}_1^3$	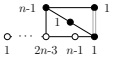 $\mathfrak{a}_{2n-2} \oplus \mathfrak{u}_1^3$
−4	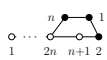 $\mathfrak{a}_{2n+1} \oplus \mathfrak{u}_1^2$	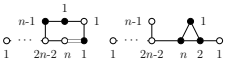 $\mathfrak{a}_{2n-1} \oplus \mathfrak{a}_1 \oplus \mathfrak{u}_1^2$	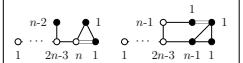 $\mathfrak{a}_{2n-2} \oplus \mathfrak{u}_1^3$	
−5	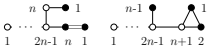 $\mathfrak{a}_{2n} \oplus \mathfrak{u}_1^2$	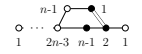 $\mathfrak{a}_{2n-2} \oplus \mathfrak{a}_1 \oplus \mathfrak{u}_1^2$		
−6	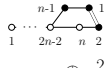 $\mathfrak{a}_{2n-1} \oplus \mathfrak{u}_1^2$			

Table A.2: UV-MQs for descendants of $SU(2n)_0 + 1\boldsymbol{AS} + (2n+6)\boldsymbol{F}$ with $N_F \geq (2n-1)$, $k = \frac{1}{2}(\Delta_+ - \Delta_-)$, $N_F = (\Delta_+ + \Delta_- + 2n + 4)$

$\Delta_\pm$	1	0	-1	-2
1	Marginal	–	–	–
0	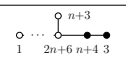 $\mathfrak{a}_{2n+7} \oplus \mathfrak{u}_1$	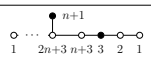 $\mathfrak{a}_{2n+4} \oplus \mathfrak{a}_2 \oplus \mathfrak{u}_1$	–	–
-1	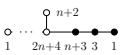 $\mathfrak{a}_{2n+5} \oplus \mathfrak{u}_1^2$	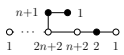 $\mathfrak{a}_{2n+3} \oplus \mathfrak{a}_1 \oplus \mathfrak{u}_1^2$	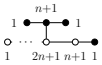 $\mathfrak{a}_{2n+2} \oplus \mathfrak{u}_1^3$	–
-2	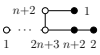 $\mathfrak{a}_{2n+4} \oplus \mathfrak{u}_1^2$	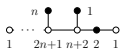 $\mathfrak{a}_{2n+2} \oplus \mathfrak{a}_1 \oplus \mathfrak{u}_1^2$	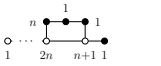 $\mathfrak{a}_{2n+1} \oplus \mathfrak{u}_1^3$	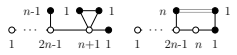 $\mathfrak{a}_{2n} \oplus \mathfrak{u}_1^3$
-3	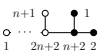 $\mathfrak{a}_{2n+3} \oplus \mathfrak{u}_1^2$	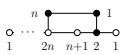 $\mathfrak{a}_{2n+1} \oplus \mathfrak{a}_1 \oplus \mathfrak{u}_1^2$	 $\mathfrak{a}_{2n} \oplus \mathfrak{u}_1^3$	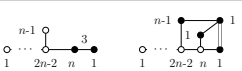 $\mathfrak{a}_{2n-1} \oplus \mathfrak{u}_1^3$
-4	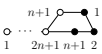 $\mathfrak{a}_{2n+2} \oplus \mathfrak{u}_1^2$	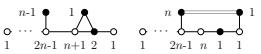 $\mathfrak{a}_{2n} \oplus \mathfrak{a}_1 \oplus \mathfrak{u}_1^2$	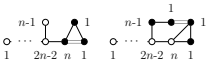 $\mathfrak{a}_{2n-1} \oplus \mathfrak{u}_1^3$	
-5	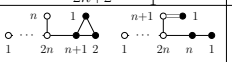 $\mathfrak{a}_{2n+1} \oplus \mathfrak{u}_1^2$	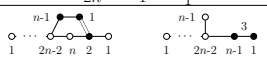 $\mathfrak{a}_{2n-1} \oplus \mathfrak{a}_1 \oplus \mathfrak{u}_1^2$		
-6	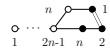 $\mathfrak{a}_{2n} \oplus \mathfrak{u}_1^2$			

Table A.3: UV-MQs for descendants of $SU(2n{+}1)_0{+}1\boldsymbol{AS}{+}(2n{+}7)\boldsymbol{F}$ with $N_F \geq (2n)$, $k = \frac{1}{2}(\Delta_+ - \Delta_-)$, $N_F = (\Delta_+ + \Delta_- + 2n + 5)$

$\Delta_\pm$	1	0	-1	-2
0	–	Marginal	–	–
-1	–	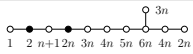 $\mathfrak{e}_7 \oplus \mathfrak{a}_1^3$	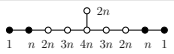 $\mathfrak{e}_6 \oplus \mathfrak{a}_1 \oplus \mathfrak{u}_1^2$	–
-2	Marginal	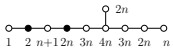 $\mathfrak{d}_6 \oplus \mathfrak{a}_1^3$	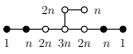 $\mathfrak{d}_5 \oplus \mathfrak{a}_1 \oplus \mathfrak{u}_1^2$	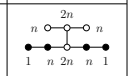 $\mathfrak{d}_4 \oplus \mathfrak{a}_1 \oplus \mathfrak{u}_1^2$
-3	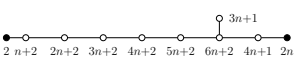 $\mathfrak{d}_8 \oplus \mathfrak{a}_1$	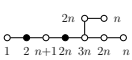 $\mathfrak{a}_5 \oplus \mathfrak{a}_1^3$	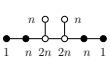 $\mathfrak{a}_4 \oplus \mathfrak{a}_1 \oplus \mathfrak{u}_1^2$	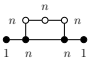 $\mathfrak{a}_3 \oplus \mathfrak{a}_1 \oplus \mathfrak{u}_1^2$
-4	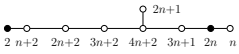 $\mathfrak{d}_6 \oplus \mathfrak{a}_1^2$	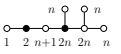 $\mathfrak{a}_3 \oplus \mathfrak{a}_1^4$	 $\mathfrak{a}_2 \oplus \mathfrak{a}_1^2 \oplus \mathfrak{u}_1^2$	
-5	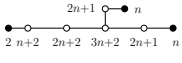 $\mathfrak{d}_5 \oplus \mathfrak{a}_1 \oplus \mathfrak{u}_1$	 $\mathfrak{a}_2 \oplus \mathfrak{a}_1^3 \oplus \mathfrak{u}_1$		
-6	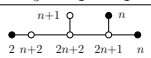 $\mathfrak{d}_4 \oplus \mathfrak{a}_1 \oplus \mathfrak{u}_1$			

Table A.4: UV-MQs for $SU(2n)_k + 2\boldsymbol{AS} + N_F\boldsymbol{F}$ with $N_F \geq 3$, $k = \frac{1}{2}(\Delta_+ - \Delta_-)$, $N_F = (\Delta_+ + \Delta_- + 8)$

$\Delta_\pm$	1	0	-1	-2
0	–	Marginal	–	–
-1	–	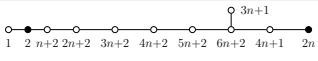 $\mathfrak{d}_8 \oplus \mathfrak{a}_1^2$	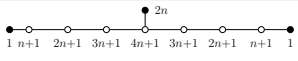 $\mathfrak{a}_7 \oplus \mathfrak{a}_1 \oplus \mathfrak{u}_1$	–
-2	Marginal	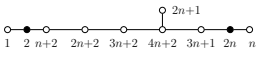 $\mathfrak{d}_6 \oplus \mathfrak{a}_1^3$	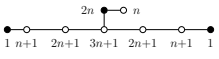 $\mathfrak{a}_5 \oplus \mathfrak{a}_1^2 \oplus \mathfrak{u}_1$	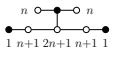 $\mathfrak{a}_3 \oplus \mathfrak{a}_1^3 \oplus \mathfrak{u}_1$
-3	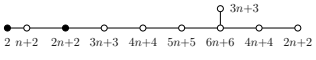 $\mathfrak{e}_7 \oplus \mathfrak{a}_1^2$	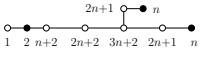 $\mathfrak{d}_5 \oplus \mathfrak{a}_1^2 \oplus \mathfrak{u}_1$	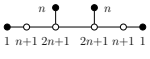 $\mathfrak{a}_4 \oplus \mathfrak{a}_1 \oplus \mathfrak{u}_1^2$	 $\mathfrak{a}_2 \oplus \mathfrak{a}_1^2 \oplus \mathfrak{u}_1^2$
-4	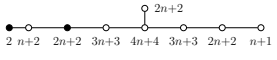 $\mathfrak{d}_6 \oplus \mathfrak{a}_1^2$	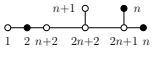 $\mathfrak{d}_4 \oplus \mathfrak{a}_1^2 \oplus \mathfrak{u}_1$	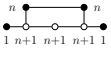 $\mathfrak{a}_3 \oplus \mathfrak{a}_1 \oplus \mathfrak{u}_1^2$	
-5	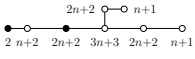 $\mathfrak{a}_5 \oplus \mathfrak{a}_1^2$	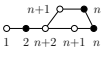 $\mathfrak{a}_3 \oplus \mathfrak{a}_1^2 \oplus \mathfrak{u}_1$		
-6	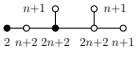 $\mathfrak{a}_3 \oplus \mathfrak{a}_1^3$			

Table A.5: UV-MQs for $SU(2n+1)_k + 2\boldsymbol{AS} + N_F\boldsymbol{F}$ with $N_F \geq 3$, $k = \frac{1}{2}(\Delta_+ - \Delta_-)$, $N_F = (\Delta_+ + \Delta_- + 8)$

n_1	4	3	2	1	0, $\theta = \pi$	0, $\theta = 0$
	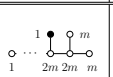 $\mathfrak{d}_{2m+3}$	 $\mathfrak{a}_{2m+2}$	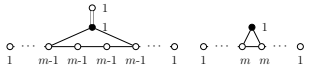 $\mathfrak{a}_{2m} \oplus \mathfrak{a}_1$	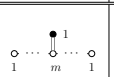 $\mathfrak{a}_{2m-1} \oplus \mathfrak{u}_1$	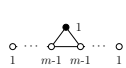 $\mathfrak{a}_{2m-2} \oplus \mathfrak{u}_1$	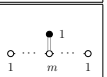 $\mathfrak{a}_{2m-1}$

Table A.6: UV-MQs for $[n_1] - SU(2)^m - [0]_{\theta=0}$

Appendix B

Appendices to Part II

B.1 Positive Curvature Seifert Manifolds

In this appendix we provide concrete specialisations of the Seifert data to three-manifolds that will be studied in chapter 5. For concreteness, we only consider Seifert manifolds fibred over a genus zero base, and with three special fibres

$$M_3 \cong [d = 0;\ g = 0;\ (p_1, q_1),\ (p_2, q_2),\ (p_3, q_3)\ ]\,. \tag{B.1}$$

We are interested in Seifert manifolds with positive scalar curvature which is equivalent to

$$\left(\frac{1}{p_1} + \frac{1}{p_2} + \frac{1}{p_3} - 1\right) > 0\,. \tag{B.2}$$

Such spaces can always be written as quotients

$$M_3 \cong S^3/(\Gamma_1 \times \Gamma_2)\,, \tag{B.3}$$

where $\Gamma_1 \times \Gamma_2$ is a finite subgroup of $SO(4)$ of which at least one is cyclic.[1] We can classify the possibilities, which come in three series:

1. $M_3 \cong [0; 0; (1, 1), (p_2, q_2), (p_3, q_3)]$ are the Lens spaces $L(p, q)$. They are given

[1] Additionally, the orders of the two groups have to be coprime.

by $\mathbb{Z}_p$ quotients of S^3 where the group action is given by

$$(z_1, z_2) \to (e^{2\pi i/p} z_1, e^{2\pi i q/p} z_2)\,, \tag{B.4}$$

where $(z_1, z_2) \in \mathbb{C}^2$. The first homology group is

$$H_1(L(p,q), \mathbb{Z}) \cong \mathbb{Z}_p\,, \tag{B.5}$$

with $p = |p_2 p_3 + p_2 q_3 + p_3 q_2|$.

2. $M_3 \cong [0; 0; (2,-1), (2,1), (p_3, q_3)]$ are the prism manifolds $M^{\text{Prism}}_{p_3,q_3}$. The fundamental group is a product of a cyclic group and a binary dihedral group $\mathbb{D}_m$. The cyclic group becomes trivial for $(p_3, q_3) = (n-2, 1)$. Then, the manifolds are $S^3/\mathbb{D}_{4(n-2)}$ with fundamental group

$$H_1(S^3/\mathbb{D}_{4(n-2)}, \mathbb{Z}) \cong \begin{cases} \mathbb{Z}_2 \times \mathbb{Z}_2 & n \text{ even} \\ \mathbb{Z}_4 & n \text{ odd} \end{cases}\,. \tag{B.6}$$

In the more general case $q_3 \neq 1$ the Γ_i depend non-trivially on q_3.

3. $M_3 \cong [0; 0; (2,-1), (3, q_2), (p_3, q_3)]$, where $p_3 = 3, 4, 5$. The fundamental group is a product of a cyclic group and one of the groups $\mathbb{T}, \mathbb{O}, \mathbb{I}$,[2] depending on p_3. Choosing $(p_3, q_3, q_2) = (m-3, 1, 1)$ leaves the cyclic group trivial. Then, the manifolds are $S^3/\{\mathbb{T}, \mathbb{O}, \mathbb{I}\}$ respectively with fundamental groups

$$H_1(S^3/\mathbb{T}) = \mathbb{Z}_3\,, \qquad H_1(S^3/\mathbb{O}) \ = \mathbb{Z}_2\,, \qquad H_1(S^3/\mathbb{I}) = 1\,. \tag{B.7}$$

The last manifold is also called the Poincaré homology sphere, and is a famous example of an integer homology sphere, i.e. it has the same homology as S^3 but different fundamental group. For simplicity we will not consider the general case with non-trivial q_i.

[2]These are the binary tetrahedral, binary octahedral and binary icosahedral groups of order $(24, 48, 120)$, respectively.

These three series are connected to the semi-simple Lie algebras by the McKay correspondence. In particular, if all the $q_i = 1$ they are known as the S^3/Γ_{ADE}

$$\begin{aligned} S^3/\Gamma_{A_k} &\cong [0;0;(\ell,1),(k-\ell+1,1)] \quad \forall \ell \\ S^3/\Gamma_{D_n} &\cong [0;0;(2,-1),(2,1),(n-2,1)] \\ S^3/\Gamma_{E_m} &\cong [0;0;(2,-1),(3,1),(m-3,1)]\,. \end{aligned} \tag{B.8}$$

B.2 Twisted Superpotential and Bethe Equations for $\widehat{T}[\Omega, SU(2)]$

Let M_3 be a Seifert manifold, with associated graph Ω and linking matrix Q_{ij}. Consider the theory $\widehat{T}[\Omega, SU(2)]$. To compute the twisted superpotential for this theory, we first need to compute the contribution from the building blocks $\varphi = T^k$ and $\varphi = S$.

Let us start with the $T(SU(2))$ theory, i.e. $\varphi = S$. It has a UV Lagrangian description as a $U(1)$ gauge theory with two hypermultiplets. This theory has a manifest $SU(2)_m$ flavour symmetry acting on the hypermultiplets, and the $U(1)_J$ topological symmetry enhances in the IR to another $SU(2)_\zeta$ flavour symmetry. We consider the $\mathcal{N} = 2^*$ version of the theory by turning on a coupling to the diagonal combination of the R-symmetry

$$U(1)_\tau = 2[U(1)_C - U(1)_H]\,, \tag{B.9}$$

where $U(1)_C$ and $U(1)_H$ are a maximal torus of the $SU(2)_C$ and $SU(2)_H$ factors of the R-symmetry. The global symmetry of the theory in the infrared is then

$$SU(2)_\zeta \times SU(2)_m \times U(1)_\tau\,. \tag{B.10}$$

The twisted superpotential can be written as

$$\mathcal{W}_S(u,\zeta,m;\tau) = \mathcal{W}_{\rm FI}(u,\zeta) + \mathcal{W}_{\rm matter}(u,m;\tau)\,, \tag{B.11}$$

where the first term is the contribution from the FI parameter

$$\mathcal{W}_{\rm FI}(u,\zeta) = 2u\zeta\,, \tag{B.12}$$

and the contribution from the matter can be written as

$$\mathcal{W}_{\rm matter}(u,m;\tau) = \mathcal{W}_\Phi(\tau \pm u \pm m) + \mathcal{W}_\Phi(-2\tau)\,. \tag{B.13}$$

Here and below we use the convention that each choice of sign in '$\pm$' is summed over. For the twisted superpotential $\mathcal{W}_\Phi$ of the chiral multiplet we adopt the $U(1)_{-1/2}$ quantisation of the CS level as discussed in [108]. For example, the chiral multiplet with charge ± 1 under the Cartan $U(1)$ contribute as

$$\begin{aligned} \mathcal{W}_\Phi(u) &= \frac{1}{(2\pi i)^2}\,\mathrm{Li}_2(x) \\ \mathcal{W}_{\widetilde{\Phi}}(u) &= \frac{1}{(2\pi i)^2}\,\mathrm{Li}_2(x^{-1}) + \frac{1}{2}u(u+1)\,, \end{aligned} \tag{B.14}$$

where Li_2 is the second polylogarithm.

As mentioned in section 5.1.4 this theory has a dual description as an $SU(2)$ theory with a $k=1$ CS term and $N_f = 2$ fundamental flavours, see figure 5.4. This dual theory has twisted superpotential

$$\widetilde{\mathcal{W}}_S(u,\zeta,m;\tau) = \mathcal{W}_\Phi(\tau \pm u \pm m \pm \zeta) + u^2 - \mathcal{W}_{\rm adj}(\zeta;\tau) - \zeta^2 - m^2\,, \tag{B.15}$$

where the first term comes from the trinion coupling. We have added an adjoint chiral multiplet (the "flip" field) charged under the $SU(2)_\zeta$ symmetry, as well as background CS terms ("contact terms") for the $SU(2)_m \times SU(2)_\zeta$ symmetries. These are both necessary for a precise duality to the usual description of $T(SU(2))$ above. Here, and in general, coupling an adjoint chiral multiplet of positive $U(1)_t$ charge corresponds to

$$\mathcal{W}_{\rm adj}(\zeta;\tau) = \mathcal{W}_\Phi(-2\tau \pm 2\zeta) + \mathcal{W}_\Phi(-2\tau)\,, \tag{B.16}$$

whereas an adjoint of negative charge contributes with $-\mathcal{W}_{\rm adj}$ (up to τ-dependent contact terms, which we ignore). In addition, we have equipped the flavour groups

in $T(SU(2))$ with a background Chern-Simons term. The corresponding contribution to the twisted superpotential is

$$\mathcal{W}_{T^k}(\zeta) = k\ \mathcal{W}_{\rm CS}(\zeta) = k\zeta^2\,, \tag{B.17}$$

where k is the background level. Gauging the flavour symmetry corresponds to promoting the FI parameter to a dynamical field $\zeta \to u$.

We may use these ingredients to construct the twisted superpotential of a general quiver theory, $\widehat{T}[\Omega, SU(2)]$. Including a copy of the twisted superpotential, $\mathcal{W}_S$, of the $T(SU(2))$ theory for each edge, and an appropriate Chern-Simons term for each node, we may write this conveniently in terms of the linking matrix Q_{ij} of (5.12), as

$$\mathcal{W}_\Omega(u_i;\tau) = \sum_{i=1}^{n}\Big(Q_{ii}u_i^2 + N_i^{\rm adj}\mathcal{W}_{\rm adj}(u_i;\tau)\Big) - \sum_{i<j}Q_{ij}\mathcal{W}_S(u_i,u_j;\tau)\,, \tag{B.18}$$

where $N_i^{\rm adj}$ is the number of adjoints attached to the ith node, which can be determined following the prescription in section 5.1.2. Here u_i is the $SU(2)$ fugacity for the ith node.

The number of vacua is given by the number of solutions to the vacuum equations using the definition (5.109)

$$\Pi_i = e^{2\pi i\partial_{u_i}\mathcal{W}_\Omega} = 1\,, \quad i = 1,...,n\,, \tag{B.19}$$

modulo the action of $\mathbb{Z}_2$ Weyl group

$$x_i \to x_i^{-1}\,, \tag{B.20}$$

where $x_i = e^{2\pi i u_i}$.

For general graphs Ω the Bethe equations correspond to a set of coupled polynomial equations. Except for some very limited cases these can not be solved analytically. However, they can be solved using Gröbner basis methods in Mathematica or SINGULAR. These methods are similar to solving systems of linear equations using Gaussian elimination: the system of polynomial equations is mapped to the Gröbner

basis, retaining the same set of solutions. The system of equations can however now be successively solved. For sufficiently small values of the Chern-Simons levels and low rank, i.e. few parameters and Bethe equations, this can be implemented in practice. This was done for linear quivers and the gauged trinion, leading to the results in (5.117) and (5.140).

B.3 One-form Symmetries and Anomalies for Bethe Vacua

In this appendix we discuss the action of 1-form symmetries on the Hilbert space of Bethe vacua on T^2. We can define linear operators on the Hilbert space associated to 1-form generators wrapping the two cycles of the torus

$$U^{\gamma}_{A,B}: \quad \mathcal{H}_{T^2} \to \mathcal{H}_{T^2}\,. \tag{B.21}$$

Then the Hilbert space must fall into representations of the group of these 1-form generators. Although the 1-form symmetry group itself is abelian, in the presence of anomalies this group need not be abelian since we have in general

$$[U^{\gamma_1}_{A}, U^{\gamma_2}_{B}] = e^{2\pi i \mathcal{A}(\gamma_1,\gamma_2)}\,, \tag{B.22}$$

where $\mathcal{A}: \Gamma \times \Gamma \to U(1)$ is the anomaly form.

To see how these operators act on the Bethe vacua, note that we may identify the centre of the gauge group with a set of transformations acting on the gauge variables, $u_i \to u_i + \gamma_i$, which are defined up to large gauge transformations. Now suppose an element $\gamma = (\gamma_1, ..., \gamma_{r_G})$ in the centre acts trivially on the matter. Then we may define the action of the 1-form operators on the basis of Bethe vacua as

$$\begin{aligned} U^{\gamma}_{A} \;&:\; |\widehat{u}_i\rangle \to \Pi^{\gamma}(\widehat{u}_i)|\widehat{u}_i\rangle, \qquad \Pi^{\gamma} \equiv \prod_i \Pi_i{}^{\gamma_i} = e^{2\pi i \gamma_i \partial_{u_i}\mathcal{W}} \\ U^{\gamma}_{B} \;&:\; |\widehat{u}_i\rangle \to |\widehat{u}_i + \gamma_i\rangle\,. \end{aligned} \tag{B.23}$$

We note both operators are well-defined when acting on the space of Bethe vacua (one can show Π^γ is a rational function, given the assumption that γ acts trivially), and satisfy the appropriate group law. One also finds their commutation relations correctly encode the anomalies of the theory

$$U_A^{\gamma_1}\, U_B^{\gamma_2} = e^{2\pi i \gamma_1 \mathcal{A} \gamma_2}\, U_B^{\gamma_2}\, U_A^{\gamma_1}\,. \tag{B.24}$$

Thus in addition to the space of vacua, we can consider the extra data of how the vacua are acted on by these symmetries. This data will be important when gauging the symmetries.

To illustrate this with a simple example, consider the $\widehat{T}[\Omega_{[k]}, SU(2)]$ theory, which is an $SU(2)$ gauge theory with level k CS term and an adjoint. The Bethe equation is

$$\Pi = x^{2k}\left(\frac{t^2x^2-1}{t^2-x^2}\right)^2 = 1\,. \tag{B.25}$$

Then the centre acts as $u \to u + \frac{1}{2}$, or $x = e^{2\pi i u} \to -x$, and so we may take $\gamma = (\frac{1}{2})$, and find from (B.23)

$$U_A^\gamma \;:\; |\widehat{u}\rangle \to -x^k\left(\frac{t^2x^2-1}{t^2-x^2}\right)|\widehat{u}\rangle, \qquad U_B^\gamma \;:\; |\widehat{u}\rangle \to |\widehat{u}+\frac{1}{2}\rangle\,. \tag{B.26}$$

These satisfy $U_A^\gamma U_B^\gamma = (-1)^k U_B^\gamma U_A^\gamma$, which is the expected anomaly coefficient. Note that the overall sign for U_A needs to be fixed by modular invariance.

In the case where the 1-form symmetry Γ is anomaly-free, we may also consider "twisted sectors" in the Hilbert space. These are sectors where we let a 1-form charge operator, U^γ, lie along the time direction, and may be labeled by the element $\gamma \in \Gamma$

$$\mathcal{H}^\gamma_{T^2} = \bigoplus_{\chi_A,\chi_B} \mathcal{H}^\gamma_{\chi_A,\chi_B}, \qquad \gamma \in \Gamma\,, \tag{B.27}$$

where the untwisted sector corresponds to $\gamma = 1$, and we may also simultaneously grade these sectors into characters of the $U_{A,B}$ operators, as above. These twisted sectors are important when gauging the 1-form symmetry. Namely, the Hilbert space

of the gauged theory is given by

$$\widetilde{\mathcal{H}}^{\text{gauged}}_{T^2} = \bigoplus_{\gamma\in\Gamma} \mathcal{H}^{\gamma}_{\chi_A=\chi_B=1} \,. \tag{B.28}$$

For each state that is fixed by the operator U_B^γ, this state also contributes to the twisted sector $\mathcal{H}^\gamma$. Conversely, if a solution, $\widehat{u}$, is fixed by U_B^γ for all γ in a subgroup, $\Gamma_{\widehat{u}}$, of Γ, then this solution contributes $|\Gamma_{\widehat{u}}|$ states, one untwisted sector and a twisted sector for each non-trivial element in $\Gamma_{\widehat{u}}$.

These twisted sector states become physical states in the theory obtained by gauging Γ. Then we can understand the counting above physically from the fact that, in this situation, $\Gamma_{\widehat{u}}$ corresponds to an unbroken subgroup of the gauge group acting on $\widehat{u}$, and so there remains a low energy $\Gamma_{\widehat{u}}$-gauge theory at this solution, which is known to have $|\Gamma_{\widehat{u}}|$ states. In the example above, we see that the non-trivial twisted sector has a single state, corresponding to the $\widehat{u} = \frac{1}{4}$ fixed point.

B.4 Flat Connections on S^3/Γ_{ADE}

According to the 3d-3d correspondence we expect that the Witten index of the theory $T[M_3, \mathfrak{g}]$ counts the number of complex flat connections on M_3. The precise statement is discussed in section 5.4. In this section we will investigate this correspondence by computing the $G_{\mathbb{C}}$-connections on $M_3 = S^3/\Gamma_{ADE}$ for $G_{\mathbb{C}} = GL(N,\mathbb{C})$ and $G_{\mathbb{C}} = PSL(2,\mathbb{C})$, which are given by the corresponding representations of the fundamental group

$$\begin{aligned} \{A|F_A = 0\}/G_{\mathbb{C}} &= \text{Hom}\left(\pi_1(M_3), G_{\mathbb{C}}\right)/G_{\mathbb{C}} \\ \pi_1(S^3/\Gamma_{ADE}) &= \Gamma_{ADE}\,. \end{aligned} \tag{B.29}$$

B.4.1 $GL(N,\mathbb{C})$

We start by computing the number of flat $GL(N,\mathbb{C})$-connections on S^3/Γ_{ADE} in order to compare them with the Witten index of the $T[M_3, U(2)]$ determined in section 5.3.3.

In principle we expect

$$I(M_3, U(N)) = \#(GL(N,\mathbb{C}) \text{ reps of } \pi_1(M_3)) \tag{B.30}$$

In the case of $M_3 = S^3/\Gamma_{ADE}$, we can compute the number of $GL(N,\mathbb{C})$-representations of $\pi_1(M_3) = \Gamma_{ADE}$ by the McKay correspondence [209]. It states that the irreducible representation of Γ_{ADE} are in one-to-one correspondence with the nodes of the ADE affine Dynkin diagram. Each node of a Dynkin diagram is assigned a Dynkin number d_i, which is the dimension of the i-th irreducible representation. The affine node represents the trivial representation with $d_0 = 1$.

The $GL(N,\mathbb{C})$-representations of Γ_{ADE} can be constructed from the linear combinations of these irreducible representations, which are labeled by a set of integers $(n_0, \cdots, n_r)$

$$\#(GL(N,\mathbb{C}) \text{ reps of } \Gamma_{ADE}) = \left\{ (n_0, \cdots, n_r) \;\middle|\; N = \sum_{i=0}^{r} d_i n_i \right\} . \tag{B.31}$$

For A_{p-1} all the p Dynkin numbers are one, so $\mathbb{Z}_p$ has p irreducible $\mathbb{C}$-connections of dimension one. The number of N-dimensional representations is thus given by the number of ways to assign N indistinguishable objects to p distinct boxes

$$\#(GL(N,\mathbb{C}) \text{ reps of } \mathbb{Z}_p) = \binom{p+N-1}{N} . \tag{B.32}$$

Similarly, we find

$$\begin{aligned} \#(GL(2,\mathbb{C}) \text{ reps of } \Gamma_{D_n}) &= n+7 \\ \#(GL(2,\mathbb{C}) \text{ reps of } \Gamma_{E_m}) &= 3(9-m) . \end{aligned} \tag{B.33}$$

All these results match the number of vacua of the corresponding theories computed in section 5.3.3, see table 5.2.

B.4.2 $PSL(2,\mathbb{C})$

We consider the $PSL(2,\mathbb{C})$ connections for the Seifert manifolds $M_3 = [0;0;(p_i,q_i)]$ with three exceptional fibres. The fundamental group is given by

$$\pi_1(M_3) = \langle x, y, h | x^{p_1} = h^{q_1}, y^{p_2} = h^{q_2}, (xy)^{-p_3} = h^{q_3} \rangle , \tag{B.34}$$

where h is a central element [210].[3]

The $PSL(2,\mathbb{C})$ connections of the groups in (B.34) are discussed in [211]. The strategy is to first consider the reducible representations which factor through the abelianisation of $\pi_1(M_3)$

$$\pi_1^{\rm ab}(M_3) = \mathbb{Z}_{c_1} \oplus \mathbb{Z}_{c_2}\,, \quad c_1 = \frac{|H_1(M_3,\mathbb{Z})|}{(p_1,p_2,p_3)}\,, \quad c_2 = (p_1,p_2,p_3)\,, \tag{B.35}$$

generated by $z_{1,2}$. Here, (p_1,p_2,p_3) denotes the gcd. The reducible $PSL(2,\mathbb{C})$-representations of the cyclic groups are given by

$$\rho_{j_1,j_2}(z_i) = \begin{pmatrix} e^{\pi i j_i/c_i} & 0 \\ 0 & e^{-\pi i j_i/c_i} \end{pmatrix}\,, \qquad j_i \in \{0,\cdots,c_i-1\}\,. \tag{B.36}$$

After accounting for Weyl symmetry we find

$$\#(\text{reducible } SL(2,\mathbb{C}) \text{ reps of } \pi_1(M_3)) = \left\lfloor \frac{|H_1(M_3,\mathbb{Z})|}{2} \right\rfloor + \begin{cases} 1 & (p_1,p_2,p_3) \text{ odd} \\ 2 & (p_1,p_2,p_3) \text{ even} \end{cases}\,. \tag{B.37}$$

To find the number of irreducible representations we use the related group

$$\Delta_{p_i} = \langle x,y | x^{p_1} = y^{p_2} = (xy)^{p_3} = 1\rangle\,, \tag{B.38}$$

as $\rho(h)$ needs to be trivial if ρ is irreducible. The irreducible representations of these groups are counted by three integers

$$\begin{aligned} &\rho_j(x) = \begin{pmatrix} \alpha_j & 0 \\ 0 & \alpha_j^{-1} \end{pmatrix}\,, \qquad \rho_{j,k,\ell}(y) = \begin{pmatrix} \gamma_{j,k,\ell} & 1 \\ \gamma_{j,k,\ell}\,(\beta_k - \gamma_{j,k,\ell}) - 1 & \beta_k - \gamma_{j,k,\ell} \end{pmatrix}\,, \\ &\alpha_j = e^{\frac{\pi i j}{p_1}}\,, \quad \beta_k = 2\cos\left(\frac{\pi k}{p_2}\right)\,, \quad \gamma_{j,k,\ell} = \frac{2\cos\left(\frac{\pi\ell}{p_3}\right) - \alpha_j^{-1}\beta_k}{2i\,\mathrm{Im}\,\alpha_j}\,, \\ &j = 1,\cdots\left\lfloor\frac{p_1}{2}\right\rfloor\,, \quad k = 1,\cdots\left\lfloor\frac{p_2}{2}\right\rfloor\,, \quad \ell = 1,\cdots p_3 - 1\,. \end{aligned} \tag{B.39}$$

[3]Note that this group reduces to a cyclic group if any of the $p_i = 1$.

After accounting for the Weyl symmetry, and including the reducible connections in (B.37) we obtain

$$\#(PSL(2,\mathbb{C}) \text{ reps of } \pi_1(M_3)) = \left\lfloor \frac{p_1}{2} \right\rfloor \left\lfloor \frac{p_2}{2} \right\rfloor \left\lfloor \frac{p_3}{2} \right\rfloor + \left\lfloor \frac{p_1-1}{2} \right\rfloor \left\lfloor \frac{p_2-1}{2} \right\rfloor \left\lfloor \frac{p_3-2}{2} \right\rfloor + \left\lfloor \frac{(p_1,p_2)}{2} \right\rfloor + \left\lfloor \frac{(p_1,p_3)}{2} \right\rfloor + \left\lfloor \frac{(p_2,p_3)}{2} \right\rfloor + 1 + \left\lfloor \frac{|H_1(M_3,\mathbb{Z})|}{2} \right\rfloor - \left\lfloor \frac{(p_1p_2,p_1p_3,p_2p_3)}{2} \right\rfloor . \tag{B.40}$$

B.5 G_2-holonomy, Associatives and Deformation Theory

This appendix gives a brief review of manifolds with holonomy group G_2 and calibrated, so-called associative, three-cycles, that play a key role in chapter 6. For more in depth reviews of these geometries in mathematics and string theory see [14, 115]. A G_2-holonomy manifold is a pair (X_7, Φ), where X_7 is an oriented manifold of real dimension seven and Φ is a harmonic three-form, the associative form. This manifold admits a metric g_Φ, constructed from Φ, with reduced holonomy group $G_2 \subset SO(7)$. Under this holonomy reduction, the spinor representation of $SO(7)$ splits as

$$\mathbf{8} \to \mathbf{7} \oplus \mathbf{1} \,, \tag{B.41}$$

such that M-theory compactified on X_7 preserves $\frac{1}{8}$ of supersymmetry, leading to a 4d $\mathcal{N} = 1$ theory. Key to the present discussion are its calibrated or supersymmetric cycles. Associative three-cycles M_3 are calibrated by Φ,[4] i.e.

$$\text{vol}(M_3) = \Phi|_{M_3} \,, \tag{B.42}$$

and their properties including the deformation theory have been discussed in [212, 213]. Most notably, it was shown that the normal bundle of M_3 is

$$N_{M_3} = \mathbb{S} \otimes V \,, \tag{B.43}$$

[4]There are also co-associative four-cycles, which are calibrated by $\star\Phi$.

where $\mathbb{S}$ is the spinor bundle of M_3 and V is a rank two $SU(2)$-bundle.

The space of linear deformations is given by sections of the normal bundle, i.e. the kernel of $\not{\mathcal{D}}$, the twisted Dirac operator on M_3 coupled to the $SU(2)$-bundle V. We denote its dimension by

$$d_{\not{\mathcal{D}}}(M_3, g) = \dim \ker \not{\mathcal{D}} \,. \tag{B.44}$$

Note that $d_{\not{\mathcal{D}}}(M_3, g)$ depends on the metric g, which descends from the G_2-metric g_Φ [214]. Although over a three-manifold every $SU(2)$-bundle is trivial, i.e. it admits a trivial connection, this does not imply that we can simply set the connection $\mathfrak{A}$ on V to zero, as the connection relevant here is the one determined by the embedding of the associative cycle into the G_2-manifold. The connection is therefore fixed, and not necessarily trivial. In the examples studied by Bryant-Salamon [114], the G_2-holonomy manifolds are constructed as the total space of the spin bundle over a constant sectional curvature three-manifold, so that $\mathfrak{A} = 0$. In fact, whenever $\mathfrak{A} = 0$ there are three distinct cases depending on the scalar curvature $\mathcal{R}$:

1. $\mathcal{R} > 0$: There are no harmonic spinors [215], i.e. M_3 is rigid.

2. $\mathcal{R} = 0$: The harmonic spinors coincide with the parallel spinors on $M_3 = T^3$.

3. $\mathcal{R} < 0$: M_3 can have non-trivial linear deformations depending on the metric g induced by the embedding.

The index of the Dirac operator vanishes on a closed three-manifold, so that its obstruction space is of the same dimension as the deformation space [180, 212]. This implies that the virtual dimension of the moduli space of associative deformations is always zero. It is believed [115, 180] that for generic M_3 there is no obstruction space, so there are also no linear deformations and $d_{\not{\mathcal{D}}}(M_3, g) = 0$. This structure is generically preserved under small deformations of the metric, or equivalently the associative form Φ. However for non-generic G_2-manifolds, the obstruction and deformation spaces can be non-trivial.

B.6 Reduction of the Abelian 6d (2,0) Tensor Multiplet to 3d $\mathcal{N}=1$

In this appendix we dimensionally reduce the abelian tensor multiplet from 6d on M_3 with the topological twist in (4.7). The tensor multiplet consists of a self-dual tensor field $H = dB$, five scalars $\Phi^{\underline{\hat{m}\hat{n}}}$ and four symplectic-Majorana-Weyl spinors $\varrho^{\underline{\alpha\hat{m}}}$ of negative chirality. We will look at them in turn. The three-form H satisfies the equations of motion

$$dH = 0\,, \qquad H_{\underline{abc}} = \frac{1}{3!}\varepsilon_{\underline{abc}}{}^{\underline{def}} H_{\underline{def}}\,. \tag{B.45}$$

We can make an ansatz for H

$$H = \frac{1}{3!}H_{xyz}e^x\wedge e^y\wedge e^z + \frac{1}{2!}H_{axy}e^a\wedge e^x\wedge e^y + \frac{1}{2!}H_{abx}e^a\wedge e^b\wedge e^x + \frac{1}{3!}H_{abc}e^a\wedge e^b\wedge e^c\,, \tag{B.46}$$

where the e^a are local coordinates of T^*M_3 and $x, y, z = 0, 1, 2$ label coordinates along $\mathbb{R}^{1,2}$. Self-duality then reads

$$H_{abc} = -\frac{1}{6}\varepsilon_{abc}\varepsilon^{xyz}H_{xyz}\,, \qquad H_{abx} = \frac{1}{2}\varepsilon_{ab}{}^{c}\varepsilon_{x}{}^{yz}H_{cyz}\,, \tag{B.47}$$

where we normalise $\varepsilon_{012345} = \varepsilon_{012} = \varepsilon_{345} = 1$. Inserting this into $dH = 0$ we obtain

$$\begin{aligned} 0 &= -\frac{1}{6}\varepsilon_{abc}\partial_w\varepsilon^{xyz}H_{xyz} - \frac{1}{2}\varepsilon_{w}{}^{xy}\partial_{[a}\varepsilon_{bc]}{}^{d}H_{dxy} \\ 0 &= \frac{1}{2}\partial_{[x}\varepsilon_{y]}{}^{wz}\varepsilon_{ab}{}^{c}H_{cwz} - \partial_{[a}H_{b]xy} \\ 0 &= \partial_{[x}H_{yz]a} - \partial_a H_{xyz}\,. \end{aligned} \tag{B.48}$$

To obtain the massless spectrum in 3d one expands H_{axy} in a basis of harmonic one-forms $\omega_{I,a}$ that depend on the local coordinates on M_3

$$H_{axy} = \sum_{I=1}^{b_1(M_3)} F^I_{xy}\,\omega_{I,a}\,, \tag{B.49}$$

where $b_1(M_3)$ is the first Betti number of M_3. The F^I_{xy} then only depend on the coordinates of $\mathbb{R}^{1,2}$. After taking H_{xyz} to be a constant on M_3 the equations of

motion take the form

$$dF^I = 0\,, \qquad d\star F^I = 0\,, \tag{B.50}$$

where $\star$ is the Hodge star on $\mathbb{R}^{1,2}$. The first equation of motion implies that locally we can write $F^I = dA^I$ and from the second equation we obtain the usual equation of motion for free gauge fields. The massless spectrum therefore consists of $b_1(M_3)$ gauge fields. Since in three dimensions a massless gauge field is dual to a massless scalar we can introduce a set of scalars α^I with

$$\partial_x \alpha^I = \frac{1}{2}\varepsilon_x{}^{yz} F^I_{yz}\,, \tag{B.51}$$

which are periodic due to the gauge symmetry of the F^I. In terms of these scalars the 3d action can be written as

$$S = \int_{\mathbb{R}^{1,2}} d\alpha_I \wedge \star\, d\alpha^I\,. \tag{B.52}$$

Now consider the equation of motion for the three-form H_{xyz} which is given by

$$d\star H = 0\,, \tag{B.53}$$

where H_{xyz} is constant on the M_3. This equation of motion can be obtained from the 3d action

$$\int_{\mathbb{R}^{1,2}} H \wedge \star H\,, \tag{B.54}$$

where $H = dB$, since H closes trivially. In terms of the scalar $H_{xyz} = -\varepsilon_{xyz} h$ dual to the three-form this action gives rise to the equation of motion [216] $h = 0$, and we obtain a scalar field which is set to zero by its equation of motion. We will see from the supersymmetry variations that this scalar can be identified with the auxiliary field in the centre of mass scalar multiplet.

By this direct reduction it is not possible to detect gauge fields with non-zero Chern-Simons term. The action of such a field takes the form

$$S = g^{-2} \int_{\mathbb{R}^{1,2}} F \wedge \star F + \frac{k}{4\pi} \int_{\mathbb{R}^{1,2}} A \wedge F\,, \tag{B.55}$$

where g is the gauge coupling and k is the integer Chern-Simons level. In the presence of such a Chern-Simons term the gauge field acquires a mass [217]

$$m = \frac{g^2 k}{4\pi} \,. \tag{B.56}$$

Despite the massive nature of the gauge field the theory is not completely trivial at low energies [104]. It was argued in [95] that the integral first homology group of the three-manifold is presented by the matrix of Chern-Simons levels in a $U(1)^R$ theory, where $R = b_1(M_3) + r$. In other words, the Chern-Simons levels induce the relation

$$k_{MN}\gamma^N = 0 \,, \tag{B.57}$$

where γ^N are the generators of the full integral homology $H_1(M_3, \mathbb{Z})$ as in (6.5).[5] Thus, given $H_1(M_3, \mathbb{Z})$, one can present it in terms of a diagonal matrix of Chern-Simons levels where the torsion numbers p_m, where $m = 1, \cdots, r$, correspond to the (non-zero) integer eigenvalues of k_{MN} and the free part of $H_1(M_3, \mathbb{Z})$, generated by the one-cycles γ^I, span the kernel of k_{MN}. The resulting theory is a $U(1)^R$ theory with $b_1(M_3)$ massless gauge fields A_I and r gauge fields A_m with level p_m Chern-Simons self-interactions.

Next, let us discuss the remaining bosonic field content coming from the five scalars $\Phi^{\underline{\hat{m}\hat{n}}}$. Under the topological twist the scalars decompose, yielding a singlet φ and a bispinor field $\phi^{\alpha\hat{\alpha}}$. The decomposition of the R-symmetry naturally leads to the identification

$$\begin{aligned} \Phi^{\alpha\beta} &= -\varphi\varepsilon^{\alpha\beta} \,, \qquad & \Phi^{\hat{\alpha}\hat{\beta}} &= \varphi\varepsilon^{\hat{\alpha}\hat{\beta}} \\ \Phi^{\alpha\hat{\alpha}} &= \phi^{\alpha\hat{\alpha}} \,, & \Phi^{\hat{\alpha}\alpha} &= \phi^{\hat{\alpha}\alpha} \,, \end{aligned} \tag{B.58}$$

where we have identified the $SU(2)_r$ index $\hat{m}$ with the spinor index α on M_3 as dictated by the topological twist. The conventions are chosen such that $\phi^{\alpha\hat{\alpha}}$ satisfies $\phi^{\alpha\hat{\alpha}} = -\phi^{\hat{\alpha}\alpha}$ and the reality condition

$$\phi^{1\hat{1}^*} = \phi^{2\hat{2}} \,, \qquad \phi^{1\hat{2}^*} = -\phi^{2\hat{1}} \,. \tag{B.59}$$

[5] This also explains why we were not able to see these fields in the reduction from 6d. In order to impose the self-duality H has to be $\mathbb{R}$-valued so the torsion part of the homology is not detected.

Since φ is a singlet the 6d equation of motion $D^2\Phi^{\underline{\hat{m}\hat{n}}} = 0$, where D is the 6d covariant derivative, reduces to

$$\left(\Delta_{M_3} + \partial^2_{\mathbb{R}^{1,2}}\right)\varphi = 0\,, \tag{B.60}$$

and we obtain a single massless scalar in 3d for φ constant on M_3. As discussed in section 6.1.1, the fields $\phi^{\alpha\hat{\alpha}}$ are identified with sections of the normal bundle of M_3. For general three-manifolds the additional $SU(2)_V$-bundle is twisted with the spin bundle and can act non-trivially. Thus, the derivative acting on $\phi^{\alpha\hat{\alpha}}$ needs to be covariantised not only with respect to the spin connection on M_3, but also an $SU(2)_V$ connection. The equation of motion for $\phi^{\alpha\hat{\alpha}}$ therefore takes the form

$$(\not{\mathcal{D}}^2\phi)^{\alpha\hat{\alpha}} + \partial^2_{\mathbb{R}^{1,2}}\phi^{\alpha\hat{\alpha}} = 0\,, \tag{B.61}$$

where $\not{\mathcal{D}}$ is the twisted Dirac operator on M_3 explicitly given by

$$(\mathcal{D}_a\phi)^{\alpha\hat{\alpha}} = \partial_a\phi^{\alpha\hat{\alpha}} + \frac{1}{4}\omega_a{}^{bc}(\sigma_{bc})^\alpha{}_\beta\phi^{\beta\hat{\alpha}} + \mathfrak{A}_a{}^{\hat{\alpha}}{}_{\hat{\beta}}\phi^{\alpha\hat{\beta}}\,, \tag{B.62}$$

where $\omega_a{}^{bc}$ is the spin connection on M_3 and $\mathfrak{A}_a{}^{\hat{\alpha}}{}_{\hat{\beta}}$ is the $SU(2)_V$ connection. Since the kernels of $\not{\mathcal{D}}$ and $\not{\mathcal{D}}^2$ agree, $\phi^{\alpha\hat{\alpha}}$ is expanded in a basis of twisted harmonic spinors $\zeta_i^{\alpha\hat{\alpha}}$

$$\phi^{\alpha\hat{\alpha}} = \sum_{i=1}^{d_{\not{\mathcal{D}}}(M_3,g)} \phi^i\zeta_i^{\alpha\hat{\alpha}}\,. \tag{B.63}$$

The number of massless modes is given by the dimension, $d_{\not{\mathcal{D}}}(M_3, g)$, of the kernel of the twisted Dirac operator $\not{\mathcal{D}}$ on the associative three-cycle. As reviewed in section B.5 this dimension depends on the metric on the associative three-cycle M_3 induced by the G_2-holonomy metric.

By $\mathcal{N} = 1$ supersymmetry the bosonic fields are supplemented by their fermionic superpartners. The negative chirality spinor $\varrho^{\underline{\alpha\hat{m}}}$ was shown in (6.4) to decompose after the twist as

$$\varrho^{\underline{\alpha\hat{m}}} \quad \to \quad i\lambda^\sigma\varepsilon^{\alpha\hat{\alpha}} + \xi^\sigma_a(\sigma^a)^\alpha{}_\beta\varepsilon^{\beta\hat{\alpha}} - i\rho^{\sigma\alpha\hat{\alpha}}\,, \tag{B.64}$$

where the prefactors have been introduced for convenience. The 6d symplectic-Majorana-Weyl condition implies a reality condition on a 3d spinor ψ^σ such that it takes the form

$$\psi^\sigma = \begin{pmatrix} \psi^1 \\ i\psi^2 \end{pmatrix} , \tag{B.65}$$

where ψ^1, ψ^2 are real. Applied to the fields $\rho^{\alpha\hat{\alpha}}$ there is an additional condition

$$\rho^{1\hat{1}^*} = \rho^{2\hat{2}} , \qquad \rho^{1\hat{2}^*} = -\rho^{2\hat{1}} . \tag{B.66}$$

Note that this is the same reality condition (B.59) as for the $\phi^{\alpha\hat{\alpha}}$. The 6d equations of motion $\not{\mathcal{D}}^{\underline{\alpha}}{}_{\underline{\beta}}\underline{\varrho^{\beta\hat{m}}} = 0$ reduce to

$$\begin{aligned} \star d \star \xi^\sigma + \not{\phi}_{\mathbb{R}^{1,2}}{}^\sigma{}_\tau \lambda^\tau &= 0 \\ d\lambda^\sigma + \star d \xi^\sigma - \not{\phi}_{\mathbb{R}^{1,2}}{}^\sigma{}_\tau \xi^\tau &= 0 \\ i(\not{\mathcal{D}}\rho)^{\sigma\alpha\hat{\alpha}} + \not{\phi}_{\mathbb{R}^{1,2}}{}^\sigma{}_\tau \rho^{\tau\alpha\hat{\alpha}} &= 0 , \end{aligned} \tag{B.67}$$

where $\star$, d and $\not{\mathcal{D}}$ denote the Hodge star, the exterior derivative and the twisted Dirac operator along M_3, respectively. As λ^σ is the superpartner of the scalar φ it is constant along M_3. The equations then decouple leading to a single massless spinor λ^σ in 3d. The massless modes from ξ^σ_a are obtained by expanding

$$\xi^\sigma_a = \sum_{I=1}^{b_1(M_3)} \xi^{\sigma I} \omega_{I,a} , \tag{B.68}$$

where the $\omega_{I,a}$ are a basis of harmonic one-forms on M_3. This yields the superpartners of the $b_1(M_3)$ massless gauge fields A^I. The superpartners of the massive gauge fields A^m also arise from the reduction of ξ^σ_a. Each of the torsion cycles $\gamma^m \in H_1(M_3, \mathbb{Z})_{\text{torsion}}$ corresponds to a massive fermion $\xi^{\sigma m}$ whose mass is governed by the respective torsion number p_m. Lastly, the massless superpartners of the ϕ^i arise from the expansion of $\rho^{\sigma\alpha\hat{\alpha}}$ in terms of twisted harmonic spinors on M_3

$$\rho^{\sigma\alpha\hat{\alpha}} = \sum_{i=1}^{d_{\not{\mathcal{D}}}(M_3,g)} \rho^{\sigma i} \zeta_i^{\alpha\hat{\alpha}} . \tag{B.69}$$

In order to properly group these fields into 3d $\mathcal{N}=1$ multiplets we consider the abelian 6d $\mathcal{N}=(2,0)$ supersymmetry transformations

$$\begin{aligned}\delta B_{\underline{ab}} &= \epsilon_{\underline{\hat{m}}}\Gamma_{\underline{ab}}\varrho^{\underline{\hat{m}}}\\ \delta\Phi^{\underline{\hat{m}\hat{n}}} &= -4\epsilon^{[\underline{\hat{m}}}\varrho^{\underline{\hat{n}}]} - \Omega^{\underline{\hat{m}\hat{n}}}\epsilon^{\underline{\hat{r}}}\varrho_{\underline{\hat{r}}}\\ \delta\varrho^{\underline{\hat{m}}} &= \frac{1}{48}H^{+}_{\underline{abc}}\Gamma^{\underline{abc}}\epsilon^{\underline{\hat{m}}} + \frac{1}{4}\not{\partial}\Phi^{\underline{\hat{m}\hat{n}}}\epsilon_{\underline{\hat{n}}}\,.\end{aligned} \tag{B.70}$$

The topological twist is implemented by requiring that the invariant supersymmetry parameter satisfies

$$(\Sigma_a)^{\underline{\alpha}}{}_{\underline{\beta}}\epsilon^{\underline{\beta\hat{m}}} + \delta_{a\hat{a}}\,(\Sigma_{\hat{a}})^{\underline{\hat{m}}}{}_{\underline{\hat{n}}}\epsilon^{\underline{\alpha\hat{n}}} = 0\,, \tag{B.71}$$

where Σ_a and $\Sigma_{\hat{a}}$ are the generators of $SU(2)_M$ and $SU(2)_r$, respectively. The solution to (B.71) is given by

$$\epsilon^{\sigma\alpha\hat{m}} = \epsilon^{\sigma}\varepsilon^{\alpha\hat{m}} \qquad \text{and} \qquad \epsilon^{\sigma\alpha\hat{\alpha}} = 0\,, \tag{B.72}$$

where $\varepsilon^{\alpha\hat{m}}$ is the anti-symmetric two-tensor and the 6d symplectic-Majorana-Weyl condition reduces to (B.65) for ϵ^{σ}. The dimensional reduction of the supersymmetry variations yields

$$\begin{aligned}\delta A^m_x &= -2\epsilon_\sigma\gamma_x{}^\sigma{}_\tau\xi^{\tau m} & \delta\xi^{\sigma m} &= -\frac{1}{8}\varepsilon^{xyz}F^m_{xy}\gamma_z{}^\sigma{}_\tau\epsilon^\tau\\ \delta\alpha^I &= -2\epsilon_\sigma\xi^{\sigma I} & \delta\xi^{\sigma I} &= -\frac{1}{4}\not{\partial}_{\mathbb{R}^{1,2}}{}^\sigma{}_\tau\alpha^I\epsilon^\tau\\ \delta\varphi &= -2\epsilon_\sigma\lambda^\sigma & \delta\lambda^\sigma &= -\frac{1}{4}\not{\partial}_{\mathbb{R}^{1,2}}{}^\sigma{}_\tau\varphi\epsilon^\tau - \frac{1}{4}h\epsilon^\sigma\\ \delta h &= -2\epsilon_\sigma\not{\partial}_{\mathbb{R}^{1,2}}{}^\sigma{}_\tau\lambda^\tau & \delta\rho^{\sigma i} &= -\frac{1}{4}\not{\partial}_{\mathbb{R}^{1,2}}{}^\sigma{}_\tau\phi^i\epsilon^\tau\,,\\ \delta\phi^i &= -2\epsilon_\sigma\rho^{\sigma i}\end{aligned} \tag{B.73}$$

which are indeed consistent 3d $\mathcal{N}=1$ supersymmetry variations. Note that it is not possible to determine the supersymmetry variation of the auxiliary scalar h by direct reduction as it only appears in the decomposition of the self-dual part of the field strength H^+, not of B itself. It is straightforward to determine $\delta H_{abc} = 3\partial_{[a}\delta B_{bc]}$ and from this the variations of $H^{\pm}$. In order for δH^- to vanish one has to impose the first equation of motion in (B.67) by hand. This ensures that the 3d supersymmetry algebra closes off-shell. Then, the variation of δH^+_{xyz} reduces to δh in (B.73).

Label	Background Field	$Sp(4)_R$	Properties
$e_{\mu'}^{a'}$	Frame	**1**	
$C_{\mu'}$	Graviphoton	**1**	$G = dC$
$V_{a'}^{\underline{\hat{m}\hat{n}}}$	R-symmetry gauge field	**10**	
$S^{\underline{\hat{m}\hat{n}}}$	Auxiliary scalar	**10**	
$T_{a'b'}^{\underline{\hat{m}\hat{n}}}$	Auxiliary 2-form	**5**	$T_{a'b'}^{\underline{\hat{m}\hat{n}}} = -T_{b'a'}^{\underline{\hat{m}\hat{n}}}, T_{a'b'}^{\underline{\hat{m}\hat{n}}} = -T_{a'b'}^{\underline{\hat{n}\hat{m}}}$
$D_{\underline{\hat{a}\hat{b}}}$	Auxiliary scalar	**14**	$D_{\underline{\hat{a}\hat{b}}} = D_{\underline{\hat{b}\hat{a}}}, D^{\underline{\hat{a}}}{}_{\underline{\hat{a}}} = 0$
$b_{a'}$	Dilaton gauge field	**1**	

Table B.1: The bosonic background fields for 5d $\mathcal{N} = 2$ supergravity

B.7 M5-branes on S^3

This appendix contains details of the reduction of M5-branes on S^3 in section 6.3.

B.7.1 Supergravity Background

We start with the bosonic 5d supergravity background fields summarised in table B.1. To determine which fields are compatible with the topological twist along the associative three-cycle we have to work out whether there are any singlets under the twisted symmetry group

$$G_{\text{twist}} = SO(2)_L \times SU(2)_{\text{twist}} \times SU(2)_\ell \,. \tag{B.74}$$

We can check explicitly that there are three singlets under (B.74)

$$V_a{}^{\underline{\hat{m}}}{}_{\underline{\hat{n}}} = -\frac{2iv}{r}\delta_{a\hat{a}}\,(\Sigma_{\hat{a}})^{\underline{\hat{m}}}{}_{\underline{\hat{n}}}\,, \quad T_{xy}^{\underline{\hat{m}\hat{n}}} = \frac{t}{r}\varepsilon_{xy}\gamma_{\hat{5}}^{\underline{\hat{m}\hat{n}}}\,, \quad D_{\underline{\hat{a}\hat{b}}} = d\ \text{diag}\,(1,1,1,1,-4)\ , \tag{B.75}$$

where the $\Sigma_{\hat{a}}$ generate the $SU(2)_r$ and the normalisations are chosen for convenience. We impose that the supersymmetry parameter solves the equation for the topological twist on M_3 (B.71), and therefore, the non-vanishing components can be written as

$$\epsilon^{\alpha'\underline{\hat{m}}} = \epsilon^{\mu}\varepsilon^{\alpha\hat{m}}\,. \tag{B.76}$$

B.7.2 The Killing Spinor Equations on $S^2 \times \mathbb{R}^3$

The Killing spinor equations for the gravitino $\psi_{a'}^{\hat{m}}$ and the dilatino $\chi^{\hat{m}\hat{n}}{}_{\underline{\hat{r}}}$ are summarised in [5, 100]. By solving them we determine the conditions on the supersymmetry parameter and the supergravity background.

First, we find that the gravitino variations along $\mathbb{R}^3$ vanish for

$$t = \frac{1}{2}(1 - v)\,, \tag{B.77}$$

and no further restrictions on ϵ^μ arise.

To solve the equations along the S^2 we have to include an explicit dependence of the supersymmetry parameter on the angles on S^2. Inserting the singlet ansatz (B.76) for the supersymmetry parameter one obtains

$$(\sigma_3 \not{\mathcal{D}}_{S^2})^\mu{}_\nu \epsilon^\nu = -\epsilon^\mu\,, \qquad \not{\mathcal{D}}_{S^2}{}^\mu{}_\nu = \left(\partial_\theta + \frac{1}{2}\cot\theta\right)(\sigma_1)^\mu{}_\nu + \frac{\partial_\phi}{\sin\theta}(\sigma_2)^\mu{}_\nu\,, \tag{B.78}$$

where $\not{\mathcal{D}}$ is the Dirac operator on the unit two-sphere. Since the operator $(\sigma_3 \not{\mathcal{D}}_{S^2})$ has two eigenvectors with eigenvalue -1 we find that the background preserves two supercharges, which transform as scalars on M_3. We can repeat this logic for the dilatino variations and find that it vanishes for

$$d = \frac{3t(t-1)}{r^2} + \frac{9v^2}{8r^2} = \frac{3\,(5v^2 - 2)}{8r^2}\,, \tag{B.79}$$

where we used (B.77) for the second equality.

B.7.3 Generalisation to Curved M_3

The 3d flat space action and supersymmetry variations can be generalised to curved M_3 by covariantising the derivatives and determining the additional terms required in the action for supersymmetry to be preserved, by first noting that the non-vanishing curvature on M_3 modifies the commutation relations satisfied by the covariant derivatives, which enters into the supersymmetry variation of the action. In addition we

gauge the flavour symmetry $SU(2)_\ell$, which is identified with $SU(2)_V$ associated with the bundle V in the normal bundle of M_3.

For the spinor $\phi^{\alpha\hat{\alpha}}$ on M_3 we obtain

$$([\mathcal{D}_a, \mathcal{D}_b]\phi)^{\alpha\hat{\alpha}} = F_{ab}\phi^{\alpha\hat{\alpha}} + \frac{1}{4}\mathcal{R}_{ab}{}^{cd}(\sigma_{cd})^{\alpha}{}_{\beta}\phi^{\beta\hat{\alpha}} + \mathfrak{F}_{ab}{}^{\hat{\alpha}}{}_{\hat{\beta}}\phi^{\alpha\hat{\beta}}\,, \tag{B.80}$$

where $\mathcal{D}$ is the covariant derivative on the three-manifold with respect to the metric, with Riemann tensor $\mathcal{R}_{ab}{}^{cd}$, the gauge connection A and the $SU(2)_V$ connection $\mathfrak{A}$, with field strength $\mathfrak{F}$. To cancel the contribution of these terms in the supersymmetry variation of the action it is necessary to add the term

$$S_\Phi^{\text{curv}} = \frac{1}{16\pi^2 r}\int d^5x\,\text{Tr}\left(\frac{\mathcal{R}}{4}\phi_{\alpha\hat{\alpha}}\phi^{\alpha\hat{\alpha}} - \frac{i}{2}\varepsilon^{abc}\mathfrak{F}_{ab}{}^{\hat{\alpha}}{}_{\hat{\beta}}(\sigma_c)^{\alpha}{}_{\beta}\phi_{\alpha\hat{\alpha}}\phi^{\beta\hat{\beta}}\right)\,. \tag{B.81}$$

No additional corrections are required for the other fields.[6] In the action the additional terms (B.81) can be combined with the covariantised kinetic term for $\phi^{\alpha\hat{\alpha}}$ using the Lichnerowicz-Weitzenböck formula for the twisted Dirac operator [218]

$$\begin{aligned}\phi_{\alpha\hat{\alpha}}\left(\mathcal{D}_a\mathcal{D}^a - \frac{\mathcal{R}}{4}\right)\phi^{\alpha\hat{\alpha}} + \frac{i}{2}\varepsilon^{abc}\mathfrak{F}_{ab}{}^{\hat{\alpha}}{}_{\hat{\beta}}(\sigma_c)^{\alpha}{}_{\beta}\phi_{\alpha\hat{\alpha}}\phi^{\beta\hat{\beta}} \\ = \phi_{\alpha\hat{\alpha}}(\not{\mathcal{D}}^2\phi)^{\alpha\hat{\alpha}} + \frac{i}{2}\varepsilon_{abc}F^{ab}(\sigma^c)^{\alpha}{}_{\beta}[\phi_{\alpha\hat{\alpha}}, \phi^{\beta\hat{\alpha}}]\,.\end{aligned} \tag{B.82}$$

B.8 Index Conventions for Section 6

In this appendix we summarise our index conventions in chapter 6 and appendices B.6 and B.7. For the conventions for gamma matrices and the spinor decomposition, see appendix A of [5].

The space-time and R-symmetry indices are given in tables B.2 and B.3, respectively. All hatted indices are associated to an R-symmetry. Note that after imposing the twist $SU(2)_{\text{twist}} = \text{diag}(SU(2)_M, SU(2)_r)$ we identify the indices $\alpha = \hat{m}$ as the

[6] Alternatively, the additional curvature terms can be determined by turning on an extra R-symmetry gauge field, to cancel the spin-connection on M_3, in the background supergravity. The terms required for preserving supersymmetry on a curved three-manifold agree, however in order to solve the supergravity Killing spinor equations M_3 is required to be Einstein.

spinor index of the $SU(2)_{\text{twist}}$. Note that the spinor components denote those of a Dirac spinor and we need to impose the symplectic-Majorana-Weyl condition, which halves the degrees of freedom.

	6d	5d	M_3	$\mathbb{R}^{1,2}$	S^2
Vector	$\underline{a}, \underline{b} = 0, \ldots, 5$	$a', b' = 0, \ldots, 4$	$a, b = 1, 2, 3$	$x, y = 0, 1, 2$	$x, y = 1, 2$
Spinor	$\underline{\alpha}, \underline{\beta} = 1, \ldots, 8$	$\alpha', \beta' = 1, \ldots, 4$	$\alpha, \beta = 1, 2$	$\sigma, \tau = 1, 2$	$\mu, \nu = 1, 2$

Table B.2: Summary of spacetime indices

	$SO(5)_R$	$SU(2)_r$	$SU(2)_\ell$
Vector	$\underline{\hat{a}}, \underline{\hat{b}} = 1, \ldots, 5$	$\hat{a}, \hat{b} = 1, 2, 3$	$\hat{a}', \hat{b}' = 1, 2, 3$
Spinor	$\underline{\hat{m}}, \underline{\hat{n}} = 1, \ldots, 4$	$\hat{m}, \hat{n} = 1, 2$	$\hat{\alpha}, \hat{\beta} = 1, 2$

Table B.3: Summary of R-symmetry indices

References

[1] M. van Beest, A. Bourget, J. Eckhard and S. Schafer-Nameki, *(Symplectic) Leaves and (5d Higgs) Branches in the Poly(go)nesian Tropical Rain Forest*, 2008.05577.

[2] M. van Beest, A. Bourget, J. Eckhard and S. Schafer-Nameki, *(5d RG-flow) Trees in the Tropical Rain Forest*, 2011.07033.

[3] J. Eckhard, S. Schäfer-Nameki and Y.-N. Wang, *Trifectas for T_N in 5d*, *JHEP* **07** (2020) 199 [2004.15007].

[4] J. Eckhard, H. Kim, S. Schafer-Nameki and B. Willett, *Higher-Form Symmetries, Bethe Vacua, and the 3d-3d Correspondence*, *JHEP* **01** (2020) 101 [1910.14086].

[5] J. Eckhard, S. Schäfer-Nameki and J.-M. Wong, *An $\mathcal{N} = 1$ 3d-3d Correspondence*, *JHEP* **07** (2018) 052 [1804.02368].

[6] P. Candelas, G.T. Horowitz, A. Strominger and E. Witten, *Vacuum Configurations for Superstrings*, *Nucl. Phys. B* **258** (1985) 46.

[7] T. Kaluza, *Zum Unitätsproblem der Physik*, *Int. J. Mod. Phys. D* **27** (2018) 1870001 [1803.08616].

[8] O. Klein, *Quantum Theory and Five-Dimensional Theory of Relativity. (In German and English)*, *Z. Phys.* **37** (1926) 895.

[9] M. Berger, *Sur les groupes d'holonomie homogènes de variétés à connexion affine et des variétés riemanniennes*, *Bulletin de la Société Mathématique de France* **83** (1955) 279.

[10] B.S. Acharya, *On Realizing N=1 superYang-Mills in M theory*, hep-th/0011089.

[11] M. Atiyah, J.M. Maldacena and C. Vafa, *An M theory flop as a large N duality*, *J. Math. Phys.* **42** (2001) 3209 [hep-th/0011256].

[12] M. Atiyah and E. Witten, *M theory dynamics on a manifold of G(2) holonomy*, *Adv. Theor. Math. Phys.* **6** (2003) 1 [hep-th/0107177].

[13] S. Gukov and J. Sparks, *M theory on spin(7) manifolds. 1*, *Nucl. Phys. B* **625** (2002) 3 [hep-th/0109025].

[14] B.S. Acharya and S. Gukov, *M theory and singularities of exceptional holonomy manifolds*, *Phys. Rept.* **392** (2004) 121 [hep-th/0409191].

[15] N. Arkani-Hamed, L. Motl, A. Nicolis and C. Vafa, *The String landscape, black holes and gravity as the weakest force*, *JHEP* **06** (2007) 060 [hep-th/0601001].

[16] H. Ooguri and C. Vafa, *On the Geometry of the String Landscape and the Swampland*, *Nucl. Phys. B* **766** (2007) 21 [hep-th/0605264].

[17] J. Polchinski, *Dirichlet Branes and Ramond-Ramond charges*, *Phys. Rev. Lett.* **75** (1995) 4724 [hep-th/9510017].

[18] O. Aharony, O. Bergman, D.L. Jafferis and J. Maldacena, *N=6 superconformal Chern-Simons-matter theories, M2-branes and their gravity duals*, *JHEP* **10** (2008) 091 [0806.1218].

[19] P. Claus, R. Kallosh and A. Van Proeyen, *M five-brane and superconformal (0,2) tensor multiplet in six-dimensions*, *Nucl. Phys. B* **518** (1998) 117 [hep-th/9711161].

[20] A. Strominger, *Open p-branes*, *Phys. Lett. B* **383** (1996) 44 [hep-th/9512059].

[21] E. Witten, *Five-branes and M theory on an orbifold*, *Nucl. Phys. B* **463** (1996) 383 [hep-th/9512219].

[22] A. Hanany and E. Witten, *Type IIB superstrings, BPS monopoles, and three-dimensional gauge dynamics*, *Nucl. Phys.* **B492** (1997) 152 [hep-th/9611230].

[23] D. Gaiotto and E. Witten, *S-Duality of Boundary Conditions In N=4 Super Yang-Mills Theory*, 0807.3720.

[24] O. Aharony and A. Hanany, *Branes, superpotentials and superconformal fixed points*, *Nucl. Phys. B* **504** (1997) 239 [hep-th/9704170].

[25] O. Aharony, A. Hanany and B. Kol, *Webs of (p,q) five-branes, five-dimensional field theories and grid diagrams*, *JHEP* **01** (1998) 002 [hep-th/9710116].

[26] O. DeWolfe, A. Hanany, A. Iqbal and E. Katz, *Five-branes, seven-branes and five-dimensional E(n) field theories*, *JHEP* **03** (1999) 006 [hep-th/9902179].

[27] P. Di Francesco, P. Mathieu and D. Senechal, *Conformal Field Theory*, Graduate Texts in Contemporary Physics, Springer-Verlag, New York (1997), 10.1007/978-1-4612-2256-9.

[28] J.M. Maldacena, *The Large N limit of superconformal field theories and supergravity*, *Int. J. Theor. Phys.* **38** (1999) 1113 [hep-th/9711200].

[29] E. Witten, *AdS / CFT correspondence and topological field theory*, *JHEP* **12** (1998) 012 [hep-th/9812012].

[30] W. Nahm, *Supersymmetries and their Representations*, *Nucl. Phys. B* **135** (1978) 149.

[31] N. Seiberg, *Five-dimensional SUSY field theories, nontrivial fixed points and string dynamics*, *Phys. Lett. B* **388** (1996) 753 [hep-th/9608111].

[32] D.R. Morrison and N. Seiberg, *Extremal transitions and five-dimensional supersymmetric field theories*, *Nucl. Phys. B* **483** (1997) 229 [hep-th/9609070].

[33] K.A. Intriligator, D.R. Morrison and N. Seiberg, *Five-dimensional supersymmetric gauge theories and degenerations of Calabi-Yau spaces*, *Nucl. Phys.* **B497** (1997) 56 [hep-th/9702198].

[34] P. Jefferson, S. Katz, H.-C. Kim and C. Vafa, *On Geometric Classification of 5d SCFTs*, *JHEP* **04** (2018) 103 [1801.04036].

[35] N. Seiberg and E. Witten, *Comments on string dynamics in six-dimensions*, *Nucl. Phys. B* **471** (1996) 121 [hep-th/9603003].

[36] A. Hanany and A. Zaffaroni, *Branes and six-dimensional supersymmetric theories*, *Nucl. Phys. B* **529** (1998) 180 [hep-th/9712145].

[37] J.J. Heckman, D.R. Morrison and C. Vafa, *On the Classification of 6D SCFTs and Generalized ADE Orbifolds*, *JHEP* **05** (2014) 028 [1312.5746].

[38] M. Del Zotto, J.J. Heckman, A. Tomasiello and C. Vafa, *6d Conformal Matter*, *JHEP* **02** (2015) 054 [1407.6359].

[39] J.J. Heckman, D.R. Morrison, T. Rudelius and C. Vafa, *Atomic Classification of 6D SCFTs*, *Fortsch. Phys.* **63** (2015) 468 [1502.05405].

[40] J.J. Heckman and T. Rudelius, *Top Down Approach to 6D SCFTs*, *J. Phys. A* **52** (2019) 093001 [1805.06467].

[41] C. Cordova, T.T. Dumitrescu and K. Intriligator, *Deformations of Superconformal Theories*, *JHEP* **11** (2016) 135 [1602.01217].

[42] F. Apruzzi, C. Lawrie, L. Lin, S. Schafer-Nameki and Y.-N. Wang, *5d Superconformal Field Theories and Graphs*, 1906.11820.

[43] F. Apruzzi, C. Lawrie, L. Lin, S. Schafer-Nameki and Y.-N. Wang, *Fibers add Flavor, Part I: Classification of 5d SCFTs, Flavor Symmetries and BPS States*, 1907.05404.

[44] F. Apruzzi, C. Lawrie, L. Lin, S. Schafer-Nameki and Y.-N. Wang, *Fibers add Flavor, Part II: 5d SCFTs, Gauge Theories, and Dualities*, 1909.09128.

[45] F. Apruzzi, S. Schafer-Nameki and Y.-N. Wang, *5d SCFTs from Decoupling and Gluing*, 1912.04264.

[46] C. Closset, S. Schafer-Nameki and Y.-N. Wang, *Coulomb and Higgs Branches from Canonical Singularities: Part 0*, 2007.15600.

[47] M. Del Zotto, J.J. Heckman and D.R. Morrison, *6D SCFTs and Phases of 5D Theories*, *JHEP* **09** (2017) 147 [1703.02981].

[48] F. Apruzzi, L. Lin and C. Mayrhofer, *Phases of 5d SCFTs from M-/F-theory on Non-Flat Fibrations*, *JHEP* **05** (2019) 187 [1811.12400].

[49] L. Bhardwaj, P. Jefferson, H.-C. Kim, H.-C. Tarazi and C. Vafa, *Twisted Circle Compactifications of 6d SCFTs*, 1909.11666.

[50] L. Bhardwaj, *Do all 5d SCFTs descend from 6d SCFTs?*, 1912.00025.

[51] M. Hubner, *5d SCFTs from (E_n, E_m) Conformal Matter*, 2006.01694.

[52] L. Bhardwaj, *Flavor Symmetry of 5d SCFTs, Part 1: General Setup*, 2010.13230.

[53] L. Bhardwaj, *Flavor Symmetry of 5d SCFTs, Part 2: Applications*, 2010.13235.

[54] P. Jefferson, H.-C. Kim, C. Vafa and G. Zafrir, *Towards Classification of 5d SCFTs: Single Gauge Node*, 1705.05836.

[55] L. Bhardwaj and P. Jefferson, *Classifying 5d SCFTs via 6d SCFTs: Rank one*, 1809.01650.

[56] L. Bhardwaj and P. Jefferson, *Classifying 5d SCFTs via 6d SCFTs: Arbitrary rank*, 1811.10616.

[57] L. Bhardwaj, *Dualities of 5d gauge theories from S-duality*, 1909.05250.

[58] L. Bhardwaj and G. Zafrir, *Classification of 5d N=1 gauge theories*, 2003.04333.

[59] D. Xie and S.-T. Yau, *Three dimensional canonical singularity and five dimensional $\mathcal{N} = 1$ SCFT*, *JHEP* **06** (2017) 134 [1704.00799].

[60] C. Closset, M. Del Zotto and V. Saxena, *Five-dimensional SCFTs and gauge theory phases: an M-theory/type IIA perspective*, *SciPost Phys.* **6** (2019) 052 [1812.10451].

[61] F. Benini, S. Benvenuti and Y. Tachikawa, *Webs of five-branes and N=2 superconformal field theories*, *JHEP* **09** (2009) 052 [0906.0359].

[62] O. Bergman, D. Rodríguez-Gómez and G. Zafrir, *5-Brane Webs, Symmetry Enhancement, and Duality in 5d Supersymmetric Gauge Theory*, *JHEP* **03** (2014) 112 [1311.4199].

[63] O. Bergman and G. Zafrir, *Lifting 4d dualities to 5d*, *JHEP* **04** (2015) 141 [1410.2806].

[64] O. Bergman and G. Zafrir, *5d fixed points from brane webs and O7-planes*, *JHEP* **12** (2015) 163 [1507.03860].

[65] H. Hayashi, S.-S. Kim, K. Lee, M. Taki and F. Yagi, *A new 5d description of 6d D-type minimal conformal matter*, *JHEP* **08** (2015) 097 [1505.04439].

[66] H. Hayashi, S.-S. Kim, K. Lee and F. Yagi, *6d SCFTs, 5d Dualities and Tao Web Diagrams*, *JHEP* **05** (2019) 203 [1509.03300].

[67] H. Hayashi, S.-S. Kim, K. Lee and F. Yagi, *5-brane webs for 5d $\mathcal{N}$ = 1 G_2 gauge theories*, *JHEP* **03** (2018) 125 [1801.03916].

[68] H. Hayashi, S.-S. Kim, K. Lee and F. Yagi, *Dualities and 5-brane webs for 5d rank 2 SCFTs*, *JHEP* **12** (2018) 016 [1806.10569].

[69] H. Hayashi, S.-S. Kim, K. Lee and F. Yagi, *Rank-3 antisymmetric matter on 5-brane webs*, *JHEP* **05** (2019) 133 [1902.04754].

[70] S. Cremonesi, G. Ferlito, A. Hanany and N. Mekareeya, *Instanton Operators and the Higgs Branch at Infinite Coupling*, *JHEP* **04** (2017) 042 [1505.06302].

[71] G. Ferlito, A. Hanany, N. Mekareeya and G. Zafrir, *3d Coulomb branch and 5d Higgs branch at infinite coupling*, *JHEP* **07** (2018) 061 [1712.06604].

[72] S. Cabrera and A. Hanany, *Quiver Subtractions*, *JHEP* **09** (2018) 008 [1803.11205].

[73] S. Cabrera, A. Hanany and F. Yagi, *Tropical Geometry and Five Dimensional Higgs Branches at Infinite Coupling*, *JHEP* **01** (2019) 068 [1810.01379].

[74] S. Cabrera, A. Hanany and M. Sperling, *Magnetic quivers, Higgs branches, and 6d N=(1,0) theories*, *JHEP* **06** (2019) 071 [1904.12293].

[75] A. Bourget, S. Cabrera, J.F. Grimminger, A. Hanany, M. Sperling, A. Zajac et al., *The Higgs mechanism — Hasse diagrams for symplectic singularities*, *JHEP* **01** (2020) 157 [1908.04245].

[76] A. Bourget, S. Cabrera, J.F. Grimminger, A. Hanany and Z. Zhong, *Brane Webs and Magnetic Quivers for SQCD*, *JHEP* **03** (2020) 176 [1909.00667].

[77] S. Cabrera, A. Hanany and M. Sperling, *Magnetic quivers, Higgs branches, and 6d $\mathcal{N}$ = (1, 0) theories — orthogonal and symplectic gauge groups*, *JHEP* **02** (2020) 184 [1912.02773].

[78] J.F. Grimminger and A. Hanany, *Hasse Diagrams for* **3d** $\mathcal{N} = 4$ *Quiver Gauge Theories – Inversion and the full Moduli Space*, 2004.01675.

[79] A. Bourget, J.F. Grimminger, A. Hanany, M. Sperling and Z. Zhong, *Magnetic Quivers from Brane Webs with O5 Planes*, *JHEP* **07** (2020) 204 [2004.04082].

[80] A. Bourget, J.F. Grimminger, A. Hanany, M. Sperling, G. Zafrir and Z. Zhong, *Magnetic quivers for rank 1 theories*, 2006.16994.

[81] M. Akhond, F. Carta, S. Dwivedi, H. Hayashi, S.-S. Kim and F. Yagi, *Five-brane webs, Higgs branches and unitary/orthosymplectic magnetic quivers*, 2008.01027.

[82] A. Bourget, S. Giacomelli, J.F. Grimminger, A. Hanany, M. Sperling and Z. Zhong, *S-fold magnetic quivers*, 2010.05889.

[83] S. Cremonesi, A. Hanany and A. Zaffaroni, *Monopole operators and Hilbert series of Coulomb branches of* $3d$ $\mathcal{N} = 4$ *gauge theories*, *JHEP* **01** (2014) 005 [1309.2657].

[84] E. Witten, *Topological Quantum Field Theory*, *Commun. Math. Phys.* **117** (1988) 353.

[85] L.F. Alday, D. Gaiotto and Y. Tachikawa, *Liouville Correlation Functions from Four-dimensional Gauge Theories*, *Lett. Math. Phys.* **91** (2010) 167 [0906.3219].

[86] N. Wyllard, *A(N-1) conformal Toda field theory correlation functions from conformal N = 2 SU(N) quiver gauge theories*, *JHEP* **11** (2009) 002 [0907.2189].

[87] D. Gaiotto, *N=2 dualities*, *JHEP* **08** (2012) 034 [0904.2715].

[88] I. Bah, C. Beem, N. Bobev and B. Wecht, *Four-Dimensional SCFTs from M5-Branes*, *JHEP* **06** (2012) 005 [1203.0303].

[89] D. Gaiotto and S.S. Razamat, $\mathcal{N} = 1$ *theories of class* $\mathcal{S}_k$, *JHEP* **07** (2015) 073 [1503.05159].

[90] V. Mitev and E. Pomoni, *2D CFT blocks for the 4D class* $\mathcal{S}_k$ *theories*, *JHEP* **08** (2017) 009 [1703.00736].

[91] A. Gadde, S. Gukov and P. Putrov, *Fivebranes and 4-manifolds*, 1306.4320.

[92] B. Assel, S. Schafer-Nameki and J.-M. Wong, *M5-branes on $S^2 x M_4$: Nahm's Equations and 4d Topological Sigma-models*, 1604.03606.

[93] T. Dimofte, D. Gaiotto and S. Gukov, *Gauge Theories Labelled by Three-Manifolds*, *Commun. Math. Phys.* **325** (2014) 367 [1108.4389].

[94] Y. Terashima and M. Yamazaki, *SL(2,R) Chern-Simons, Liouville, and Gauge Theory on Duality Walls*, *JHEP* **08** (2011) 135 [1103.5748].

[95] S. Cecotti, C. Cordova and C. Vafa, *Braids, Walls, and Mirrors*, 1110.2115.

[96] O. Aharony, A. Hanany, K.A. Intriligator, N. Seiberg and M. Strassler, *Aspects of N=2 supersymmetric gauge theories in three-dimensions*, *Nucl. Phys. B* **499** (1997) 67 [hep-th/9703110].

[97] C. Closset, T.T. Dumitrescu, G. Festuccia and Z. Komargodski, *The Geometry of Supersymmetric Partition Functions*, *JHEP* **01** (2014) 124 [1309.5876].

[98] V. Pestun et al., *Localization techniques in quantum field theories*, *J. Phys. A* **50** (2017) 440301 [1608.02952].

[99] C. Closset, H. Kim and B. Willett, *Seifert fibering operators in 3d $\mathcal{N} = 2$ theories*, *JHEP* **11** (2018) 004 [1807.02328].

[100] C. Cordova and D.L. Jafferis, *Five-Dimensional Maximally Supersymmetric Yang-Mills in Supergravity Backgrounds*, 1305.2886.

[101] C. Cordova and D.L. Jafferis, *Complex Chern-Simons from M5-branes on the Squashed Three-Sphere*, 1305.2891.

[102] T. Dimofte, D. Gaiotto and S. Gukov, *3-Manifolds and 3d Indices*, *Adv.Theor.Math.Phys.* **17** (2013) 975 [1112.5179].

[103] S. Gukov and D. Pei, *Equivariant Verlinde formula from fivebranes and vortices*, *Commun. Math. Phys.* **355** (2017) 1 [1501.01310].

[104] E. Witten, *Supersymmetric index of three-dimensional gauge theory*, hep-th/9903005.

[105] N.A. Nekrasov and S.L. Shatashvili, *Supersymmetric vacua and Bethe ansatz*, *Nucl. Phys. Proc. Suppl.* **192-193** (2009) 91 [0901.4744].

[106] N.A. Nekrasov and S.L. Shatashvili, *Bethe/Gauge correspondence on curved spaces*, *JHEP* **01** (2015) 100 [1405.6046].

[107] C. Closset and H. Kim, *Comments on twisted indices in 3d supersymmetric gauge theories*, *JHEP* **08** (2016) 059 [1605.06531].

[108] C. Closset, H. Kim and B. Willett, *Supersymmetric partition functions and the three-dimensional A-twist*, *JHEP* **03** (2017) 074 [1701.03171].

[109] F. Benini and A. Zaffaroni, *Supersymmetric partition functions on Riemann surfaces*, *Proc. Symp. Pure Math.* **96** (2017) 13 [1605.06120].

[110] H.-J. Chung, T. Dimofte, S. Gukov and P. Sulkowski, *3d-3d Correspondence Revisited*, *JHEP* **04** (2016) 140 [1405.3663].

[111] D. Gaiotto, A. Kapustin, N. Seiberg and B. Willett, *Generalized Global Symmetries*, *JHEP* **02** (2015) 172 [1412.5148].

[112] Y. Tachikawa, *On the 6d origin of discrete additional data of 4d gauge theories*, *JHEP* **05** (2014) 020 [1309.0697].

[113] S. Gukov, P.-S. Hsin and D. Pei, *Generalized Global Symmetries of $T[M]$ Theories. I*, 2010.15890.

[114] R.L. Bryant and S.M. Salamon, *On the construction of some complete metrics with exceptional holonomy*, *Duke Math. J.* **58** (1989) 829.

[115] D. Joyce, *Compact Manifolds with Special Holonomy*, Oxford mathematical monographs, Oxford University Press (2000).

[116] A. Kovalev, *Twisted connected sums and special Riemannian holonomy*, math/0012189.

[117] A. Corti, M. Haskins, J. Nordström and T. Pacini, *Asymptotically cylindrical Calabi-Yau 3-folds from weak Fano 3-folds*, *Geom. Topol.* **17** (2013) 1955.

[118] A. Corti, M. Haskins, J. Nordström and T. Pacini, *G_2-manifolds and associative submanifolds via semi-Fano 3-folds*, *Duke Math. J.* **164** (2015) 1971 [1207.4470].

[119] F. Benini and S. Benvenuti, *$\mathcal{N}$=1 dualities in 2+1 dimensions*, 1803.01784.

[120] D. Gaiotto, Z. Komargodski and J. Wu, *Curious Aspects of Three-Dimensional $\mathcal{N} = 1$ SCFTs*, *JHEP* **08** (2018) 004 [1804.02018].

[121] F. Benini and S. Benvenuti, *N=1 QED in 2+1 dimensions: Dualities and enhanced symmetries*, 1804.05707.

[122] C. Choi, M. Roˇ cek and A. Sharon, *Dualities and Phases of $3DN = 1$ SQCD*, *JHEP* **10** (2018) 105 [1808.02184].

[123] B.S. Acharya and C. Vafa, *On domain walls of N=1 supersymmetric Yang-Mills in four-dimensions*, hep-th/0103011.

[124] A. Ritz, M. Shifman and A. Vainshtein, *Counting domain walls in N=1 superYang-Mills*, *Phys. Rev. D* **66** (2002) 065015 [hep-th/0205083].

[125] V. Bashmakov, F. Benini, S. Benvenuti and M. Bertolini, *Living on the walls of super-QCD*, *SciPost Phys.* **6** (2019) 044 [1812.04645].

[126] J. Halverson and D.R. Morrison, *The landscape of M-theory compactifications on seven-manifolds with G_2 holonomy*, *JHEP* **04** (2015) 047 [1412.4123].

[127] J. Halverson and D.R. Morrison, *On gauge enhancement and singular limits in G_2 compactifications of M-theory*, *JHEP* **04** (2016) 100 [1507.05965].

[128] T.C.d.C. Guio, H. Jockers, A. Klemm and H.-Y. Yeh, *Effective action from M-theory on twisted connected sum G_2-manifolds*, 1702.05435.

[129] A.P. Braun and S. Schafer-Nameki, *Compact, Singular G2-Holonomy Manifolds and M/Heterotic/F-Theory Duality*, 1708.07215.

[130] A.P. Braun, M. Del Zotto, J. Halverson, M. Larfors, D.R. Morrison and S. Schafer-Nameki, *Infinitely Many M2-instanton Corrections to M-theory on G_2-manifolds*, 1803.02343.

[131] A.P. Braun, S. Cizel, M. Hübner and S. Schäfer-Nameki, *Higgs bundles for M-theory on G_2-manifolds*, *JHEP* **03** (2019) 199 [1812.06072].

[132] O. DeWolfe, T. Hauer, A. Iqbal and B. Zwiebach, *Constraints on the BPS spectrum of N=2, D = 4 theories with A-D-E flavor symmetry*, *Nucl. Phys. B* **534** (1998) 261 [hep-th/9805220].

[133] A. Iqbal, *Selfintersection number of BPS junctions in backgrounds of three-branes and seven-branes*, *JHEP* **10** (1999) 032 [hep-th/9807117].

[134] O. Bergman and D. Rodriguez-Gomez, *The Cat's Cradle: Deforming the higher rank E_1 and $\tilde{E}_1$ theories*, 2011.05125.

[135] H. Kraft and C. Procesi, *Minimal singularities in gl n*, *Inventiones mathematicae* **62** (1980) 503.

[136] H. Kraft and C. Procesi, *On the geometry of conjugacy classes in classical groups*, *Commentarii Mathematici Helvetici* **57** (1982) 539.

[137] D. Maclagan and B. Sturmfels, *Introduction to Tropical Geometry*, vol. 161 of *Graduate Studies in Mathematics*, American Mathematical Society, Providence, RI (2015).

[138] K. Altmann, *The versal deformation of an isolated toric Gorenstein singularity*, *Invent. Math.* **128** (1997) 443.

[139] K. Altmann, *Infinitesimal deformations and obstructions for toric singularities*, *arXiv preprint alg-geom/9405008* (1994) .

[140] G. Pick, "Geometrisches zur Zahlenlehre." Sonderabdr. Naturw.-medizin. Verein f. Böhmen "Lotos" Nr. 8, 9 S. 8° (1899)., 1899.

[141] O. Bergman and A. Fayyazuddin, *String junction transitions in the moduli space of N=2 SYM*, *Nucl. Phys. B* **535** (1998) 139 [hep-th/9806011].

[142] G. Zafrir, *Brane webs, 5d gauge theories and 6d $\mathcal{N}=(1,0)$ SCFT's*, *JHEP* **12** (2015) 157 [1509.02016].

[143] N. Mekareeya, K. Ohmori, Y. Tachikawa and G. Zafrir, *E_8 instantons on type-A ALE spaces and supersymmetric field theories*, *JHEP* **09** (2017) 144 [1707.04370].

[144] A. Bourget, A. Hanany and D. Miketa, *Quiver origami: discrete gauging and folding*, 2005.05273.

[145] H. Hayashi, Y. Tachikawa and K. Yonekura, *Mass-deformed T_N as a linear quiver*, *JHEP* **02** (2015) 089 [1410.6868].

[146] E. Witten, *Constraints on Supersymmetry Breaking*, *Nucl. Phys.* **B202** (1982) 253.

[147] F. Benini, P.-S. Hsin and N. Seiberg, *Comments on global symmetries, anomalies, and duality in (2 + 1)d*, *JHEP* **04** (2017) 135 [1702.07035].

[148] E. Witten, *SL(2,Z) action on three-dimensional conformal field theories with Abelian symmetry*, hep-th/0307041.

[149] P.-S. Hsin, H.T. Lam and N. Seiberg, *Comments on One-Form Global Symmetries and Their Gauging in 3d and 4d*, *SciPost Phys.* **6** (2019) 039 [1812.04716].

[150] P. Orlik, *Seifert manifolds*, Lecture Notes in Mathematics, Vol. 291, Springer-Verlag, Berlin-New York (1972).

[151] H.M. Pedersen, *Splice diagram determining singularity links and universal abelian covers*, *Geom. Dedicata* **150** (2011) 75.

[152] M. Scharlemann, *Heegaard splittings of compact 3-manifolds*, in *Handbook of geometric topology*, pp. 921–953, North-Holland, Amsterdam (2002).

[153] N. Saveliev, *Lectures on the topology of* 3*-manifolds*, De Gruyter Textbook, Walter de Gruyter & Co., Berlin (1999), 10.1515/9783110806359.

[154] D. Gaiotto and E. Witten, *Janus Configurations, Chern-Simons Couplings, And The theta-Angle in N=4 Super Yang-Mills Theory*, *JHEP* **1006** (2010) 097 [0804.2907].

[155] D. Gaiotto and E. Witten, *Supersymmetric Boundary Conditions in N=4 Super Yang-Mills Theory*, 0804.2902.

[156] S. Gukov, P. Putrov and C. Vafa, *Fivebranes and 3-manifold homology*, *JHEP* **07** (2017) 071 [1602.05302].

[157] S. Gukov, D. Pei, P. Putrov and C. Vafa, *BPS spectra and 3-manifold invariants*, 1701.06567.

[158] L.F. Alday, P. Benetti Genolini, M. Bullimore and M. van Loon, *Refined 3d-3d Correspondence*, *JHEP* **04** (2017) 170 [1702.05045].

[159] F. Aprile, S. Pasquetti and Y. Zenkevich, *Flipping the head of $T[SU(N)]$: mirror symmetry, spectral duality and monopoles*, *JHEP* **04** (2019) 138 [1812.08142].

[160] F. Benini, Y. Tachikawa and D. Xie, *Mirrors of 3d Sicilian theories*, *JHEP* **1009** (2010) 063 [1007.0992].

[161] D. Pei, *3d-3d Correspondence for Seifert Manifolds*, Ph.D. thesis, Caltech, 2016.

[162] A. Kapustin, H. Kim and J. Park, *Dualities for 3d Theories with Tensor Matter*, *JHEP* **12** (2011) 087 [1110.2547].

[163] D. Jafferis and X. Yin, *A Duality Appetizer*, 1103.5700.

[164] S.S. Razamat and B. Willett, *Star-shaped quiver theories with flux*, *Phys. Rev. D* **101** (2020) 065004 [1911.00956].

[165] A. Giveon and D. Kutasov, *Seiberg Duality in Chern-Simons Theory*, *Nucl.Phys.* **B812** (2009) 1 [0808.0360].

[166] B. Willett and I. Yaakov, *N=2 Dualities and Z Extremization in Three Dimensions*, 1104.0487.

[167] J. Teschner and G. Vartanov, *6j symbols for the modular double, quantum hyperbolic geometry, and supersymmetric gauge theories*, *Lett. Math. Phys.* **104** (2014) 527 [1202.4698].

[168] E. Witten, *Geometric Langlands From Six Dimensions*, 0905.2720.

[169] D.S. Freed and C. Teleman, *Relative quantum field theory*, *Commun. Math. Phys.* **326** (2014) 459 [1212.1692].

[170] D. Gang and K. Yonekura, *Symmetry enhancement and closing of knots in 3d/3d correspondence*, *JHEP* **07** (2018) 145 [1803.04009].

[171] S. Gukov, D. Pei, P. Putrov and C. Vafa, *4-manifolds and topological modular forms*, 1811.07884.

[172] S. Monnier, *The anomaly field theories of six-dimensional (2,0) superconformal theories*, *Adv. Theor. Math. Phys.* **22** (2018) 2035 [1706.01903].

[173] E. Witten, *Five-brane effective action in M theory*, *J. Geom. Phys.* **22** (1997) 103 [hep-th/9610234].

[174] O. Aharony, N. Seiberg and Y. Tachikawa, *Reading between the lines of four-dimensional gauge theories*, *JHEP* **08** (2013) 115 [1305.0318].

[175] D. Pei and K. Ye, *A 3d-3d appetizer*, *JHEP* **11** (2016) 008 [1503.04809].

[176] M.C.N. Cheng, S. Chun, F. Ferrari, S. Gukov and S.M. Harrison, *3d Modularity*, *JHEP* **10** (2019) 010 [1809.10148].

[177] F. Benini, D. Gang and L.A. Pando Zayas, *Rotating Black Hole Entropy from M5 Branes*, 1909.11612.

[178] S. Gukov, *Gauge theory and knot homologies*, *Fortsch. Phys.* **55** (2007) 473 [0706.2369].

[179] P.S. Howe, E. Sezgin and P.C. West, *Covariant field equations of the M theory five-brane*, *Phys. Lett.* **B399** (1997) 49 [hep-th/9702008].

[180] D. Joyce, *Riemannian holonomy groups and calibrated geometry*, in *Calabi-Yau Manifolds and Related Geometries*, pp. 1–68, Springer (2003).

[181] E. Witten, *Quantum Field Theory and the Jones Polynomial*, *Commun. Math. Phys.* **121** (1989) 351.

[182] E. Witten, *Elliptic Genera and Quantum Field Theory*, *Commun. Math. Phys.* **109** (1987) 525.

[183] V. Bashmakov, J. Gomis, Z. Komargodski and A. Sharon, *Phases of $\mathcal{N} = 1$ Theories in 2+1 Dimensions*, 1802.10130.

[184] R. Gopakumar and C. Vafa, *Branes and fundamental groups*, *Adv. Theor. Math. Phys.* **2** (1998) 399 [hep-th/9712048].

[185] E. Witten, *Topology Changing Amplitudes in (2+1)-Dimensional Gravity*, *Nucl. Phys.* **B323** (1989) 113.

[186] D. Birmingham, M. Blau and G. Thompson, *Geometry and Quantization of Topological Gauge Theories*, *Int. J. Mod. Phys.* **A5** (1990) 4721.

[187] B. Geyer and D. Mulsch, *N(T) = 4 equivariant extension of the 3-D topological model of Blau and Thompson*, *Nucl. Phys.* **B616** (2001) 476 [hep-th/0108042].

[188] M. Blau and G. Thompson, *Aspects of N(T) ≥ 2 topological gauge theories and D-branes*, *Nucl. Phys.* **B492** (1997) 545 [hep-th/9612143].

[189] R. Dijkgraaf and G.W. Moore, *Balanced topological field theories*, *Commun. Math. Phys.* **185** (1997) 411 [hep-th/9608169].

[190] A. Haydys and T. Walpuski, *A compactness theorem for the Seiberg-Witten equation with multiple spinors in dimension three*, *Geom. Funct. Anal.* **25** (2015) 1799.

[191] M. Blau and G. Thompson, *N=2 topological gauge theory, the Euler characteristic of moduli spaces, and the Casson invariant*, *Comm. Math. Phys.* **152** (1993) 41 [hep-th/9112012].

[192] E. Bergshoeff, E. Sezgin and A. Van Proeyen, *(2,0) tensor multiplets and conformal supergravity in D = 6*, *Class.Quant.Grav.* **16** (1999) 3193 [hep-th/9904085].

[193] T. Kugo and K. Ohashi, *Supergravity tensor calculus in 5-D from 6-D*, *Prog. Theor. Phys.* **104** (2000) 835 [hep-ph/0006231].

[194] T. Kitao, K. Ohta and N. Ohta, *Three-dimensional gauge dynamics from brane configurations with (p,q)-fivebrane*, *Nucl. Phys. B* **539** (1999) 79 [hep-th/9808111].

[195] O. Bergman, A. Hanany, A. Karch and B. Kol, *Branes and supersymmetry breaking in three-dimensional gauge theories*, *JHEP* **10** (1999) 036 [hep-th/9908075].

[196] D. Xie, *M5 brane and four dimensional N = 1 theories I*, *JHEP* **04** (2014) 154 [1307.5877].

[197] A. Hashimoto, P. Ouyang and M. Yamazaki, *Boundaries and defects of $\mathcal{N} = 4$ SYM with 4 supercharges. Part I: Boundary/junction conditions*, *JHEP* **10** (2014) 107 [1404.5527].

[198] A. Hashimoto, P. Ouyang and M. Yamazaki, *Boundaries and defects of $\mathcal{N} = 4$ SYM with 4 supercharges. Part II: Brane constructions and 3d $\mathcal{N} = 2$ field theories*, *JHEP* **10** (2014) 108 [1406.5501].

[199] C. Cordova, T.T. Dumitrescu and K. Intriligator, *Multiplets of Superconformal Symmetry in Diverse Dimensions*, *JHEP* **03** (2019) 163 [1612.00809].

[200] D.R. Morrison, S. Schafer-Nameki and B. Willett, *Higher-Form Symmetries in 5d*, *JHEP* **09** (2020) 024 [2005.12296].

[201] F. Albertini, M. Del Zotto, I.n. García Etxebarria and S.S. Hosseini, *Higher Form Symmetries and M-theory*, 2005.12831.

[202] L. Bhardwaj and S. Schäfer-Nameki, *Higher-form symmetries of 6d and 5d theories*, 2008.09600.

[203] K. Ohmori, H. Shimizu, Y. Tachikawa and K. Yonekura, *6d $\mathcal{N} = (1, 0)$ theories on T^2 and class S theories: Part I*, *JHEP* **07** (2015) 014 [1503.06217].

[204] M. Del Zotto, C. Vafa and D. Xie, *Geometric engineering, mirror symmetry and* $6\mathrm{d}_{(1,0)} \to 4\mathrm{d}_{(\mathcal{N}=2)}$, *JHEP* **11** (2015) 123 [1504.08348].

[205] S.S. Razamat, C. Vafa and G. Zafrir, *4d $\mathcal{N} = 1$ from 6d (1, 0)*, *JHEP* **04** (2017) 064 [1610.09178].

[206] I. Bah, A. Hanany, K. Maruyoshi, S.S. Razamat, Y. Tachikawa and G. Zafrir, *4d $\mathcal{N} = 1$ from 6d $\mathcal{N} = (1, 0)$ on a torus with fluxes*, *JHEP* **06** (2017) 022 [1702.04740].

[207] H.-C. Kim, S.S. Razamat, C. Vafa and G. Zafrir, *Compactifications of ADE conformal matter on a torus*, *JHEP* **09** (2018) 110 [1806.07620].

[208] K. Yonekura, *Instanton operators and symmetry enhancement in 5d supersymmetric quiver gauge theories*, *JHEP* **07** (2015) 167 [1505.04743].

[209] G.W. Mackey, *Graphs, singularities, and finite groups*, *Uspekhi Matematicheskikh Nauk* **38** (1983) 159.

[210] W. Jaco, *Lectures on three-manifold topology*, vol. 43 of *CBMS Regional Conference Series in Mathematics*, American Mathematical Society, Providence, R.I. (1980).

[211] L. Ben Abdelghani and S. Boyer, *A calculation of the Culler-Shalen seminorms associated to small Seifert Dehn fillings*, *Proc. London Math. Soc. (3)* **83** (2001) 235.

[212] R.C. McLean, *Deformations of calibrated submanifolds*, *Comm. Anal. Geom.* **6** (1998) 705.

[213] R. Harvey and H.B. Lawson, Jr., *Calibrated geometries*, *Acta Math.* **148** (1982) 47.

[214] N. Hitchin, *Harmonic spinors*, *Advances in Math.* **14** (1974) 1.

[215] A. Lichnerowicz, *Spineurs harmoniques*, *C. R. Acad. Sci. Paris* **257** (1963) 7.

[216] N. Kaloper, *Topological mass generation in three-dimensional string theory*, *Phys. Lett.* **B320** (1994) 16 [hep-th/9310011].

[217] J.F. Schonfeld, *A Mass Term for Three-Dimensional Gauge Fields*, *Nucl. Phys.* **B185** (1981) 157.

[218] A.J. Moreno and H.N.S. Earp, *The Weitzenböck formula for the Fueter-Dirac operator*, 1701.06061.